The RNA-binding activity of glycolytic enzymes in melanoma

Ana Luisa Dian

THESE DE DOCTORAT

NNT : 2024UPASL058

The RNA-binding activity of glycolytic enzymes in melanoma

L'activité de liaison à l'ARN des enzymes de la glycolyse dans le mélanome

Thèse de doctorat de l'université Paris-Saclay

École doctorale n° 582, Cancérologie : Biologie, Médecine, Santé (CBMS)
Spécialité de doctorat : Sciences du cancer
Graduate School : Life Science and Health. Référent : Faculté de Médecine

Thèse préparée dans l'unité de recherche **Intégrité du génome, ARN et cancer** (Institut Curie, CNRS, Université Paris Saclay), sous la direction de **Stéphan VAGNER**, directeur de recherche.

Thèse soutenue à Paris-Saclay, le 27 septembre 2024, par

Ana Luisa DIAN

Composition du Jury

Membres du jury avec voix délibérative

Virginie MARCEL Directrice de recherche, Centre de Recherche en Cancérologie de Lyon	Présidente
Frederick BOST Directeur de recherche, Université Côte d'Azur	Rapporteur & Examinateur
Michele TRABUCCHI Directeur de recherche, Université Côte d'Azur	Rapporteur & Examinateur
Fátima GEBAUER Directrice de recherche, Universitat Pompeu Fabra Centre for Genomic Regulation (CRG)	Examinatrice

université
PARIS-SACLAY

ÉCOLE DOCTORALE
Cancérologie : biologie - médecine - santé (CBMS)


institut
Curie

MSCA

Fondation pour la
Recherche
Médicale

LA LIGUE
CONTRE LE CANCER

cnrs

Inserm
La science pour la santé
From science to health

Titre : L'activité de liaison à l'ARN des enzymes de la glycolyse dans le mélanome

Mots clés : Mélanome, protéine de liaison à l'ARN, ARN, glycolyse, traduction, hexokinase

Résumé : Au cours de la dernière décennie, le développement de nouvelles approches a permis d'identifier un répertoire plus complet de protéines liant l'ARN (RBP), qui comprenait diverses enzymes glycolytiques. En effet, les enzymes glycolytiques sont des protéines étonnamment complexes et à multiples facettes qui remplissent également des fonctions non glycolytiques. Il a été démontré que GAPDH et PKM, par exemple, se lient directement aux ARNm et, dans certains cas, régulent leur traduction. La dérégulation de la traduction des ARNm est fréquemment décrite dans le cancer. Il existe déjà de nombreuses données démontrant que l'altération de la fonction d'une RBP a un impact significatif sur le phénotype du cancer. Étant donné l'importance critique de la traduction de l'ARNm et de la glycolyse dans les cellules cancéreuses à croissance rapide, le rôle des enzymes glycolytiques utilisées en tant que RBP doit encore être élucidée dans le contexte du cancer. Nous montrons ici que l'Hexokinase II (HK2), une glucose kinase qui catalyse la première étape de la glycolyse dans les cellules cancéreuses, est une nouvelle RBP qui régule la traduction des ARNm dans le mélanome. En particulier, nous avons découvert que HK2 régule la traduction de l'ARNm codant SOX10, un facteur de transcription de la lignée de la crête neurale dont l'expression est impliquée dans la prolifération des cellules de mélanome, la croissance tumorale, l'invasion et la résistance aux médicaments. La régulation de la traduction de l'ARNm SOX10 par HK2 dépend de la région 5' non traduite (5'UTR). Nous avons également identifié que la régulation de la traduction de SOX10 dépendante de HK2 est impliquée dans la formation de colonies et les propriétés de prolifération des cellules de mélanome. En conclusion, nos données mettent en évidence une fonction non métabolique de HK2, indiquant que les cellules cancéreuses peuvent augmenter la glycolyse à des fins autres que le simple anabolisme. Une meilleure compréhension des rôles respectifs des activités de liaison à l'ARN et kinase de HK2 pourrait fournir des indices sur la coordination entre le métabolisme et l'expression génétique.

université PARIS-SACLAY | ÉCOLE DOCTORALE Cancérologie : biologie - médecine - santé (CBMS)

Title : The RNA-binding activity of glycolytic enzymes in melanoma

Keywords : Melanoma, RNA-binding protein, RNA, glycolysis, translation, hexokinase

Abstract : Over the past decade, the development of new approaches has allowed the identification of a more complete repertoire of RNA-binding proteins (RBPs), which included various glycolytic enzymes. Indeed, glycolytic enzymes are unexpectedly complex, multifaceted proteins shown to also perform non-glycolytic functions. GAPDH and PKM, for example, have been demonstrated to bind directly to mRNAs and, in some instances, regulate their translation. The dysregulation of mRNA translation is a frequent feature in cancer and there is already ample experimental evidence that altered RBP function has a significant impact on cancer phenotype. Given the critical importance of mRNA translation and glycolysis in rapidly growing cancer cells, the significance of glycolytic enzymes moonlighting as RBPs still needs to be elucidated in the cancer context. Here, we report that Hexokinase II (HK2), a glucose kinase that catalyses the first step of glycolysis in cancer cells, is a novel bona-fide RBP that regulates mRNA translation in melanoma. In particular, we found that HK2 regulates the translation of the mRNA encoding SOX10, a neural crest lineage transcription factor whose expression has been implicated in melanoma cell proliferation, tumour growth, invasion and drug resistance. The translation regulation of the SOX10 mRNA mediated by HK2 occurs in a manner dependent on the 5' untranslated region (5'UTR). We further identified that HK2-dependent SOX10 translational regulation is involved in colony formation and proliferation properties of melanoma cells. Collectively, our data highlight a non-metabolic function of HK2, indicating that cancer cells may enhance glycolysis for purposes beyond simple anabolism. A better understanding of the respective roles of the HK2 RNA binding and kinase activities will potentially provide some clues on the coordination between metabolism and gene expression.

université PARIS-SACLAY | ÉCOLE DOCTORALE Cancérologie : biologie - médecine - santé (CBMS)

ACKNOWLEDGMENT

First, I would like to express my deepest gratitude to my supervisor, Dr. Stephan VAGNER, for giving me this life-changing opportunity. I cannot thank you enough for your guidance, patience, kindness, and for generously sharing your invaluable knowledge with me. Thank you for opening the doors of your lab to me and for believing in me, even during times when I struggled to believe in myself. In your lab, I had the privilege of meeting many incredible people who were essential throughout the development of my thesis. In fact, each lab and unit colleague supported me in countless ways. In particular, I would like to thank Drice CHALLAL for the crucial help at the beginning of my PhD. I also thank Lucilla FABBRI, who was not only kind enough to support me from start to finish, but who also served as a true example of resilience, honesty, and generosity. Thank you for your friendship. Along those lines, I would like to thank Alexandre DEVAUX for the time we spent together during the PhD. I'll miss our conversations and, most importantly, spotting squirrels with you! To Sidhant KALIA, thank you for your friendship, especially during my fourth year. You arrived at such an important time and reminded me that friendship (and PhD life) doesn't need to be overly complicated. I can't wait to see you shine in your defense! To Clara BONNET, or Clarinha, we started our thesis journey together, and from day one, we knew we were going to be friends. Thank you for the good moments inside and outside the lab.

However, none of this would have been possible without my family. Aos meus pais, Aloisio e Elisabete, eu não tenho palavras para expressar a imensa gratidão que sinto por vocês. Todas as minhas conquistas são frutos de suas vidas que foram e são repletas de muitas batalhas, mas também de muito amor e companheirismo. Obrigada por embarcarem em mais um desafio comigo, mesmo que dessa vez tenha sido a quase 10.000 km de distância e que tenha começado na turbulência de uma inimaginável pandemia. To my beloved sisters and best friends, Livia and Natalia, thank you for being my lifesaving jackets and personal cheerleaders throughout all these years. You were always there for me. To my boyfriend, Lucas, moving to France and starting our PhD journey together once felt like an unimaginable dream, but we made it! I know it wasn't always easy, but thank you for choosing to embark on this adventure with me. You, more than anyone, know that I couldn't have achieved any of this without you. You were, and always will be, my rock. Congratulations, Dr. Lucas, we did it! And always, together.

I would also like to thank the members of my Thesis Monitoring Committee, Dr. Sebastien APCHER and Dr. Olivier NAMY, for their guidance and support throughout my doctorate. Finally, I would like to thank Dr. Virginie MARCEL, Dr. Frederick BOST, Dr. Michele TRABUCCHI, and Dr. Fátima GEBAUER for kindly accepting the invitation to serve as jury members for my PhD defense. Your expertise provided invaluable insights and contributed significantly to my work.

My eternal gratitude to all of you!

RÉSUMÉ DÉTAILLÉ

INTRODUCTION

La biologie de l'ARN est coordonnée par l'interaction des ARN avec des protéines spécialisées possédant une activité de liaison à l'ARN. Ces protéines sont appelées protéines liant l'ARN (RBPs), et leur interaction avec l'ARN varie de l'interaction protéine-ARN unique à l'assemblage de complexes dynamiques comprenant plusieurs RBPs et molécules d'ARN. Ces complexes sont appelés particules ribonucléoprotéiques (RNP) et ils sont principalement impliqués dans la régulation de l'expression génique. Cette régulation est essentielle pour maintenir l'homéostasie cellulaire, et les complexes RNP le font en coordonnant les étapes de traitement co- et post-transcriptionnelles, de la synthèse à la dégradation, de toutes les classes d'ARN. En tant qu'effecteurs critiques de l'expression génique, il n'est pas surprenant que des altérations aberrantes de l'expression et de la fonction des RBPs soient liées à plusieurs maladies, y compris le cancer.

Le nombre de protéines identifiées comme RBPs a considérablement augmenté au cours de la dernière décennie. En 2010, le premier catalogue des RBPs humains comprenait un total de 422 protéines. En 2021, ce nombre a augmenté à plus de 6000 RBPs potentiels, et il continue d'augmenter grâce au développement d'un éventail polyvalent de méthodes permettant d'identifier et de caractériser les interactions ARN-protéine. Les approches disponibles pour étudier ces interactions peuvent être divisées en deux grandes catégories en fonction de la question biologique abordée : les méthodes centrées sur l'ARN et les méthodes centrées sur la protéine. Les méthodes centrées sur l'ARN, comme leur nom l'indique, se concentrent sur un ARN d'intérêt pour caractériser les protéines qui lui sont liées. Les méthodes centrées sur la protéine, en revanche, sont utilisées pour examiner les ARN liés par une protéine d'intérêt. Chaque méthode possède évidemment son propre ensemble de forces et de limitations. Comprendre ces nuances permet de sélectionner l'approche la plus optimale pour l'application.

Ces dernières années, plusieurs méthodes quantitatives à grande échelle ont été développées pour examiner le protéome global lié à l'ARN (RBPome) afin de cataloguer un répertoire de RBPs plus complet et d'obtenir des informations sur les caractéristiques qui régulent les interactions ARN-protéine dans les processus physiologiques et pathologiques. Dans ces méthodes, les RBPs sont identifiés par spectrométrie de masse, tandis que leurs ARN correspondants liés et leurs sites de liaison sont identifiés par séquençage à haut débit. Ensemble, ces méthodes ont permis l'identification de RBPs déjà connus mais aussi de nouveaux. De manière intrigante, de nombreux nouveaux candidats identifiés ne possèdent pas les caractéristiques connues des RBPs, telles que la fonction de régulation du destin de l'ARN et des caractéristiques architecturales bien établies (RBDs). Cependant, ces protéines contenaient une diversité d'autres domaines, y compris des régions

intrinsèquement désordonnées (IDRs) et des domaines associés à différentes fonctions moléculaires (par exemple, la liaison à l'ADN et les interactions protéine-protéine). Remarquablement, de nombreuses enzymes métaboliques identifiées comme RBPs non conventionnelles ont été proposées pour lier l'ARN à travers des régions à proximité de leurs poches de liaison aux substrats. Ces domaines multifonctionnels proposés semblent donc être monnaie courante et non l'exception parmi les RBPs non conventionnelles. De nouvelles études promettent de dévoiler comment cette nouvelle classe de RBPs se lie à l'ARN, la spécificité de cette liaison et comment cette interaction est régulée. En effet, une étape importante pour la découverte de RBPs non canoniques est la caractérisation impartiale des régions de liaison à l'ARN. De tels efforts promettent une meilleure compréhension des mécanismes moléculaires derrière la fonction des RBPs associées aux maladies, et la conceptualisation de nouvelles interventions thérapeutiques.

Ces nouvelles RBP dépourvues de RBD canoniques ou de liens connus avec la biologie de l'ARN ont été récemment appelées « enigmRBP », et leur découverte suggère l'existence d'interactions inexplorées entre l'expression des gènes et d'autres processus biologiques. Les énigmRBP couvrent un large éventail de protéines qui, à leur tour, remplissent diverses fonctions biologiques. Par exemple, des études ont montré que les enzymes glycolytiques sont des protéines étonnamment complexes et à multiples facettes, plutôt que de simples composants de la voie glycolytique. Il a été démontré que ces enzymes remplissent des fonctions non glycolytiques, notamment la régulation des réponses inflammatoires, l'expression des gènes et d'autres processus cellulaires, tels que l'apoptose, le cycle cellulaire, l'autophagie et la dynamique du cytosquelette. Outre ces fonctions, plusieurs études sur l'interaction avec l'ARN ont montré que les enzymes glycolytiques se lient directement à l'ARN. Dans certains cas, il a été démontré que la liaison des enzymes glycolytiques à l'ARN contrôlait le destin de l'ARN ou même la fonction de la protéine.

L'aldolase, par exemple, se lie à l'UTR 3'de l'ARNm du *NF-L in vitro* et *in vivo*, et cette liaison est impliquée dans la régulation de la stabilité de l'ARNm. Une autre enzyme glycolytique, la GAPDH, se lie à la region 3′UTR d'une grande variété d'ARNm, en particulier au niveau des éléments riches en AU (ARE). La liaison de la GAPDH à l'ARNm de l'*IFN-γ*, par exemple, inhibe la traduction de l'ARNm. La liaison de l'enzyme glycolytique PGK1 à la région CDS de l'ARNm du *uPAR* diminue la stabilité de la transcription. En outre, il a été proposé que l'activité RBP non canonique de la PKM favorise le blocage de la traduction. En revanche, il a été démontré que la liaison d'ENO1 à l'ARN inhibait spécifiquement son activité enzymatique à la fois *in vitro* et *in vivo*. Cependant, alors que des rapports sporadiques ont montré que certaines enzymes glycolytiques sont effectivement des RBP, d'autres restent des RBP putatives (par exemple, les hexokinases) chez l'homme en raison de l'absence de preuves expérimentales supplémentaires de leur activité de liaison à l'ARN.

Les enzymes glycolytiques ne sont pas les seules protéines métaboliques à avoir été identifiées comme des RBP non conventionnelles. En effet, de nombreuses enzymes

impliquées dans d'autres voies métaboliques classiques ont également été identifiées à plusieurs reprises comme des liants d'ARN dans des études d'interactome d'ARN, suggérant une fois de plus l'existence d'interconnexions étendues entre la régulation des gènes et le métabolisme. Bon nombre de ces enzymes, notamment les aconitases, les enzymes du cycle TCA/OXPHOS, des métabolisme des acides gras, des cycle de synthèse du thymidylate, entre autres, ont été validées comme liant directement l'ARN et régulant le destin de l'ARN. Dans certains cas, il a également été démontré que cette liaison régulait la stabilité et la fonction de l'enzyme.

Il ne fait aucun doute que les enzymes métaboliques peuvent jouer le rôle de régulateurs des ARN(m), en assumant des fonctions cruciales dans la régulation des étapes co- et post-transcriptionnelles de l'expression des gènes, en agissant comme des facteurs de trans-action pour contrôler le destin de l'ARN. La découverte que ces enzymes métaboliques apparemment bien caractérisées peuvent également lier l'ARN constitue la base de l'hypothèse ARN-enzyme-métabolite (REM, de l'anglais RNA–enzyme–metabolite). Cette hypothèse propose l'existence de liens régulateurs entre l'expression des gènes et le métabolisme intermédiaire, médiés par l'activité de liaison à l'ARN des enzymes métaboliques, dont les fonctions sont régulées par des cofacteurs et des métabolites. De futures études visant à comprendre pourquoi, quand et comment ces complexes ARN-enzyme sont formés pourraient donner un aperçu des caractéristiques qui régulent ces interactions et élucider le rôle de ces enzymes en tant que régulateurs de l'expression génétique.

Avec la disponibilité croissante d'analyses transcriptomiques et protéomiques à haut débit, de plus en plus de données font état de divergences entre les concentrations d'ARNm et de protéines. Cela suggère que les niveaux d'ARNm ne suffisent pas à expliquer entièrement le comportement cellulaire et que des mécanismes post-transcriptionnels sont également nécessaires pour le contrôle de la fonction cellulaire. La traduction est un mécanisme essentiel pour l'expression des gènes, qui contrôle dynamiquement la synthèse des protéines et contribue ainsi à la détermination du phénotype cellulaire. Le processus de traduction de l'ARNm peut être divisé en quatre étapes : 1) l'initiation, l'étape la plus étroitement régulée ; 2) l'élongation ; 3) la terminaison ; et 4) le recyclage des ribosomes. La traduction étant l'étape finale de la synthèse des protéines, sa régulation permet de modifier immédiatement les niveaux de protéines des ARNm globaux et spécifiques, ce qui est donc plus avantageux pour les cellules que d'autres niveaux de manipulation.

En période de stress, les cellules atténuent la traduction globale des ARNm afin de réduire le coût énergétique élevé du processus et de donner la priorité à la traduction des ARNm qui répondent au stress. Il convient de noter qu'environ 50 à 75 % de l'énergie totale d'une cellule est consacrée à la synthèse des protéines. Il n'est donc pas surprenant qu'une régulation efficace de la traduction des ARNm soit vitale pour maintenir l'homéostasie cellulaire. En fait, le dérèglement du contrôle de la traduction a été désigné comme un facteur critique pour l'émergence de plusieurs troubles, y compris le cancer, les maladies neurodégénératives et les troubles métaboliques. Ces

résultats soulignent l'importance d'une connaissance plus approfondie des mécanismes impliqués dans la traduction des ARNm et de son remaniement par les cellules cancéreuses, en plus de la compréhension des caractéristiques impliquées dans la régulation de la biogenèse et de la fonction des ARNm. Plusieurs techniques, telles que le profilage des polysomes, ont été mises au point pour étudier les changements dans les niveaux de traduction des protéines, ce qui permet d'étudier le mécanisme moléculaire potentiel de la dérégulation de la traduction des ARNm.

Les facteurs communs affectant la traduction comprennent les facteurs d'initiation de la traduction, différentes caractéristiques de l'ARN (séquence, structure et modifications post-transcriptionnelles), les ARN non codants et les RBP, mais aussi les ARNt et les codons utilisés lors de la phase d'élongation de la traduction. C'est par la modulation de ces facteurs que la traduction est recomposée en réponse à différents stimuli, ce qui est vital non seulement pour la survie cellulaire, mais aussi pour la (dé)différenciation cellulaire, la tumorigenèse et l'agressivité du cancer. Bien que les mécanismes associant certains facteurs et régulateurs de la traduction au cancer ne sont pas entièrement élucidés, ils ont indubitablement lié ces caractéristiques aux processus oncogéniques. En outre, des altérations sélectives de la traduction des ARNm sont également observées dans les cellules soutenant les tumeurs, ce qui leur permet d'adapter leur protéome et, par conséquent, leur fonction cellulaire en cas de stress. En fin de compte, ces altérations pourraient contribuer au soutien des tumeurs et à l'apparition de métastases, mais aussi potentiellement faciliter l'activité antitumorale des cellules non cancéreuses présentes dans le microenvironnement tumoral.

Le ciblage de la machinerie de traduction et des protéines associées au sein de l'ETM au sens large ne conduit pas toujours à une réponse antitumorale directe, car les cellules cancéreuses et d'autres cellules des microenvironnement tumoral peuvent adopter des mécanismes compensatoires lorsqu'une voie de signalisation importante est perturbée. La compréhension des rôles des facteurs de traduction et d'autres régulateurs de la traduction dans le cancer peut révéler de nouvelles possibilités de cibler spécifiquement ces cellules cancéreuses et d'autres aspects malins des microenvironnement tumoral tout en équilibrant l'impact de l'inhibition de la traduction. En conclusion, les mécanismes de contrôle de la traduction sont à l'origine de la progression tumorale et de la résistance à la thérapie, ce qui constitue une vulnérabilité pouvant être ciblée.

OBJECTIFS DE LA THESE

Comme largement décrit dans l'introduction, les enzymes impliquées dans les voies métaboliques classiques ont été identifiées de manière récurrente comme jouant un rôle secondaire en tant que protéines de liaison à l'ARN (RBP, du anglais RNA-binding protein) impliquées dans la régulation post-transcriptionnelle des gènes. Compte tenu de l'importance cruciale de la glycolyse et de la traduction des ARNm dans les cellules cancéreuses, nous avons proposé d'explorer l'activité de liaison non canonique à l'ARN des enzymes glycolytiques dans le contrôle de la traduction des ARNm et d'élucider la signification de cette activité secondaire dans le contexte du cancer. L'hexokinase II (HK2), la première enzyme du métabolisme du glucose, est fortement exprimée dans les cellules cancéreuses. Bien que le rôle de HK2 dans la tumorigénèse a été attribué à son activité glycolytique, cette enzyme a montré des fonctions non canoniques qui régulent souvent des processus hautement pertinents pour la transformation cellulaire et le développement du cancer. De manière intrigante, HK2 a été identifiée de manière récurrente comme liant l'ARN dans diverses lignées cellulaires humaines par des méthodes quantitatives orthogonales à grande échelle. Ces découvertes nécessitent cependant une validation expérimentale supplémentaire par des recherches complémentaires. Néanmoins, bien que les hexokinases de levure (Hxks) ont montré qu'elles se lient directement aux acides nucléiques, une étude récente a révélé que de nombreuses protéines de liaison au glucose peuvent lier l'ARN dans les lignées cellulaires humaines. Ensemble, ces découvertes corroborent l'hypothèse que HK2 est une RBP non canonique dont l'activité de liaison à l'ARN pourrait être exploitée par les cellules cancéreuses.

Le laboratoire, en collaboration avec le groupe de Caroline Robert à l'Institut Gustave Roussy, a découvert par des expériences 2C que HK2 se lie à l'ARN. De plus, ils ont également trouvé par profilage des polysomes que HK2 régule la traduction des ARNm codant des gènes clés impliqués dans les propriétés de transition épithélio-mésenchymateuse (EMT). Ensemble, ces résultats ont servi de fondation pour mon projet de thèse. Nous pensons que l'activité de liaison à l'ARN de HK2 pourrait être impliquée dans le contrôle de la traduction des ARNm dans le mélanome. Étant donné que des études supplémentaires sont nécessaires pour valider HK2 en tant que RBP non canonique impliqué dans la régulation de l'expression des gènes, nous visons à explorer l'activité potentielle de liaison à l'ARN de HK2, à évaluer la signification de l'interaction de HK2 avec l'ARN dans le contrôle de l'expression génique post-transcriptionnelle et à déterminer si le contrôle post-transcriptionnel médié par HK2 a un impact sur les phénotypes liés au cancer.

RÉSULTATS

Moya-Plana (2020) a découvert que HK2 régule la traduction des ARNm dans les cellules de mélanome. Par exemple, dans la lignée cellulaire de mélanome A375, il a montré par profilage des polysomes que la déplétion de HK2 diminue la traduction des ARNm liés au cancer, tels que l'ARNm de *SOX10*, qui code pour un facteur de transcription jouant un rôle clé non seulement dans le développement des mélanocytes, mais aussi dans l'agressivité du mélanome. Nous avons émis l'hypothèse que cette régulation pourrait se faire par l'activité de liaison à l'ARN de HK2. Pour explorer si HK2 est une RBP non canonique, nous avons réalisé des essais 2C et CLIP dans des cellules vivantes. Ces essais sont complémentaires et reposent tous deux sur l'utilisation d'une irradiation UV-C pour lier de façon covalente et purifier les complexes ARN-RBP. Ensemble, ces techniques ont confirmé que HK2 se lie directement à l'ARN dans les cellules de mélanome et que cette liaison est globalement indépendante de l'activité enzymatique de HK2. Pour étudier plus précisément les interactions HK2-ARN, nous avons soumis des lysats de cellules A375 traités ou non par RNase à une ultracentrifugation en gradient de densité de saccharose et une fractionnement, identifiant ainsi que la composition des complexes contenant HK2 dépend partiellement de l'ARN.

En réalisant des analyses RIP-qPCR, nous avons identifié que HK2 se lie à l'ARNm de *SOX10*, spécifiquement à la 5'UTR de cet ARNm. Cette interaction a également été confirmée *in situ* à l'aide de techniques d'imagerie, telles que le RNA-PLA. Nous avons également constaté que l'interaction HK2-ARNm de *SOX10* est altérée en l'absence de glucose (en présence de galactose ou de l'analogue de glucose 2-DG). De manière intrigante, les expériences d'ultracentrifugation en gradient de densité de saccharose indiquent également que la composition des complexes contenant HK2 dépend moins de l'ARN en présence de galactose. Nous avons également étudié si HK2 pouvait se lier à l'ARNm de SOX10 de manière dépendante de la PKA, car il a été récemment démontré que HK2 interagit directement avec cette kinase dans le cancer du sein. Cependant, ni l'inhibition de la formation intracellulaire de l'AMPc ni l'induction et l'accumulation de l'AMPc n'ont eu d'impact sur l'association de HK2 avec l'ARNm de *SOX10*. Il est à noter que l'AMPc est nécessaire à l'activation de la PKA. De même, la déplétion de la PKA par siRNA n'a pas affecté l'interaction HK2-*SOX10* ARNm. Cependant, nous avons trouvé qu'un inhibiteur réversible compétitif de l'ATP de la PKA réduisait l'association HK2-ARNm de *SOX10*.

Pour évaluer le contrôle de la traduction des ARNm médié par HK2, Moya-Plana (2020) a réalisé des RT-qPCR sur l'ARNm de *SOX10* isolé des fractions polysomales des cellules A375 après déplétion de HK2. Nous avons également mis en evidence que la régulation à la baisse de la traduction de l'ARNm de *SOX10* après déplétion de HK2 a pu être observée au niveau de la protéine SOX10 par western blot dans différentes lignées cellulaires de mélanome. De plus, des essais de luciférase couplés à des RT-qPCR ont été réalisés pour définir les éléments cis-régulateurs sur l'ARNm de *SOX10* impliqués dans la régulation traductionnelle par HK2. Nous avons identifié que la

délétion de la moitié 3' de la region 5'UTR de *SOX10* conduit à une diminution de l'efficacité de la traduction. De manière frappante, les délétions dans cette région ont également diminué l'association entre HK2 et l'ARNm de *SOX10* dans les experiences de RIP. Nous avons ensuite étudié la possibilité que la traduction de l'ARNm de *SOX10* dépendante de HK2 soit impliquée dans les phénotypes liés au cancer, y compris la résistance aux therapies ciblées. Des essais fonctionnels ont été menés dans différentes lignées cellulaires de mélanome surexprimant SOX10, générées par la transduction de particules lentivirales portant la séquence ORF de SOX10 humain.

En utilisant des essais de cicatrisation des plaies 2D IncuCyte et des inserts de culture ibidi pour évaluer la capacité des cellules à migrer, nous avons observé que les cellules après déplétion de HK2 migraient significativement moins que les contrôles. Cependant, l'expression ectopique de SOX10 n'a pas réduit l'effet observé après la déplétion de HK2. Au contraire, la déplétion de HK2 dans les cellules transduites par SOX10 a montré une diminution encore plus importante de la capacité migratoire des cellules par rapport aux cellules de contrôle. Bien que nos résultats suggèrent que le rôle de HK2 dans la migration des cellules de mélanome peut ne pas impliquer SOX10, nous avons démontré que l'expression ectopique de SOX10 réduit l'effet de la déplétion de HK2 sur la clonogénicité et la prolifération.

Nous avons également étudié la possibilité que l'interaction HK2-ARNm de *SOX10* soit impliquée dans la résistance aux inhibiteurs de BRAF et de MEK dans les essais clonogéniques. Nous avons trouvé que la déplétion de HK2 ou l'incubation des cellules avec des inhibiteurs de BRAFi (vemurafenib) et de MEKi (cobimetinib) réduisait la formation de colonies. En fait, l'incubation des cellules avec BRAFi/MEKi a réduit la clonogénicité dans la même mesure, voire plus que les cellules qui sont knockdown de HK2 incubées dans le DMSO. L'effet du traitement médicamenteux semble indépendant de l'expression de HK2, car la déplétion de HK2 n'a pas eu d'effet supplémentaire sur la formation de colonies. De manière intrigante, l'expression ectopique de SOX10 après traitement médicamenteux a fortement inhibé la formation de colonies. Ces résultats suggèrent que HK2 n'est pas impliqué dans la résistance aux therapies ciblées, tandis que l'expression de SOX10 semble rendre les cellules plus sensibles à l'inhibition de BRAF et de MEK.

DISCUSSION ET PERSPECTIVES

Le rôle de HK2 dans la tumorigénèse a été attribué à son activité glycolytique et, plus récemment, à ses fonctions non canoniques. En collaboration avec le laboratoire de Caroline Robert à l'Institut Gustave Roussy, nous avons découvert que HK2 est non seulement une nouvelle enzyme glycolytique associée aux polysomes dans les cellules de mélanome, mais nous avons également trouvé que cette enzyme régule spécifiquement la traduction de l'ARNm de *SOX10*, qui code pour un important facteur de transcription impliqué dans l'agressivité et la résistance aux therapies ciblées du mélanome. En effet, d'autres enzymes glycolytiques ont été trouvées pour réguler la traduction des ARNm soit par liaison directe aux ARNs et/ou en interagissant avec les ribosomes. Bien que HK2 ne possède aucun domaine de liaison à l'ARN reconnaissable, cette enzyme a été récurrentement proposée comme se liant aux ARNs dans les cellules humaines lors d'études à grande échelle de l'interactome des ARN. En accord avec ces études, nous avons montré que HK2 se lie directement à l'ARN in vivo. De manière frappante, les expériences de gradient de sucrose ont également suggéré que les complexes contenant HK2 montrent une dépendance plus grande à l'ARN que les complexes contenant d'autres enzymes glycolytiques connues pour se lier à l'ARN. Par conséquent, nos résultats suggèrent fortement que HK2 est une nouvelle protéine de liaison à l'ARN authentique, dont la fonction secondaire encore non identifiée doit être caractérisée.

Nous avons aussi découvert que HK2 se lie et affecte la traduction de l'ARNm de *SOX10* via sa région 5'UTR. Étant donné l'importance des 5'UTR pour l'initiation de la traduction, ainsi que des observations antérieures selon lesquelles des enzymes glycolytiques spécifiques se lient aux polysomes et modulent la traduction des ARNm, il est concevable que HK2 puisse faciliter l'initiation de la traduction de l'ARNm de *SOX10* en promouvant l'association des ribosomes avec l'ARNm. En conséquence, nous observons que la déplétion de HK2 diminue l'association de l'ARNm de *SOX10* avec les polysomes fonctionnellement actifs dans les cellules de mélanome. Cependant, des études supplémentaires sont nécessaires pour tester si HK2 facilite l'assemblage ribosomal, par exemple, via le recrutement de facteurs eIF4F au niveaux de la région 5'UTR de *SOX10*. De plus, notre étude n'exclut pas la possibilité que la régulation de la traduction de l'ARNm de *SOX10* se produise par la liaison indirecte de HK2. Par conséquent, d'autres tests sont également nécessaires pour confirmer la liaison potentielle directe entre HK2 et l'ARNm de *SOX10*, en plus d'aider à identifier la base structurelle impliquée dans cette interaction.

Plusieurs rapports ont démontré que le contrôle de la traduction exercé par l'activité de liaison à l'ARN des enzymes glycolytiques peut être régulé par les substrats glycolytiques, les métabolites ou les états métaboliques cellulaires. En conséquence, l'inhibition de la glycolyse a diminué l'interaction de HK2 avec *SOX10*, même si l'activité de liaison à l'ARN de HK2 ne nécessite pas nécessairement son activité catalytique, comme observé dans les expériences CLIP. Cependant, nos expériences suggèrent également que la composition des complexes contenant HK2 peut être moins

dépendante de l'ARN dans les cellules nourries avec du galactose plutôt qu'avec du glucose. Par conséquent, des approches pour étudier la traduction des ARNm et les interactions ARN-protéines *in vivo* et *in vitro* sont nécessaires pour enquêter davantage sur la façon dont les substrats et les métabolites glycolytiques sont impliqués dans le contrôle de la traduction des ARNm médié par l'activité de liaison à l'ARN de HK2. De plus, des études supplémentaires sont nécessaires pour explorer si HK2 perd globalement sa capacité à se lier à l'ARN en l'absence de glucose ou si l'enzyme se lie sélectivement à différents ARNm en fonction de l'état métabolique de la cellule. Néanmoins, nos données suggèrent l'existence d'un lien sophistiqué entre le métabolisme et la régulation génique.

Dans le but d'identifier les éléments clés impliqués dans la régulation traductionnelle de l'ARNm de SOX10 médiée par HK2, nous avons testé si l'activité de liaison à l'ARN de cette enzyme glycolytique dépend de son interaction avec la protéine kinase A (PKA), puisque HK2 a récemment été montré comme interagissant avec cette kinase pour exécuter des activités extra-métaboliques en présence de glucose. Bien que nos résultats indiquent que la liaison de HK2 à l'ARNm de SOX10 ne nécessite pas PKA, nous avons trouvé qu'un inhibiteur réversible compétitif de l'ATP de cette enzyme, H89, a entravé cette association. Nous émettons l'hypothèse que l'effet observé du traitement par H89 est dû à son action sur des cibles non spécifiques. En effet, il a été démontré que H89 affecte directement et indirectement l'activité de kinases autres que PKA, en particulier les kinases basophiles telles que AKT. Il a été montré que cette kinase impacte directement la localisation et la fonction de HK2, par conséquent, l'implication d'AKT dans l'activité de liaison à l'ARN de HK2 doit être davantage étudiée. En outre, des études récentes ont également révélé que HK2 possède des activités de kinase protéique dans les cellules de glioblastome, suggérant que cette enzyme peut également fonctionner comme une kinase basophile dans certains contextes cellulaires. Cela fait de HK2 une cible potentielle de H89. Étant donné que cet inhibiteur réduit l'interaction HK2-ARNm de SOX10, l'effet de H89 sur la traduction de SOX10 doit également être étudié.

L'enzyme glycolytique HK2 a déjà été montrée comme impliquée dans la migration et l'invasion des cellules de mélanome, potentiellement via des fonctions extra-métaboliques. Moya-Plana (2020) a démontré que la déplétion de HK2 dans les cellules suite à l'inhibition de la glycolyse (en cultivant les cellules dans du galactose) avait un impact négatif plus important sur les deux phénotypes par rapport aux cellules cultivées en présence de glucose. Nos résultats suggèrent cependant que l'interaction HK2-ARNm de *SOX10* ne joue pas de rôle dans l'invasion et dans la migration des cellules. Ces résultats sont en accord avec différents rapports démontrant que l'expression de SOX10 est inversement corrélée avec la migration et l'invasion des cellules. Cependant, la diminution de l'expression de SOX10 induit une diminuition de la prolifération et la clonogénicité des cellules de mélanome. En effet, nous avons trouvé que la régulation traductionnelle dépendante de HK2 de *SOX10* est (au moins en partie) impliquée dans la capacité des cellules de mélanome à proliférer et former

des colonies. Nous émettons donc l'hypothèse que HK2 régule la traduction d'autres ARNm codant pour des protéines clés impliquées dans la migration et l'invasion des cellules, tout en régulant la traduction de l'ARNm de *SOX10* pour soutenir la prolifération des cellules. Une compréhension plus approfondie des processus cellulaires influencés par les activités non canoniques de HK2 et leurs mécanismes moléculaires sous-jacents pourrait conduire au développement de nouvelles thérapies, offrant ainsi de nouvelles perspectives dans le traitement du cancer.

Alors que la réponse aux thérapies ciblées visant la voie MAPK des patients atteints de mélanome $BRAF^{V600E}$ est généralement élevée, ces patients acquièrent fréquemment une résistance aux médicaments en raison de mutations génétiques et de mécanismes d'adaptation non génétiques. Bien que nos résultats suggèrent que HK2 n'est pas impliqué dans la résistance aux thérapies ciblées, l'expression ectopique de SOX10 a rendu les cellules plus sensibles à l'inhibition de BRAF et de MEK. En conséquence, deux études indépendantes ont proposé que les cellules de mélanome déficientes en SOX10 étaient significativement moins sensibles à la thérapie ciblée. De plus, il a été montré que les cellules de mélanome $BRAFV^{600E}$ tolérantes aux inhibiteurs de BRAFi/MEKi changent leur métabolisme de la glycolyse à la respiration mitochondriale par plusieurs mécanismes, y compris le reprogrammation traductionnelle et la régulation transcriptionnelle permettant la baisse du niveau d'expression des enzymes glycolytiques clés (par exemple, HK2). Cela pourrait expliquer pourquoi la déplétion de HK2 n'a pas eu d'impact sur la clonogénicité des cellules. Bien que la traduction de l'ARNm de SOX10 dans ces cellules reste à être évaluée, une diminution de l'expression de SOX10 a été précédemment détectée dans la population de cellules de mélanome A375 survivantes après 14 jours de traitement avec BRAFi/MEKi.

Nos résultats soulignent une fonction non métabolique de l'enzyme glycolytique HK2, indiquant que les cellules cancéreuses peuvent augmenter la glycolyse à des fins au-delà du simple anabolisme. Étant donné que de nombreuses enzymes métaboliques sont également des protéines de liaison à l'ARN impliquées dans leur régulation post-transcriptionnelle, et compte tenu du fait que la traduction aberrante des ARNm est une caractéristique des tumeurs, il est crucial d'investiguer l'importance des interactions de HK2 avec l'ARN au-delà de *SOX10*. Nous croyons que HK2 régule la traduction de nombreux ARNm clés impliqués dans les voies de signalisation pertinentes pour le cancer. Par conséquent, comprendre les processus cellulaires influencés par l'activité de liaison à l'ARN de HK2 représente des directions prometteuses pour les recherches futures.

TABLE OF CONTENTS

LIST OF FIGURES

LIST OF TABLES

LIST OF ABBREVIATIONS

1,3-BPG	1,3-bisphosphoglycerate
2C	Complex Capture
2-DG	2-deoxyglucose
2-DG6P	2-deoxyglucose-6-phosphate
2-PG	2-phosphoglycerate
3-PG	3-phosphoglycerate
4E-BP	eIF4E-binding proteins
4SU	4-thiouridine
6SG	6-thioguanosine
aa-tRNA	Activated amino acid tRNA
ACO1	Aconitase 1
ACTB	β-actin
ADAR	Adenosine deaminase
ADP	Adenosine diphosphate
AHA	L-azidohomoalanine
AHAribo	AHA-mediated ribosome isolation
AKAP	A-kinase anchoring protein
AKT	Protein kinase B
ALDO	Aldolase
ALDOA/C	Fructose-bisphosphate aldolase A/C
AMPK	AMP-kinase
APEX2	Apurinic/Apyrimidinic Endodeoxyribonuclease 2
ARE	AU-rich elements
A-site	Ribosomal aminiacyl site
ASOs	Antisense oligonucleotides
AT1R	Angiotensin II type I receptor
ATF4	Activating transcription factor 4
ATP	Adenosine triphosphate
AUBP	AU-binding protein
BAG-1	BAG cochaperone 1
BaMV	Bamboo mosaic virus
BRAFi	BRAF inhibitor
CAESAR	Cis-acting element of structure-anchored repression
CAF	Cancer-associated fibroblast
cAMP	Cyclic adenosine monophosphate
cCL	Conventional UV crosslinking

ccn2	Cellular Communication Network Factor 2
Cdc19	Saccharomyces cerevisiae Pyruvate kinase 1
CDH1	E-cadherin
cDNAs	Complementary DNA
CDS	Coding sequence
CELF1	CUGBP Elav-Like Family Member 1
CHART	Capture hybridization analysis of RNA targets
ChIRP-MS	Comprehensive identification of RNA-binding proteins by mass spectrometry
CHX	Cycloheximide
circRNA	Circular RNA
CLIP	Crosslinking immunoprecipitation
CLUH	Clustered mitochondria protein homolog
COX-2	Cyclooxygenase-2
CSDE1	Cold Shock Domain Containing E1
CSF-1	Colony stimulating factor-1
CTGF/CCN-2	Connective tissue growth factor
CUL4A	Cullin 4A
Cy5	Cyanine5
CYFIP1	Cytoplasmic FMR1-interacting protein 1
DBD	DNA-binding domain
dCas13	Dead Cas 13
DDX3X	DEAD-Box Helicase 3 X-Linked
DHAP	Dihydroxyacetone phosphate
DIG	Digoxigenin
DNA	Deoxyribonucleic acid
DNase	Deoxyribonuclease
DSP	Dithio-bis(succinimidyl propionate)
E. coli	Escherichia coli
ECAR	Extra-cellular acidification rate
eCLIP	Enhanced CLIP
eEF2K	eEF2 kinase
eIF	Eukaryotic translation initiation factor
EJC	Exon junction complex
ELAV L1	Embryonic Lethal Abnormal Vision L1
EMT	Epithelial-to-mesenchymal transition
ENO1	α-Enolase
Eno1p	Saccharomyces cerevisiae enolase 1
Eno2p	Saccharomyces cerevisiae enolase 2

ER	Endoplasmic reticulum
eRIC	Enhanced RNA interactome capture
E-site	Ribosomal exit site
ET-1	Endothelin-1
F-1,6-B	Fructose-1,6-bisphosphate
F-6-P	Fructose-6-phospate
Fba1	Saccharomyces cerevisiae fructose-bisphosphate aldolase
FEZF1-AS1	FEZ family zinc finger 1-antisense transcript 1
FGF-2	Human fibroblast growth factor 2
FGF9	Fibroblast growth factor 9
FL	Full-length
FMRP	Fragile X Messenger Ribonucleoprotein 1
G-3-P	Glyceraldehyde-3-phosphate
G4	G-quadruplexes
G-6-P	Glucose-6-phosphate
GAPDH	Glyceraldehyde-3-phosphate dehydrogenase
G-body	Glycolytic body
GE	Glycolytic enzyme
gLINC	GlycoLINC
GLU	Glucose
GLUT1	Glucose transporter type 1
GM-CSF	Granulocyte macrophage colony stimulating factor
GO	Gene Ontology
GPI	Glucose-6-phosphate isomerase
Gpm1	Saccharomyces cerevisiae phosphoglycerate mutase
GSK3β	Glycogen synthase kinase 3
HADH	Hydroxyacyl-CoA dehydrogenase
HCC	Hepatocellular carcinoma
HIF1α	Hypoxia inducible factor 1α
HITS-CLIP	High-throughput sequencing of RNA isolated by CLIP
HK1/2	Hexokinase I/II
hnRNP A1	Heterogeneous nuclear ribonucleoprotein A1
HOXD10	Homo Sapiens homeobox D10
HSD17B10	Mitochondrial 3-hydroxyacyl-CoA dehydrogenase type 2
Hsp70	Heat-shock protein 70
HuR	Human antigen R
Hxk	Saccharomyces cerevisiae hexokinase
HyPro	Hybridization-Proximity
iCLIP	Individual-nucleotide-resolution CLIP

IDRs	Intrinsically disordered regions
IFN-γ	Interferon-γ
IL-2	Interleukin-2
IMP3	IMP U3 Small Nucleolar Ribonucleoprotein 3
IP	Immunoprecipitation
IRES	Iron-responsive elements
IRP1	Iron-responsive element-binding protein 1
ITAF	IRES trans-acting factor
iTRAPP	Individual-nucleotide-resolution TRAPP
JEV	Japanese encephalitis virus
KH	K-homology
LDHA/B	Lactate dehydrogenase A/B chain
LNA	Locked nucleic acid
lncRNA	Long non-coding RNA
m6A	N6-methyladenosine
m7G	7-methylguanosine
MAPK	RAS–mitogen-activated protein kinase
MDH	Malate dehydrogenase
MEKi	MEK inhibitor
mESCs	Mouse embryonic stem cells
miRNA	MicroRNA
MITF	Microphthalmia-associated transcription factor
MNK	MAP kinase-interacting protein kinases
mRNA	Messenger RNA
mRNPs	mRNA-protein complexes
MS	Mass spectrometry
MS2-BioTRAP	MS2 in vivo biotin-tagged RAP
mTOR	Mechanistic target of rapamycin
MyHC	Myosin heavy chain
NAD	Nicotinamide adenine dinucleotide
NADH	NAD + hydrogen (H)
NADP	NAD phosphate
NBD	Nucleotide-binding domain
ncRNAs	Non-coding RNAs
NF-L	Light neurofilament
non-poly(A)	Non-polyadenylated
NU	Nuclease
OCR	Oxygen consumption rate
OMM	Outer mitochondrial membrane

OOPS	Orthogonal organic phase separation
ORF	Open reading frame
OXPHOS	Oxidative phosphorylation
PABP	Poly(A) tail-binding protein
PABPC1	Poly(A) binding protein cytoplasmic 1
PACCE	Photo-Activatable-Competition and Chemoproteomic Enrichment
PAIR	Peptide-nucleic-acid-assisted identification of RBPs
PAR-CL	Photoactivatable-ribonucleoside-enhanced UV crosslinking
PAR-CLIP	Photoactivatable-ribonucleoside-enhanced CLIP
PAR-TRAPP	Photoactivatable-ribonucleoside-enhanced TRAPP
PDE	Phosphodiesterase
PDIA6	Protein Disulfide Isomerase Family A Member 6
PD-L1	Programmed death ligand 1
PEP	Phosphoenolpyruvate
PFK	ATP-dependent 6-phosphofructokinase
PFK-1.1	Caenorhabditis elegans phosphofructokinase 1
Pfk1p	Saccharomyces cerevisiae phosphofructokinase subunit 1p
Pfk26p	Saccharomyces cerevisiae phosphofructokinase subunit 26p
Pfk2p	Saccharomyces cerevisiae phosphofructokinase subunit 2p
PFKL	Phosphofructokinase liver isoform
PGAM1	Phosphoglycerate mutase 1
Pgi1	Saccharomyces cerevisiae phosphoglucose isomerase 1
PGK1	Phosphoglycerate kinase 1
PI3K	Phosphatidylinositol 3-kinase
PIC	Pre-initiation complex
PKA	Protein kinase A
PKM	Pyruvate kinase
PLA	Proximity Ligation Assay
PNK	T4 Polynucleotide Kinase
poly(A)	Polyadenylated
PRC2	Polycomb repressive complex 2
PRKAR1a	Regulatory subunit α of PKA
PRTE	Pyrimidine-rich translational element
P-site	Ribosomal peptidyl site
PTC	Ribosomal peptidyl transferase centre

PTex	Phenol Toluol extraction
ptsG	E. coli glucose PTS permease PtsG subunit
Puro-PLA	Puromycin-based PLA
RAP	RNA affinity purification
RBD	RNA-binding domain
RBP	RNA-binding protein
RBPDB	RNA-Binding Protein DataBase
RBPome	RNA-binding proteome
REM	RNA–enzyme–metabolite
RIC	RNA Interactome Capture
RIP	RNP/RNA immunoprecipitation
RIP-Chip	RNP immunoprecipitation–microarray
RIPiT	RNA immunoprecipitation in tandem
RNA	Ribonucleic Acid
RNA Pol II	RNA polymerase II
RNase	Ribonuclease
RNP	Ribonucleoprotein
RP	Ribosomal protein
RPL35	60S ribosomal protein 35
RRM	RNA recognition motif
rRNA	Ribosomal RNA
RT-PCR	Reverse transcription Polymerase Chain Reaction
S. Typhimurium	Salmonella Typhimurium
SCN1A	Voltage gated sodium channel type 1α subunit
Scn1a	Mouse voltage gated sodium channel type 1α subunit
SCN3A	Voltage gated sodium channel type 3α subunit
Scn3a	Mouse voltage gated sodium channel type 3α subunit
SDS	Sodium dodecyl sulfate
SDS-PAGE	Sodium dodecyl sulfate–polyacrylamide gel electrophoresis
Seq	Sequencing
SeV	Sendai virus
shRNA	Small hairpin RNA
SILAC	The Stable Isotope Labeling by Amino Acids in Cell Culture
snRNAs	Small nuclear RNAs
snRNP	Small nuclear ribonucleoprotein
SOX10	SRY-box transcription factor 10
ssRNA	Single-stranded RNA
STAMP	Surveying targets by APOBEC-mediated profiling

STAU1	Staufen-1
SUnSET	The Surface Sensing of Translation
TCA	Tricarboxylic acid
Tdh3	Saccharomyces cerevisiae glyceraldehyde-3-phosphate dehydrogenase
TERC	Telomerase RNA component
TfR1	Transferrin receptor
TNF-α	Tumor necrosis factor-alpha
TOP	5′ terminal oligopyrimidine sequence
Tpi	Saccharomyces cerevisiae triosephosphate isomerase
TPI1	Triosephosphate isomerase
TRAPP	Total RNA-associated protein purification
TRIBE	Targets of RBPs identified by editing
TRIP	Tandem RNA isolation procedure
tRNA	Transfer RNA
$tRNA_i^{Me}$	Methionyl-tRNAi
UNR	Upstream of N-RAS
uORF	Upstream ORF
uPAR	Urokinase-type plasminogen activator receptor
UPF1	Upframeshift 1
UTR	Untranslated region
UV	Ultraviolet
VARS	Valine aminoacyl-tRNA synthetase
VCL	Vinculin
VDAC-1	Voltage-dependent anion-selective channel 1
VEGF	Vascular endothelial growth factor
Viral RNA	vRNA
WT	Wild-type
XRNAX	XRNAX (protein-crosslinked RNA extraction
YAP	Yes-associated protein
YTH	YT521-B homology
ZBP1	Zipcode protein binding protein sites

1 INTRODUCTION

1.1 RNA-PROTEIN INTERACTIONS

The ribonucleic acid (RNA) biology is coordinated by the interplay of RNAs with specialized proteins that possess RNA-binding activity. These proteins are termed as RNA-binding proteins (RBPs), and their interaction with RNA range from a single-protein-RNA interaction to the assembly in dynamic complexes of multiple RBPs and RNA molecules. These complexes are referred to as ribonucleoprotein (RNPs) particles and they are principally involved in the regulation of gene expression[1–6]. This regulation is essential to sustain cellular homeostasis, and the RNP complexes do so by coordinating co- and post-transcriptional processing steps, from synthesis to degradation, of all classes of RNAs (Fig. 1)[4,7,8].

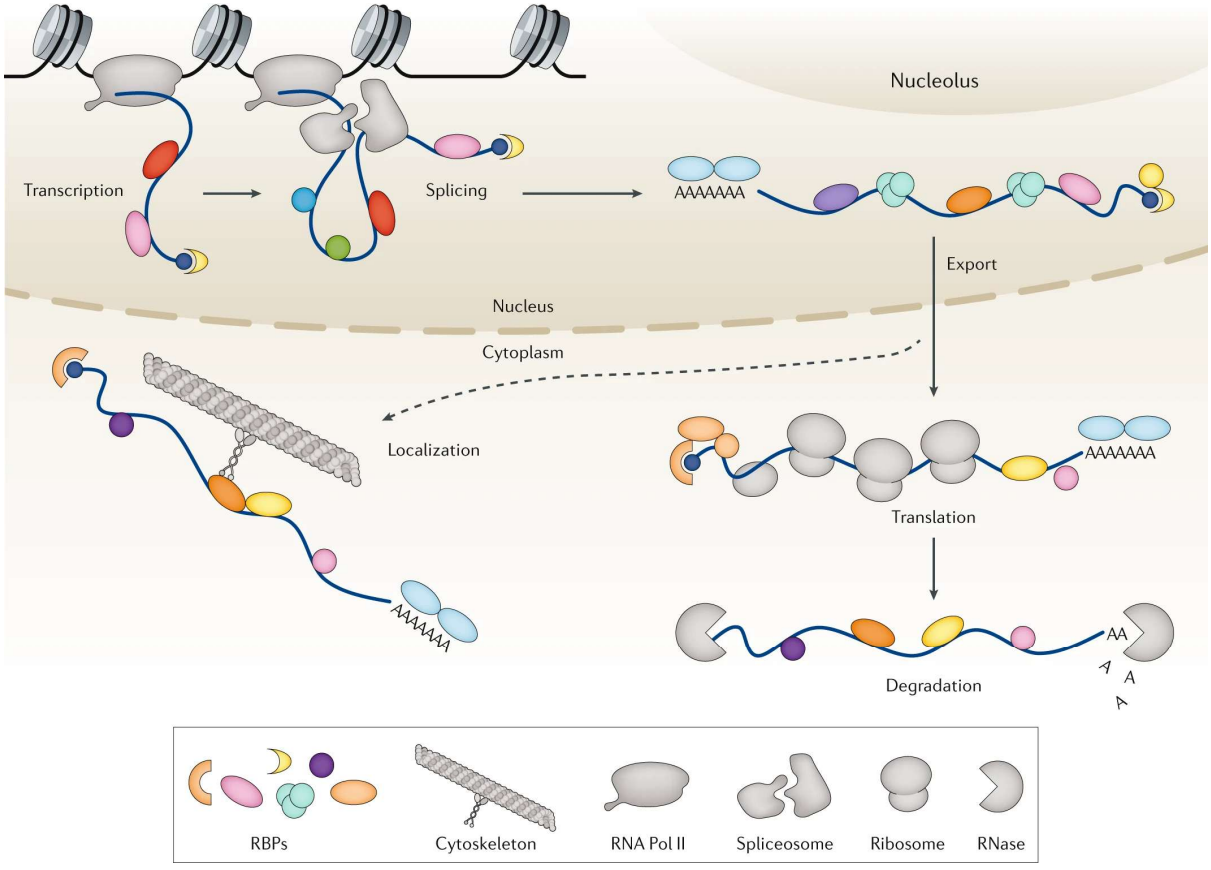

Figure 1. RNA-binding proteins coordinate RNA metabolism. Illustration of the nuclear processes of mRNA metabolism, including transcription, splicing, capping, and polyadenylation, as well as the cytoplasmic steps such as transport, localization, translation, and degradation. RBP, RNA-binding protein. RNA Pol II, RNA polymerase II. From Gebauer *et al.*, 2021 (ref [7]).

While specific RBPs are assembled during transcription, other subsets of nuclear RBPs are engaged in co-transcriptional RNA-processing reactions, such as splicing, polyadenylation and RNA stabilization. After exported from the nucleus, some RNPs

are transported to the cytoplasm to specific regions of subcellular localization. In turn, cytoplasmic RBP complexes undergo structural rearrangements to ensure the translation of coding and non-coding RNAs (ncRNAs), and, ultimately, RNA degradation[2,6–9]. Thus, the components of each RNPs are remodelled according to the maturation or functional state of the RNA. This remodelling plays a significant role in controlling each step of the RNA metabolism. Therefore, unravelling all the features that regulate the dynamic and complex RNA-protein interaction events is fundamental for a better understanding of the control of gene expression.

As stated above, RNA-protein interactions are often transient, but essential for proper cellular function. Both the RBP repertoire and RBP activities are remodelled according to cellular cues and environmental stimuli[3]. Therefore, as critical effectors of gene expression, it is unsurprising that aberrant alterations in the expression and function of RBPs have been linked to several diseases, including cancer[10–13], neuropathies[14], cardiovascular diseases[15], and genetic disorders[7,16,17]. Nevertheless, RNA–protein interactions have been therapeutically exploited through the use, for example, of small molecules and (antisense)oligonucleotides capable of altering or blocking the access of RBPs to their cognate binding sites[18]. Certainly, the development and fine tuning of new molecules capable of targeting RNA-RBP interactions hold promise for more relevant RBP-targeting therapeutics.

The widely held assumption that RBPs regulate the fate and function of RNAs has a broad but not universal applicability. Similarly to how post-translational modifications impact proteins, the direct and specific binding of RNAs can regulate the activity, stability, interaction and localization of RBPs[4]. This process of protein regulation by RNA is termed as "riboregulation"[4]. One recent example of this regulation involves the long non-coding RNA (lncRNA) *SNHG1* and the RBP hnRNPL in prostate cancer, in which *SNHG1* impaired hnRNPL-dependent translation of mRNAs by competitive interaction with the RBP, activating the epithelial-to-mesenchymal transition (EMT) and consequent cellular growth and metastasis[19]. Another striking example is the glycolytic enzyme (GE) α-Enolase (ENO1), which has been recently found to be riboregulated[20,21]. While the enzyme activity of ENO1 is repressed by the competitive interaction of *lncRNA-6195* with its substrate-binding site in hepatocellular carcinoma (HCC) cells[21], acetylation-driven riboregulation of ENO1 by the direct interaction with messenger RNAs (mRNAs) was demonstrated as a physiological mechanism of regulation of stem cell differentiation[20]. Hence, future work is needed to profoundly explore the role of riboregulation in biology. If taken into consideration, it offers an additional rationale for the classification of proteins as RBPs. If proteins can be regulated by RNAs, they could therefore transiently or stably interact with these molecules for regulatory purposes.

The number of proteins identified as RBPs, including many with already well-characterized functions (e.g., ENO1), has drastically increased during the past three

decades (Figure 2). In 2010, the first catalogue of human RBPs comprised a total of 422 proteins[22]. This catalogue, assembled in the RNA-Binding Protein DataBase (RBPDB), contained only well-characterized RBPs or predicted RBPs that possessed well-established architectural features, such as known RNA-binding domains (RBDs), or an RNA-binding annotation. Consequently, these criteria limited the pool of known human RBPs by systematically excluding those that were poorly characterized or deemed unconventional. Urging for a broader cataloguing of the RNA-binding proteome (RBPome) and a better characterization of the features that regulate the RNA-RBP interactions, the introduction of unbiased large-scale quantitative methods and modern protein mass spectrometry has been developed. In 2014, the number of putative human RBPs increased to 1,542 proteins[8], and then to 1,914 proteins in 2018[4]. More recently, this number increased to more than 6000 potential RBPs[23], and it is constantly increasing as a result of the development of a versatile array of methods to identify and characterize RNA-protein interactions.

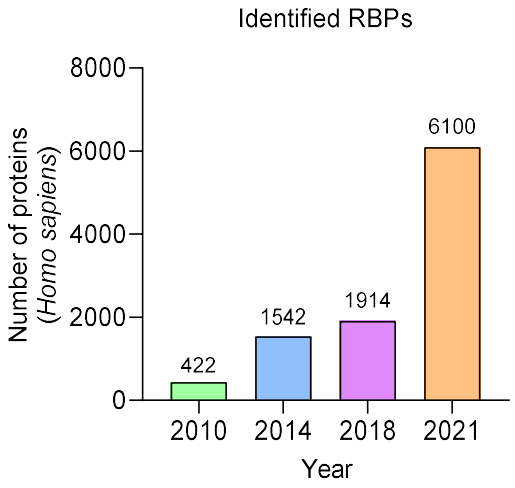

Figure 2. Human RBPs identified over the past three decades. Total number of annotated and novel RBPs identified in different human cell lines by the combination of RBP detection studies[4,8,22,23].

Together, these methods allowed the discovery of many putative RBPs, revealing proteins that do not harbour well-established RBDs nor a known link to the RNA biology[6,7]. Still, these proteins seem to possess RNA-binding abilities, in contrast with what was known about classical RBPs. Indeed, the RNA-related functions of some of them have been shown to be involved in perturbations in the cellular homeostasis, which will be further discussed in session 1.2. These discoveries underscore the critical need to comprehensively characterize unconventional RNA-protein interactions, alongside the expansion of the RBP repertoire. Such efforts hold promise for a better understanding of the molecular mechanisms behind the function of disease-associated RBPs, and in the conceptualization of novel therapeutic interventions.

1.1.1 APPROACHES TO STUDY RNA-PROTEIN INTERACTIONS

Recent efforts have expanded the number of methods available for studying RNA–protein interactions. Indeed, they allowed the identification of hundreds of new RBPs, and many of them lacked any known RBDs or RNA-related functions[6,7], therefore highlighting the diversity and complexity of the RNA-protein interactions. The approaches available to study these interactions can be divided in two main categories based on the biological question being addressed: RNA-centric and protein-centric methods. RNA-centric methods, as the name suggests, focus on an RNA of interest in order to characterize the proteins bound to it. Protein-centric methods, however, is used to examine the RNAs that are bound by a protein of interest. Each method evidently possesses its own set of strengths and limitations. Understanding these nuances enables the selection of the most optimal approach for application.

1.1.1.1 RNA-CENTRIC METHODS

RNA is dynamically bound to proteins throughout its entire life cycle[7]. To unravel the most important proteins bound to a specific RNA, RNA-centric methods are preferred[24,25]. Such methods generally use proximity-based protein labelling or RNA affinity capture purification, and they can be performed *in vivo* with the use or not of crosslinking agents, or *in vitro* to study the RNA-protein interactions outside of the cellular environment[24,25].

In vitro methods

RNA affinity capture methods are mainly *in vitro* assays based on the tagging of endogenous RNAs or on the modification of *in vitro* transcribed/synthesized RNAs, aiming for an easy RNA pulldown and subsequent identification of interacting proteins[25]. The simplest method used for this purpose is the biotinylating of the 5′ or 3′ ends, or both ends of the RNA[24–26] (Figure 3A). End-labelled biotinylated RNAs can be bound to solid surfaces, such as streptavidin beads[27]. Then, cellular extracts (e.g., total, nuclear or cytoplasmic) are added, and the beads are washed and boiled in sodium dodecyl sulfate (SDS) elution buffer for downstream mass spectrometry analysis[27]. Alternatively, RNA aptamers can be used to tag the RNA of interest[24–26]. The aptamers are short single-stranded nucleic acids that bind the tagged RNA to a resin support[28,29] (Figure 3B). Cellular proteins bind non-specifically to resin, therefore the elution of the RNA from the resin (and consequently the RBPs bound to it) reduces the background noise from downstream analysis by excluding nonspecific resin-bound proteins. Another alternative approach is the use and hybridization of dye-labelled (e.g., Cyanine5, Cy5) *in vitro* transcribed RNAs to recombinant protein microarrays (e.g.,

Human ProtoArray)[30] (Figure 3C). In this assay, only proteins that are directly bound to the RNA can be detected via fluorescence reading. This method does not require cellular extracts and yet it enables the discovery of direct RNA–protein interactions[30].

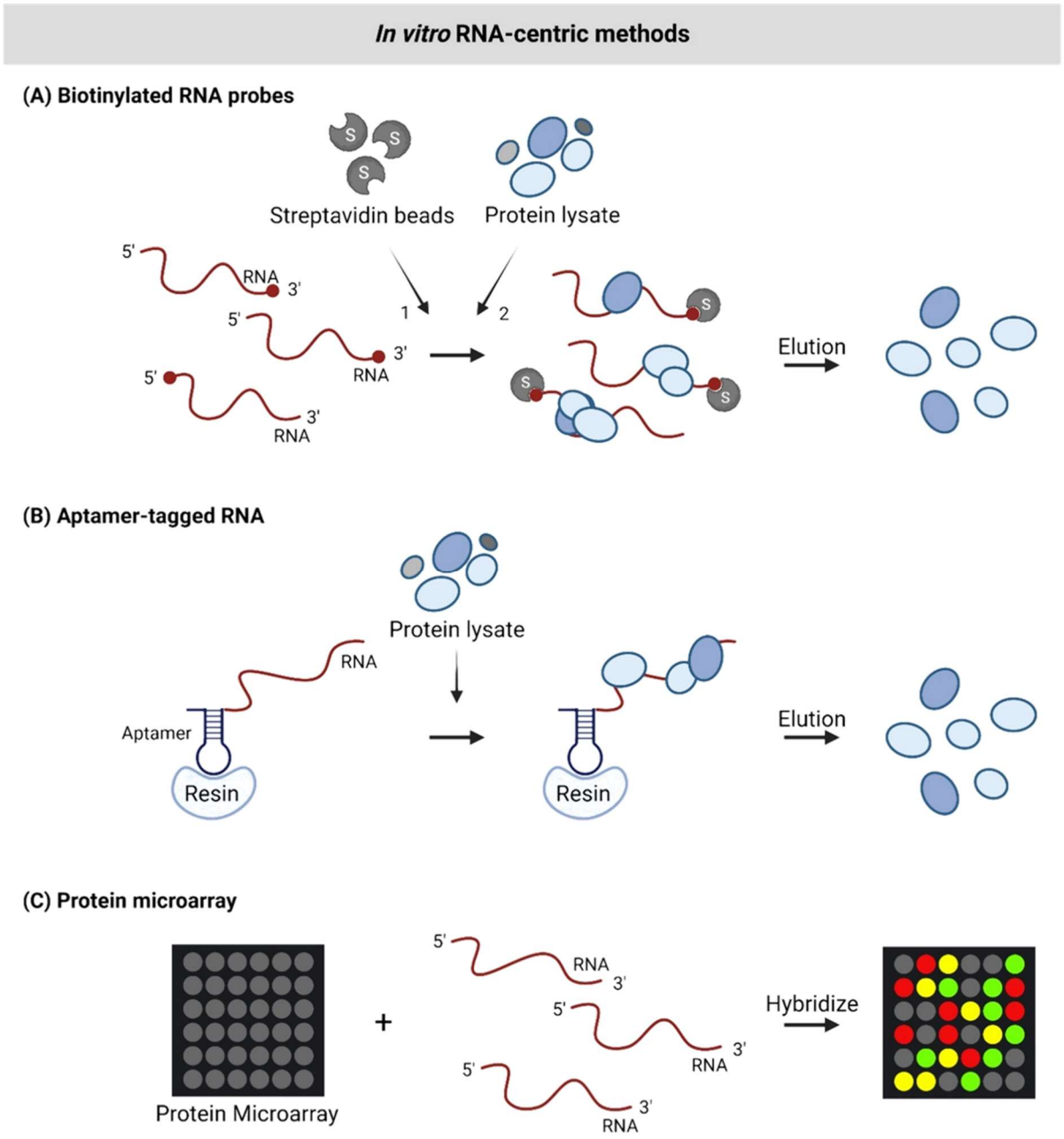

Figure 3. Schematic workflow of *in vitro* RNA-centric methods. (**A**) End-biotinylated-RNA pulldown. Biotin-tagged RNA at the 5′ or 3′ end (red) is immobilized on streptavidin beads. Recombinant or cellular protein extracts are incubated with the RNA. After stringent washes, RNA-unbound proteins are removed, and RNA-bound proteins are eluted. The eluted RNA-bound proteins are further processed for western blot or mass spectrometry analysis. (**B**) Aptamer-tagged-RNA pulldown. The RNA of interest is *in vitro*–transcribed with a short single-stranded nucleic acid tag (aptamer, blue). The aptamer tag binds the RNA (red) to a resin support. Recombinant or cellular protein extracts are incubated with the RNA. After stringent washes, RNA-bound proteins are eluted and further processed for western blot or mass spectrometry analysis. (**C**) Protein microarray. Cy5-labelled *in vitro* transcribed RNA. The RNA (red) is then added to a human protein microarray. Fluorescence is used to detect and quantitate the RNA

bound on spotted proteins. Adapted from Ramanathan *et al.*, 2019 (ref **24**).

As a category of methods, *in vitro* approaches are useful for characterizing specific RNA–protein interactions. However, the RNA of interest may not harbour the same structures or modifications when in cells. Likewise, interacting proteins may lack important post-translational modifications for RNA association[24,25], and the use of high concentrations of recombinant proteins may potentially promote nonspecific interactions[24]. Nevertheless, the use of cellular extracts may partially overcome some of these matters, at least regarding protein post-translational modifications[24]. Aiming to overcome these limitations, a new technique has been developed, uncovering interactors and other spatial neighbours of the RNA of interest in genetically unmodified samples. This technique is termed as Hybridization-Proximity (HyPro) labeling[31,32], and it allows the identification of proteins and RNAs associated with the RNA of interest by mass spectrometry (HyPro-MS) and deep sequencing (Hypro-Seq), respectively. It relies on the hybridization of digoxigenin(DIG)-labelled deoxyribonucleic acid (DNA) oligonucleotide probes complementary to the RNA molecules of interest in cells fixed with thiol-cleavable dithio-bis(succinimidyl propionate) (DSP) crosslinking reagent[33,34], a cell-permeant and reversible crosslinker that primary reacts and links amino groups. The DIG-labelled DNA probe is bound by its digoxigenin groups to a custom-designed HyPro enzyme that contains apurinic/apyrimidinic endodeoxyribonuclease 2 (APEX2), an engineered peroxidase that can rapidly tag proteins and RNAs in spatial proximity with biotin and H_2O_2[35,36], and DIG-binding domains connected by a flexible linker[31,32]. RNAs and proteins co-localized with the RNA of interest are then biotinylated *in situ* and, following crosslink reversal, are captured using streptavidin beads and analysed[31,32]. HyPro then emerges as an alternative RNA-centric approach to map molecular interactions and complexes within cells, offering new insights into cellular organization and function, thereby promoting a more comprehensive understanding of the RNA interactome.

In vivo methods

To study the protein binding partners of an RNA of interest in its cellular context, RNA proximity-based methods can be applied without the need for any cross-linking agents[24,25] (Figure 4A). These methods are particularly interesting for the study of transient protein interactions or to study RNPs from poorly soluble cellular compartments (e.g., chromatin), that are more prone to precipitate during the affinity capture methods described above[24,25]. In the RNA-directed proximity-based methods, a labelling enzyme is recruited to the RNA of interest to covalently modify proteins found in close proximity to the RNA[24,25]. The RNA can be endogenously tagged by the tethering of biotin ligases (BirA*), as performed in the RNA-BioID technique[37]. Alternatively, labelling enzymes can be recruited to the RNA by the use of aptamers[26], or by the use of antisense guide RNAs coupled with a modified CRISPR–Cas system[38].

Split proximity-based tools, such as split APEX2[35,36], can be potentially applied in order to reduce the background noise generated by the excess of enzymes not recruited to the targeted RNA. In split APEX2, the co-localization of two inactive APEX2 subunits is required to restore the peroxidase activity and biotinylate the proteins in the vicinity of the RNA[39].

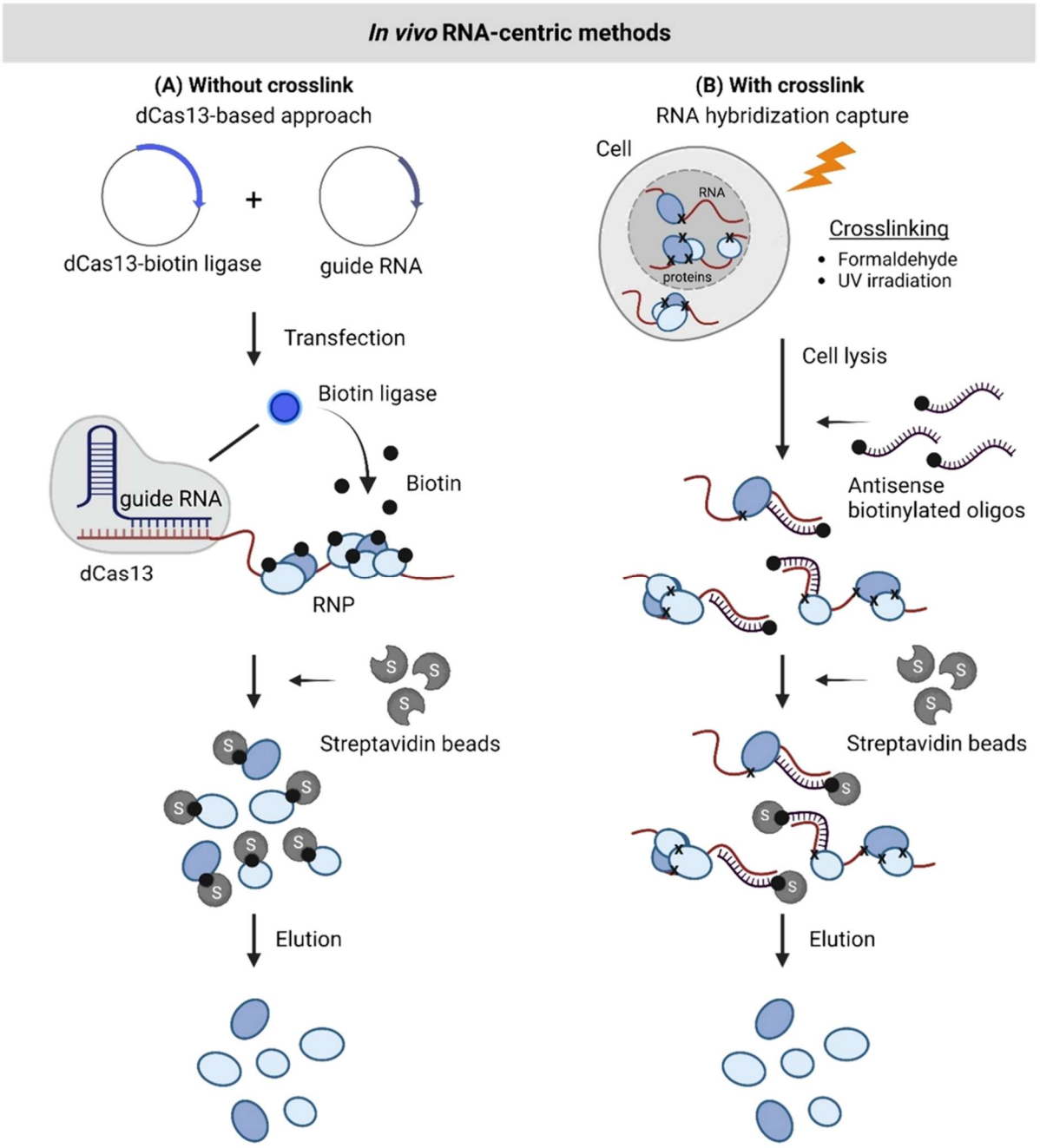

Figure 4. Schematic workflow of *in vivo* RNA-centric methods. (**A**) Non-crosslinking dCas13-based approach. Cells are co-transfected with guide RNAs and catalytically dead Cas 13 (dCas13) systems with biotin ligases. The RNA of interest is then recognized by the antisense guide RNAs coupled with dCas13-biotin ligase. The proximity-labelling enzyme biotinylates proteins found in close proximity to

the target RNA upon addition of biotin. Biotin-labbled proteins are immobilized and isolated on streptavidin beads, then eluted and further processed for western blot or mass spectrometry analysis. (**B**) Crosslinking based RNA hybridization capture approach. RNA–protein interactions in cells are preserved by crosslinking. Crosslinking sites are indicated by a black cross. After lysis, target RNA–protein complexes hybridize with biotinylated DNA antisense oligonucleotides, which allows the purification of the complexes by streptavidin beads. After stringent washes, RNA-bound proteins are eluted. Adapted from Gräwe *et al.*, 2021 (ref [25]).

A disadvantage of not performing any crosslink between interacting RNA and proteins is the possibility to detected false-positive RNA-RBPs associations due to post-lysis reorganization of the RNPs[40]. To avoid that, proteins can be crosslinked to interacting RNAs by the use of crosslinking agents *in vivo*, which allows the purification of crosslinked RNA-protein complexes and the removal of noncovalent interactions. Several methods[41–46] mainly rely on the use of two crosslinking agents to crosslink RNPs in cultured cells prior to cell lysis: ultraviolet (UV) irradiation or formaldehyde. Formaldehyde is a small crosslinking agent able to easily permeates cells, forming reversible covalent linkages between proteins and DNA/RNA-protein complexes within 2 Å[47]. Since formaldehyde promotes crosslinking between other molecules in addition to RNA-protein interactions, the distinction of the proteins that interact directly with RNA from those whose interaction is indirect becomes challenging[47]. In contrast, UV irradiation is a more specific crosslinker than formaldehyde. It irreversibly crosslinks interacting nucleic acids and proteins at direct contact ("zero" distance) by the formation of covalent bonds between them[48,49]. However, its crosslinking efficiency is lower compared to formaldehyde, and double-stranded RNAs are usually poorly crosslinked[25]. Besides, UV crosslinking has a slight preference for uridine residues[50].

In recent years, RNA hybridization capture approaches have been used to identify crosslinked RNA–protein interactions occurring in cells by using biotin-tagged antisense DNA oligonucleotides to pull down the RNA of interest[26] (Figure 4B). Examples of methods include the capture hybridization of analysis of RNA targets (CHART)-MS[41], comprehensive identification of RNA-binding proteins by mass spectrometry (ChIRP-MS)[42], and RNA affinity purification (RAP)[43]. The first two methods, CHART-MS and ChIRP-MS, use formaldehyde to crosslink the RNA-protein interactions, while RAP, in contrast, uses UV irradiation. Interestingly, all three methods have been used to explore the interactome of the lncRNA *Xist*[51]. However, the overlapping between the identified proteins was low, which could be explained by the use of different crosslinking reagents, use of different antisense oligonucleotides, and parameters used to identify statistically significant protein interactors[51].

Besides RAP, many other methods use UV crosslinking to unravel the proteins bound to a specific RNA. These methods include tandem RNA isolation procedure (TRIP)[44], MS2 *in vivo* biotin-tagged RAP (MS2-BioTRAP)[45] and peptide-nucleic-acid-assisted identification of RBPs (PAIR)[46]. Although all four methods share the same crosslinking

approach, they differ in experimental setup. As mentioned above, RAP uses oligonucleotide probes to capture the RNA–RBP complexes[43]. PAIR, in contrast, uses peptide nucleic acid probes to hybridize to RNA, after which the RNA–RBP complexes are purified[46]. MS2-BioTRAP takes advantage of the stable formation of the MS2 hairpin loop and MS2 coat protein complex to purify the MS2-containing RNA[45]. TRIP, on the other hand, focus on the study of polyadenylated (poly(A)) RNAs and uses two strategies for the purification of the RNA-protein complexes[44]. The poly(A) RNAs are first purified with the use of oligo$(dT)_{25}$ beads under stringent washing conditions, and then they are hybridized with biotinylated antisense oligonucleotides (ASOs). The ASO-RNA–protein complexes are then purified with the use of streptavidin beads[44].

Given the diversity of RNA-centric methods available, a few criteria warrant consideration when selecting the most suitable method to address the biological question at issue. The abundance of the RNA of interest is critical for the detection of the RNA–protein interactions. The higher the RNA copy number, the easier it is to detect *in vivo* the RNA–protein interactions, and with the use of fewer cells. For RNAs with lower copy number, *in vitro* assays rise as a good alternative to explore these interactions[24]. Besides, *in vitro* approaches are also helpful for determining which amino acids or nucleotides contribute to the RNA–protein interactions[24]. *In vivo* approaches, in contrast, are particularly interesting for the study of RNA-protein interactions within the cellular environment, where RNA and protein modifications, as well as subcellular localization and dynamic range of local concentrations may have an effect in the interactions in study[24,25]. The strength of the RNA–protein interactions should also be considered. In general, UV crosslinking is less likely to capture weak interactions as opposed to formaldehyde[24,25].

Collectively, the RNA-centric methods available for studying the proteome associated with a particular RNA transcript offer new insights into the RNA biology[26]. Recent advancements in these methods hold promise for a more profound comprehension of the RNA interactomes. However, the integration of complementary approaches is required to validate the identified protein interactors and gain a deeper understanding of their biological significance.

1.1.1.2 PROTEIN-CENTRIC METHODS

To characterize the RNAs bound to a specific protein, protein-centric methods are preferred. These approaches commonly start with either the direct purification of the protein of interest with the use of antibodies, or by chemically modifying the RNAs in a way that they rely on the association with the protein under investigation[24]. Despite the existence of these two different strategies, most of the studies relies on the immunoprecipitation (IP) of the protein for identifying the associated RNAs. Several

methods can be used for the identification of endogenous RNA-protein interactions, and they vary on the sensitivity and specificity of the detection. The commonly used strategies can be categorized as RNP/RNA immunoprecipitation (RIP) or crosslinking immunoprecipitation (CLIP) approaches[25,52].

RNP/RNA immunoprecipitation approaches

RIP approaches can be applied to purify RNA–protein complexes under native conditions[53] or under the use of crosslinking agents, being formaldehyde the most used for this purpose[54]. Therefore, this approach relies on the identification of the RNAs bound to a protein of interest after the IP of this protein under conditions that preserve the RNP complexes, and this can be achieved by crosslinking the RNA-protein interactions, as mentioned above, or by the use of mild washing conditions during the IP[53,54]. In 1979, this method was first used by Lerner and Steitz[53] to identify small nuclear RNAs (snRNAs) that interact with proteins present in small nuclear ribonucleoprotein (snRNP) complexes. The method was later modified and referred to for the first time as RIP by Niranjanakumari et collaborators[54], who took advantage of the efficient and reversible formaldehyde crosslinking to identify RNA–protein interactions *in vivo*[54]. Subsequent studies developed a RIP derived approach termed RNP immunoprecipitation–microarray (RIP-Chip)[55,56]. This technique allows the identification of RNAs globally associated with multi-targeted proteins in RNP complexes or in the context of cell extract. It can also be used to provide information regarding the regulation of RNAs by these proteins, identify RNAs with related functions, and determine relative levels of gene expression.

In 2010, RIP was combined with high-throughput sequencing (RIP-seq) to identify the genome-wide Polycomb repressive complex 2(PRC2)-bound RNAs in embryonic stem cells[57]. This technique was further modified and refined, allowing the mapping of RBP binding sites in the transcripts (RIP-seq footprinting)[58]. The principle of this technique is to identify the sequences directly bound by proteins, and this can be achieved by the inclusion and optimization of a nuclease degradation (ribonuclease – RNase – digestion) step. The sites occupied by proteins (binding sites) will be protected against the degradation (RNA footprinting). For example, this technique has been used to gain insights into the binding sites and functions of the Fragile X protein (FMRP) and the ATP-dependent RNA helicase upframeshift 1 (UPF1) *in vivo*, including in instance when these two proteins are in direct interaction[59–61]. In fact, RIP-seq footprinting has been successfully applied to isolate footprints of multiunit RNPs. A modified RNP footprinting approach coupled to high-throughput sequencing (RIPiT)[58,62] was developed to reveal the *in vivo* binding landscape of the exon junction complex (EJC), a multiprotein complex that plays a major role on the post-transcriptional regulation of mRNAs[63], to understand the multitude of the complex functions. It did not only

allow the obtention of footprints associated to the core complex, but also its distinction from footprints of when the core is bound to different peripheral proteins[58].

While RIP approaches allow the identification of RNAs bound to an RNP, they are not well suited to the study of direct interactions between a single protein and RNAs. This is because these techniques, as previously mentioned, were developed to characterize the RNA–protein interactions under native conditions, therefore preserving the RNP complexes formed *in vivo*[53]. Moreover, in some instances, the RNA-protein interactions found by RIP do not reflect the *in vivo* interactions, but are artificially generated after cell lysis[40]. Therefore, appropriated methods to characterize direct endogenous RNA-protein interactions involving a single RBP are needed, including those capable of identifying the nucleotides or amino acids involved in the interaction. For the identification of the direct RNA-protein interactions, CLIP methods have been widely used [25,52].

Crosslinking immunoprecipitation approaches

CLIP make use of the UV irradiation of living cells to irreversibly crosslink proteins to nucleic acids at direct contact by the formation of covalent bonds between them[48,49]. The covalent crosslink therefore forms very stable RNA-protein complexes, allowing the use of stringent purification steps followed by the determination of single protein interactions across the transcriptome. Of note, many other techniques take advantage of the UV crosslink to isolate nucleic acid–bound proteins, such as the Complex Capture (or 2C[64]), an RNA-centric approach that uses silica-based solid-phase extraction to purify crosslinked nucleic acids–RBP complexes. Besides the use of UV light, CLIP and CLIP-based methods allow the use of limited RNase treatment (RNA fragmentation) to isolate the RNA fragments occupied by the interacting RBP at the time of the crosslinking[25]. These fragments can then be sequenced to identified the RBP binding sites, and, in some instances, help in the inference of the RBP function based on the comparison to binding sites of other RBPs or *cis*-acting elements[25]. Indeed, the advancements on the high-throughput sequencing of the RNA isolated by CLIP (e.g.: HITS-CLIP[65]) has allowed a comprehensive, transcriptome-wide examination of the RNA binding sites at a single-nucleotide resolution.

All CLIP-based methods share the following core workflow (Figure 5) for determining the RNA-binding landscape of an RBP on a transcriptome-wide scale. The first step is the UV crosslinking of RNAs and proteins in direct interaction. Of note, almost all the amino acids are well crosslinked, apart from the aspartic acid, glutamic acid, asparagine, and glutamine[24,25,50]. Normally, UV-C light at λ = 254 nm is employed, but the amount of the UV crosslink energy needs to be optimized depending on the samples to be crosslinked (e.g.: cell monolayers, dissociated tissue suspension or whole organisms)[24,25,66]. After the crosslinking step, the RNA is digested into short fragments by RNase digestion[66]. The optimal RNA sizes range from 30 to 200 nts[52]. This step is

crucial to avoid co-purification of multiple RBPs crosslinked to the same RNA fragment, which decreases the specificity of the sequenced data. Besides, these RNA fragments contain the crosslink sites, therefore providing insights into the position of the binding[52]. Then, the RBP of interest is further purified by IP under denaturing conditions to also remove other interactors (including other RBPs) from the target protein[25]. Another alternative approach is to use affinity tags, such as FLAG-tag, to maximize the stringency to fully dissociate very stable RNPs[25]. The RNA fragments are ligated to a 3′ adapter and/or radiolabelled, and the RNA-protein complexes are purified by denaturing polyacrylamide gel electrophoresis (SDS-PAGE) and transfer to nitrocellulose for further purification by size selection[25,66]. The radiolabelled RNAs allow the visualization of the RNA-RBP complexes by autoradiography. The crosslinked RNA fragments are then released from the RBP by proteinase K digestion and converted by reverse transcription to cDNA libraries for high-throughput sequencing. Sequenced reads are then mapped to the genome and possible binding sites are computationally identified[25].

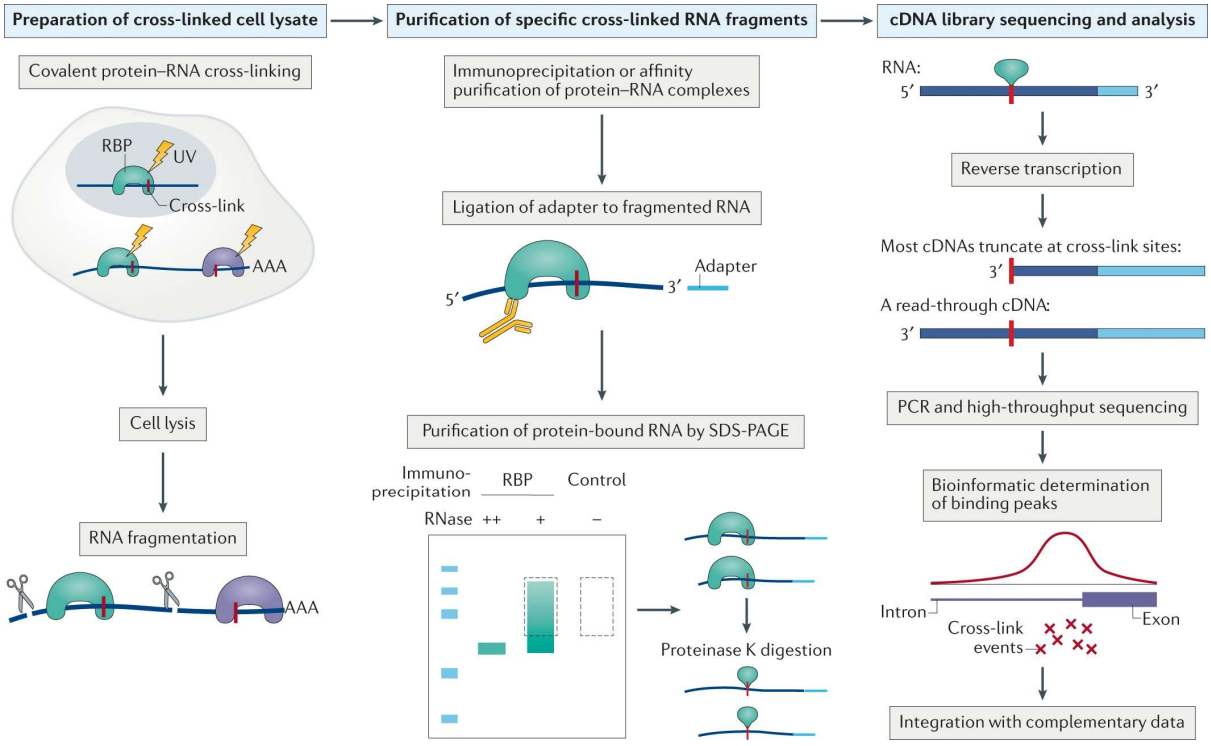

Figure 5. Schematic core workflow of CLIP-based methods. CLIP protocols commonly follow these 3 core steps: (1) preparation of the crosslinked cell lysates, which includes an RNA-fragmentation step to remove other RBPs than the one of interest crosslinked to the same RNA fragment; (2) purification of the crosslinked RNA fragments, which includes the IP of the RNAs bound to the protein of interest, ligation of a 3′adapter on the RNA fragments, further purification of the RNA-protein complexes by denaturing polyacrylamide gel electrophoresis (SDS-PAGE), and purification of the RNAs by size selection; (3) cDNA library preparation, which can differs within CLIP protocols. Typically, the computational determination of protein-RNA crosslink sites relies on the amplification of truncated cDNAs. RBP, RNA-binding protein. From Hafner et al., 2021 (ref [25]).

When coupled with high-throughput sequencing, further developments in the CLIP protocols allowed the identification *in vivo* of the RNA binding sites with single-nucleotide level resolution. Such developments include the identification of crosslink sites through analysis of mutations in reads, such as in photoactivatable-ribonucleoside-enhanced CLIP (PAR-CLIP)[67,68], or by capturing cDNAs whose elongation terminate at the crosslinking site during reverse transcription, such as in individual-nucleotide-resolution CLIP (iCLIP)[69,70]. In PAR-CLIP, cells are incubated with nucleotide analogues, such as the photoactivatable ribonucleosides 4-thiouridine (4SU) or 6-thioguanosine (6SG), which are then incorporated into nascent RNAs. These analogues allow UV crosslinking with a lower energy (UVA/B, $312 \leq \lambda \leq 365$ nm) than in the classical CLIP methods[67]. During reverse transcription, crosslinked 4SU typically pairs with guanosine, resulting in T to C transitions in the sequenced cDNA (and G to A transitions when using 6SG[67]). Specific genomic regions enriched in such transitions indicates bona fide RNA–RBP interaction sites. iCLIP, in contrast, take advantage of the tendency of the reverse transcriptase to terminate at the crosslinked peptide for the identification of the crosslink sites at nucleotide-level resolution[69,70]. Moreover, the development of dedicated bioinformatics workflows has been undoubtedly enabling the determination of the binding sites[71,72]. Many other CLIP methods exist (e.g.: eCLIP[73], and they are reviewed in [25,52]). However, they are all still very technically challenging, with high experimental failure rates[52]. A common challenge when performing CLIP-seq is the immunopurification of sufficient crosslinked RNAs for sequencing[24]. Indeed, the yield of RNA fragments purified in CLIP is typically low, which might be an issue when considering RNA-RBP interactions of mild abundance, poorly crosslinked complexes, inefficient library preparation, non-specific antibodies, or combinations thereof[24,25].

Enzymatic tagging approaches

Aiming to overcome some of the challenges encountered in CLIP methods, other techniques based on the editing of RBP targets have been developed. Without the requirement of any crosslinking step, biochemical IP or, in some instances, the preparation of cDNA libraries, enzymatic tagging approaches have emerged as alternative strategies for the transcriptome-wide identification of endogenous RNA-RBP interactions[52]. An example of enzymatic tagging approach is the STAMP (surveying targets by APOBEC-mediated profiling)[74]. In this technique, RBPs of interest are fused with APOBEC enzymes that produce clusters of mutations on cytosine bases in single-stranded RNAs with high coverage. Another example is TRIBE (the targets of RBPs identified by editing)[75], in which the RBP of interest is fused *in vivo* with the catalytic domain of the adenosine deaminase (ADAR, a RNA-editing enzyme) or its hyperactive mutant (HyperTRIBE)[76]. The catalytic domain of ADAR irreversibly edit adenosine to inosine near the RNA-binding sites, which is subsequently read as

guanosine by reverse transcriptase. The binding sites are therefore recognized by the excess of A to G conversions. Although both approaches, STAMP and TRIBE, are less technically challenging (with less manipulation step) and with minimal number of required cells to perform the protocols than CLIP, the fusion of proteins with the RBP of interest can compromise its localization and activity. Besides, the binding sites identified by these techniques are commonly distributed within hundreds of nucleotides apart from the sites identified by CLIP[75,76].

Significant efforts were certainly dedicated to developing this wide range of techniques that are currently available for identifying and analysing RNA-protein interactions. However, considerable challenges remain to be addressed. For example, while CLIP is known to have a higher signal-to-noise ratio than other techniques due to the removal of noncovalent interactions, it might not be suitable for the study of poorly crosslinked proteins[24]. Therefore, it is important to be aware of the advantages and limitations of each method, as well as the steps that can be modified and tailored for the study of a specific RBP while maintaining the commonly used standards for quality control[25]. New CLIP applications are expected to be developed in the coming years, and the integration of the data generated by these methods with others that do not rely on crosslinking or protein purification can potentially improve the interpretation of the data generated[25,52]. Additionally, the integration of data produced by both protein-centric and RNA-centric methods may help uncover a more complete RBP repertoire and define the roles of the identified RBPs in regulating RNA processing step[67,68].

1.1.1.3 LARGE-SCALE QUANTITATIVE METHODS: THE ERA OF RNA INTERACTOMES

Intensive efforts have been made to enhance our knowledge on RBPs. Indeed, several large-scale quantitative methods have been developed in recent years to examine the global RBPome in order to catalogue a more complete RBP repertoire and gain insights into the features that regulate the RNA-protein interactions in both physiological and pathological contexts. In these methods, RBPs are identified by mass spectrometry, while their correspondent bound RNAs and binding sites are identified by high-throughput sequencing. Together, they have been applied in many different cell types[3,6,10,13,77–84], tissues[79], organs[85] and organisms[78,79,81,86], increasing the number of RBP candidates.

Silica-based approaches

These unbiased large-scale studies rely on the use of UV irradiation to crosslink and preserve the *in vivo* RNA-protein interactions prior to cell lyses and purification of the complexes. In fact, the purification of cellular RNA–protein complexes can be performed in various ways. For example, TRAPP (total RNA-associated protein purification) and TRAPP-based methods (e.g.: PAR-TRAPP and iTRAPP) use silica beads that bind nucleic acids to purify cellular RNA–protein complexes[86]. In principle, both RNA- and DNA-bound proteins can be enriched by silica binding; however, UV crosslinking of double-stranded DNA to proteins is expected to be inefficient[25]. Nevertheless, TRAPP allowed the identification of 1,434 significantly enriched proteins in eukaryotes (*Saccharomyces cerevisiae*) and 1,106 enriched proteins in bacteria (*Escherichia coli, E. coli*)[86]. In both RBPomes, TRAPP and PAR-TRAPP (in a lesser extent) identified many unexpected RBPs, including metabolic enzymes from glycolysis, gluconeogenesis, purine biosynthesis, and pentose phosphate pathways[86].

Organic phase separation approaches

Other methods, such as XRNAX (protein-crosslinked RNA extraction)[77], OOPS (orthogonal organic phase separation)[78,87] and PTex (Phenol Toluol extraction)[79], purify the crosslinked RNA–protein complexes by their physicochemical properties using organic phase separation (Figure 6). As in the previous strategy, this purification method allows the capture of RNA-binding proteins interacting with both poly(A) and non-poly(A) RNAs. In XRNAX and OOPS, the complexes are extracted from whole-cell lysates using acidic guanidinium thiocyanate-phenol-chloroform, commercially known as TRIzol[77,78,87]. Under normal extraction conditions, free RNA molecules migrate to the upper, aqueous phase. Conversely, non-crosslinked proteins are retained in the lower, organic phase. The RNA-protein complexes therefore contain the physicochemical properties of both protein and RNA molecules and are thus retained at the aqueous-organic interphase[77,78,87].

XRNAX was performed in UV crosslinked MCF7, HeLa and HEK293 human cell lines, and the RNA-protein complexes were collected from the interphase, washed and deoxyribonuclease (DNase)-digested to eliminate any DNA contaminates[77]. Then, partial tryptic digestion of the XRNAX extracts and silica enrichment of RNA-bound proteins were followed by mass spectrometry to characterize the RBPome of these cell lines[77]. This strategy revealed that 1,207 proteins were enriched for MCF7, 1,239 proteins for HeLa, and 1,357 proteins for HEK293 cells. All three cell lines shared the enrichment of 858 proteins[77]. Regarding the OOPS strategy, it was applied to MCF10A, U2OS and HEK293 human cell lines, and also in *E. coli*[78]. After a few rounds of TRIzol phase separation and protease digestion, mass spectrometry analysis was performed to identify the RNA interactomes. In the human cell lines, OOPS identified a total of 1,838 RBPs, including 926 putative novel RBPs[78]. Since OOPS is not restricted to poly(A)

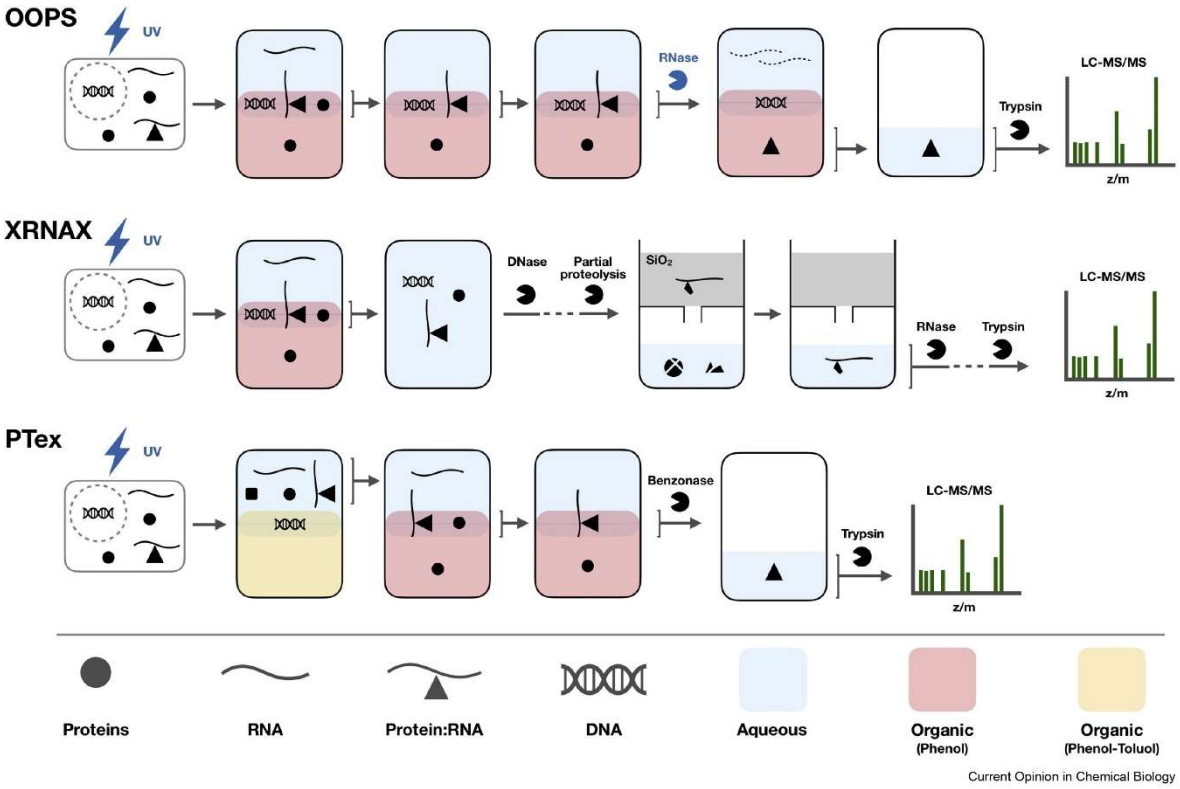

Figure 6. Organic phase separation-based methods. The first step of each method consists in the UV crosslinking of direct RNA-protein interactions in live cells, which is followed by at least one round of TRIzol phase separation to separate the crosslinked complexes from unwanted free RNAs and proteins. Steps for obtaining the final sample are different for each method, and only significant steps are shown. Potential control points are represented in blue. From Smith *et al.*, 2020 (ref [88]).

RNAs, it also allowed the identification of 364 putative RBPs in *E. coli,* in which 234 proteins were not previously annotated with any RNA-related Gene Ontology (GO) terms[78]. PTex, in contrast to XRNAX and OOPS, uses a combination of TRIzol extraction and a modified extraction chemistry mixture (phenol:toluol) to purify the crosslinked RNA-protein complexes[79]. This strategy was successfully applied in HEK293 cells, mouse brain tissues and in the bacteria *Salmonella Typhimurium*. In HEK293 cells, 3,037 proteins were found directly associated with RNA, which is nearly a third of the expressed cellular proteome[79]. In *S. Typhimurium*, 172 proteins were identified, and 113 of them had unknown links to the RNA biology[79]. Moreover, western blot analysis of PTex performed on UV crosslinked mouse brain samples revealed the enrichment of the known RBP Embryonic Lethal Abnormal Vision (ELAV) L1/Human antigen R (HuR), thus demonstrating that this technique can also be applied to mammalian tissue samples[79]. Together, all 3 approaches (XRNAX, OOPS and PTex) allowed the recovery of a global RNA-bound proteome, identifying canonical and putative RBPs associated with poly(A) and non-poly(A) RNAs in different cell types, tissues, and organisms by the purification of crosslinked RNA–protein complexes using organic phase separation[77–79,87].

Oligo(dT)-based approaches

Alternatively to purifying complexes by their physicochemical properties, direct poly(A) RNA-RBP interactions can be purified using oligo-dT beads (Figure 7). In 2012, two groups independently developed a new strategy to assess the *in vivo* eukaryotic RBPome using UV irradiation to crosslink interacting RNAs and proteins, followed by extraction of protein-RNA complexes with oligo(dT) beads, RNase treatment and, finally, quantitative proteomics to identify the extracted proteins[3,80,88]. This strategy is termed as RNA Interactome Capture (RIC), and it was designed to enrich poly(A)-binding RBPs, thereby not suitable to identify protein binding partners of non-poly(A) RNAs. Together, these two studies identified 860 and 791 proteins as part of the HeLa and HEK293 cells mRNA interactomes, respectively[3,80]. The two cell lines shared a total of 545 proteins, and most of the proteins detected in both interactomes were well known RBPs. However, the analyses also revealed that half of the proteins identified lacked know RBDs, and hundreds of them had no RNA-related ontology (e.g., metabolic enzymes)[89].

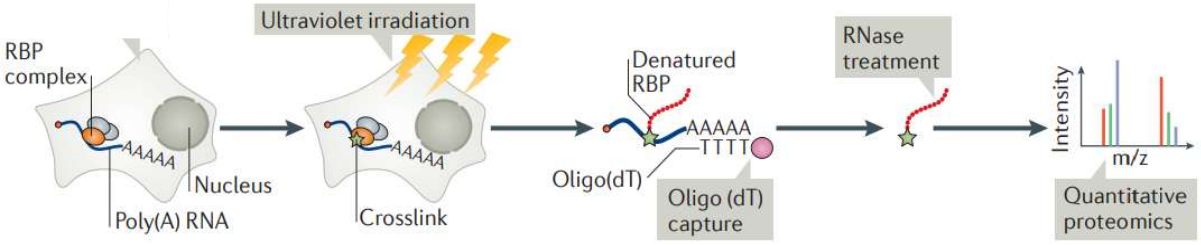

Figure 7. Oligo(dT)-based method. RIC and RIC-like methods are high-throughput approaches designed to isolate RBPs bound to poly(A) RNAs. These methods start with the UV crosslinking of RBPs to RNAs, followed by the capture of poly(A) RNA-RBP complexes by oligo(dT) beads. The proteins are then identified by quantitative mass spectrometry. Adapted from Hentze *et al.*, 2013 (ref [83]).

Since its development, RIC and RIC-based methods have been applied in samples from different sources. In 2015, RIC was used to determine the RNA interactome from the yeast *Saccharomyces cerevisiae* and the human hepatocytic HuH-7 cells, identifying 678 RBPs and 729 RBPs, respectively[81]. By combining these analyses with published RBPomes, a conserved eukaryotic mRNA interactome was defined and comprised 243 yeast RBPs and 256 human RBPs. This conserved interactome included well-studied RBPs with well-defined RBDs and functions in RNA biology[81]. In contrast, when analysed individually, 40% of the yeast and 27% of the human RBPs were unknown or lacked structural motifs related to RNA binding[81]. RIC has also been used to uncover RBPs involved in melanoma progression. Comparison of RIC profiles of melanoma cell lines with distinct aggressiveness revealed changes in RNA-binding activities[13]. Indeed, 216 out of 477 RBPs identified in the melanoma RBPome showed increased RNA-binding activity in the metastatic cell line and decreased activity in the non-tumoral cell line, thus demonstrating that changes on RNA-binding activity can be explored to

assess the tumorigenic potential of RBPs[13].

In the following years, an enhanced RNA interactome capture (eRIC) method was developed aiming to increase the detection of RNA-binding proteins while decreasing contaminants and material requirement[82,90]. eRIC is based on use of locked nucleic acid (LNA)-modified capture probes as a substitute of oligo-dT probes for a more specific and sensitive capture of mRNA interactomes, as demonstrated by comparative analysis in Jurkat cells[82]. This method was used to explore RNA-protein interactions relevant to osteosarcoma by comparative studies of the RNA-bound proteome of malignant bone tumours, normal mesenchymal stem cells and osteoblasts[10]. These analyses revealed 583 common RBPs within cell lines and uncovered systematic changes on RNA-binding activities, therefore providing insights into potential clinically relevant RBP-dependent mechanisms in osteosarcoma[10]. eRIC was also shown to be compatible with the analyses of mRNA interactomes in different subcellular compartments. Preceded by nucleocytoplasmic fractionation of HuH7 cells, eRIC revealed 197 nuclear RBPs and 746 cytoplasmic RBPs, being 155 common to both fractions and 247 novel RBPs that were missed by earlier mRNA interactome captures using non-fragmented cells[83]. Likewise, cell fractionation followed by eRIC was presented as an interesting approach for the study of dynamic changes in RBPs from specific subcellular compartments upon cellular stress[83].

Recently, a refinement of the eRIC technology allowed the characterization of the mRNA-bound proteome of mouse organs. The *ex vivo* eRIC identified 622, 1,345, and 1,238 candidate RBPs in brain, kidney and liver, respectively[85]. Surprisingly, only few RBPs were found exclusively in one organ[85]. In fact, 648 RBPs were identified in both kidney and liver, while 589 RBPs were shared between all the three organs[85]. As expected, the enriched organ poly(A) RBP dataset of 1,349 proteins was found mostly associated with terms related to RNA metabolism. Conversely, 291 RBPs of the dataset had not been previously identified in cultured cells, and more than one third of them corresponded to metabolic enzymes[85]. Together, these studies allowed the identification of both known and unexpected RBPs, therefore enabling a more complete characterization of the global RNA-bound proteome[26].

RNA-labelling approaches

In order to expand the knowledge on the function of RNA-protein interactions, other methods have been developed to systematically map how RNA and proteins assemble in RNP complexes. These methods may potentially contribute in the concomitant study of RNA-protein and protein-protein interactions, as well as in the obtention of a more accurate subcellular location of RBPs and their dynamic changes in biological process[24,25,84]. For example, a subcellular-specific RNA labelling method was developed

aiming for a deeper enrichment and profiling of nuclear and cytoplasmic RBPs without the need of cellular fragmentation[84]. Using nuclear/cytoplasm RNA targeting (furocoumarin) probes, this method revealed a total of 1,221 nuclear RNPs and 1,333 cytoplasmic RNPs in HeLa cells[84]. Interestingly, the RBPs identified displayed enhanced RNA-binding activity in nucleus and reduced RNA association in cytoplasm upon ferroptosis induction, which allowed the discovery of nucleocytoplasmic translocation candidates, including translation-related proteins and metabolic enzymes[84]. Another method was applied in HeLa cells to specific study how mRNA-protein complexes (mRNPs) are remodelled from RNA synthesis to degradation[6]. By performing pulse metabolic labelling with photoactivatable ribonucleoside at specific time points, this approach identified more than 800 RBPs. Most of them were largely consistent with previous reports regarding their subcellular locations and molecular interactions. However, this technique also identified RBPs with unexpected dynamics[6].

All these large-scale methods allowed the identification of known and novel RBPs by exploring different aspects of the RNA-protein complexes. Intriguingly, many of the newly identified candidates lack known hallmarks of RBPs, such as well-established architectural features (RBDs) and function in regulating the RNA fate[6,7]. Nevertheless, the quantification of the dynamic RBP association with RNA will ultimately provide a better understanding of the function of this interaction, including how, when and where the RNA-protein complexes assemble to modulate cellular function.

1.1.1.4 RNA-BINDING DOMAINS AND UNCONVENTIONAL TYPES OF RNA BINDING

RBPs can recognize hundreds of transcripts in the cells, and they do so by binding to specific sequences or structural motifs present in the RNAs[4,7]. Classic RNA-protein interactions occurs via a limited set of structurally well-defined RBDs[8], such as the K-homology domain (KH), RNA recognition motif (RRM), DEAD/DEAH helicase domain, and zinc-finger domains, in addition to approximately 30 other domains of lesser abundance (reviewed in [1]). Interestingly, classic RBPs often harbour multiple RBDs, which ensures RNA-binding selectivity and affinity[91–93].

Recent unbiased RIC and RIC-like methods have revealed additional unconventional RBPs that lack discernible RBDs. Considering a superset of 3,470 human RBPs, only ~25% of them (859 RBPs) harbour known RBDs[7]. The RBPomes analysis of specific human cell lines also presented impressive ratios. For example, 47,3% of the RBPs identified in the human cervical carcinoma HeLa interactome do not harbour any discernible RBD, being them classical (e.g., RRM, KH, and DEAD box helicase) or

nonclassical (e.g., LSM and YTH)[3]. Similarly, almost half of the melanoma RBPome (43%)[13] and half of the bone/mesenchymal-cell RNA interactome proteins[10] lack recognizable RBDs. These proteins, however, contained a diversity of other domains, some of which are present in translation factors or regulators of RNA metabolism, including intrinsically disordered regions (IDRs) that participate in RNA binding[13]. Interestingly, the ratio of RBPs harbouring or not conventional RBDs seems to also depend on the subcellular compartment of the RBP. While two thirds of nuclear RBPs contained classical RBDs, approximately three quarters of the cytoplasmic RBPs lacked recognizable RBDs in the human hepatoma-derived HuH7 cells[83]. In other organisms, such as in yeast, 40% of the identified RBPs lacked both known RBDs and RNA-related functions[81]. Likewise, no more than one-fifth of the RBPs identified in mouse organs bore known RBDs[85].

It's evident that, despite the increasing amount of data collected on RBPs, many domains engaged in native interactions with RNAs remain to be identified and characterized. Aiming for a better understanding of the RNA-binding architectures *in vivo*, RBDmap was applied in HeLa cells for the identification of RBDs on a proteome-wide scale[93]. RBDmap is an extension of the RIC method[88], and combines UV cross-linking and oligo(dT) capture with mass spectrometry analysis. By this means, it allowed the identification of 1,174 mRNA-binding sites in 529 RBPs, showing that more than half of these proteins had no domain or functional annotation related to the RNA biology[93]. However, it was possible to identify that unconventional RBDs were associated with different molecular functions, including DNA binding and protein-protein interactions[93,94]. Remarkably, numerous metabolic enzymes identified as unconventional RBPs were proposed to bind RNA through regions in the vicinity of their substrate-binding pockets[93]. Specifically, the Rossmann fold[95] (di-nucleotide) binding domain, among other folds (e.g., mono-nucleotide), emerged as a *bona fide* RBD[93], in accordance to previous observations[96–99]. These proposed multifunctional domains thus appear to be a commonplace and not an exception among unconventional RBPs[94].

Other methods, such as PACCE (Photo-Activatable-Competition and Chemoproteomic Enrichment)[100], have been recently developed to detect any RNA-protein interactions *in vivo* by quantifying the sensitivity of probe-modified sites in competition with photoactivatable cellular RNA. PACCE not only allowed the profiling of RNA-binding regions on known RBPs (including those with specificity for non-poly(A) RNA), but also enabled the discovery of novel proteins with non-canonical RNA-binding activity (1,658 out of the 3,018 putative RBPs identified)[100]. Importantly, PACCE analysis revealed that well-characterized RBDs were prominently enriched within know RBPs; however, these proteins were also found to harbor functional non-canonical RNA-binding regions as well as IDRs[100].

Collectively, these studies demonstrate that, for a protein to specifically interact with

RNAs, it does not necessarily need to harbour classic RBDs[93], once more highlighting the need of suitable methods for a better comprehension of the regulatory mechanisms involved in these interactions. New studies hold promise to unravel how this new class of RBPs binds RNA, the specificity of this binding and how this interaction is regulated. Indeed, an important step for the discovery of non-canonical RBPs is the unbiased characterization of the RNA-binding regions.

1.2 UNCONVENTIONAL RNA-BINDING PROTEINS

As discussed in the previous chapter, various approaches have been developed to characterize RNA-protein interactions. These approaches, with a particular focus on the large-scale quantitative methods (e.g., RIC[88]), have generated an unprecedented atlas of RBPs. Confirming the robustness of these extensively used methods, the majority of the well-established RBPs were detected, with a strong enrichment of classical RBDs, such as the RRM, KH, DEAD box helicase and some zinc-finger domains[7]. Remarkably, these approaches also revealed, with high confidence, the existence of RNA-binding activities in proteins involved in biological processes with no apparent relation to the RNA biology[7]. Overall, this can be observed, for example, in the most recently published superset of Human RBPs, in which almost half of the identified candidate RBPs had not been previously annotated (Figure 8A), and more than 75% of them harboured unknown RBDs[7] (Figure 8B). These novel RBPs lacking canonical RBDs or known links to the RNA biology were recently termed as "enigmRBPs", and their discovery suggests the existence of unexplored interactions between gene expression and other biological processes[81].

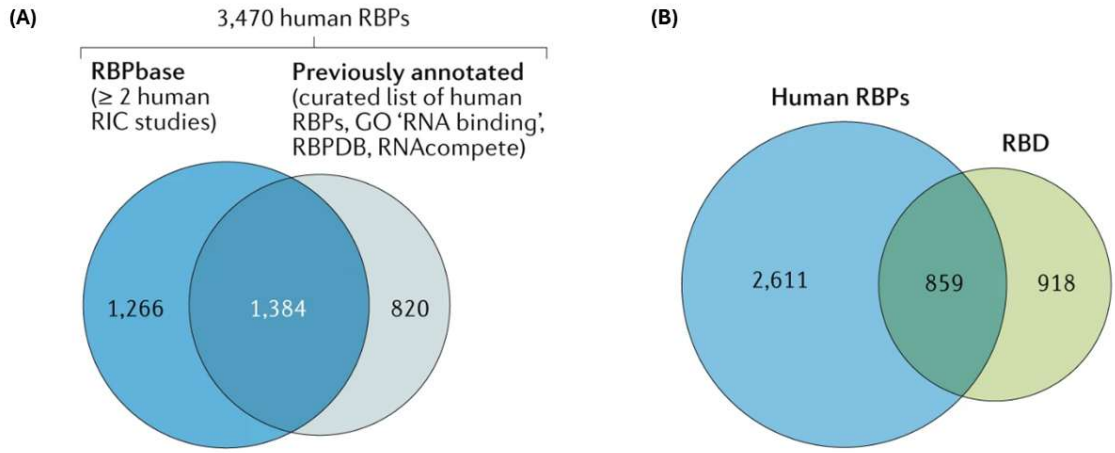

Figure 8. Human RBP superset. (**A**) The human RBP superset is composed of RBPs identified in at least 2 independent RIC studies within a compilation of 16 high-throughput studies (2,650 RBPs in total), in addition to a previous curated list of human RBPs[8] and annotated RBPs, therefore totalizing 3,470 RBPs. (**B**) Comparison of the known RBDs with the predicted RBDs within the human RBP superset. Adapted from Gebauer *et al.*, 2021 (ref [7]).

The enigmRBPs cover a broad spectrum of proteins that, in turn, perform diverse biological functions. Strikingly, these unorthodox RBPs include chromatin- and DNA-associated proteins (e.g.: histone modifiers and proteins involved in chromosome/chromatin organization, DNA replication and nucleosome assembly)[83,84], SUMO proteins, ATP-binding proteins, chaperones and enzymes[81,83,84]. Indeed, several of these enigmRBPs have been validated by orthogonal methods[3,80]. For example, the Protein Disulfide Isomerase Family A Member 6 (PDIA6), an endoplasmic reticulum(ER)-lumen chaperone, was found to display RNA-binding activities in

melanoma by RIC and OOPS, which was further validated by CLIP (PNK assay). Its interaction with RNA was proposed to sustain the tumour-promoting properties of the protein[13]. Additionally, enzymes from classic metabolic pathways that have previously been identified as non-canonical RBPs[101,102] have also been detected in RNA-bound proteome studies. While some of these enzymes were implicated in directing co-transcription processes[103], others (or, in some instances, the same enzymes) were shown to play important roles in sculpting cellular proteomes by participating in the post-transcriptional control of mRNAs[97]. Indeed, these and many other metabolic enzymes have been recurrently identified to 'moonlight' as RBPs in RNA interactome studies. Many of them are enzymes that participate in a wide range of metabolic pathways, and catalyse different reactions[4].

1.2.1 METABOLIC ENZYMES

Metabolism is a fundamental aspect of living cells, and involves a wide range of pathways and chemical reactions in order to convert energy into usable forms, synthesize molecular building blocks (amino acids, lipids, and nucleotides), and eliminate toxins and degradation products[104]. Therefore, the metabolic network is essential for cell growth, maintenance, division, and responsiveness to environmental changes. Anabolic and catabolic processes are catalysed by specialized proteins termed enzymes, which accelerate chemical reactions within these processes, and they can be subject to regulation[104].

Over the past decades, enzymes involved in the intermediary metabolism were shown to make up a significant portion of the RBPome in cells. For example, when analyzing the human RBPome in HuH-7 cell line, 9%, of the RBPs were found to be metabolic enzymes[81]. In accordance to this study, many others detected enzymes of the intermediary metabolism as RBPs[3,10,13,80,84,100]. These findings were extended to mouse organs, where RNA-binding metabolic enzymes were even more prevalent[85]. In an integrated atlas of published RNA interactomes derived from studies conducted in human or mouse cell lines, enzymes constituted 19% of the RBPome, with 7% being metabolic enzymes, whereas in mouse organs these figures were 29% and 16%, respectively[85]. This study also revealed that enzymes of intermediary metabolism bind to both poly(A) and non-poly(A) RNAs across various metabolic pathways, with 60% of the identified enzyme-RBPs binding mono- or di-nucleotide cofactors, such as the nicotinamide adenine dinucleotide phosphate (NADP)[85]. Many of the glycolytic enzymes (GEs) shown to bind RNA in *Homo sapiens* were also shown to bind RNA in *E. coli*[78]. In other organisms, such as *Saccharomyces cerevisiae* and *Arabidopsis thaliana*, a significant fraction of 5% of the proteins found in their RBPomes were involved in the carbohydrate metabolism[104]. Altogether, these studies indicate that the RNA-binding activity of the metabolic enzymes is a ubiquitous phenomenon rather than an exception.

Beyond doubt, metabolic enzymes can moonlight as regulators of (m)RNAs, as demonstrated by several well explored examples (e.g., the glyceraldehyde-3-phosphate dehydrogenase (GAPDH) and the iron-responsive element-binding protein 1 (IRP1)), and hold crucial functions in regulating co- and post-transcriptional steps of gene expression by acting as trans-acting factors to control the RNA fate[104]. The discovery that these seemingly well-characterized metabolic enzymes can also bind RNA forms the basis of the "REM (RNA–enzyme–metabolite) hypothesis"[105] (Figure 9). This hypothesis proposes the existence of regulatory links between gene expression and intermediary metabolism mediated by the 'moonlighting' RNA-binding activity of metabolic enzymes[105]. Theses links are therefore proposed to exist to direct post-transcriptional gene regulation. Thus, it is hypothesized that the metabolic enzymes might be bi-functional proteins, meaning that they might act as both enzymes and RNA-binding proteins, and have their functions regulated by cofactors and metabolites[105].

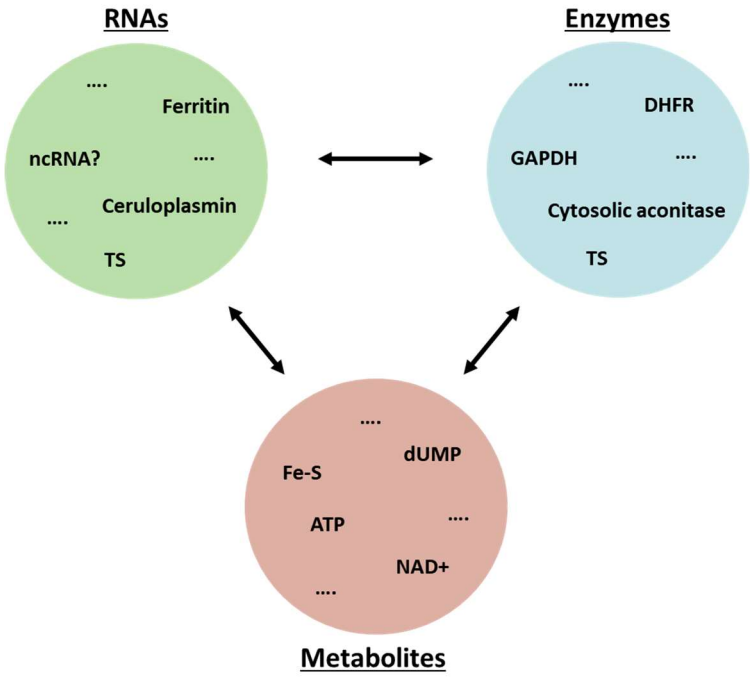

Figure 9. RNA–enzyme–metabolite network. Schematic representation of regulatory links between enzymes, RNAs and metabolites of the intermediary metabolism. Proteins with dual-function (as enzymes and RNA-binding) might be regulated by metabolites and cofactors. Adapted from Hentze & Preiss, 2010 (ref [102]).

Previous RNA interactome studies revealed that many of the newly identified RBPs do not harbour well-defined RBDs. Indeed, numerous metabolic enzymes were found to bind RNA in the vicinity of their substrate-binding pockets, as mapped by RBDmap and in accordance with previous observations[94,97]. For example, Rossmann fold is a di-nucleotide domain typically associated with the binding of nucleotides such as the nicotinamide adenine dinucleotide (NAD)[95]. This fold has been shown to play a crucial role in the function of many enzymes, particularly dehydrogenases, which catalyze

oxidation-reduction reactions. Interestingly, this same domain has been pointed to mediate binding to RNA[97]. In parallel, RBDmap mapped RNA-binding regions in the vicinity of substrate-binding pockets of many other enzymes, such as for the Aldolase (ALDO) A and C at the fructose-1,6-bisphosphate interacting domain[94]. This, and many other domains, remains to be validated regarding their ability to direct enzyme binding to RNA.

Future studies aiming to understand how these RNA-enzyme complexes are formed and respond to cellular cues may give insights into the features that regulate their interactions, as well as elucidate the role of these enzymes as regulators of gene expression. Likewise, these studies could potentially unravel novel roles of the RNA in regulating enzyme functions (riboregulation)[4] (as competitive inhibitors or allosteric regulators, for example), therefore revealing with greater extension the regulatory links between enzymes, RNAs and metabolites.

1.2.1.1 GLYCOLYTIC ENZYMES

Differentiated mammalian cells normally obtain the energy needed for cellular processes in the form of adenosine 5′-triphosphate (ATP). In these cells, ATP is primarily generated through a series of enzymatic reactions in the mitochondria by oxidative phosphorylation (OXPHOS)[106,107]. However, most of the cancer cells rely on aerobic glycolysis, even in the presence of oxygen. This process is termed as the 'Warburg effect'[108]. Aerobic glycolysis is inefficient in terms of ATP generation when compared to OXPHOS. While OXPHOS generates 36 ATPs, glycolysis generates only 2 ATP molecules from glucose break down[106]. However, glycolysis can generate ATP faster, and provides glycolytic intermediates that are required for biosynthesis of nucleic acids, lipids, and amino acids. Glycolysis also generates lactate, which maintains the balance between NAD oxidation (NAD^+) and reduction (NADH), also known as NAD+/NADH redox balance[106]. Therefore, glycolysis is an advantageous process for cells in rapid growth and proliferation, accounting for 60% of the total cellular ATP production in cancer cells[109]. Of note, some cancer cells have been shown to "reactivate" mitochondrial respiration when the tricarboxylic acid (TCA) cycle is activated, which suggests that these cells are able to modulate their metabolism according to their needs[107,110].

Aerobic glycolysis takes place in the cytosol and involves the coordinated action of different GEs to generate ATP molecules throughout the split of glucose into pyruvate, the final product of glycolysis. Although highly conserved among species, studies have shown that some GEs are unexpectedly complex, multifaceted proteins, rather than merely simple components of the glycolytic pathway. These enzymes were shown to perform non-glycolytic functions, including regulation of inflammatory responses[111], gene expression and other cellular processes, such as apoptosis, cell cycle, autophagy,

cytoskeleton dynamics[104]. In addition to these functions, GEs have been recurrently identified to direct bind RNA by several RNA interactome studies (Table 1).

Table 1. GEs identified in RNA interactome studies. All the main enzymes of the glycolytic pathway have been listed at least once as candidate RBPs in the RBP2GO database. Only RNA interactome studies performed in human cell lines are listed. GEs experimentally validated as non-canonical RBPs are marked by an asterisk (*) in the "PROTEIN NAME" field.

PROTEIN NAME	GENE NAME	APPROACH	CELL TYPE	REFERENCES (DOI)
HEXOKINASE I/II	HK1/2	OOPS, Non-Poly(A)-Based	MCF10A, U2OS	10.1038/s41587-018-0001-2
		XRNAX, Non-Poly(A)-Based *(only HK2)*	HEK293	10.1016/j.cell.2018.11.004
		PTex, Non-Poly(A)-Based	HEK293	10.1038/s41467-019-08942-3
		eRIC (cytoplasmic), Poly(A)-Based	HuH-7	10.1093/nar/gkaa256
GLUCOSE-6-PHOSPHATE ISOMERASE	GPI	pCLAP, Poly(A)-Based	HEK293	10.1021/acs.jproteome.7b00042
		CARIC, Non-Poly(A)-Based	HeLa	10.1073/pnas.1718406115
		OOPS, Non-Poly(A)-Based	HEK293, U2OS	10.1038/s41587-018-0001-2
		PTex, Non-Poly(A)-Based	HEK293	10.1038/s41467-019-08942-3
		eRIC (cytoplasmic), Poly(A)-Based	HuH-7	10.1093/nar/gkaa256
ATP-DEPENDENT 6-PHOSPHOFRUCTOKINASE	PFK	R-DeeP, Non-Poly(A)-Based	HeLa	10.1016/j.molcel.2019.04.018
		pCLAP, Poly(A)-Based	HEK293	10.1021/acs.jproteome.7b00042
		CARIC, Non-Poly(A)-Based	HeLa	10.1073/pnas.1718406115
		cRIC, Poly(A)-Based	HEK293	10.1016/j.molcel.2019.01.017
		XRNAX, Non-Poly(A)-Based	MCF7	10.1016/j.cell.2018.11.004
		PTex, Non-Poly(A)-Based	HEK293	10.1038/s41467-019-08942-3
		eRIC (cytoplasmic), Poly(A)-Based	HuH-7	10.1093/nar/gkaa256
FRUCTOSE-BISPHOSPHATE ALDOLASE A/C (*)	ALDOA/C	R-DeeP, Non-Poly(A)-Based	HeLa	10.1016/j.molcel.2019.04.018
		PAR-CLIP, Poly(A)-Based *(only ALDOA)*	HEK293	10.1016/j.molcel.2012.05.021
		RBDmap, Poly(A)-Based	HeLa	10.1016/j.molcel.2016.06.029
		pCLAP, Poly(A)-Based	HEK293	10.1021/acs.jproteome.7b00042
		RICK, Poly(A)-Based	HeLa	10.1038/nmeth.4595

		CARIC, Non-Poly(A)-Based	HeLa	10.1073/pnas.1718406115
		eRIC, Poly(A)-Based *(only ALDOA)*	Jurkat	10.1038/s41467-018-06557-8
		cRIC, Poly(A)-Based *(only ALDOA)*	HEK293	10.1016/j.molcel.2019.01.017
		XRNAX, Non-Poly(A)-Based *(only ALDOA)*	MCF7, HEK293, HeLa	10.1016/j.cell.2018.11.004
		PTex, Non-Poly(A)-Based *(only ALDOA)*	HEK293	10.1038/s41467-019-08942-3
		eRIC (cytoplasmic), Poly(A)-Based	HuH-7	10.1093/nar/gkaa256
TRIOSEPHOSPHATE ISOMERASE	TPI1	pCLAP, Poly(A)-Based	HEK293	10.1021/acs.jproteome.7b00042
		CARIC, Non-Poly(A)-Based	HeLa	10.1073/pnas.1718406115
		OOPS, Non-Poly(A)-Based	HEK293, U2OS, MCF10A	10.1038/s41587-018-0001-2
		PTex, Non-Poly(A)-Based	HEK293	10.1038/s41467-019-08942-3
		eRIC (cytoplasmic), Poly(A)-Based	HuH-7	10.1093/nar/gkaa256
GLYCERALDEHYDE-3-PHOSPHATE DEHYDROGENASE (*)	GAPDH	pCLAP, Poly(A)-Based	HEK293	10.1021/acs.jproteome.7b00042
		RICK, Poly(A)-Based	HeLa	10.1038/nmeth.4595
		CARIC, Non-Poly(A)-Based	HeLa	10.1073/pnas.1718406115
		eRIC, Poly(A)-Based	Jurkat	10.1038/s41467-018-06557-8
		cRIC, Poly(A)-Based	HEK293	10.1016/j.molcel.2019.01.017
		DIF-FRAC, Non-Poly(A)-Based	HEK293	10.1016/j.celrep.2019.09.060
		OOPS, Non-Poly(A)-Based	HEK293, U2OS, MCF10A	10.1038/s41587-018-0001-2
		XRNAX, Non-Poly(A)-Based	MCF7, HEK293, HeLa	10.1016/j.cell.2018.11.004
		PTex, Non-Poly(A)-Based	HEK293	10.1038/s41467-019-08942-3
		eRIC (cytoplasmic), Poly(A)-Based	HuH-7	10.1093/nar/gkaa256
PHOSPHOGLYCERATE KINASE 1 (*)	PGK1	pCLAP, Poly(A)-Based	HEK293	10.1021/acs.jproteome.7b00042
		RICK, Poly(A)-Based	HeLa	10.1038/nmeth.4595
		CARIC, Non-Poly(A)-Based	HeLa	10.1073/pnas.1718406115

		eRIC, Poly(A)-Based	Jurkat	10.1038/s41467-018-06557-8
		cRIC, Poly(A)-Based	HEK293	10.1016/j.molcel.2019.01.017
		OOPS, Non-Poly(A)-Based	HEK293, U2OS, MCF10A	10.1038/s41587-018-0001-2
		XRNAX, Non-Poly(A)-Based	MCF7, HEK293, HeLa	10.1016/j.cell.2018.11.004
		PTex, Non-Poly(A)-Based	HEK293	10.1038/s41467-019-08942-3
		eRIC (cytoplasmic), Poly(A)-Based	HuH-7	10.1093/nar/gkaa256
PHOSPHOGLYCERATE MUTASE 1	PGAM1	pCLAP, Poly(A)-Based	HEK293	10.1021/acs.jproteome.7b00042
		CARIC, Non-Poly(A)-Based	HeLa	10.1073/pnas.1718406115
		cRIC, Poly(A)-Based	HEK293	10.1016/j.molcel.2019.01.017
		OOPS, Non-Poly(A)-Based	HEK293, U2OS, MCF10A	10.1038/s41587-018-0001-2
		PTex, Non-Poly(A)-Based	HEK293	10.1038/s41467-019-08942-3
		eRIC (cytoplasmic), Poly(A)-Based	HuH-7	10.1093/nar/gkaa256
ALPHA-ENOLASE (*)	ENO1	RIC, Poly(A)-Based	HeLa	10.1016/j.cell.2012.04.031
		RIC, Poly(A)-Based	HuH-7	10.1038/ncomms10127
		RIC, Poly(A)-Based	Jurkat	10.1038/s41467-018-06557-8
		RBDmap, Poly(A)-Based	HeLa	10.1016/j.molcel.2016.06.029
		pCLAP, Poly(A)-Based	HEK293	10.1021/acs.jproteome.7b00042
		RICK, Poly(A)-Based	HeLa	10.1038/nmeth.4595
		CARIC, Non-Poly(A)-Based	HeLa	10.1073/pnas.1718406115
		eRIC, Poly(A)-Based	Jurkat	10.1038/s41467-018-06557-8
		cRIC, Poly(A)-Based	HEK293	10.1016/j.molcel.2019.01.017
		DIF-FRAC, Non-Poly(A)-Based	HEK293	10.1016/j.celrep.2019.09.060
		OOPS, Non-Poly(A)-Based	HEK293, U2OS, MCF10A	10.1038/s41587-018-0001-2
		XRNAX, Non-Poly(A)-Based	MCF7, HEK293, HeLa	10.1016/j.cell.2018.11.004
		PTex, Non-Poly(A)-Based	HEK293	10.1038/s41467-019-08942-3
		eRIC (cytoplasmic), Poly(A)-Based	HuH-7	10.1093/nar/gkaa256
PYRUVATE KINASE (*)	PKM	RIC, Poly(A)-Based	HeLa	10.1016/j.cell.2012.04.031

		RIC, Poly(A)-Based	HuH-7	10.1038/ncomms10127
		pCLAP, Poly(A)-Based	HEK293	10.1021/acs.jproteome.7b00042
		PAR-CLIP, Poly(A)-Based	HEK293	10.1016/j.molcel.2012.05.021
		RICK, Poly(A)-Based	HeLa	10.1038/nmeth.4595
		CARIC, Non-Poly(A)-Based	HeLa	10.1073/pnas.1718406115
		eRIC, Poly(A)-Based	Jurkat	10.1038/s41467-018-06557-8
		cRIC, Poly(A)-Based	HEK293	10.1016/j.molcel.2019.01.017
		DIF-FRAC, Non-Poly(A)-Based	HEK293	10.1016/j.celrep.2019.09.060
		OOPS, Non-Poly(A)-Based	HEK293, U2OS, MCF10A	10.1038/s41587-018-0001-2
		XRNAX, Non-Poly(A)-Based	MCF7, HEK293, HeLa	10.1016/j.cell.2018.11.004
		PTex, Non-Poly(A)-Based	HEK293	10.1038/s41467-019-08942-3
		eRIC (cytoplasmic), Poly(A)-Based	HuH-7	10.1093/nar/gkaa256
LACTATE DEHYDROGENASE A/B CHAIN	LDHA/B	RIC, Poly(A)-Based *(only LDHA)*	HuH-7	10.1038/ncomms10127
		RBDmap, Poly(A)-Based *(only LDHB)*	HeLa	10.1016/j.molcel.2016.06.029
		pCLAP, Poly(A)-Based	HEK293	10.1021/acs.jproteome.7b00042
		RICK, Poly(A)-Based	HeLa	10.1038/nmeth.4595
		CARIC, Non-Poly(A)-Based	HeLa	10.1073/pnas.1718406115
		eRIC, Poly(A)-Based	Jurkat	10.1038/s41467-018-06557-8
		cRIC, Poly(A)-Based	HEK293	10.1016/j.molcel.2019.01.017
		OOPS, Non-Poly(A)-Based	HEK293, U2OS, MCF10A	10.1038/s41587-018-0001-2
		XRNAX, Non-Poly(A)-Based	HEK293	10.1016/j.cell.2018.11.004
		PTex, Non-Poly(A)-Based	HEK293	10.1038/s41467-019-08942-3
		eRIC (cytoplasmic), Poly(A)-Based	HuH-7	10.1093/nar/gkaa256

In some instances, GEs' binding to RNA have been shown to control the RNA fate[6] or even the protein function[20]. However, while sporadic reports have shown that some of these GEs indeed moonlight as RBPs (e.g., GAPDH and ENO1), others remain as

putative RBPs (e.g., hexokinases) in humans due to a lack of further experimental evidence of their RNA-binding activity. Examples of enzyme-mediated regulation of RNAs and/or riboregulation of glycolytic enzymes are summarized in Figure 10. Reports describing the RNA-binding activity of each of these enzymes are discussed below.

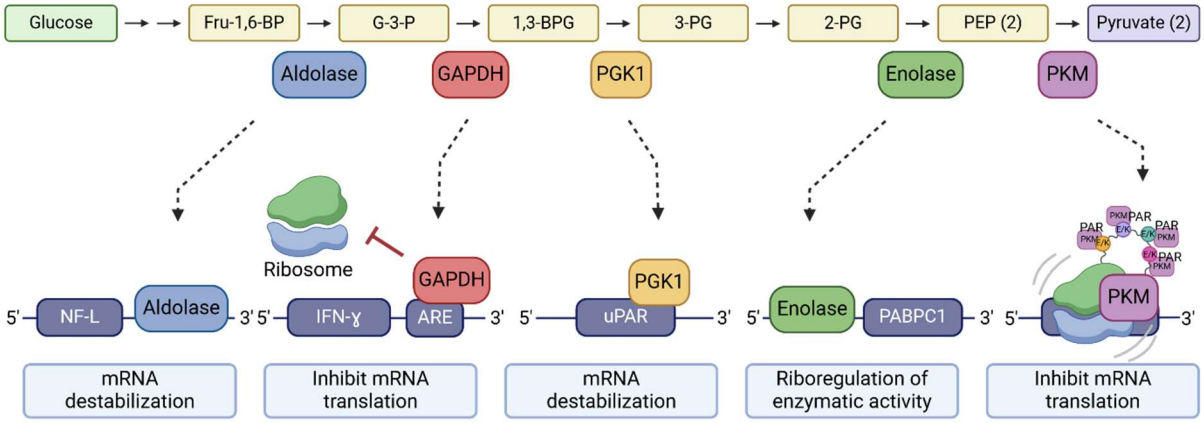

Figure 10. GEs moonlight as RBPs. GEs have been shown to bind RNA *in vitro* and *in vivo* using human cell lines. Aldolase was found to bind to the 3'UTR of the *light neurofilament* (*NF-L*) mRNA in *vitro* and *in vivo*, and this binding was implicated in the regulation of the transcript stability[112]. GAPDH was found to bind to the 3'UTR of a wide variety of mRNAs, particularly at the AU-rich elements (ARE) found in the *interferon-γ* (*IFN-γ*) 3'UTR [97,102]. GAPDH binding to *IFN-γ* mRNA was shown to inhibit its translation. PGK1 binding to the CDS region of the *urokinase-type plasminogen activator receptor* (*uPAR*) mRNA was shown to lower the stability of the transcript[113]. ENO1 was shown bind to hundreds of cellular mRNAs, including the *poly(A) binding protein cytoplasmic 1* (*PABPC1*) mRNA at its 5'UTR[20]. The RNA regulation of ENO1, also known as riboregulation[4], was demonstrated to specifically inhibit ENO1's enzymatic activity both *in vitro* and *in vivo*[20]. PKM non-canonical RBP activity was proposed to induce translational stalling[114]. PKM was found to primarily bind to the CDS of mRNAs, particularly downstream regions encoding lysine- and glutamate-enriched tracts[114].

Hexokinase, glucose-6-phosphate isomerase (GPI), triosephosphate isomerase (TPI1) and phosphoglycerate mutase 1 (PGAM1)

Both hexokinase and GPI are GEs responsible for the first and second reaction steps of glycolysis, respectively. While hexokinases catalysis the phosphorylation of glucose (GLU) to glucose-6-phosphate (G-6-P), GPI interconverts G-6-P into fructose-6-phospate (F-6-P). TPI1, in turn, catalyses dihydroxyacetone phosphate (DHAP) into glyceraldehyde-3-phosphate (G-3-P), while PGAM1 catalyses the conversion of 3-phosphoglycerate (3-PG) and 2-phosphoglycerate (2-PG). Although all these enzymes have been proposed to moonlight as RBPs in large-scale quantitative studies, further analyses are required to validate these findings and determine the biological relevance of the RNA-GE interactions. Nonetheless, hexokinases (Hxks) and triosephosphate isomerase (Tpi) were found to direct interact with nucleic acids by using the 2C

method[64] in yeast. In this technique, Hxk and Tpi were found specifically enriched in UV crosslinked samples, meaning that these enzymes were retained on a silica matrix column by their association with nucleic acids. Indeed, proteins that do not associate with nucleic acids were removed from the column after purification steps[64]. Of note, DNA is usually poorly crosslinked[25], which suggests that Hxks and Tpi were retained on the silica matrix mainly, if not only, by their direct interaction with RNA. Additionally, a recent study on epidermal tissue differentiation in human cell lines identified that many glucose-binding proteins are, in fact, RBPs[115]. Together, these studies support the hypothesis that hexokinases could bind to RNAs in human cells. The RNA-binding activity of these enzymes could potentially be involved in the control of gene expression. In fact, hexokinases have already been associated with post-transcriptional control of RNAs in human cells; however, this control was shown to occur indirectly by the regulation of the subcellular localization of the highly conserved RBP heterogeneous nuclear ribonucleoprotein A1 (hnRNP A1) during hypertonic stress and viral infection[116].

Phosphofructokinase (PFK)

PFK catalyses the phosphorylation of F-6-P, forming fructose-1,6-bisphosphate (F-1,6-B). The first indication that this enzyme could bind to nucleic acids was the discovery, in 2004, that the yeast phosphofructokinase subunit Pfk26p moonlights as a double-stranded DNA-binding protein by the use of proteome microarrays and DNA probes[117]. In 2010, another screening study performed in yeast, but this time for RBPs, identified that Pfk26p binds RNA[118]. In this study, yeast RBPs were identified using high-density protein microarrays and fluorescently labelled RNAs. This technique allowed for the identification of not only Pfk26p, but also other metabolic enzymes. The RNA-binding activity of Pfk26p was then further validated by RIP-CHIP, and this enzyme was found to bind to its own mRNA. This binding is in accordance with other studies demonstrating that unconventional RNA-binding GEs bind to their own mRNAs as well as functionally related mRNAs[119–121], which suggests that these proteins might associate with RNAs for autoregulation.

Pfk2p was also demonstrated to form, together with other GEs (Pfk1p, Fba1p, Eno2p, and Cdc19p), a single, non-membrane-bound granule termed as “glycolytic body” (G-body) in response to hypoxia in yeast[120,122]. The formation of G-bodies in hypoxia was shown to be essential for the cell growth and viability. Cells containing G-bodies displayed high glucose consumption and low levels of glycolytic intermediates[122]. Accordingly, human hepatocarcinoma HepG2 cells were also shown to form G-bodies under hypoxia (1% oxygen), containing, as in yeast, the liver isoform of the human phosphofructokinase isoform (PFKL). In *Caenorhabditis elegans*, the glycolytic protein phosphofructokinase-1 (PFK-1.1) was also shown to be recruited to G-body-like condensates in response to hypoxia-induced energy stress[123]. Some of these glycolytic

G-body components were shown to contain IDRs, including the phosphofructokinase[122]. In fact, the IDR was demonstrated to be essential, but not sufficient, for Pfk2 localization to yeast G-bodies[120,122]. Of note, these regions have been recurrently found within conventional and unconventional RBPs, raising the hypothesis of the involvement of RNA on G-body formation. Indeed, RNA was demonstrated as necessary for the formation and stabilization of G-bodies[120,122]. Many of the glycolysis enzymes found in yeast G-bodies were identified as non-canonical RBPs that bind to many shared mRNAs, which were also identified as components of the G-body[120]. Indeed, PAR-CLIP performed in yeast identified glycolytic enzymes as mRNA-binding proteins (mRBPs), in which 10 (Pgi1, Pfk1, Pfk2, Fba1, Tdh3, Pgk1, Gpm1, Eno1, Eno2, Cdc19) of them were shown to localize at G-bodies in hypoxia. Pfk2, in particular, was shown to preferentially bind to AU-rich elements (ARE) located in the 3′UTR of its mRNA targets[120]. As previously observed[118], these mRNA were enriched in metabolic processes, including glycolysis, and many of them were shared by other GEs (Eno1 and Fba1). RNA binding by other RBPs in G-bodies may promote G-body formation under hypoxia, considering that these RNAs correlate with the RNAs bound to these enzymes under normoxic conditions[120].

Fructose-bisphosphate aldolase

The fructose-bisphosphate aldolase catalyses the interconversion of F-1,6-BP into G-3-P and DHAP. This enzyme has been reported to bind RNA, particularly the isoforms A and C (ALDOA and ALDOC, respectively). In fact, studies demonstrate the RNA-binding activity of these enzymes, exploring their binding to mRNA[112] and viral RNAs (vRNAs)[124,125]. Both ALDOA and C were shown to bind the *light neurofilament* (*NF-L*) mRNA *in vitro* and *in vivo*, and to regulate the stability of the transcript[112]. The direct binding of ALDOA to vRNAs was demonstrated in different studies. For example, ALDOA binding to *Japanese encephalitis virus* (*JEV*) RNAs at both 5′ and 3′UTRs was determined via RNA affinity capture and gel mobility shift assays[124]. This aldolase isoform has also been shown to bind to the *simian hemorrhagic fever virus* at a stemloop in its 3′-UTR[125] [29]. However, the function of this binding is still not known. Additionally, ALDOA was shown to bind to the 3′-UTR of the *myosin heavy chain* (*MyHC*) mRNA in synergy with GAPDH. This binding was implicated in the post-transcriptional regulation of *MyHC*[126].

Glyceraldehyde-3-phosphate dehydrogenase (GAPDH)

GAPDH is a GE responsible for the oxidative phosphorylation of glyceraldehyde-3-phosphate G-3-P to 1,3-bisphosphoglycerate (1,3-BPG), using NAD+ as cofactor. This enzyme was first described to moonlight as an RBP already in 1979, when the human GAPDH was isolated by poly(A)-sepharose chromatography from HeLa cells[127]. Not so

long after that, GAPDH emerged as a non-canonical RBP that binds to a wide variety of RNA types, including transfer RNAs (tRNAs)[98], mRNAs[96,97,99,102,128–138] and vRNAs[126,139–143]. Among its various targets, GAPDH selectively binds RNAs containing AU-rich sequences (AREs) and is therefore classified as an AU-binding protein (AUBP)[97]. Indeed, most of the GAPDH's targets are ARE-RNAs containing three to eight AUUUA pentanucleotide motifs and U-rich regions[144]. It was also demonstrated that the human GAPDH selectively recognizes structural features, as observed on tRNAs[98]. In this context, GAPDH was demonstrated to discriminate *in vitro* between wild-type (WT) tRNA and two tRNA mutants that differs from the WT by single nucleotide substitutions[98]. These mutants are defective in nuclear export, which suggests that the enzyme may participate in tRNA export from the nucleus to the cytoplasm.

RNA-GAPDH interactions were assessed both *in vitro* and *in cellulo*, using a combination of qualitative experiments (e.g., RNA affinity pull-down, co-immunoprecipitation, mobility shift assays, native PAGE, luciferase assays, among others). By these means, GAPDH was found to bind to the 3'UTR of a wide variety of mRNAs, specifically the *interferon-γ* (*IFN-γ*)[97,102], *granulocyte macrophage colony stimulating factor* (*GM-CSF*)[97], *c-myc*[97], *interleukin-2* (*IL-2*)[97], *colony stimulating factor-1* (*CSF-1*)[128,129], *endothelin-1* (*ET-1*)[130], *cyclooxygenase-2* (*COX-2*)[96], *connective tissue growth factor* (*CTGF/CCN-2*)[131], *voltage gated sodium channel type 1α subunit* (*SCN1A*)[132,133], *voltage gated sodium channel type 3α subunit* (SCN3A)[133], *hypoxia inducible factor 1α* (*HIF1α*)[135], *angiotensin II type I receptor* (*AT1R*)[136], and *tumor necrosis factor-alpha* (*TNF-α*)[99,134], *glucose transporter type 1* (*GLUT1*)[137] and the *telomerase RNA component* (*TERC*)[138] mRNAs. Similarly, GAPDH was shown to bind to vRNAs, such as the *hepatitis A*, *B* and *C* viral RNAs[139–141,145], *antigenomic hepatitis D* RNA[143] and the *human papilloma virus* RNA[142]. Regarding the biological relevance of these interactions, the RNA-binding activity of GAPDH has been extensively reported as involved in the control of post-transcriptional gene expression by directly influencing mRNA stability and translation.

In malignant ovarian cancer cells, GAPDH binding to the AREs of the *CSF-1* 3'UTR was shown to increase *CSF-1* stability[128] (Figure 11). Indeed, GAPDH knockdown decreased *CSF-1* mRNA half-live by 50%, and mutations or deletions in the AREs abrogated GAPDH binding[129]. Moreover, the stabilization of the *CSF-1* mRNA consequently increased its translation, and its overexpression was shown to increase metastatic properties of the ovarian epithelial cells[128]. In contrast, GAPDH binding to the AREs of the *ET-1* 3'UTR was shown to increase mRNA decay by destabilizing the mRNA[130]. The mRNA destabilization, however, was found to be modulated by oxidative stress. The incorporation of glutathione (S glutathionylation), a major antioxidant in the cell, to the catalytically active residue Cys 152 of GAPDH mitigated the binding of the enzyme to the *ET-1* mRNA[130]. Likewise, GAPDH was demonstrated to negatively regulates *COX-2* mRNA in hepa1c1c7 cells by binding to the AREs present in the 3'-UTR of the mRNA through its NAD+ binding domain[96]. Interestingly, LPS-induced oxidative stress

induced GAPDH disappearance from the nucleus and dissociation from the *COX-2* ARE, which led to the stabilization of the mRNA[96]. However, further studies are required to investigate whether the *COX-2*-GAPDH dissociation is due to a direct effect of the oxidative stress or by preventing GAPDH's nuclear localization[96]. Of note, recent time-resolved profiling of RNA-binding proteins throughout the mRNA life cycle in HeLa cells indicated that GAPDH-containing mRNPs exhibits the maximal level of mRNA interaction in the nucleus[6].

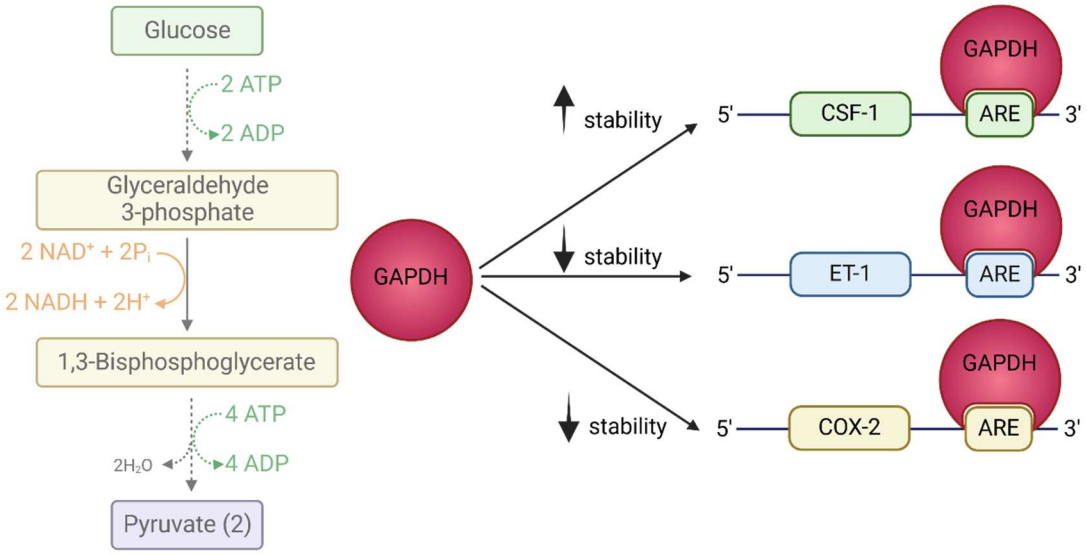

Figure 11. GAPDH regulates mRNA stability. Binding of GAPDH to the AREs at the 3'UTR of the *CSF-1*[128,129], *ET-1*[130] and *COX-2*[96] mRNAs and regulate their stability. GAPDH binding to *CSF-1* mRNA was shown to increase *CSF-1* stability, leading to an increase in its translation[128,129]. Conversely, GAPDH binding to the *ET-1* and *COX-2* mRNAs was shown to decrease mRNAs stability, increasing their decay[96,130].

In these examples, GAPDH was shown to bind to regions within the 3'UTR of mRNAs that are AU rich. However, other studies demonstrated that GAPDH can also bind to non-AU-rich regions and still modulate the stability of its targets[131–133]. For example, this enzyme was shown to bind to the cis-acting element of structure-anchored repression (CAESAR) in the 3'-UTR of the *ccn2* mRNA in hypoxic HCS-2/8 cells. This binding was shown to stabilize the mRNA, leading to ccn2 overexpression and promotion of angiogenesis[131]. As observed in GAPDH's binding to *ET-1* and *COX-2* mRNAs, the *ccn2*-GAPDH interactions could be modulated by oxidative stress. In addition, this interaction could also be regulated by NAD+ in a dose-dependent manner[131]. Other examples also demonstrated the GAPDH binds to non-AU-rich element which are conserved between genes[133] or a new binding sites formed by structural rearrangements as a consequence of mutations[132]. In *SCN1A* and *SCN3A* genes, GAPDH was found to bind to a conserved region in 3' UTRs of human and mouse mRNAs[133]. This binding increased and decreased the genes' expressions by affecting the mRNA stability of *Scn3a* and *Scn1a* mRNAs, respectively[133]. This expression profile was found in acute seizure mice[133]. Interestingly, ketogenic diet, a

high-fat and low-carbohydrate treatment for intractable epilepsy in children, was shown to weaken the GAPDH's binding to the conserved elements in the *Scn3a* and *Scn1a* mRNAs[133]. In a Dravet syndrome patient, a single mutation on the *SCN1A* 3'UTR was shown to form a new GAPDH-binding site. The c.*1794C>T was predicted to alter the secondary structure of the 3' UTR, which allowed the binding of GAPDH. This binding was described to negatively regulate the mRNA stability[132], as observed in mice[133].

In addition to regulating mRNA stability, GAPDH has also been found to control the translation of certain target mRNAs[102,134–136,145]. This regulatory activity seems to be in coordination with the enzyme's metabolic functions, and this is best exemplified in the context of T lymphocytes activation[102] (Figure 12). In T lymphocytes, cells are able to switch their metabolism from OXPHOS to aerobic glycolysis depending on their activation status[102]. In fact, aerobic glycolysis is only required for an effective cytokine production and is therefore not needed for T cell proliferation or survival[102]. In active T lymphocytes, cells are engaged in glycolysis, and GAPDH is fully involved in its metabolic activity. In this context, the *IFN-γ* mRNA is being translated and the cytokine produced[102]. Following T lymphocyte inactivation and metabolic switch to OXPHOS, translation of the *IFN-γ* mRNA was shown to be repressed by the direct binding of GAPDH to the AREs found in the 3'UTR of the mRNA[102]. Similarly, GAPDH was shown to negatively regulate *HIF1A* mRNA translation by binding to the AREs of the *HIF1α* 3'UTR in naïve and central memory T cells, which are less glycolytic[135]. In effector memory T cells, which have an increased glycolytic activity, GAPDH is fully engaged in glycolysis and *HIF1α* mRNA translation is restored[135]. GAPDH was also found to be a translational suppressor of the *TNF* mRNA in THP-1 monocytes by decreasing the *TNF* mRNA association with polysomes through its binding to the AREs present in *TNF* 3'-UTR. As shown in previous studies, GAPDH binding to *TNF* mRNA only occurs when the cells are in a low glycolytic state. Accordingly, the binding could be reversed by increasing glycolysis, thus allowing TNF cytokine production[134].

Despite its lack of canonical RNA binding motif, GAPDH was found to bind *in vitro* and *in vivo* to numerous mRNAs. However, how this non-canonical RBP binds to RNAs is not completely solved. GAPDH contains a di-nucleotide binding domain, known as Rossmann fold, which is a binding site for its cofactor NAD+[95]. This binding site, which is highly conserved among dehydrogenases, was also proposed to mediate RNA-binding[93,96–99]. Indeed, this hypothesis was supported by several papers demonstrating that the RNA-binding activity of GAPDH could be modulated by NAD+, NADH, and ATP in a dose-dependent manner[96–98,130,131]. Recently, the Rossmann fold emerged as a *bona fide* RBD engaged in native interactions with RNA *in vivo*[93]. This observation could potentially be extended to the RNA binding activity attributed to other dehydrogenases and enzymes[97]. A few studies, however, have suggested the involvement of other regions outside the Rossmann fold in the RNA-binding activity

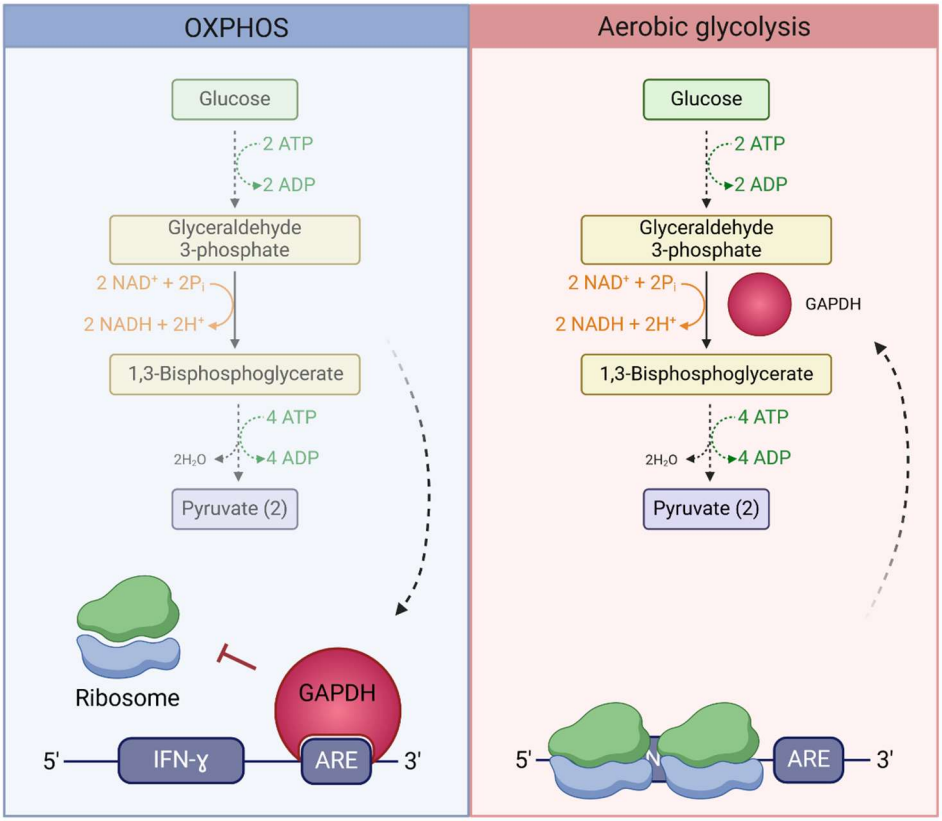

Figure 12. GAPDH regulates *IFN-γ* mRNA translation in T lymphocytes[102]. When T lymphocytes are in their active state, the cells are engaged in glycolysis and GAPDH is fully involved in its metabolic activity. In this context, *IFN-γ* mRNA is being translated and the cytokine produced. During T lymphocytes inactivation, cells switch their metabolism from glycolysis to OXPHOS. Now, GAPDH is not engaged in glycolysis and represses *IFN-γ* mRNA translation by its direct binding to the AREs found in the 3'UTR of the mRNA.

of GAPDH[99,130]. Clearly, more studies are needed to fully elucidate GAPDH-binding to RNA, and these studies must consider both subcellular localization of GAPDH and cellular context (e.g., metabolic, and redox status) to unravel all the features involved in the GAPDH-dependent regulation of gene expression, in addition to its well described role in glycolysis.

Phosphoglycerate kinase (PGK) 1

The GE PGK1 reversibly converts 1,3-BPG into 3-PG, generating ATP molecules. In 2001, this enzyme was proposed to be essential for *in vitro* mRNA synthesis of RNA virus genomes, such as the *Sendai* virus (*SeV*)[146]. However, its regulatory role on the transcription of the *SeV* genome was proposed to be dependent on protein-protein interactions with proteins from the transcription initiation complex and not by the direct interaction with the vRNA[146]. In contrast, gel shift assays and LC-MS analysis revealed that the chloroplast PGK directly bind to vRNAs *in vitro*, specifically at the 3' poly(A) tail of the *Bamboo mosaic virus* (*BaMV*) RNA. This binding was proposed to be

essential for the minus-strand RNA synthesis and efficient *BaMV* accumulation in plants[147,148]. Moreover, the chloroplast PGK binding to *BaMV* RNA was shown to mediate the localization of the vRNA to the chloroplast in an early stage of infection, which was shown to be necessary for efficient virus replication[147].

PGK was also shown to bind to RNA in yeast and in humans cell lines. Indeed, PGK1 was validated as part of both yeast and human HuH-7 mRNA interactome by photo-activatable crosslinking (PAR-CL) and CLIP (PNK assay), respectively[81]. The human PGK1 activity in mRNA-binding and post-transcriptional regulation has been further explored. Using conventional chromatography combined with gel mobility shift and northwestern assays, PGK1 was found to bind to the coding sequence (CDS) region of the *urokinase-type plasminogen activator receptor (uPAR*) mRNA in human bronchial epithelial (Beas2B) cells[113]. This finding was further validated *in vivo* by RIP-qPCR using both Beas2B and human lung carcinoma (H157) cells. The RNA-binding activity of PGK1 was proposed to be dependent on the phosphorylation of the enzyme[149], and its binding to the *uPAR* mRNA was shown to inhibit the transcript expression by regulating the destabilization of the mRNA. Indeed, *uPAR* mRNA was shown to degrade faster in H157 cells overexpressing PGK1[113]. This enzyme was later proposed to lower the stability of the *COX-2* mRNA in lung cancer cells by the interaction of its nucleotide-binding domain (NBD) with the CDS region of the *COX-2* mRNA[150]. The overexpression of PGK1 or its NBD was indeed demonstrated to reduce the mRNA stability and protein expression in lung cancer cells; however, the direct binding of PGK1 to the *COX-2* mRNA still remains to be determined[150].

Enolase

Enolase is a GE responsible for catalysing the interconversion between 2-PG and phosphoenolpyruvate (PEP). Together with PGK, this enzyme was proposed to be essential for the transcription of *SeV* RNA genome[151]. Although ENO1 was demonstrated to be part of the viral transcription initiation complex, its regulatory role on the transcription of the *SeV* genome was proposed to be dependent on its direct interaction with tubulin, another component of the complex, and not with the vRNA[151]. Similarly, enolase was identified as a component of the RNA degradosome complex from *E. coli* by protein-protein interactions with the C-terminal scaffold region of the ribonuclease E (RNase E)[152–155]. While the role of enolase in the *E. coli* degradosome still remains to be fully elucidated, the enzyme was proposed to regulate mRNA degradation according to the metabolic state of the cell. Indeed, degradation of the *ptsG* mRNA, which encodes the major glucose transporter in *E. coli*, was shown to be dependent on enolase[156]. Both removal of the scaffold region of RNase E and depletion of enolase suppressed the rapid degradation of *ptsG* mRNA in response to the metabolic (phosphosugar) stress[156].

One of the first reports of the direct binding of enolase to RNA demonstrated that this enzyme binds to tRNAs *in vitro* and *in vivo* using the yeast *S. cerevisiae*[157,158]. This binding was implicated in the tRNA targeting towards the mitochondrial outer membrane[158], and enolase 2 (Eno2p) was proposed to act as a tRNA chaperone inducing deep tRNA conformational changes[157]. Of note, *in vitro* assays also demonstrated that human enolases are also implicated in tRNA mitochondrial import by similar mechanisms[159]. Yeast α-enolase (Eno1p) was later shown to also bind to tRNAs using an adapted UV-crosslinking technique termed CRAC[160], which allowed for a stringent transcriptome-wide recovery of the RNAs in direct interaction with Eno1p. In fact, tRNAs corresponded to ~25% of the recovered RNAs, with a specific enrichment of cytoplasmic tRNAs over mitochondrial tRNAs. Interestingly, fluorescence-based mRNA-protein interaction assays in yeast demonstrated that Eno1p, along with other GEs, binds to its own mRNA and the mRNAs coding for other glycolytic proteins[119,120].

One of the first reports in mammals of ENO1's RNA-binding activity demonstrated that this enzyme could bind to CUG repeats containing transcripts[161]. ENO1 was isolated from L6 rat myoblasts using $(CUG)_{10}$ ssRNA probes and its RNA-binding activity was further verified by EMSA using radiolabelled RNA probes[161]. However, the biological relevance of these interactions, if any, remains to be elucidated. The human α-enolase (ENO1) was later demonstrated to interact with poly(A) RNA in HeLa cells using a dual fluorescence method and CLIP-Seq[3]. Similarly to its proposed role in *E. coli*, ENO1 was shown to promote the *iron regulatory protein 1* (*IRP1*) mRNA degradation in HCC cell lines[162]. IRP1 is an important metabolic enzyme involved in the iron homeostasis, and ENO1 was shown to directly bind to *IRP1* mRNA at the CpG-rich region present in the mRNA 5' UTR via its DNA-binding domain (DBD). Indeed, deletions of the ENO1's DBD domain or the CpG-rich region of the *IRP1* 5' UTR abolished the inhibitory effect of ENO1 on IRP1[162]. *IRP1*-ENO1 interaction allowed the recruitment of CNOT6, a member of the CCR4–NOT deadenylase complex, via its interaction with ENO1 C-terminal domain, whereby the nuclease (NU) domain of CNOT6 promotes the deadenylation of the IRP1-3' UTR and consequent degradation[162]. The suppression of the *IRP1* mRNA expression by ENO1 was then demonstrated to regulate the iron homeostasis and survival of HCC cells[162].

Recently, ENO1 was shown to not only bind to hundreds of cellular mRNAs by eCLIP, but also to have its enzymatic activity modulated by the binding to some of them[20]. The RNA regulation of ENO1, also known as riboregulation[4], was demonstrated to specifically inhibit ENO1's enzymatic activity both *in vitro* and *in vivo*, and in a competitive-manner with the enzyme's glycolytic substrates (2-PG and PEP)[20]. Interestingly, post-translational lysine modifications, particularly the acetylation of ENO1's K89 amino acid, was shown to increase the enzyme's RNA-binding activity. In contrast, deletion of K343 generated an ENO1 mutant with decreased binding to RNA[20]. ENO1 interaction with RNA was further implicated in the rewiring of the

metabolism of cultured human cells and mouse embryonic stem cells (mESCs). Indeed, this binding was shown to diminish glycolysis, specifically altering glycolytic metabolite levels and serine synthesis[20].

To explore the biological relevance of the RNA-ENO1 interaction, the inhibitory effect on the enzyme activity was evaluated in mESCs. During stem cell differentiation, the metabolism of the cells was demonstrated to shift from glycolysis to OXPHOS. Concomitantly to this shift, both acetylation levels and RNA-binding activity of ENO1 increased[20]. Stem cells expressing ENO1's RNA-binding mutants displayed impaired germ layer differentiation. Indeed, mESCs expressing the ENO1 mutant with increased RNA-binding activity, therefore hyper-inhibited by RNA, showed a defective differentiating toward the definitive endoderm and neuroectoderm, phenocopying differentiating ENO1-depleted mESCs[20]. In contrast, mESCs expressing the ENO1 mutant with decreased RNA-binding activity, where ENO1's enzymatic activity escapes riboregulation, showed an increased differentiation toward the definitive endoderm[20]. Taken together, these findings uncover a new regulatory mechanism of stem cell differentiation through ENO1's riboregulation, especially for the formation of the endodermal germ layer[20]. Structural studies, however, are still needed to elucidate how ENO1's binding to RNA inhibits its catalytic function and how acetylation controls this binding, in addition to determine whether other post-translational modifications contribute to ENO1-RNA interaction.

The pyruvate kinase M (PKM)

PKM is a GE that catalyses the conversion of PEP to pyruvate by the transfer of a phosphate from PEP to the adenosine diphosphate (ADP)[163]. This enzyme has been constantly reported to bind RNA, particularly the M2 isoform (PKM2). Indeed, several studies have shown that PKM can bind to both coding and non-coding RNAs. In 2012, Castello *et al.* ([3]) demonstrated that PKM2 interaction with poly(A) RNA in cells using a dual fluorescence method, which brought into question the role of this protein in gene expression regulation. Recently, two independent studies reported the non-canonical RBP activity of PKM on the regulation of mRNA translation[114,164]. To identify possible PKM-associated RNAs *in vivo*, iCLIP analyses on endogenous PKM tagged with FLAG HA in mESCs was performed[164]. This analysis revealed that PKM binds to two major classes of RNAs: ribosomal RNAs (rRNAs) (29% of reads) and protein coding RNAs (23% of reads), with enrichment at 3'UTRs and CDSs of mRNAs[164]. Moreover, PKM was found to interacts with ER-associated ribosomes, functioning as an RBP in the translation of ER-destined mRNAs[164]. Next, ribosome profiling revealed that the most enriched PKM2 mRNA targets exhibited the greatest decrease in translational efficiency upon PKM2 knockdown. In other words, ribosome occupancy of PKM2-bound mRNAs was lower in PKM2-depleted cells compared to the control cells[164]. These results suggested that PKM2 acts as a translational activator of its direct,

physiological mRNA targets. In human cell lines, PKM was found to associate with cytosolic polysomes in a poly-ADP ribosylation dependent manner and influence mRNA translation[114]. Of note, other GEs (ENO1 and GAPDH) were found associated to cytosolic polysomes. In contrast to the previous study[164], PKM moonlighting activity induced translational stalling. It was found through eCLIP that PKM binds primarily to the CDS of mRNAs, particularly in the downstream of regions that encode lysine- and glutamate-enriched tracts[114]. Interestingly, ribosome footprint revealed translational stalling near these sequences, and this event was shown to be dependent on the recruitment of PKM to ribosomes in a poly-ADP ribosylation dependent manner. However, current data is insufficient to conclude whether PKM stalls translation in cis (by binding to the ribosome) or in trans (neighbouring ribosomes)[114].

The binding of PKM to RNA, however, is not restricted to protein coding RNAs or rRNAs. Several reports have demonstrated that PKM2 also directly interacts with lncRNAs which, in turn, can modulate the protein activity, stability and localization. For example, while the lncRNA *FEZ family zinc finger 1-antisense transcript 1* (*FEZF1-AS1*) was shown to bind to PKM2 and increase the enzyme stability in both nucleus and cytoplasm in colorectal cancer[165], the binding of the exosomal lncRNA *HOTAIR* protected PKM2 against ubiquitination degradation in colorectal cancer[166]. Another recent example demonstrated that the lncRNA *VAL* strengthens the enzymatic activity of PKM2 through directly binding, protecting PKM2 against Parkin-induced polyubiquitination in gastric cancer[167].

Lactate dehydrogenase (LDH)

LDH is the last enzyme in the glycolytic pathway, and it catalyses the conversion of pyruvate to lactate using NAD+ as cofactor. This enzyme exists as homo- or heterotetramers, and it consists of the combination of two different subunits: A (or M) and B (or H). Although LDH has been recurrently identified as an RBP in large-scale RBPome studies, little is known about its RNA-binding activity. Nonetheless, LDH was shown to harbour a di-nucleotide binding domain (Rossmann fold), which has been proposed to mediate RNA-binding[93,96–99]. Moreover, LDHA was identified to selectively bind to the AREs present in the 3′-UTR of the *GM-CSF* mRNA in murine erythroleukemia cells using both UV crosslinking and nitrocellulose filter binding assays[168], being therefore classified as an AUBP. Incubation of purified LDHA with NAD+ inhibited the AU-binding activity in a concentration-dependent manner, indicating that the enzyme binds to AREs of the *GM-CSF* mRNA through the Rossmann fold[168]. Interestingly, LDHA was also found associated to polysomes of human lymphoid and monocytic cells using discontinuous (10–40%) sucrose density gradient analysis, and this association was shown to be dependent on RNA[168]. However, its direct association with actively translated mRNAs and its role in post-transcriptional gene regulation remains to be demonstrated. Recently, LDHA was shown to form non-

covalent complexes (metabolons) with other glycolytic enzymes (PGK1, PGAM1, ENO1, and PKM2) by its interaction with RNA in cancer cells[169]. A c-Myc-responsive lncRNA termed as *glycoLINC* (*gLINC*). *gLINC* was shown to be essential for the formation of these metabolons, and all the mentioned glycolytic enzymes, except PGAM1, were shown to direct bind to this lncRNA. *gLINC* acts as a backbone for the metabolon formation, resulting in enhanced catalytic efficiency[169]. The formation of this multi-enzyme complex was thus shown to enhance the glycolytic flux, increase ATP and lactate production, as well as promote cell survival under serine deprivation[169]. The regulatory control of *gLINC* over PGK1, ENO1, and PKM2, and LDHA through RNA-protein interactions emerges as another example of riboregulation of metabolic enzymes.

In summary, GEs have emerged as critical regulators of post-transcriptional gene expression, revealing unexpected functions beyond their canonical metabolic roles[104]. These enzymes have been shown to interact with RNA, influencing processes such as RNA stability, localization, translation, and degradation. Additionally, several reports demonstrate that some of these RNA-enzyme interactions can be regulated by glycolytic substrates, metabolites, and cellular metabolic states, suggesting the existence of a sophisticated link between metabolism and gene regulation to directly control gene expression[20,96–98,130,131,168]. Strikingly, direct and specific binding of RNAs was also shown to regulate GEs activity, stability, interaction and localization[20,165–167,169]. The discovery of these moonlighting activities not only expands our understanding of glycolytic enzymes but also provides new perspectives on the integration of metabolic and gene regulatory networks.

1.2.1.2 OTHER METABOLIC ENZYMES

Glycolytic enzymes are not the only metabolic proteins that have been identified as unconventional RBPs. In fact, numerous enzymes involved in other classic metabolic pathways have also been repeatedly identified as RNA binders in RNA interactome studies, once more suggesting the existence of extensive interconnections between gene regulation and metabolism[81]. Many of these enzymes, including aconitases, enzymes of the TCA cycle/OXPHOS, fatty acid metabolism, thymidylate synthesis cycle, among others[170], have been validated to directly bind RNA and to regulate the RNA fate. In some instances, this binding has also been shown to regulate the enzyme stability and function[171,172]. Examples of metabolic enzymes outside of the glucose metabolism moonlighting as RBPs are described below.

Aconitase 1 (ACO1/IRP1)

ACO1, also known as IRP1, is one of the best examples of RNA-binding metabolic enzymes whose interaction with the binding site of its RNA targets is regulated by metabolic signals[170]. To be active as a cytosolic aconitase, ACO1 requires the binding of a tetranuclear iron–sulfur cluster (cubane-type; 4Fe-4S) in its active site, which prevents its association with RNA[173]. Indeed, the aconitase and RNA-binding activities are mutually exclusive, meaning that ACO1 can only associate with RNAs when the intracellular levels of iron are scarce, therefore while the iron clusters are disassembled[174]. The loss of 4Fe-4S was then shown to allow for the binding of the enzyme to mRNAs containing iron-responsive elements (IREs) in their UTRs. IREs are RNA stem loop structures found, for example, in the 5'UTR of the *ferritin* mRNA[175,176] and in the 3' UTR of *transferrin receptor* (*TfR1*) mRNA[177,178]. These structures have also been found in other mRNAs, particularly those encoding proteins involved in the iron homeostasis and related processes[101,179,180]. Therefore, ACO1 has been shown to specifically bind to IREs of mRNAs in iron-deficient cells, and this binding was shown to block mRNA translation or to induce mRNA stabilization (Figure 13).

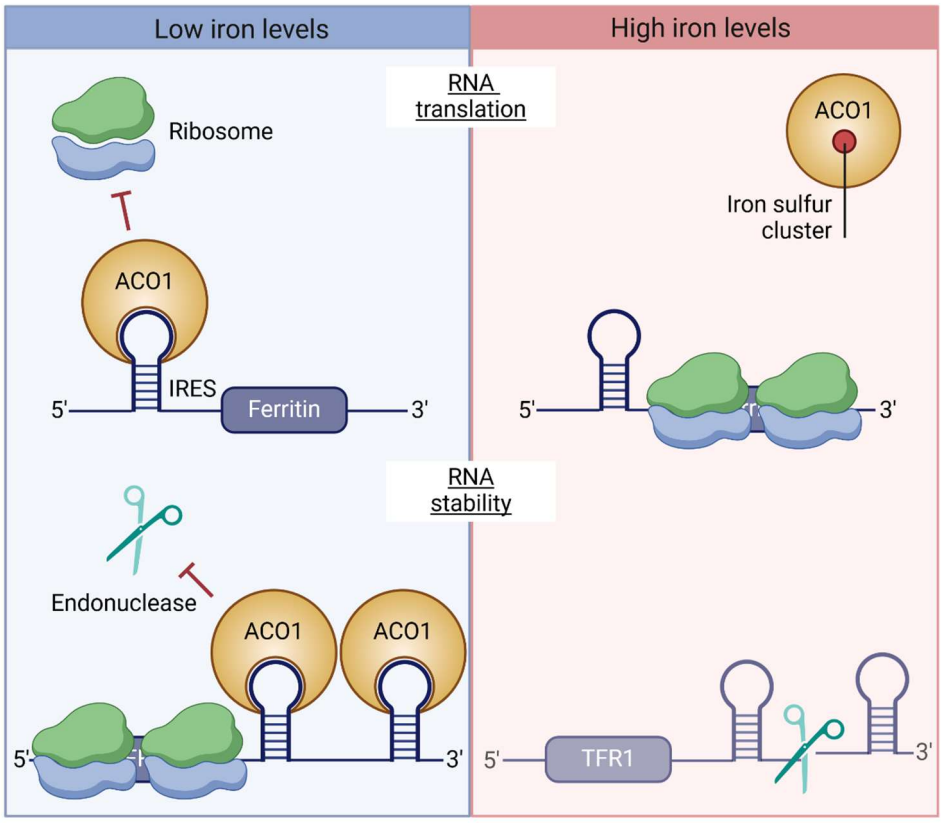

Figure 13. ACO1 functions as a cytosolic aconitase and as an RBP. In low intracellular iron levels, ACO1, also known as IRP1, binds mRNAs that encode cellular factors involved in iron homeostasis, thereby regulating their fate. Among the best-studied examples is the binding of ACO1 to the IRES in the ferritin and TFR1 mRNAs. ACO1 binds to the IRES in the 5'UTR of the ferritin mRNA to repress its translation[175,176]. In contrast, binding of ACO1 to IREs in the 3' UTR of the TFR1 mRNA increases the stability of the mRNA and, consequently, translation[177,178]. In high iron levels, the iron–sulfur cluster is synthesized, and ACO1 is no longer binding RNA. In this context ACO1 assembles with the iron–sulfur cluster to catalyse the interconversion between citrate and isocitrate. Adapted from Castello *et al.*, 2015

(ref [174]).

Among the best-studied examples, binding of ACO1 to the IRE present in the 5'UTR of the *ferritin* mRNA was shown to repress the mRNA translation by preventing the assemble of the small ribosomal subunit (43S preinitiation complex) with the mRNA even in the presence of the cap binding complex eIF4F[175,176]. The *ferritin* mRNA encodes for an iron-storage protein; therefore, this decreased in the protein expression was shown to not only diminished the intracellular ferritin levels, but also promote an increase of free iron. In contrast, the binding of ACO1 to the IREs in the 3' UTR of the *TfR* mRNA was shown to increase the mRNA stability, therefore promoting cellular iron uptake[177,178]. However, in instances when the intracellular iron concentration is high, the 4Fe–4S cluster is assemble. ACO1 then bears this cluster and becomes active as an aconitase, catalysing the conversion of citrate into isocitrate. Thus, the translation of the *ferritin* mRNA is resumed[175,176], while the half-life of the *TfR* mRNA is shorten by endonucleolytic cleavage[177,178]. By these means, ACO1 presents itself as a crucial post-transcriptional regulator of the expression of genes involved in the maintenance of appropriate intracellular iron levels by increasing iron uptake and decreasing iron storage, utilization and export[173,181].

Malate dehydrogenase (MDH)

MDH has recurrently been identified to interact with RNAs in large-scale RNA interactome studies. Together, the cytosolic and mitochondrial isoforms of MDH (MDH1 and MDH2, respectively) are responsible for part of the malate aspartate shuttle by transporting metabolites and reducing equivalents across the mitochondrial membrane, thus supporting the preservation of the cellular redox state across the cytosolic and mitochondrial compartments[182]. MDH2 catalyses the interconversion of malate to oxaloacetate with the reduction of NAD+ to NADH. This enzyme has been implicated in the post-transcriptional regulation of *SCN1A* and *SCN3A* mRNA by binding to their 3'UTR in HEK293 cells[183]. As for GAPDH[133], MDH2 overexpression decreased *SCN1A* gene expression by affecting mRNA stability under seizure condition. Additionally, MDH2 has been reported to be stabilized by the lncRNA *AC020978* binding, consequently promoting non-small cell lung cancer progression[172], and to regulate TCA cycle by binding to the lncRNA *GAS5* in response to cellular stress, which led to the disruption of the 'MDH2-fumarate hydratase-citrate synthase' metabolon complex[171]. Recently, eCLIP was employed in Huh7 cells to analyse the MDH2's RNA-binding properties and to determine the scope of RNAs bound by MDH2[182]. Strikingly, a major proportion of the RNAs identified as MDH2 targets were RNAs expressed outside of the mitochondria (cytosolic RNAs), particularly tRNAs[182]. This is in accordance with studies in yeast showing that the yeast MDH2 acts as an RBP that predominantly binds to small RNAs[184], as well as the tRNA-binding activity of GAPDH, another NAD-dependent dehydrogenase. In addition, MDH2 was shown to

preferentially bind to RNAs in the cytosol, and the RNA-enzyme interactions were shown to respond to modulations in NAD+ levels[182].

Mitochondrial 3-hydroxyacyl-CoA dehydrogenase type 2 (HSD17B10)

HSD17B10 is a mitochondrial enzyme involved in the oxidation of isoleucine, metabolism of xenobiotics, branched-chain fatty acids, sex hormones and neuroactive steroids[185]. This enzyme was found as a component of the mitochondrial RNase P complex[186], a complex required to processes mitochondrial tRNAs, being later identified to directly bind RNA[81]. iCLIP data revealed that HSD17B10 binds to mitochondrial tRNAs, preferentially at 5′ ends, and regions of D-loop, D-stem, anticodon stem and other loop regions[81]. Mutations in this enzyme, particularly the mutation R130C, have been associated with classical cardiomyopathy and neuropathy phenotypes[187]. Interestingly, iCLIP data also reviewed that HSD17B10 bearing the mutation R130C displays reduced RNA-binding abilities[81], suggesting that dysfunctional association of HSD17B10 with RNA might contributes to the phenotype of these diseases.

Serine hydroxymethyltransferase (SHMT)

The human SHMT is an enzyme of the one-carbon metabolism, being in the intersection of the amino acid and folic acid metabolic pathways. This enzyme catalyses the transfer of one-carbon units from serine to tetrahydrofolate (THF), generating glycine and 5,10-methylene-THF (CH2-THF). Besides their canonical metabolic role, both cytosolic and mitochondrial isoforms of SHMT (SHM1 and SHM2, respectively) have been shown to specifically bind to poly(A) RNAs[3,88]. In 2012, Castello *et al.* ([3]) applied a dual fluorescence method and CLIP-Seq analysis in HeLa cells, revealing that SHMT2 binds to specific and distinct subsets of mRNAs. And, as expected from a *bona fide* RBP, SHMT2 was also found enriched in RNA interactome eluate samples of HeLa cells upon conventional UV crosslinking (cCL) and PAR-CL, being undetectable in western blot analysis of control eluates (nonirradiated cells) using antibodies against SHMT2[88]. Regarding SHMT1, the first evidence of its RNA-binding activity emerged in 2000, when Liu *et al.* ([188]) demonstrated that the human SHMT could bind to the 5′UTR of its own mRNA *in vitro*, regardless of the presence or absence of its substrates. Additionally, *in vitro* translation of the *SHMT1* 5′UTR was inhibited by the presence of the enzyme, and this inhibition was also shown to occur independently of the amino acid and folate substrate binding to the SHMT1 enzyme[188].

Previous reports have demonstrated that some metabolic enzymes are able to bind to their own mRNAs and other mRNAs encoding proteins of related metabolic pathways[118–120]. In this context, SHMT1 was shown to not only bind to its mRNA[188], but also to the mRNA encoding its mitochondrial counterpart[189]. SHMT1 was shown to

control the expression of SHMT2 by binding to the *SHMT2* 5'UTR[189]. In contrast to the binding of the enzyme to the *SHMT1* mRNA, binding to *SHMT2* 5'UTR was modulated by metabolites *in vitro*. Strikingly, the formation of the *SHMT2* 5'UTR-SHMT1 complex was shown to inhibit the serine cleavage activity of the enzyme *in vitro* and in H1299 lung cancer cells[189]. Together, these results suggest a potential mechanism of SHMT control, with the involvement of regulatory links between the enzyme, metabolites and RNAs for the control of the serine metabolism between the cytosolic and mitochondrial compartments.

In conclusion, the moonlighting role of metabolic enzymes in the regulation of post-transcriptional gene expression underscores a sophisticated interplay between metabolism and gene regulation[105]. These enzymes, traditionally recognized for their catalytic functions within metabolic pathways, have emerged as vital players in RNA binding and post-transcriptional control[81]. This dual functionality not only highlights the versatility and complexity of cellular processes, but also opens new avenues for understanding how metabolic states can influence gene expression[105]. Future research into these multifaceted roles will likely reveal deeper insights into cellular regulation, with potential implications for therapeutic strategies targeting metabolic and gene regulatory pathways.

1.3 mRNA TRANSLATION

Translation is a process in which proteins are synthesized by the decoding of the genetic information stored in mRNA molecules. These molecules exist as intermediates between genetic information (DNA) and cellular 'workhorses' (proteins), being therefore highly regulated by a variety of RNA-processing reactions in eukaryotic cells[2]. It is vital that the genetic information stored in the mRNAs is properly translated, since both cell fate and function depend on the protein sequence, composition and abundance. Experimental evidence has shown that translation can be highly heterogeneous[2,190], which is supported by studies indicating that mRNA and protein concentrations correlate poorly[191,192]. The mRNA translation can not only differ within the cells/tissues of origin, but also depends on the genes they derived from. In fact, even different gene isoforms can show translational heterogeneity[190]. The control of mRNA translation relies on the involvement of many different features, including cis-regulatory elements (e.g., heterogeneity in primary mRNA sequence, RNA modifications and structure) and the coordinated action of trans-acting factors (e.g., translation initiation factors and RBPs)[190,193]. Since translation is the final step of protein synthesis, its regulation allows for immediate changes in the protein levels of both global and specific mRNAs, being therefore more advantageous for cells than other layers of manipulation.

Translational control allows cells to promptly and dynamically adapt to a variety of stimuli (e.g., aberrant oncogenic signalling, and environmental and intracellular stresses) as an attempt to create favourable conditions to survive[194]. During stress, cells attenuate their global mRNA translation to reduce the expensive energetic cost of the process, and to prioritize the translation of stress-responsive mRNAs[194]. Of note, around 50-75% of a cell's total energy goes to protein synthesis[195,196]. It is thus unsurprising that an efficient regulation of mRNA translation is vital for an appropriate control of gene expression and, consequently, to maintain cell homeostasis. In fact, dysregulation in the translational control has been appointed as a critical factor for the emergence of several disorders, including cancer, neurodegenerative diseases and metabolic disorders[2,197]. These findings underscore the importance of a deeper knowledge on the mechanisms involved in mRNA translation and its rewiring by cancer cells, besides understanding the features involved in the regulation of mRNA biogenesis and function[2,197].

1.3.1 OVERVIEW OF THE mRNA TRANSLATION PROCESS

Translation is the last major regulatory step of gene expression, being therefore one of the most important processes in cells. This process involves a coordinated interplay between tRNAs, ribosomes, translation factors, and amino acids to decode mature mRNAs and synthesize correspondent proteins[194,197]. The mRNA translation process

can be divided into four stages: 1) initiation, the most tightly regulated step; 2) elongation; 3) termination; and 4) ribosome recycling (Figure 14).

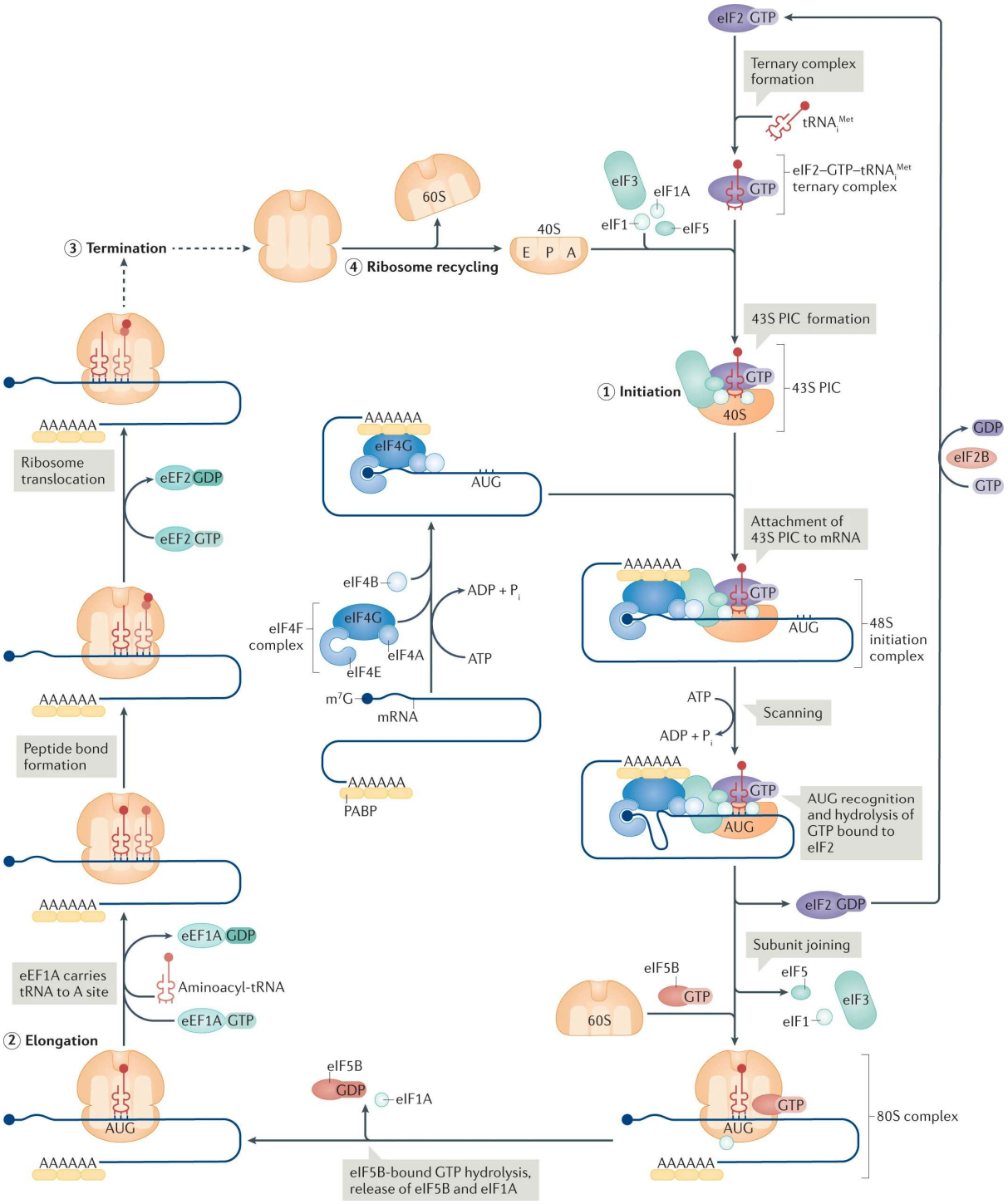

Figure 14. Cap-dependent translation process of eukaryotic mRNAs. Schematic representation of the four stages of cap-dependent mRNA translation: (1) initiation, (2) elongation, (3) termination, and (4) ribosome recycling. (1) Initiation of the cap-dependent mRNA translation involves the formation of the 43S pre-initiation complex (PIC), and its recruitment to the 7-methylguanosine (m7G) cap located at the 5'UTR of mRNAs in an eIF4F dependent-manner. This recruitment leads to the assembly of the 48S initiation complex[193,194]. The 48S initiation complex then scans the mRNA 5'UTR until it recognizes

the first start codon (AUG), triggering the recruitment of the 60S ribosomal subunit and the formation of a functional 80S complex. The elongation step of protein synthesis (2) begins with the decoding of the first three nucleotides (codon) after the start codon by the binding of the corresponding activated amino acid tRNA into the A-site of the ribosome. Then, the ribosome mediates the formation of a peptide bond between both tRNAs, which is followed by ribosome translocation[190,198]. This process is repeated continuously to proper synthesize the polypeptide chain, and it is terminated (3) once a stop codon enters the ribosome A-site. After translation termination, the ribosomes dissociate from the mRNA, and its subunits are recycled (4) for the translation of other mRNAs[194,198]. From Fabbri *et al.*, 2021 (ref [194]).

The translation initiation stage involves the assembly of the ribosome and (eukaryotic) translation initiation factors ((e)IFs). The majority of the total eukaryotic cellular mRNAs, likely 95–97%, are translated via the cap-dependent pathway[199]. Of note, cap-independent translation of mRNAs is commonly explained by the use IRESs; however, this mechanism cannot always be explained by the IRES concept[200]. In the cap-dependent pathway, translation initiation requires the assembly of the eIF4F complex on the m^7G cap located at the 5′UTR of the mRNAs, which also interacts with the poly(A) tail-binding protein (PABP) bound to the 3′ poly(A) end of the mRNAs[193,194]. The eIF4F complex is composed by the RNA helicase eIF4A, which unwinds the RNA into a single strand through eIF4B, the cap-binding protein eIF4E and the scaffolding protein eIF4G, that interacts with PABP. After the assemble of the translation initiation complex, another complex termed 43S pre-initiation complex (43S PIC) , is recruited to the capped mRNA by the mediation of eIF4F to form the 48S initiation complex[193,194]. Of note, the 43S PIC is composed by the 40S small ribosomal subunit, the GTP–bound eIF2 and the initiator methionyl-tRNAi ($tRNA_i^{Me}$) (eIF2-GTP- $tRNA_i^{Me}$ ternary complex), and eIF3, eIF1, eIF1A and eIF5. After its assembly to the 5′ end of the mRNA, the 48S initiation complex scans the 5′ UTR (from 5′ to 3′) until it recognizes the first start codon (AUG), that enters the ribosomal peptidyl (P) site via $tRNA_i^{Me}$. Meanwhile, the GTP bound to eIF2 is hydrolysed, leading to the release of eIF2-GDP and other initiation factors, such as eIF1, eIF3 and eIF5. This triggers the recruitment of the 60S ribosomal subunit and eIF5B-bound GTP to the 48S initiation complex, forming an 80S complex. The GTP bound to eIF5B is then hydrolysed, leading to the release of eIF5B–GDP and eIF1A. The 80S complex is now functional and ready to progress into the elongation stage of protein synthesis[193,194].

It is during the elongation stage of the translation process that the polypeptide chain is synthetized. At this stage, the open reading frame (ORF) of the mRNA sequence is decoded in steps of three nucleotides (one codon) to synthesize each amino acid. With the $tRNA_i^{Me}$ bound to the P-site of the 80S complex, a new activated amino acid (aa-tRNA) is selected and bound to the ribosomal aminoacyl (A) site just downstream of the first start codon through base-pairing between the codon in the mRNA and the aa-tRNA anticodon[198]. Then, the ribosome catalyses the formation of a first peptide bond by the transfer of the methionyl group from its tRNA to the amino group of the newly bound aa-tRNA at the A-site, respectively resulting in a deacylated-tRNA and a peptidyl-tRNA. Both tRNAs and the mRNA move along the ribosome in a process

termed as translocation. Now, the peptidyl-tRNA is bound to the P-site, and a new aa-tRNA binds the next mRNA codon in the A-site[190,198]. This process occurs repeatedly in order to synthesize the correct amino acid sequence in the peptide chain, and with the help of elongation factors (e.g., eEF1A, for codon decoding; and eEF2, for ribosome translocation) that transiently associate with the other elements involved in the process. Once the ribosome encounters a stop codon (UGA, UAA or UAG) in the mRNA at the A-site, translation is terminated, the tRNAs are released and the ribosomal subunits are dissociated from the mRNA and recycled for further use in the translation of other mRNAs, a process called ribosome recycling[194,198].

1.3.2 Approaches to study mRNA translation

With the increasing availability of high-throughput transcriptomic[201] and proteomic[202] analyses, growing evidence reports discrepancies between mRNA and protein concentrations[191,192], particularly in tumors[203]. This suggests that mRNA levels alone are not sufficient to fully explain cell behaviour, and that post-transcriptional mechanisms, including those regulating mRNA translation, are also required for the control of cell function[203]. Indeed, along with the overall quantification of mRNAs or proteins in cells, there is significant interest in studying the dynamics of protein synthesis[204]. The past decades have witnessed the rapid development of experimental technologies to study translation and its regulators. Indeed, translation can be affected by various factors, including well-recognized players, such as RBPs and factors of the translation initiation complex, as well as novel players, such as mRNA post-transcriptional modifications and non-coding RNAs[193]. Several techniques, such as polysome[205] and ribosome profilings[206,207], have been developed to investigate changes in protein translation levels, allowing for the study of the potential molecular mechanism of mRNA translation dysregulation in tumor biology[193,208].

Translation assays in living cells provide valuable insights into the dynamics of mRNA translation. In order to study translational dynamics in real time and in individual cells, both mRNA and nascent peptide chains can be labelled for live cell imaging[204,209]; however, methods that depend on this strategy often suffer from high image background intensity, offering a low signal-to-noise ratio[209]. To overcome these challenges, many methods have explored other strategies to improve mRNA labelling, including chemically labelled synthetic probes or aptamers[204,210], and incorporation of fluorescently labelled dUTP into nascent mRNA[210]. However, the dyes used for labelling, although offered low background intensity, were not easily permeabilized into cells[204]. Another simple strategy to measure translation levels in cells relies on the direct detection of nascent peptides. For this aim, the antibiotic puromycin is commonly used[204]. The structure of this antibiotic is similar to the tyrosyl-tRNA, enabling puromycin to bind to the nascent peptide chains at their C-terminal regions during translation near the ribosomal peptidyl transferase centre (PTC), a region

responsible for peptide bond formation and peptide release[211]. By taking advantage of the mechanism of action of puromycin in cells, various methods to detect novel peptide chains have been developed, such as The Surface Sensing of translation (SUnSET) assay[212], which relies on the use of puromycin antibodies to measure the global amount of nascent polypeptide chains, as well as other assays developed to detect the translation of a specific mRNAs, such as puromycin-based PLA assays (Puro-PLA)[213]. Although many methods exist to study translational dynamics using cell imaging, it is important to recognize that there is still significant room for improvement, especially as advancements in microscopy techniques continue to enhance data resolution.

During protein synthesis, multiple ribosomes can be bound to mRNAs forming polysomes. Many methods have been developed for the study of translation based on the association of mRNAs and ribosomes (Figure 15). The most used method to study is termed as Polysome Profiling[205] (Figure 15A). In this assay, the first step to analyse the mRNA translation rate in cells or tissues is the separation of the mRNAs that are being translated from those that are not being translated based on their association with polysomes. And this can be achieved by the use of sucrose density gradient ultracentrifugation[214]. Then, the sucrose gradient can be fractionated and the RNA from the fractions purified. Finally, the mRNA translation levels can be analysed by RT-PCR analysis of ribosome-bound mRNAs or through high-throughput sequencing[215]. Although polysome profiling has many advantages (e.g., assessment of global and specific changes in the translatome; accurate measurement of translation efficiency based on measures of ribosome density on mRNAs; etc), it still is a very labour intensive method that requires specialized equipment and large amounts of starting material, besides not providing individual nucleotide resolution[195]. Another widely used method to analyse the extent of protein translation is Ribosome Profiling[206,207] (Figure 15B). This approach has been used to investigate mRNA translation at multiple levels of regulation, including at translation initiation, elongation and arrest, being able to measure translation efficiency, and to identify codon bias and new reading frames[216]. Ribosome profiling start with the cell lysis and treatment with RNase[217]. Then, the ribosome-bound mRNA fragments are isolated and used to generate an RNA database (cDNA library), which is followed by high-throughput sequencing and analysis. However, as for the polysome profiling, this method also has its disadvantages, such as by being labour intensive and by requiring a large amount of starting material[195].

Antibiotics are frequently used in translation studies, and their selection is based on their impact on the translation process and on their binding position on the ribosome[218]. Cycloheximide (CHX), for example, is the most used antibiotic, and it has been shown to block the elongation stage of the translation process by binding to the Exit (E)-site of the 60S large ribosomal subunit, thereby blocking the movement of tRNAs in ribosomes[219]. Therefore, the use of antibiotics in ribosome-based experiments can potentially introduce variations in the results. For example, while CHX

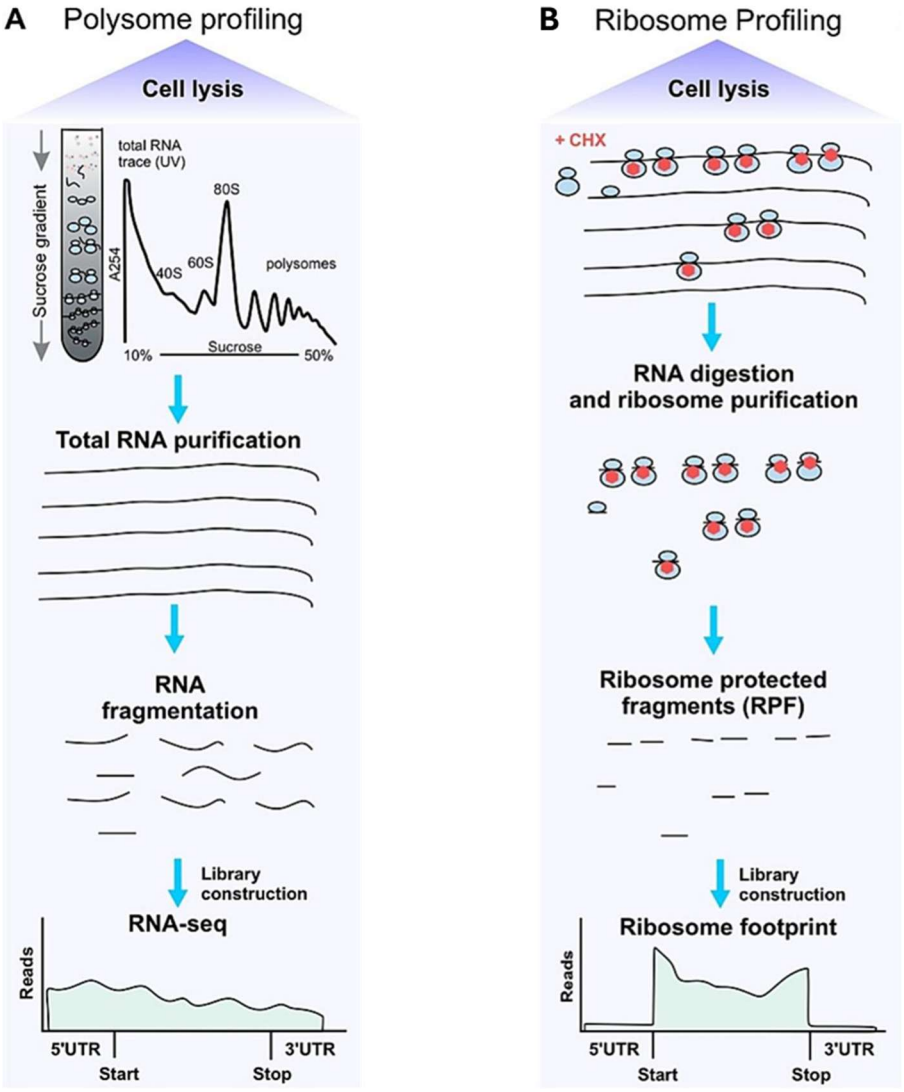

Figure 15. Ribosome-based strategies to study mRNA translation. (**A**) Polysome profiling. After cell lysis, cells are subjected to sucrose density gradient ultracentrifugation. The RNA is purified and prepared for high-throughput sequencing and analyses. (**B**) Ribosome profiling. After cell lysis, ribosome-bound mRNA is purified and partially digested upon RNase treatment. Ribosome protected fragments are used for the preparation of libraries for high-throughput sequencing and analyses. In both strategies, cells are often treated with CHX to stabilize mRNA-ribosomes interactions. Adapted from Zhang *et al.*, 2024 (ref [204]).

might block the translational elongation step during the experiments, it does not prevent translational initiation and termination. Thus, the use of CHX may lead to an accumulation of translation initiation events, and a partial decrease in translation termination[218]. In addition, different antibiotics can exhibit different translation inhibition rates. Therefore, these events cannot be entirely disregarded when interpreting the result of the ribosome-based experiments.

In order to study local mRNA translation, different methods have been developed, including the proximity-specific ribosome profiling[220,221]. In this assay, BirA, an *E. coli* biotin ligase, is fused to an organelle localization protein. When in close proximity to ribosomes targeted with AviTag peptide, BirA can covalently attach biotin to the AviTag

on the ribosomal protein[222,223]. By combining this approach with ribosome profiling, the biotin-labelled ribosomes can be purified using streptavidin beads and thereby detecting translation in specific regions (mitochondria, endoplasmic reticulum) of the cell[222,224]. Other methodologies have been applied to study the mitochondrial translation system, including the use of antibodies to enrich labelled mitochondrial ribosomal proteins[225], and by using sucrose density gradient centrifugation to isolate mitochondrial ribosomes from cytoplasmic ribosomes based on their distinct sedimentation coefficients[225–227]. These techniques can potentially broad the knowledge on the regulatory network governing the mitochondrial translation system.

In the past few years, mass spectrometry proteomics has become a powerful tool for investigating dynamic changes in protein synthesis and identifying key regulatory players[208]. Techniques like SILAC and click-reactive amino acids/puromycin labelling allow for the assessment of protein synthesis and degradation. Mass spectrometry can compare protein levels between healthy and diseased cells, revealing translation defects[228]. Additionally, chemical labelling and pulse-chase assays track protein synthesis kinetics, uncovering abnormalities in translation disorders[229]. Integrating mass spectrometry with other omics approaches may enhance our understanding of protein translation dysregulation[208]. Continued advancements in this technology will further unravel the complex mechanisms involved in translational dysregulation.

1.3.3 Mechanisms of translational control

Translation of mRNAs into proteins mediates the formation of cellular proteomes through the decoding of genomic information. Many mechanisms have been described to regulate translation, and they can be divided into two main modes of control: global and specific control. In the global mode of control, translational control is applied to most of the cellular mRNAs. In contrast, mRNA-specific control can be envisaged as the translational control of a defined set of mRNAs, without generally affecting the translation of the whole cellular transcriptome[230]. While global regulation relies mainly on the modulation of translation initiation factors, mRNA-specific regulation is performed via the recognition by regulatory complexes (*trans*-acting factors) of elements found in the target mRNAs (*cis*-regulatory elements) or by performing local regulation of translation. *Cis*-regulatory elements include regulatory sequences and structural features within the mRNAs. These elements are involved in the control of mRNA translation, particularly in the translation initiation step. Interestingly, transcript isoforms originated from the same genes frequently present different translation rates, which can be explained by the inclusion or exclusion of specific regulatory sequences and structures, post-transcriptional modifications or usage of variable transcription start sites[190]. The control of mRNA translation is, in fact, performed by trans-acting factors, such as ncRNAs, RBPs, ribosomal proteins and translation initiation factors, among others, that interact with the *cis*-regulatory

elements present in the mRNAs to promote or inhibit their translation. Both *trans*-acting factors and *cis*-regulatory elements can be selectively rewired as a response to microenvironmental stresses and oncogenic signalling pathways. Indeed, several aspects of translational control are remodelled to define more selective stress-response/oncogenic proteomes (Figure 16)[194].

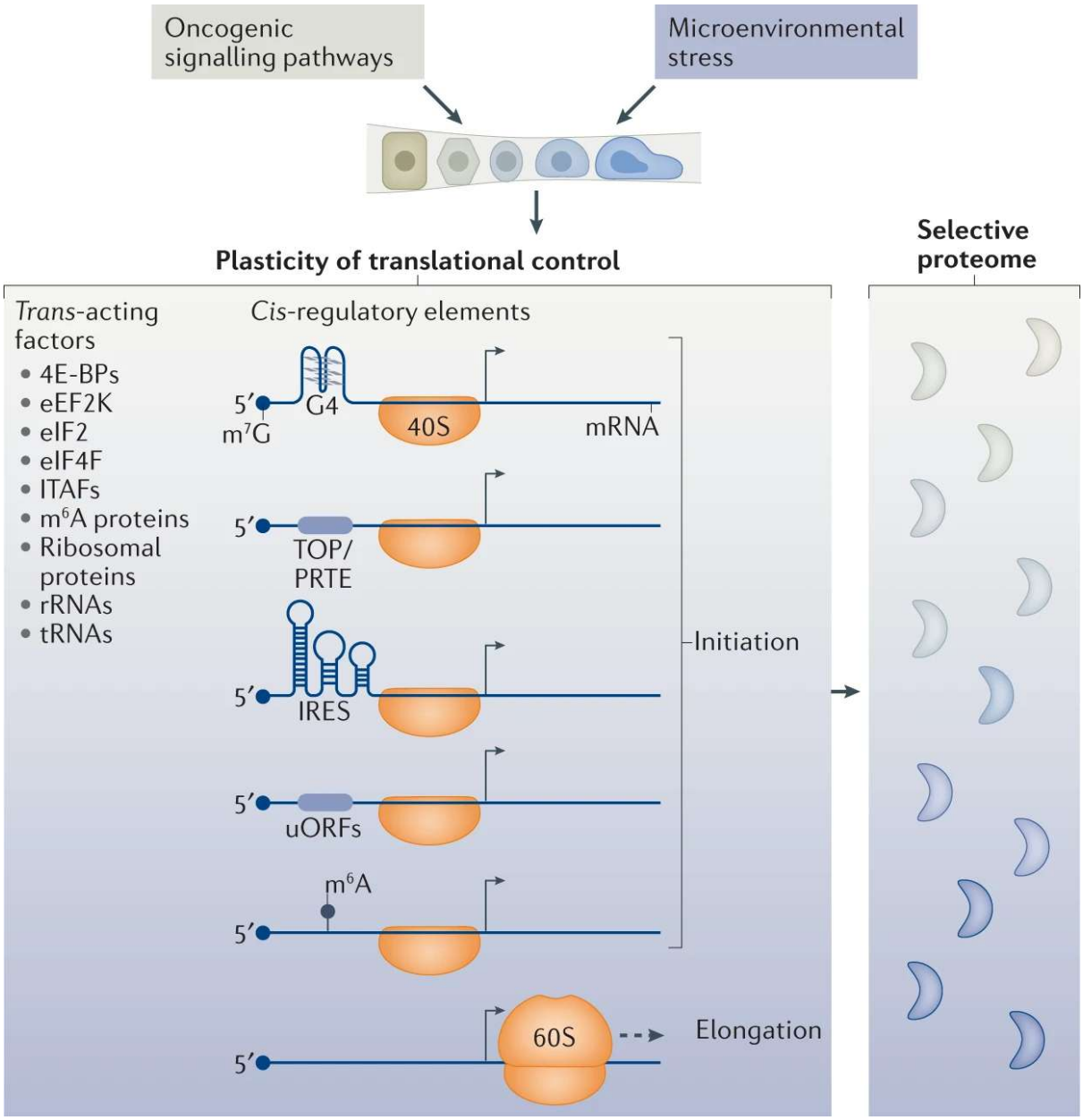

Figure 16. Aspects of translational control. The control of mRNA translation is performed through *cis*-regulatory elements and *trans*-acting factors, which are remodelled in response to cellular stress and oncogenic signalling to define a more selective cellular proteome. rRNAs, ribosomal RNAs; m7G, 7-methylguanosine; m6A, N6-methyladenosine; G4, G-quadruplexes; IRES, internal ribosome entry site; TOP, 5′ terminal oligopyrimidine sequence; PRTEs, pyrimidine-rich translational elements; uORFs, upstream open reading frames; ITAFs, IRES trans-acting factors; eIF4F, eukaryotic initiation factor 4F; eIF2, eukaryotic translation initiation factor 2; eEF2K, eukaryotic elongation factor 2 kinase; 4E-BPs, eukaryotic initiation factor 4E-binding proteins. Adapted from Fabbri *et al.*, 2021 (ref [194]).

mRNA sequence

Many eukaryotic genes encode multiple mRNA isoforms with distinct primary nucleotide sequences. For example, sequence motifs, such as the pyrimidine-rich translational elements (PRTEs) or 5′ terminal oligopyrimidine (TOP) sequences, have been shown to participate in the control of mRNA translation[194]. The usage of variable transcription start sites that generate alternative 5′ UTRs can also affect the translation rate of different mRNAs and mRNA isoforms. Of note, the usage of variable transcription start sites can also affect the sequence of the synthesized proteins. For example, the presence of alternative transcription start sites can lead to the synthesis of truncated proteins, short peptides, or N-terminally extended proteins if located downstream or upstream the traditional translation initiation sites[231]. While splicing events can also cause protein sequence heterogeneity, the occurrence of these events within the 5′UTR can impact the translation rate of mRNAs[232]. Over half of human genes express isoforms with distinct 3′UTRs due to alternative cleavage and polyadenylation events. Since many RBPs and microRNAs (miRNAs) bind to 3′ UTRs and influence the mRNAs' fate, these alternative sequences can result in altered mRNA translation rates[233]. Besides the usage of alternative transcription initiation sites and splicing events, upstream ORFs (uORFs) have also been suggested to contribute to the differences observed in the translation rate of mRNAs[190,194]. For example, the insertion of uORFs in the mRNA 5′UTRs revealed that general translational inhibition of the main downstream ORF can be achieved during or after the translation of the uORF by ribosome stalling or dissociation, respectively. However, under certain cellular stresses, the translation of the main ORF can be resumed via 'leaky scanning' of the uORF by PIC[194].

mRNA structure

Secondary structures in mRNAs, such as G-quadruplex structures and stable hairpins, have been shown to affect translation in multiple ways. These structures can physically inhibit translation by blocking the scanning of the transcript sequence by PIC, or even promote translation by either the recruitment of eIF3 to specific hairpin structures or by direct recruitment of ribosomes to IRESs. The IRES elements, in particular, are present in ~10% of the mammalian mRNAs[234], and they have been shown to regulate mRNA translation in a cap-independent manner by recruiting the 40S small ribosomal subunit directly to the internal region of the mRNA 5′UTR. Translation elongation can also be impacted by ribosome stalling due to structures present in the coding sequence of the mRNAs[190]. mRNA secondary structures are likely highly dynamic, which might contribute to the translational heterogeneity of mRNAs. For example, the *β-actin* (*ACTB*) mRNA has been shown to adopt different structural conformations *in vivo*, which affects its accessibility to the RBP Zipcode Protein Binding Protein Sites (ZBP1). ZBP1 binding has been shown to mediate *ACTB* mRNA localization and

translational control[235]. Other studies have also shown that mRNAs can dynamically change their conformation during their lifetime, during their translocation from the nucleus to the cytoplasm, or even during translation[236–239]. Thus, it is necessary to understand the impact of the structures adopted by different mRNAs, as well as their dynamics, on mRNA translation.

mRNA post-transcriptional modifications

More than 170 chemically distinct types of post-transcriptional nucleotide modifications have been described for mRNAs. Together, these modifications have been referred as the 'epitranscriptome'[240]. The most prevalent post-transcriptional modification is the adenosine methylation at the nitrogen-6 position (n6-methyladenosine, m^6A), with an average of 3–5 modifications per mRNA in one-third of the total mammalian mRNAs[241]. Additionally, this modification can also be found in almost every type of RNA. The m^6A is installed by methyltransferase complexes (named m^6A writers), including METTL16, METTL14, METTL3, KIAA1429, RBM15, WTAP, and ZC3H13. In contrast, this modification can be removed by erasers, such as the demethylases FTO and ALKBH5. Proteins that can recognize m^6A-modified RNAs are called m^6A readers, which include members of the YT521-B homology (YTH) domain-containing family and others RBPs. Together, these proteins have been shown to play important roles in the regulation of many aspects of the m^6A-modified RNA biology, including RNA splicing, stability, translocation and translation[241]. Regarding translation, m^6A has been documented to increase the initiation rate and protein synthesis by recruiting translation initiation factors (e.g., eIF3), m^6A writers (e.g., METTL3) and readers (e.g., YTHDF1) to the mRNA, and to inhibit translation by slowing down the elongation step[190,194]. For example, m^6A in the mRNA 5'UTR can promote cap-independent translation initiation by directly interacting with eIF3 for ribosome recruitment[242]. When in the 3'UTR, binding of METTL3 to internal m^6A favours cap-dependent translation by promoting mRNA circularization and interaction with eIF3H[243]. Interactions of the m^6A reader YTHDF1 with m^6A-modified transcripts was also found to promote mRNA translation in response to neuronal stimuli[244]. m^6A within the coding sequence, however, was shown to block tRNA accommodation and inhibit translation elongation[245].

ncRNAs (miRNA/lncRNA/circRNA)

Many ncRNAs, which includes miRNAs, lncRNA and circular RNAs (circRNAs), have been described to regulate mRNA translation. miRNAs are small ncRNAs of about 22 nucleotides, and they have been shown to bind to mRNA UTRs by complementary base-pairing. Intriguingly, this binding has been associated with the regulation of translation or degradation of its mRNA targets. Regarding translation, miRNAs have

been shown to inhibit cap-dependent translation initiation by inducing the dissociation of translation initiation factors from the mRNA[246,247]. The involvement of miRNAs in translation has also been widely explored in cancer. For example, *miR-10b* was shown to inhibit the translation of the *Homo Sapiens homeobox D10* (*HOXD10*) mRNA in metastatic breast cancer cells by interacting with the mRNA 3′UTR. This inhibition was shown to promote cell migration and invasion[248]. The *miR-10a*, in contrast, was shown to bind to the 5′UTR of the *ribosomal protein* (*RP*) mRNA and promote its translation in the context of amino acid starvation[249]. The interplay between miRNAs and RBPs has also been shown to regulate mRNA translation. The RBP HUR, for example, was shown to promote *STAT3* mRNA translation by preventing the binding and consequent translation inhibition of *miR-330* in tumor-induced cachexia[250].

LncRNAs, in contrast to miRNAs, contain about 200 nucleotides. These ncRNAs have been shown to play a vital role in gene expression by regulating every step of the RNA life cycle, including transcription, stability, translation, and post-translational modifications[193]. Many reports indeed demonstrate the translational control of lncRNAs, particularly in cancer. The antisense lncRNA of the proapoptotic gene *PYCARD* (*PYCARD-AS1*) was shown to bind to *PYCARD* 5′UTR and inhibit the mRNA translation by preventing ribosome assembly in breast cancer cells[251]. Conversely, the *lncNB1* was demonstrated to bind to the 60S ribosomal protein 35 (RPL35) and promotes the protein synthesis of the E2F1 protein, required for N-Myc-driven oncogenesis in human neuroblastoma cells[252]. As for the miRNAs, lncRNAs can also regulate mRNA translation by interacting with RBPs. For example, the lncRNA *SNHG1* was found to competitively bind to the RBP hnRNPL to impair the translation of the *E-cadherin* (*CDH1*) mRNA in prostate cancer[19]. Moreover, lncRNAs can also interfere with miRNA activities to regulate translation. For example, the *LINC00460* was shown to antagonize *miR-149-5p* to inhibit the translation of *cullin 4A* (CUL4A) mRNA, affecting colorectal cancer cells growth and apoptosis[253].

CircRNAs are another class of ncRNAs, which is characterized by the presence of covalent closed loops formed by reverse splicing events on the precursor mRNA. Strikingly, circRNAs can also be transcribed and translated into proteins[193]. The *Circ-FBXW7*, for example, is highly expressed in human brain cells and it translates a 21 kDa protein (FBXW7-185aa) through IRES-driven translation of the ORF. In gliomas, the upregulation of FBXW7-185aa was shown to inhibit cell cycle and cell proliferation[254]. In addition to synthesize proteins, circRNAs can regulate mRNA translation by regulating the initiation step. For example, *circYap* was shown to inhibit the translation of the *yes-associated protein* (*YAP*) mRNA by competing with eIF4G for binding to PABP, therefore preventing the assembly of the translation initiation machinery on the *YAP* mRNA in non-cancer cells. In liver and breast cancer cells, *circYap* overexpression lower YAP levels, suppressing cell proliferation, migration and colony formation[255]. As for lncRNAs and circRNAs, circRNAs was demonstrated to interact with RBPs to

regulate translation. The *circPABPN1*, for example, was shown to inhibit *PABPN1* mRNA translation by preventing the binding of HUR to the mRNA[256].

eIF4F

Global control of mRNA translation is generally accomplished by modifications in the activity of initiation factors or the regulators that interact with them. The eIF4F complex controls the initiation of mRNA translation, and modulations in the availability or activity of its components can have a direct impact in this important process[203]. The binding of eIF4G to eIF4E is considered as a key step in the formation of the complex; however, this interaction has been shown to be repressed by eIF4E-binding proteins (4E-BPs)[197,203]. Repression by the 4EBP CYFIP1 (cytoplasmic FMR1-interacting protein 1), for example, was shown to form a repressive complex with FMRP (FMRP-CYFIP1-eIF4E complex) to decrease the translation initiation of its target mRNAs[257]. In addition to being regulated by 4E-BPs, eIF4E activity can be modulated by the MAP kinase-interacting protein kinases 1 and 2 (MNK1 and MNK2), which are activated downstream of the p38 and ERK pathways. Both kinases phosphorylate eIF4E at serine 209, which is believed to promote translation initiation by increasing the affinity of the eIF for the mRNA cap[197,203]. The eIF4F complex seems to also have a selective impact in the translation of mRNAs with distinct features within their 5′ UTR. For instance, inhibition of eIF4E (and not EIF4A) activity disproportionally reduces the translation of mRNAs with very short 5′ UTRs when compared to the global mRNA translation rates. Conversely, the translation of mRNAs with long and structured 5′ UTRs is sensitive to both eIF4E and eIF4A availability[203]. Additionally, the scaffold protein eIF4G has been shown to mediate cap-independent translation by enabling the interaction of PIC with IRESs found in the 5′ UTR of certain mRNAs, and it is commonly activated under cellular stress[203].

RBPs

RBPs are one of the most widely studied post-transcriptional regulators of gene expression[1–6]. These proteins were found to be involved in every aspect of the RNA biology, including RNA maturation, localization and degradation. Many RBPs were also found to play vital roles in the regulation of mRNA translation[4,7,8]. However, both ‘selection’ of the RNA target and affinity for its binding by RBPs depend on the RNA sequence, secondary structure, and other cis-acting RNA elements. By binding directly to these regulatory sequences, RBPs have been shown to control mRNA translation initiation by modulating (promoting or inhibiting) the capability of the ribosomes to associate with the bound mRNA. For example, specific RBPs called ‘IRES trans-acting factors’ (ITAFs) were shown to bind to IRESs-containing mRNAs and control their translation[194]. Interestingly, even the same RPB can regulate both cap- and IRES-

dependent (cap-independent) translation. For example, the double-stranded RBP Staufen-1 (STAU1) was shown to binds to the 5'UTR of the *HIV-1* vRNA and promote its cap-dependent translation[258]. Recently, the same RBP was identified as an ITAF, promoting the *HIV-1* IRES-dependent translation initiation[259]. Besides vRNAs, RBPs have been shown to bind and regulate the translation of many eukaryotic mRNAs, orchestrating of the expression of immune-modulating cytokines[260–262], inflammatory responses[263–265] and angiogenesis[266–268].

Certain RBPs were shown to regulate mRNA translation by controlling its localization in the cell. The cytosolic mRBP clustered mitochondria protein homolog (CLUH), for example, was shown to bind to mRNAs of nuclear-encoded mitochondrial proteins and regulate their (localized) translation by the ribosomes present in the vicinity of the mitochondria[269–271]. The main advantage of local translation is that proteins are synthesized close to the site where they are needed, thus avoiding their expression throughout the cell while reducing the highly energetic cost of this process. Accordingly, changes on RBPs' localization can also impact their RNA-binding activity, including, therefore, their control on mRNA translation. Indeed, RNA-proteins interactions are highly dynamic, and they have been shown to be modulated by many factors, including cellular stresses. Upon ferroptosis induction in HeLa cells, many translation-related RBPs were found accumulated in nucleus and/or disassociated from their RNA targets in the cytoplasm[84]. The translation initiation factor eIF5, for example, enhanced its RNA-binding activity in the nucleus upon ferroptosis; however, this was explained by its nucleocytoplasmic translocation. In contrast, while FXR1 protein levels remained unchanged in both subcellular compartments, this RBP showed an enhanced RNA-binding activity in the nucleus and disassociation from its RNA targets in the cytoplasm. Of note, ACO1, a bifunctional protein associated with the maintenance of iron homeostasis, also decreased its association with RNAs in the cytoplasm upon ferroptosis induction[84]. This enzyme was found to bind and regulate mRNA translation upon low intracellular levels of iron[174]. Additionally, many of the stress-regulated RBPs identified upon arsenite stress in MCF7 and HuH-7 cells were ribosome-associated proteins (both cytoplasmic and mitochondrial) and translation initiation factors, among other translation-related proteins[77,83]. In response to vincristine-induced chemotoxic stress, PTB and PCBP1 were shown to translocate from the nucleus to the cytoplasm to activate the IRES-mediated translation of the *BAG cochaperone 1* (*BAG-1*) mRNA in HeLa cells, therefore promoting tumorigenesis and chemoresistance[272]. Together, these studies demonstrate how stress can alter RBP localization and/or RNA-binding activity, and the impact of these alterations on mRNA translation.

Many RBPs have also been shown to play a vital role in the regulation of mRNA translation in tumorigenesis. For example, HUR was shown to bind to the 5'UTR of the pro-apoptotic *caspase-2L* mRNA and inhibit its translation in colorectal cancer, therefore promoting tumor cell antiapoptotic activities[273]. LARP1 was demonstrated as

involved in the translational control of mRNAs containing 5'TOP sequence motifs[274–276], including those encoding ribosomal proteins. The Musashi proteins (Musashi-1, MSI1; and Musashi-2, MSI2) were shown to inhibit or promote the translation of mRNAs of oncogenes and tumor suppressor genes in numerous cancer types[277]. Additionally, RBPs have been shown to increase the translation of mRNAs encoding glycolytic enzymes in order to promote cancer cell survival[278]. Based on these studies, it is evident that RBPs participate in tumorigenesis by influencing the translation of target mRNAs. Differential RNA-binding activity of translation-related RBPs has also been described within cancer cells[10]. For example, RNA interactome analyses identified that translation-related RBPs are predominantly elevated in more aggressive osteosarcomatas, thus indicating that these cells exhibit a more active global translation than less aggressive osteosarcomatas and normal bone/mesenchymal cells[10]. Besides identifying enriched RBPs associated with the regulation of global translation, the RNA-binding activity of RBPs involved in the translation of more selective mRNAs was also enhanced. For example, the RNA-binding activity of tumorigenic-associated RBPs, such as PUM1 and PUM2, Y-box proteins (YBX1 and YBX3), La-related proteins (LARP1, LARP4, LARP4B) and the IGF2BP family (IGF2BP1 and IGF2BP3), was enriched in aggressive osteosarcomatas[10]. It is thus not surprising that these aggressive tumors characterized by high translation rates were found more susceptible to the use of translation inhibitors[10]. These findings demonstrate that translation represents a potential therapeutic target for "translation-hungry" tumors.

In conclusion, translation control is an essential mechanism for gene expression, dynamically controlling protein synthesis and thereby contributing to the determination of the cellular phenotype[193,194]. The common factors affecting this procedure include translation initiation factors, different RNA features (sequence, structure and post-transcriptional modifications), non-coding RNAs and RBPs, but also tRNAs and codons used at the elongation phase of translation. It is through the modulation of these factors that translation is rewired in response to different stimuli, which is vital for not only cell survival, but also cell (de)differentiation, tumorigenesis and cancer aggressiveness[194]. Indeed, dysregulation in mRNA translation is commonly reported in tumors, thus having the potential to be therapeutic targeted to specifically kill cancer cells while preserving their normal (non-malignant) counterparts. Therefore, a deeper understanding of how translation is rewired in cancer cells and in the tumor microenvironment (TME) might uncover attractive new targets for drug development.

1.3.4 Cellular stress rewires translation

Translation can be rewired upon stress to define a more selective proteome to allow cells, particularly cancer cells, to adapt to potentially lethal stresses (Figure 15). While

the cap-dependent translation initiation is commonly inhibited under stress, other alternative mechanisms involved in translation initiation arise, allowing the translation of a select group of stress-responsive mRNAs. In response to stress, some mRNAs were shown to be preferentially translated through uORF-mediated mechanisms. For example, the translation of the *activating transcription factor 4* (*ATF4*) mRNA is vital for the transcription of genes involved in the response against amino acids depravation, endoplasmic reticulum stress, hypoxia, oxidative and genotoxic stress[194,279]. This mRNA contains two uORFs upstream the main ORF in the 5′ UTR, preventing its translation; however, under stress, the ribosomal 40S subunit bypasses the two uORFs, reinitiating the translation of the main ORF[279].

Another 'strategy' commonly used to initiate translation under stress is the use of alternative translation initiation codons. This phenomenon is particularly interesting for the generation of protein isoforms with cancer cell-specific or stress-specific functions. This is the case, for example, of the CUG-initiated isoforms of the human fibroblast growth factor 2 (FGF-2)[280] and vascular endothelial growth factor (VEGF)[281] that have critical roles in cell transformation and in the stress response. Although it is still not clear what are the feature involved in the activation of non-AUG translation, ribosome profiling approaches revealed that this phenomenon is a widespread mechanism for translation initiation[282,283]. In addition, redistribution of m^6A modifications within mRNA 5′ UTRs during stress has been appointed to potentially favour the translation of stress-responsive mRNAs in a cap-independent manner. For example, translation of the *heat-shock protein 70* (*Hsp70*) mRNA, which contains an m^6A site within its 5′UTR, was induced upon heat shock in an m^6A-dependent manner[284]. IRES-mediated translation has also been implicated in the translation of stress-responsive mRNAs. This mechanism, however, requires the involvement of ITAFs. In colon cancer cells under hypoxia, for example, the IRES-mediated translation of the *fibroblast growth factor 9* (*FGF9*) mRNA, which encodes for an important mitogen involved in tumor progression, was shown dependent on the ITAF hnRNP M[285,286].

The influence of stress on translation, however, is not restricted to modulations in translation initiation. During nutrient deprivation, translation elongation can be blocked via the AMP-kinase (AMPK)-dependent activation of the eEF2 kinase (eEF2K), followed by eEF2K-mediated inhibition of the translation elongation factor eEF2, which is a factor responsible for the translocation step of translation elongation[287]. Moreover, elongation pausing can also be triggered by stress, directly impacting protein synthesis. During severe heat shock in both mouse and human cells, for example, ribosomes were found to often pause at ~200 nts in most ORFs, resulting in the upstream accumulation of ribosomes while decreasing their accumulation upstream this point[288]. Additionally, the pool of tRNAs can also be reprogrammed to enable the translation of stress-responsive mRNAs in mammals[289], demonstrating another example of how the synthesis of stress-induced proteins can be control at the elongation stage of translation. In summary, cells can employ various mechanisms to

modulate translation under stress in order to promote their survival and, in the case of cancer cells, drive cancer progression. The rewiring of mRNA translation therefore gives to these cells the flexibility to adapt to a hostile microenvironment.

1.3.4.1 TRANSLATION DYSREGULATION OF CANCER CELLS AND CELLS OF THE TME

In recent years, increasing evidence has shown that, alongside dysregulations in transcription and post-translational modifications, dysregulations in translation also play a crucial role in the development and progression of various cancers.[193,208]. Alterations in components of the translation machinery, for example, were proven critical for cancer development by enabling cellular adaptation to intra- or extracellular stimuli, environmental changes and activation of stress responses[290]. These stimuli reshape the cellular translational landscape during tumorigenesis and, as a result, conventional and unconventional mechanisms of mRNA translation become crucial for cancer cell proliferation, resistance, and metastasis[194,195,290]. Many decades of research indicate that uncontrolled cell growth and proliferation are commonly caused by aberrant mRNA translation controlled by the RAS–mitogen-activated protein kinase (MAPK), phosphatidylinositol 3-kinase (PI3K)-protein kinase B (AKT)-mechanistic target of rapamycin (mTOR) (Figure 17), and/or MYC signalling pathways[194,195,290]. For example, activation of the RAS-MAPK pathway triggers MNK1/2-depedent phosphorylation and activation of eIF4E to initiate cap-dependent translation[197,203]. RAS proto-oncogenes can also stimulate the PI3K-Akt-mTORC1 pathway, triggering the formation of the eIF4F complex through the phosphorylation of 4E-BP, therefore enabling translation initiation[195,290]. Not surprisingly, increase in abundance and phosphorylation of components of the translation initiation complex have been described in various types of cancers[279,291–294]. High expression of the eIF4F complex in $BRAF^{V600E}$-mutated tumors, for example, has been associated with resistance to anti-BRAF/MEK therapy and occurrence of metastasis. Particularly in melanoma cells, persistent formation of the eIF4F complex was proposed to be used as an indicator of resistance to $BRAF^{V600E}$-targeted therapy[293]. Phosphorylation of eIF4E, for example, was shown to enable cancer cells to escape immune surveillance by promoting the *programmed death ligand 1* (*PD-L1*) mRNA translation[294]. Accordingly, increased phosphorylation of eIF2α was proposed to promote tumorigenesis by increasing the translation of certain mRNAs (e.g., ATF4[194,279]). However, eIF2α phosphorylation was also shown to inhibit angiogenesis and tumor proliferation, and to promote tumor cell apoptosis[291,292].

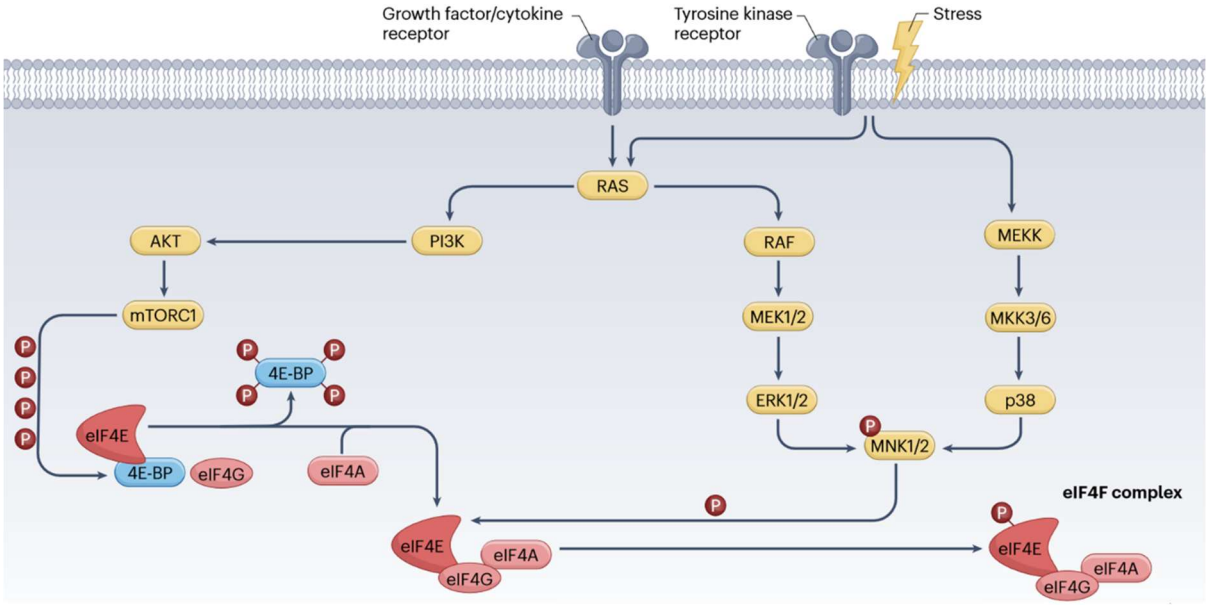

Figure 17. Oncogenic signalling pathways. The eIF4F complex is the key factor for cap-dependent translation initiation. The availability of free mRNA cap-binding protein eIF4E is controlled by 4E-BP, downstream the PI3K–AKT–mTORC1 kinase pathway. 4E-BP phosphorylation by mTORC1 prevents its binding to eIF4E, allowing the formation of the eIF4F complex. The phosphorylation of eIF4E, although not essential for its role in translation initiation, is controlled by MNK1 and MNK2 kinases downstream of the ERK and p38 pathways. In cancer cells, the described pathways are commonly dysregulated due to the hyperactivation and/or overexpression of cell surface receptors, as well as a result of specific external stimuli, such as cytokine and growth/stress signals. Adapted from Bartish *et al.*, 2023 (ref [203]).

In cancer cells, the hyperactivation of oncogenic signalling pathways can also affect the elongation step of translation. Indeed, activation of the RAS–MAPK, PI3K–AKT–mTOR, and MYC signalling pathways was shown to regulate the tRNA expression[194]. Translation elongation rates are highly dependent on the regulation of tRNAs, and growing evidence has demonstrated that dysregulation of tRNA abundance might be involved in tumor progression. In breast cancer cells, for example, nuclear-and mitochondrial-encoded tRNA expression presented 3- and 5-fold increase, respectively[295]. This increase was proposed to facilitate the translational regulation of specific regulatory genes. Additionally, tRNA epitranscriptome was also proposed to control the codon-specific translation of mRNAs encoding oncogenic proteins. In melanoma cells, codon-specific translational control of *HIF1α* mRNA was suggested to enhance the glycolytic metabolism, promoting cell survival[296]. Likewise, aberrant oncogenic signalling pathways were also shown to control mRNA translation by modulating the expression of ribosomal components (e.g., rRNAs)[194].

Cancer cells may also take advantage of their ability to rewire translation to switch between distinct and interconvertible phenotypes, thereby rendering them more invasive and resistant to therapy. Indeed, cancer cells appear to regulate the translation of mRNAs associated to the EMT process. At the initiation stage of translation, phosphorylation of eIF4E was shown to upregulate the translation of *Mmp3* and *Snai1* mRNAs, which encode for key inducers of EMT[297]. Similarly, phosphorylation of eIF2α

was shown associated to EMT, dedifferentiation and breast cancer cell invasion in a ATF4-dependent manner[298,299]. In other studies, the RBP CUGBP Elav-Like Family Member 1 (CELF1) was shown to bind to EMT-related mRNAs and promote their translation in a cap-dependent manner[300].

At the elongation stage of translation, the Upstream of N-RAS (UNR) RBP (also known as Cold Shock Domain Containing E1, CSDE1), for example, was shown to promote the translation elongation of the *VIM* and *RAC1* mRNAs, which encode EMT markers, and therefore the EMT-like (invasive) behaviour of melanoma cells[301]. Acquisition and maintenance of stem-like phenotypes also depend on translational control. Cancer stem cells have a slow proliferation rate, which implies that these cells are characterized by low global translation rates. Accordingly, haematopoietic and muscle stem cells exhibit reduce protein synthesis, potentially due to hypo-phosphorylation of 4E-BP1 and phosphorylation of eIF2α[302,303]. Moreover, in triple-negative breast cancer, the RBP IMP U3 Small Nucleolar Ribonucleoprotein 3 (IMP3) was proposed to maintain breast cancer stemness by promoting the translation of *SNAI2* mRNA and thereby SOX2 upregulation[304]. IMPs may also induce the translation of mRNA targets by acting as m^6A readers[305]. Indeed, m^6A methylation mediated by m^6A readers and writers have been associated with the promotion of stability and translation of mRNAs relevant for cancer stemness maintenance[306,307].

In non-epithelial cancers (e.g., melanoma), the transition between a proliferative state to an invasive drug-resistant dedifferentiated (mesenchymal) phenotypic state is associated with the translational control of the microphthalmia-associated transcription factor (MITF)[308]. MITF is a key regulator of the melanocyte lineage, and its expression can be controlled, for example, by the DEAD-Box Helicase 3 X-Linked (DDX3X)-IRES-dependent translation of the *MITF* mRNA[309]. Altered DDX3 levels drive a proliferative-to-invasive (and therapy-resistant) phenotypic switch in melanoma cells through reduction in MITF expression. Similarly, translational reprogramming dependent on the phosphorylation of eIF2α in melanoma cells under nutrient deprivation was described to represses the expression of MITF, therefore inducing melanoma phenotypic switch to a more invasive phenotype[310]. These studies thereby suggest translational reprogramming as a crucial factor for phenotypic switching in melanoma, contributing to cancer aggressiveness and resistance to targeted therapy.

Indeed, translational reprogramming has been demonstrated to enable cancer cells to adapt during therapy and, therefore, overcome drug efficacy[194]. Activation of alternative pathways or even reactivation of the pathway that is being targeted by therapy are the major causes of resistance. In $BRAF^{V600E}$-mutated melanoma, for example, modulation of the eIF4F complex formation via the activation of different oncogenic pathways was shown to mediate resistance to anti-BRAF and anti-MEK inhibitors[293]. Similarly, targeted MAPK therapy in $BRAF^{V600E}$-mutated melanoma was recently shown to rewire the tumour proteome by promoting a codon-biased translation reprogramming through the increase of the valine aminoacyl-tRNA

synthetase (VARS) expression[311]. VARS was shown to favour the translation of valine codon-enriched mRNAs, including the hydroxyacyl-CoA dehydrogenase (HADH) mRNA, enhancing fatty acid oxidation in mitochondria and therapy resistance[311].

In addition to cancer cells, other cells of the TME participate actively in tumor progression through constant communication with cancer cells, therefore a deeper understanding of the TME translational control is also needed[194,203]. Indeed, mRNA translation has been implicated in the crosstalk between cancer cells and cancer-associated fibroblasts (CAFs), which are cells derived from the normal stromal fibroblasts. Recently, co-culture of murine fibroblasts with breast cancer cells enhanced the ability of cancer cells to invade due to an increase in eIF4E phosphorylation in fibroblasts, and elevated translation and secretion of fibroblast-derived IL-33[312]. Additionally, the transition between normal fibroblasts and CAFs is also regulated by translation. Knockdown of eIF3e, for example, was shown to induce CAF-like properties on normal fibroblasts[313]. Tumor vascularization is a process orchestrated by a range of signaling pathways and secreted factors, which involves the participation of endothelial and non-endothelial cells. In tumors, the formation of new vascular network, a process termed neoangiogenesis, is dynamically remodelled in response to hypoxia to sustain cancer cells with metabolic substrates[314]. Following hypoxia, translation reprogramming was shown to sustain angiogenesis by regulating the expression of the angiogenic factor *VEGF*, *BCL-2* and *HIF1α* mRNAs in an IRES-dependent manner. Similarly, IRES-dependent translation of *VEGF-C* mRNA stimulates lymphangiogenesis[315].

Immune cells are also vital components of the TMEs. These cells use translational control to maintain plasticity and adapt their function in the context of cancer by triggering an immune response against cancerous cells or by conferring immune tolerance. The switch from naïve to effector T cells is regulated, at least in part, at the translational level. In coordination with the metabolic status of the cell, the glycolytic enzyme GAPDH, also a non-canonical RBP, play a key role in T cell activation by regulating *IFN-γ* mRNA translation[102]. In dendritic cells, the m^6A-binding protein YTHDF1 recognized mRNAs encoding lysosomal proteases that were marked by m^6A[316]. Binding of YTHDF1 to these mRNAs was shown to increase the translation of lysosomal proteases and subsequent degradation of tumour neoantigens, thereby decreasing immunoreactivity to tumours[316]. Recently, tumour-infiltrating T CD8+ cells in human postpartum breast cancer were characterized by high levels of phosphorylated eIF4E and the Programmed Cell Death Protein 1 (PD-1), an exhaustion marker associated with self-tolerance, in comparison to T CD8+ cells in tumours of non-postpartum cancers[312]. Overall, these studies demonstrate how translational control can shape the TME, regulating its composition and thereby influencing cancer progression.

Although the mechanisms associating certain translation factors and translation regulators with cancer are not fully elucidated, they undoubtedly linked these features to oncogenic processes. Indeed, dysregulation or altered expression of the translation factors/regulators appears to promote tumorigenesis and tumor progression by promoting changes in protein diversification through selective mRNA translation under harsh microenvironmental conditions[195]. These changes are frequently involved in the promotion of cell survival, proliferation, hypoxia responses, neoangiogenesis and immune evasion[195,290]. Additionally, selective alterations in mRNA translation are also found in tumour-supportive cells, allowing them to adapt their proteome and, consequently, cellular function under stress. Ultimately, these alterations might contribute to tumor support and metastases, but also potentially facilitate the antitumour activity of non-cancer cells present in the TME[203]. However, targeting the translational machinery and associated proteins within the larger TME may not always lead to a straightforward antitumour response, since cancer cells and other cells in the TME can adopt compensatory mechanisms when an important signalling pathway is disrupted[203]. Understanding the roles of translation factors and other translation regulators in cancer may reveal novel opportunities to specifically target these cancer cells and other malignant aspects of the TME while balancing the impact of inhibiting translation, in combination or not with the use of immune checkpoint inhibitors[195,203]. In conclusion, mechanisms of translational control are pivotal in driving tumor progression and conferring resistance to therapy. Consequently, these mechanisms represent potential targetable vulnerabilities for therapeutic intervention.

2 OBJECTIVES

As vastly described in the introduction, enzymes involved in classic metabolic pathways have been recurrently identified to moonlight as RBPs[174]. This discovery led to the hypothesis that the intermediary metabolism mediated by RNA-binding metabolic enzymes is involved in post-transcriptional gene regulation[105]. Indeed, some glycolytic enzymes have been shown to moonlight as RBPs and regulate the translation of their mRNA targets[102,164]. This observation is particularly noteworthy, considering that both conventional and unconventional RBPs have been found to play vital roles in the control of mRNA translation, including within the context of cancer[194]. Therefore, given the critical importance of both glycolysis and mRNA translation in cancer cells, we propose to explore the non-canonical RNA-binding activity of GEs on the control of mRNA translation in order to elucidate the significance of this moonlighting activity in the cancer context. We believe that these proteins might execute both enzymatic and RNA-binding functions, and that the shift between the two activities may drive oncogenic changes in melanoma cells.

The Hexokinase II (HK2), which is the first enzyme in the glucose metabolism, is highly expressed in cancer cells. Although HK2's role in tumorigenesis has been attributed to its glycolytic activity, this enzyme has been shown to execute non-canonical functions that often regulate processes that are highly relevant for cell transformation and cancer development. In particular, Blaha *et al*. (2022) demonstrated a novel non-catalytic mechanism by which HK2 contributes to SNAIL-mediated EMT and metastasis in breast cancer[317]. Intriguingly, HK2 has been recurrently identified to bind RNA in various human cell lines by orthogonal large-scale quantitative methods[77–79,83]. Together, these studies suggest that HK2 moonlights as an RBP, binding to both poly(A)[83] and non-poly(A)[77–79] RNAs. These findings, however, require additional experimental validation through further research. Nonetheless, yeast hexokinases (Hxks) were shown to bind nucleic acids[64]. Together, these studies, along with a recent evidence that many glucose-binding proteins can bind RNA in human cell lines[115], corroborates the hypothesis that HK2 is a non-canonical RBP, whose RNA-binding activity could be exploit by cancer cells.

The laboratory, in collaboration with Caroline Robert's group at Institut Gustave Roussy, has found by 2C experiments that HK2 binds RNA. Additionally, they have also found by polysome profiling that HK2 regulates the translation of mRNAs encoding key-genes involved in EMT properties[318]. Together, these findings served as the foundation for my thesis project. We believe that HK2's RNA binding activity might be involved in the control of mRNA translation in melanoma. Since further studies are needed to validate HK2 as non-canonical RBP involved in the regulation of gene expression, we pursued the following objectives (Figure 18) to study HK2-RNA interactions:

1) Explore the RNA-binding activity of HK2.
2) Assess the significance of HK2's interaction with RNA in the control of post-transcriptional gene expression.
3) Evaluate whether HK2-mediated post-transcriptional control has an impact in cancer-related phenotypes.

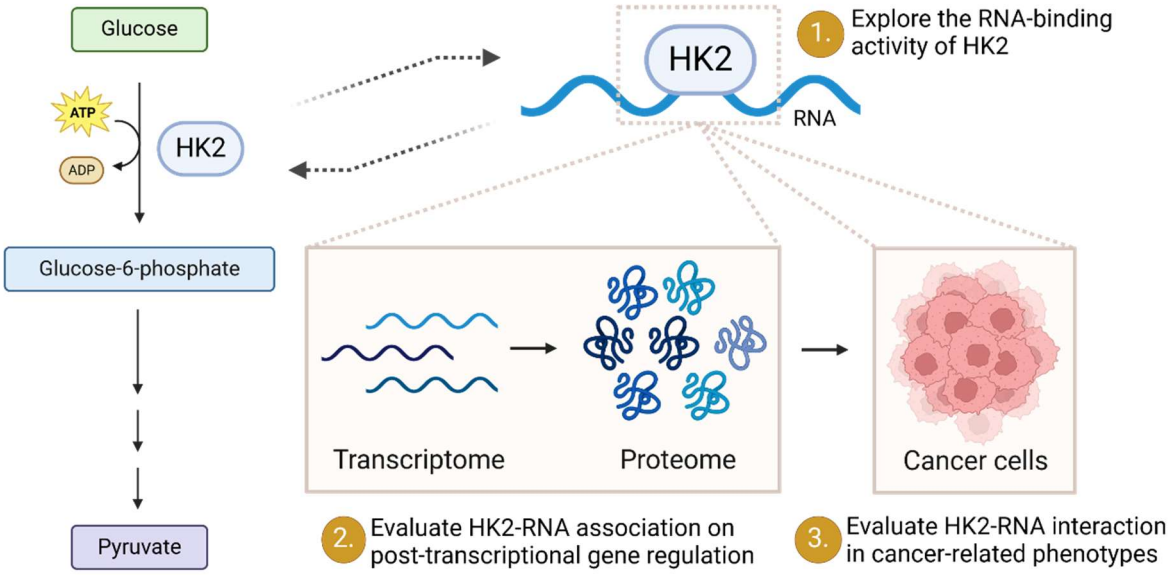

Figure 18. Objectives of the thesis

3 RESULTS

3.1 ARTICLE: AN EXTRA-GLYCOLYTIC FUNCTION FOR HEXOKINASE 2 AS AN RNA-BINDING PROTEIN REGULATING MRNA TRANSLATION IN MELANOMA

To explore the potential RNA-binding activity of HK2, we performed protein- and RNA-centric assays. We employed the Cross-linking immunoprecipitation (CLIP) assay, a protein-centric method that makes use of UV irradiation of living cells to irreversibly crosslink proteins to RNAs at direct contact by the formation of stable covalent bonds between them. This crosslink therefore allows the use of stringent steps to purify single protein interactions across the transcriptome. Similarly, we employed another technique that takes advantage of the UV crosslink to isolate RNA–bound proteins, the Complex Capture (2C) assay. 2C is an RNA-centric approach that uses silica-based solid-phase extraction to purify crosslinked RNA–RBP complexes. Despite complementing each other, both techniques are not suitable for the characterization of RNA–protein interactions under native conditions, since RNP complexes formed *in vivo* are not preserved under stringent conditions. Nonetheless, alternative techniques were also used, as the density gradient centrifugation to further study proteins with RNA-dependent interactions (including RNP complexes). Moreover, RNA immunoprecipitation (RIP) approaches were also applied to purify RNA–protein complexes under native conditions, thereby allowing the identification of RNAs bound to HK2 in the context of RNP. These interactions could also be assessed *in situ* using imaging approaches, such as the RNA-Proximity Ligation Assay (RNA-PLA).

Once identified that HK2 binds to RNA in melanoma cells, we evaluated the HK2-dependent control of mRNA translation. To this end, we used Polysome Profiling, a method developed for the study of mRNA translation rate in living cells based on their association with ribosomes. Western blot assays coupled with RT-qPCR analysis were also used as complementary methods. Additionally, luciferase assays coupled with RT-qPCR were performed to further investigate the cis-acting elements involved in the mRNA translational regulation by HK2. The impact of HK2-mediated post-transcriptional control in cancer-related phenotypes was evaluated through functional assays, such as the clonogenic assay and the Incucyte proliferation assay. While the clonogenic assays are widely used to assess the ability of single cells to grow into colonies *in vitro*, Incucyte proliferation assays allow the measurement of cell proliferation through a live-cell time-lapse imaging approach.

Together, these techniques enabled the identification of HK2 as a novel RNA-binding protein that regulates mRNA translation. In particular, we demonstrate that this enzyme specifically binds and regulates the translation of the mRNA encoding for SOX10, a transcription factor shown to play a key role not only in the development of melanocytes, but also in melanoma aggressiveness. We show that the HK2-dependent

SOX10 mRNA translational regulation is involved in clonogenic and proliferation properties of melanoma cells.

An extra-glycolytic function for hexokinase 2 as an RNA-binding protein regulating *SOX10* mRNA translation in melanoma

Ana Luisa Dian[1,2,3], Antoine Moya-Plana[4,5,6], Giuseppina Claps[4,5], Céline M. Labbé[1,2,3], Virginie Quidville[4,5], Dorothée Baille[1,2,3], Séverine Roy[4,5], Virginie Raynal[7], Sylvain Baulande[7], Caroline Robert[4,5*], Stéphan Vagner[1,2,3,*]

[1]Institut Curie, PSL Research University, CNRS UMR 3348, INSERM U1278, Orsay, France.
[2]Université Paris-Saclay, CNRS UMR 3348, INSERM U1278, Orsay, France.
[3]Equipe labellisée Ligue contre le Cancer.
[4]INSERM U981, Gustave Roussy, Villejuif, France.
[5]Université Paris Sud, Université Paris-Saclay, Kremlin-Bicêtre, France.
[6]Head and Neck Oncology Department, Gustave Roussy, Villlejuif, France
[7]Institut Curie Genomics of Excellence (ICGex) Platform, PSL Research University, Institut Curie Research Center, Paris, France

[*]co-corresponding authors:
stephan.vagner@curie.fr, caroline.robert@gustaveroussy.fr

bioRxiv preprint doi: https://doi.org/10.1101/2024.08.13.607712

ABSTRACT

Several studies have reported the importance of aerobic glycolysis in melanoma development. Although metabolic benefits of glycolysis have been extensively described in tumor cells, the extra-metabolic functions linked to this energetic pathway in melanoma growth and proliferation have not been clearly established yet. Recently, some key glycolytic enzymes, such as GAPDH and PKM2, were reported to regulate mRNA translation. Translational control of gene expression is considered as a critical effector in cancer biology, representing a highly promising area of research. Here, we report that Hexokinase 2 (HK2), a glucose kinase that catalyzes the first step of glycolysis, is an RNA binding protein (RBP) that regulates mRNA translation in melanoma. We show that siRNA-mediated HK2 depletion changes the translational landscape of melanoma cells. Polysome profiling experiments and RNA-Seq indicate that the translational regulation exerted by HK2 is partly independent of the metabolic status or the glycolytic pathway. We found that HK2 specifically regulates the translation of the mRNA encoding SOX10, a transcription factor implicated in the regulation of tumor initiation, maintenance and progression in melanoma. RNA-protein interaction assays, including crosslinking immunoprecipitation (CLIP), indicate that HK2 is an RBP whose interaction with RNA is independent of its hexokinase activity or subcellular localization. We also show that HK2 specifically associates with the 5' untranslated region (5'UTR) of the *SOX10* mRNA, and that several deletions in this region decreases both HK2-*SOX10* mRNA association and *SOX10* 5' UTR-mediated translation. We further show that HK2-dependent SOX10 translational regulation is involved in melanoma cell proliferation and colony formation. Collectively, our data highlight a non-metabolic function of HK2, indicating that melanoma cells may enhance glycolysis for purposes beyond simple anabolism.

bioRxiv preprint doi: https://doi.org/10.1101/2024.08.13.607712

INTRODUCTION

Aerobic glycolysis, in which glucose is converted into lactate, is a key metabolic pathway in tumorigenesis. This pathway is usually promoted by cancer cells even when local conditions are suitable to utilize the oxidative phosphorylation (OXPHOS), a more efficient mechanism to generate ATP. This specific metabolic process is called the Warburg effect (Warburg, 1956; DeBerardinis & Chandel, 2020). Although metabolic benefits of glycolysis have been established for sustaining biosynthesis and cellular proliferation in tumor cells (Lunt & Vander Heiden, 2011; Vander Heiden *et al*, 2009) some data suggest that extra-metabolic functions are linked to this energetic pathway.

Over the past decades, several enzymes involved in the intermediary metabolism were shown to directly interact with RNAs (Castello *et al*, 2015). Indeed, several metabolic enzymes were found to bind RNA in the vicinity of their substrate-binding pockets (Castello *et al*, 2016; Nagy & Rigby, 1995). One example is the Rossmann fold, a di-nucleotide domain typically associated with the binding of nucleotides such as the nicotinamide adenine dinucleotide (NAD) (Rossman *et al*, 1975). This fold plays a crucial role in the function of many enzymes, particularly dehydrogenases such as GAPDH, which catalyze oxidation-reduction reactions. Interestingly, this same domain has been implicated in mediating RNA-binding (Nagy & Rigby, 1995).

Beyond dehydrogenases, several other enzymatic activities are found in the glycolytic pathway including kinases for glucose (HK1/2), pyruvates (PKM1/2), and enolases (ENO1/2/3). While PKM2 and ENO1 have been found to bind RNAs, the possible RNA-binding activity of hexokinase 2 (HK2), the first and limiting glycolysis enzyme catalyzing the irreversible phosphorylation of glucose to form glucose-6-phosphate, has never been addressed. High levels of HK2 expression have been reported in many different types of cancer, and this upregulation is typically associated with poor outcomes in patients (Wang *et al*, 2017; Wolf *et al*, 2011; Patra *et al*, 2013; Kudryavtseva *et al*, 2016; Liu *et al*, 2013). Although the role of HK2 in tumorigenesis has been attributed to its glycolytic activity, HK2 has also been shown to execute non-canonical functions that often regulate processes that are highly relevant for cell transformation and cancer development. In particular, Blaha *et al*. (2022) demonstrated a novel non-catalytic mechanism by which HK2 contributes to SNAIL-

mediated EMT and metastasis in breast cancer (Blaha *et al*, 2022). Intriguingly, HK2 has also been identified as a candidate RBP by orthogonal large-scale quantitative methods (Trendel *et al*, 2019; Queiroz *et al*, 2019; Urdaneta *et al*, 2019; Backlund *et al*, 2020) and many glucose-binding proteins were recently reported to bind RNA in human cell lines (Miao *et al*, 2023). Together with recent evidences showing that some key-glycolytic enzymes, such as GAPDH (glyceraldehyde-3-phosphate dehydrogenase) and PKM (pyruvate kinase) were able to regulate the translation of mRNAs (Simsek *et al*, 2017; Chang *et al*, 2013) in human T-cells and mouse embryonic stem cells respectively, we explored the role of HK2 as an RBP regulating mRNA translation in human cancer cells.

Here we describe a novel extra-glycolytic function of HK2 in melanoma cell lines chosen due to the critical role of glycolysis and OXPHOS in melanoma development (Scott *et al*, 2011; Qin *et al*, 2010). We demonstrate that the HK2 glucose kinase is a *bona-fide* RBP that regulates the translation of the *SOX10* mRNA, thereby regulating cell proliferation.

RESULTS

HK2 regulates mRNA translation

Upon stress stimuli and/or acquisition of mutations, melanocytes evolve from early superficial melanoma with radial growth (RGP) to early invasive melanoma (VGP) and metastatic tumor. We evaluated the level of HK2 in a variety of melanoma cell lines. We observed increased levels of HK2 in invasive cell lines (A375, WM35, SKMel10) compared to VGP (WM793), RGP (SBCL2) or normal human melanocytes (Figure S1A). In addition, in patients with cutaneous melanoma, HK2 expression was significantly higher in stages III-IV compared to stages I-II ($p=0.026$) (Figure S1B).

Since PKM2 and GAPDH were shown to associate with polysomes (Kejiou *et al*, 2023; Simsek *et al*, 2017), we analyzed whether HK2 could also be associated with polysomes. To this end, we performed western blot analysis on polysome fractions isolated from A375 cells, one of the melanoma cell lines with the highest level of HK2 (Figure S1C). We found that, as for PKM2 and GAPDH, HK2 is present in ribosome-containing fractions (Figure 1A). This is specific since another glycolytic enzyme, LDHB (lactate dehydrogenase B), is not associated to ribosome-containing fractions.

To investigate whether HK2 is involved in the translational regulation of specific mRNAs, we depleted (siRNA) HK2 in A375 melanoma cells. Of note, depletion of HK2 did not lead to a decrease in the levels of GAPDH and PKM2 (Figure 1B). We used RNA sequencing to simultaneously quantify the abundance of total transcripts and those that are being actively translated, i.e. that are associated with polysomes (>4 ribosomes). The analysis of mRNAs that are differentially recruited to heavy polysome fractions in HK2-depleted cells under normoglucidic conditions showed that the translation status of 101 mRNAs was changed (log2(fold change) > 0.7; pvalue < 0.05) (Figure 1C and Table S1).

To determine if this translational regulation is linked to the metabolic status, we cultured A375 cells in medium containing galactose instead of glucose for 24 h. The metabolism of galactose eventually converges with the glucose metabolism through the Leloir pathway. However, because this conversion occurs at a much slower rate than glucose entry into glycolysis, culture with galactose favours oxidative phosphorylation (OXPHOS) (Zhang *et al*, 2013; Wang *et al*, 2018; Weinberg *et al*, 2010). To confirm that A375 cells switch their metabolic profile in the presence of galactose, we employed the Seahorse metabolic flux assay to measure the oxygen consumption rate (OCR) and the extra-cellular acidification rate (ECAR) of living cells in culture. We observed that the ECAR, an indicator of aerobic glycolysis, was significantly higher in A375 cells cultured in glucose-containing medium compared to cells cultured in galactose. On the other hand, the OCR, an indicator of OXPHOS, was higher than ECAR in cells cultured in galactose-containing medium (Figure S2). These results therefore confirmed the metabolic switch of the melanoma cells from glycolysis to mitochondrial respiration. We found that modifying the metabolic status of cells by growing them in the presence of galactose instead of glucose impacted the translation of 312 mRNAs (Figure 1C and Table S1). Only about 20% of mRNAs regulated by HK2 are also regulated by galactose indicating that translation regulation by HK2 is partly independent of the metabolic status of the cells (Figure 1C). We also compared the subsets of mRNAs translationally regulated by HK2, PKM2 and GAPDH. We found that 59 mRNAs are specifically regulated by HK2, but not by the other tested glycolytic enzymes (i.e. PKM2 or GAPDH) (Figure 1D).

In parallel, we performed RT-qPCR (reverse transcription quantitative Polymerase Chain Reaction) on a panel of 84 cancer-relevant mRNAs (Table S2). By comparing the presence of mRNAs on heavy polysomes fractions according to HK2

expression (siHK2 vs siCTRL), we identified 6 mRNAs that were specifically translationally downregulated upon siRNA-mediated HK2 depletion (Figure S3A-B). Among them, we were particularly interested on the *SOX10* mRNA that encodes the Sex Determining Region Y (SRY)-Box Transcription Factor 10 (SOX10) because of its well-known activity as a transcription factor regulating tumor initiation, maintenance and progression in melanoma (Han *et al*, 2018; Graf *et al*, 2014; Cronin *et al*, 2018). Of note, the *SOX10* mRNA was not found in the list of 101 candidate mRNAs regulated by HK2 (Table S1) because of lack of statistical significance (p=0.3). We compared SOX10 expression in different types of malignancies and normal tissues in human in the TCGA database and found that cutaneous melanoma highly expressed SOX10 compared to other cancers (Figure S4A). Moreover, we confirmed that the prognosis of melanoma was correlated to SOX10 expression. In a cohort of melanoma patients, the quartile low-SOX10 group had a significantly higher overall survival than the quartile high-SOX10 group (p=0.012) (Figure S4B). Interestingly, when the patients were stratified according to their mutational profile, SOX10 expression appeared to be a potential prognostic factor of oncologic outcomes in patients with BRAF-mutated melanoma (as A375 cell line) while no prognostic value was observed for RAS, NF1 and triple-negative melanomas (Figure S4C). This could be explained by the fact that aerobic glycolysis is upregulated in human $BRAF^{V600}$ melanoma cells via a transcriptional regulation of HK2 and GLUT1 (Parmenter *et al*, 2014). Thus, the transcriptional activation of HK2 by the MAPK/ERK pathway may lead to a translational activation of *SOX10*.

To confirm the *SOX10* mRNA translational regulation mediated by HK2, we monitored the level of *SOX10* mRNA isolated from all polysome fractions of A375 cells upon siRNA-mediated depletion of HK2. We found that *SOX10* mRNA shifted from heavy polysome fractions to lighter polysome fractions upon HK2 depletion, indicating that the depletion of the enzyme decreases the translation of the *SOX10* mRNA in melanoma cells (Figure 2A). Conversely, the translation of the *HPRT* mRNA (negative control) was not affected by HK2 depletion (Figure 2A). In agreement with our polysome data suggesting that HK2 is required for the translation of the *SOX10* mRNA, HK2 depletion decreased SOX10 protein levels, as observed in western blot analyses of different BRAF-mutated (V600E) melanoma cell lines (Figure 2B). This regulation appears to be specific to HK2 as the depletion of GAPDH did not affect SOX10 expression (Figure 2B). In addition, the *SOX10* mRNA level, which was

evaluated by RT-qPCR, remained unchanged upon HK2 depletion (Figure 2C). Collectively, our results demonstrate that HK2 regulates the translation of cancer-relevant mRNAs, and more specifically of the *SOX10* mRNA.

HK2 directly binds RNA

To test the hypothesis that HK2 directly interacts with RNA, we first performed Complex Capture experiments (2C) (Asencio *et al*, 2018). This approach takes advantage of the ability of negatively charged nucleic acids to bind silica matrix-based columns, consequently retaining UV-crosslinked RNA-RBP complexes. HK2 was retained on the column in extracts of UV-C irradiated cells, but not detected in RNase A-treated samples, demonstrating that HK2 was retained on the column due to its UVC-induced covalent interaction with RNAs (Figure 3A). The well-characterized RBP HuR was used as a positive control in this assay, as well as the non-canonical RNA-metabolic enzymes GAPDH and PKM2. The metabolic enzymes ACOT1/2 and HSC70 were used as negative controls. To gain more evidence that HK2 binds to RNA, we performed CrossLinking ImmunoPrecipitation (CLIP) assay (Hafner *et al*, 2021; Lee & Ule, 2018). This assay relies on the UVC-dependent crosslinking of RNA-RBP complexes in living cells followed by cell lysis and partial RNA digestion with RNase I. The RNA molecules crosslinked to HK2 were then recovered through HK2 immunoprecipitation and radioactively labelled with ^{32}P-yATP and T4 polynucleotide kinase (PNK). We observed a radioactive signal at the molecular size of HK2 in UVC-treated samples (Figure 3B). The signal was not detected in the non-crosslinked conditions or in IgG-immunoprecipitated conditions (negative controls) (Figure 3B). The signal was modulated according to the RNase I concentration used in UV-crosslinked cells; at higher concentrations, the radioactive signal collapsed to a sharp band at the molecular mass of HK2. These results indicate that HK2 directly interacts with RNA in living A375 melanoma cells.

We next examined whether the RNA-binding activity of HK2 was dependent on its hexokinase activity or subcellular localization. We ectopically expressed GFP-tagged HK2, either wild-type (HK2-WT) or mutants in HEK293T cells and performed the CLIP assay. We used the HK2-MBD mutant, which carries a deletion of the first 15 amino acids that are critical for the association of HK2 with the outer membrane of the mitochondria through its interaction with the voltage-dependent anion-selective channel 1 (VDAC-1) (Wolf *et al*, 2016). This binding has been shown to enhance

glycolysis due to privilege access of HK2 to newly synthesized ATP generated by the mitochondria. However, HK2 has been shown to alternate between cytoplasmic and mitochondrial-bound states in response to environmental and metabolic stress (Guo *et al*, 2022). The second tested mutant was the HK2-DA mutant, in which alanine is substituted to two aspartic acid residues in both the amino- and carboxy-terminal domains of HK2 (D209A/D657A). Mutations in both sites inhibit HK2 binding to glucose (Nawaz *et al*, 2018). Additionally, we tested whether the catalytic activity of HK2 is necessary for its binding to RNA. To this end, alanine was substituted for two serine residues in both the amino- and carboxy-terminal domains of HK2 (HK2-SA mutant; S155A/S603A) (Guo *et al*, 2022). As expected, we observed a sharp radioactive signal at the molecular size of HK2-FL-GFP (~129 kDa), which corresponds to the upper band (Figure 3C). The lower band, labelled with an asterisk, corresponds to a non-specific signal. Strikingly, all mutants retained their ability to bind RNA, indicating that the interaction of HK2 with RNA is independent of its enzymatic activity, its ability to bind to glucose or its subcellular localization.

To further study HK2-RNA interaction, we subjected RNase-treated or untreated lysates of A375 cells to sucrose density gradient (5-25%) ultracentrifugation and fractionation. By these means, we found that 18% of the total cellular HK2 changed its distribution in the sucrose gradient following RNase treatment, indicating that the composition of HK2-containing complexes is partially dependent on RNA (Figure 3D). Intriguingly, complexes containing either GAPDH or PKM2 showed less sensitivity to RNase treatment (Figure S5). In contrast to HUR, HK2 presented an RNA-dependent shift to more dense fractions suggesting that the presence of RNA might prevent the formation of heavy HK2-containing complexes.

HK2 associates with the *SOX10* mRNA

We next determined whether HK2 could specifically associate with the *SOX10* mRNA, which was identified to be translationally regulated by HK2. By performing HK2 immunoprecipitation (IP) followed by RT-qPCR (RNA ImmunoPrecipitation-RIP analysis), we identified an enrichment of the *SOX10* mRNA in HK2 IP over the control IP using IgG antibodies of the same isotype (Figure 4A). mRNAs of similar or higher abundance such as *GAPDH*, *TBP* and *actin* were less enriched in the HK2 IP indicating that HK2 specifically binds to the *SOX10* mRNA (Figure 4A and S7A). To delineate the HK2 binding site on the *SOX10* mRNA, *CatRAPID* fragment prediction

(Armaos *et al*, 2021) was employed and revealed a significant binding site of HK2 to the *SOX10* sequence located between nucleotides 206 and 321. This region corresponds to the 5′ untranslated region (5′ UTR) of the *SOX10* mRNA (Figure 4B). We transfected A375 cells with plasmids containing either the *SOX10* 5'UTR, the 3'UTR or no *SOX10* sequences (empty vector) and performed RIP experiments. Consistent with the *in silico* prediction, we observed a significant enrichment of the 5'UTR-containing mRNA over the 3'UTR-containing mRNA (Figure 4C and S6). To provide additional evidence that HK2 associates with the 5'UTR of the *SOX10* mRNA, we used an immunofluorescence-based RNA-Proximity Ligation Assay (RNA-PLA) (Zhang *et al*, 2016). The RNA-PLA assay enables the study of the association of proteins of interest with their target RNAs *in situ*. The association of HK2 with the *SOX10* mRNA was observed by a robust RNA-PLA signal (Figure 4D), which was generated by the use of an antibody that specifically recognizes HK2, in combination with an antisense probe that hybridize close to the predicted HK2-*SOX10* interaction region within the 5'UTR. To further confirm the specificity of the PLA signal, we depleted HK2 or SOX10 using target-specific siRNAs. As expected, siRNA-mediated depletion of HK2 or *SOX10* mRNA resulted in a loss of proximity signal when compared to the cells transfected with control siRNA (Figure 4D and S6C), demonstrating the specificity of the signal for HK2-*SOX10* 5'UTR interactions. Together, these results indicate that HK2 preferentially associates with *SOX10* via its 5'UTR.

The 3' half of the *SOX10* 5'UTR is essential for *SOX10* 5'UTR-driven translation and HK2 association

Next, we sought to define the *cis*-acting elements on the *SOX10* mRNA involved in the translational regulation by HK2. To this end, we performed a luciferase assay coupled with RT-qPCR using constructs containing the full-length (FL) 5′ and 3' UTR of *SOX10* mRNA, which were cloned upstream and downstream of a Renilla ORF, respectively. We also generated six *SOX10* 5'UTR deletion mutants containing distinct deletions of ~50 nucleotides each (Δ1 to Δ6, based on the region of the deletion) (Figure 5A). In this assay, we transiently transfected the Renilia reporters together with a control Firefly luciferase expressing plasmid into A375 cells and quantified the relative Renilia over Firefly luciferase activities (Rluc/Fluc ratio). We observed a higher Rluc/Fluc ratio for the construct containing the 5'UTR compared to the 3'UTR or no

UTR ("empty") showing the importance of the 5'UTR in the translation of the *SOX10* mRNA. We also observed that the constructs expressing the Δ4, Δ5 and Δ6 deletions (but not the Δ1, Δ2 and Δ3 deletions) presented a reduced Rluc/Fluc ratio when compared to the 5'UTR-containing plasmid (Figure 5B). Of note, the different *SOX10* vectors expressed a similar level of RNA (Figure 5C), suggesting that the 3' half of the *SOX10* 5'UTR (152-301 nts) is essential for efficient translation. We next explored the possibility that the observed translation effects were mediated by HK2 association to the *SOX10* 5'UTR. Using RIP experiments, we found a reduced association between HK2 and the Δ4, Δ5 and Δ6 deletion mutants of the 5'UTR RNA (with a significant effect for the Δ4 deletion) (Figure 5D). Together, these results indicate that the 3' half of the *SOX10* 5'UTR is crucial for HK2 association and for driving *SOX10* 5'UTR-mediated translation.

HK2-dependent *SOX10* translational regulation is involved in colony formation and proliferation properties of melanoma cells

We next investigated the possibility that the HK2-*SOX10* 5'UTR interaction is involved in cancer-related phenotypes. Functional assays were conducted in A375 and A2058 melanoma cell lines upon HK2 knock down. To investigate whether the effects observed by depleting HK2 are mediated by the 5'UTR-dependent translation regulation of the *SOX10* mRNA, we ectopically expressed SOX10 in both cell lines through the transduction of lentivirus particles carrying the sequence of the human SOX10 open reading frame (ORF) (Figure 6A), without the 5′UTR. We found that HK2 knock down led to decreased colony formation and proliferation of melanoma cells (Figure 6B-C). As expected, SOX10 ectopic expression reduced the effect of HK2 depletion on colony formation, while rescuing the proliferation properties of the melanoma cells (Figure 6B-C). Collectively, our findings indicate that the oncogenic functions of HK2 in melanoma cells are, at least in part, dependent on the translational regulation of the *SOX10* mRNA via its 5' UTR.

DISCUSSION

The glycolytic enzyme HK2 has recently been found to perform non-glycolytic activities in cancer, including regulation of transcription (Wang *et al*, 2017), anti-apoptotic (Zheng *et al*, 2023; AZOULAY-ZOHAR *et al*, 2004), scaffolding activities (Blaha *et al*,

2022), and protein kinase activities mediating tumour immune evasion (Guo *et al*, 2022). In yeast, hexokinases have been shown to directly bind to nucleic acids (Asencio *et al*, 2018), thus suggesting unexpected DNA- or RNA-binding activities. Although HK2 does not harbour any recognisable RNA-binding domain, this kinase has been proposed to bind to poly(A) and non-poly(A) RNAs in human cells in large-scale RNA interactome studies (Backlund *et al*, 2020; Trendel *et al*, 2019; Queiroz *et al*, 2019; Urdaneta *et al*, 2019). In this work, we demonstrated that HK2 is a novel *bona-fide* RNA-binding protein implicated in the control of mRNA translation in melanoma. We found that HK2 specifically binds the *SOX10* mRNA, a key transcriptional factor involved in tumour initiation, and regulates mRNA translation initiation in a 5'UTR-dependent manner. We found that the *SOX10* 5'UTR is essential for HK2 association and translation.

Some reports have demonstrated the involvement of the RNA-binding activity exerted by GAPDH in the control of mRNA stability through interaction with 3'UTRs of several mRNAs in cancer cells (Kondo *et al*, 2011; Bonafé *et al*, 2005; Zhou *et al*, 2008; Ikeda *et al*, 2012). In addition, PKM has been shown to promote ribosome stalling in the vicinity of glutamate- and lysine-encoding regions in ORFs, thereby inhibiting translation elongation (Kejiou *et al*, 2023). Our findings extend these studies, providing new evidence that the moonlighting RNA-binding activity of glycolytic enzymes (*i.e.* HK2) plays a key role in translational initiation through an interaction with a 5'UTR.

Since (i) regulation of translation initiation is a crucial mechanism for gene expression, dynamically regulating protein synthesis and thereby contributing to the determination of the cellular phenotype (Song *et al*, 2021; Fabbri *et al*, 2021), and (ii) our results demonstrate that the HK2-*SOX10* 5'UTR RNA-protein interaction is involved in cancer-relevant processes such as the ability of melanoma cells to proliferate and form colonies, further research is needed to unravel the factors involved in the regulation of *SOX10* mRNA translation by HK2. This is particularly important since HK2 is an attractive target in cancer (Shan *et al*, 2022) and since SOX10 is not only critical in melanoma proliferation but also a factor of resistance to immunologic cell death (Rosenbaum *et al*, 2024).

Our findings underscore a non-metabolic function of HK2, indicating that cancer cells may enhance glycolysis for purposes beyond simple anabolism. While aerobic

glycolysis provides significant advantages for rapidly growing and proliferating cells, contributing to 60% of total cellular ATP production in cancer cells (Busk *et al*, 2008) and supplying glycolytic intermediates necessary for the biosynthesis of nucleic acids, lipids, and amino acids (Vander Heiden *et al*, 2009), its role extends further. Given that many glycolytic enzymes also serve as RNA-binding proteins engaged in post-transcriptional RNA-processing reactions and considering that aberrant mRNA translation is a hallmark of tumours, it is crucial to investigate the significance of HK2 interactions with RNA beyond the *SOX10* mRNA. HK2 might regulate the translation of several other key mRNAs involved in cancer-relevant signalling pathways. Understanding the cellular processes influenced by HK2 RNA-binding activity and uncovering their underlying molecular mechanisms represent promising directions for future research. Such studies could lead to the development of novel therapeutics that specifically block HK2-RNA interaction in cancer cells while sparing non-malignant counterparts, offering new perspectives in cancer treatment.

METHODS

Cell culture, transfection and transduction

M249 cells were grown in RPMI 1640 (Biowest, #L0500) supplemented with 10% FBS (Gibco™, #A5256701) and 2 mM L-glutamine (Eurobio-Scientific, #CSTGLU00-0U). MALME 3M cells were grown in high glucose (4.5 g/L) DMEM supplemented with 20% FBS. HEK293T, A375, A258 and other melanoma cells were grown in high glucose DMEM (Biowest, #L0101-500) supplemented with 10% FBS and 2 mM L-glutamine. All cells were grown in 5% CO2 humidified incubator at 37°C. When indicated, the high glucose medium of A375 cells was replaced with glucose-free DMEM (Gibco™, #11966025) containing 10% FBS and 2 mM L-glutamine and supplemented with 5 g/L galactose (Sigma-Aldrich, #G5388) or 16mM 2-DG (MedChemExpress, #HY-13966) when indicated. The cells were washed with PBS before the medium was replaced. Cells were regularly tested for mycoplasma and authenticated by short tandem repeat (STR) profiling.

Cells were plated one day before for siRNA and plasmid transfections. The siRNAs were purchased from Dharmacon (ON-TARGETplus technology), and siRNA transfections were performed using Lipofectamine RNAiMAX (Invitrogen™, #13778150) according to manufacturer's instructions. Transfected cells were either

harvested at 48h or re-plated 24 h after transfection, as indicated in the figure legends. Plasmid transfections were performed using Lipofectamine 2000 (Invitrogen™, #11668019) or JetPEI (Polyplus Transfection, #101000020), and the transfection was performed according to manufacturer's instructions. At 48 h post-transfection, cells were harvested for further analysis. Lipofectamine 2000 was used for the transfection of Renilla and Firefly luciferase reporters in A375 cells. The cDNA for human *SOX10* 5'UTR and 3'UTR were subcloned into the pRP(Exp)-EGFP-CMV vector upstream and downstream a Renilla sequence, respectively, and they were kindly provided by Prof Caroline Robert (Gustave Roussy, France). Site-directed mutagenesis of *SOX10* 5'UTR was performed using Q5® Site-Directed Mutagenesis Kit (New England Biolabs, #E0554) according to the manufacturer's instructions. JetPEI was used for transient transfection of HK2 plasmids in HEK293T cells. HK2 (NM_000189.5) plasmids were purchased from VectorBuilder. HK2-WT (wild-type; #VB220927-1092xyz), DA (D209A/D657A, a non-glucose-binding mutant; #VB221214-1257apk), SA (S340A/S788A, a catalytically inactive mutant; #VB221214-1258ubs), and MBD (deletion of 1–15aa, mitochondrial-binding deficient; #VB221214-1255ezg) were cloned into a pLV[Exp]-Puro-CMV EGFP expressing vector.

To establish the stable overexpression of SOX10 (Myc-DDK tagged; OriGene, #RC203545L3V) in A375 and A2058 cell lines, cells were transduced with pLenti-C-Myc-DDK-P2A-Puro vector expressing SOX10 (NM_006941) ORF nucleotide sequence (OriGene, #RC203545L3V) according to manufacturer's instructions. Lentivirus infection was performed during 48h, and cells were selected with puromycin (2 µg/ml). Western blot and RT-qPCR analyses were performed to confirm the ectopic expression of SOX10 in the stable cells. The stablished cell lines were cultured in high glucose DMEM medium with 10% FBS and 2 mM L-glutamine supplemented with puromycin (2 µg/ml).

Polysome profiling

Polysome profiling was performed as previously described (Shen *et al*, 2019; Boussemart *et al*, 2014). Briefly, A375 cells were incubated with 100 µg/mL cycloheximide in fresh medium at 37 °C for 5 min. Cells were then washed, scraped into ice-cold PBS supplemented with 100 µg/mL cycloheximide (Sigma-Aldrich, #C4859), and centrifuged for 10 min at 3000 rpm. The cell pellets were re-suspended

into 400 µL of LSB buffer (20 mM Tris, pH 7.4, 100 mM NaCl, 3 mM MgCl2, 0.5 M sucrose, 1 mM DTT, 100 U/mL RNasOUT and 100 µg/mL cylcoheximide). After homogenization, 400 µL LSB buffer supplemented with 0.2 % Triton X-100 and 0.25 M sucrose was added. Samples were incubated on ice for 30 min, and then centrifuged at 12,000 × g for 15 min at 4 °C. The supernatant was adjusted to 5 M NaCl (Sigma-Aldrich, #S6546) and 1 M MgCl2 (Invitrogen™, AM9530G). The lysates were then loaded onto a 5–50% sucrose density gradient and centrifuged in an SW41 Ti rotor (Beckman) at 36,000 rpm for 2 h at 4 °C. Polysome fractions were monitored and collected using a gradient fractionation system (Isco). The sucrose gradient fractions were stored at -80°C or directly processed for western blot analysis or RNA extraction. For RT-qPCR analysis, RNAs from each fraction were extracted using TRIzol-LS (Invitrogen™, #10296028) according to manufacturer's procedure and were quantified using RNA 2100 Bioanalyzer (Agilent Genomics). The expression of a panel of 84 EMT-associates genes was measured using RT^2 Profiler PCR Array (qPCR Qiagen EMT array, #330231) in both total RNA and polysomal RNA levels of A375 cells transfected with siRNAs targeting HK2 or control.

RNA sequencing and bioinformatic analysis

RNA sequencing libraries were prepared from 500ng to 1µg of total RNA or mRNA-enriched from heavy polysome fractions using the Illumina TruSeq Stranded mRNA Library preparation kit which allows to perform a strand specific sequencing. Nanodrop spectrophotometer was used to assess purity of RNA based on absorbance ratios (260/280 and 260/230) and BioAnalyzer for RNA integrity (RIN>9). A first step of polyA+ selection using magnetic beads is done to focus sequencing on polyadenylated transcripts. After fragmentation, cDNA synthesis was performed and resulting fragments were used for dA-tailing followed by ligation of TruSeq indexed adapters. PCR amplification was finally achieved to generate the final barcoded cDNA libraries. The libraries were equimolarly pooled and subjected to qPCR quantification using the KAPA library quantification kit (Roche). Sequencing was carried out on the NovaSeq 6000 instrument from Illumina based on a 2*100 cycle mode (paired-end reads, 100 bases) to obtain around 30 million clusters (60 million raw paired-end reads) per sample. Finally, Fastq files were generated from raw sequencing data using bcl2fastq pipeline performing data demultiplexing based on index sequences.

RNA-seq data were analyzed with the Institut Curie RNA-seq Nextflow pipeline (Servant *et al*, 2023) (v3.1.4). Briefly, raw reads were first trimmed with Trimgalor. Reads were aligned on the human reference genome (hg19) using STAR (STAR_2.6.1a_08-27). Genes abundances were then estimated using STAR, and the Gencode v34 annotation. Differential analysis between conditions were done using the R package Xtail (Xiao *et al*, 2016) only on protein coding genes.

We used the variance stabilizing transformation (VST) offered by *DESeq2* (Love *et al*, 2014) on the raw count data to stabilize the variance across the mean and then performed a principal components analysis (PCA). The PCA plots (Figure S7) were built using the ggplot2 package (Wickham, 2009).

Complex Capture (2C)

A375 cells were irradiated with UV-C light at 254 nm and lysed in HMGN150 buffer (20 mM HEPES pH 7,5; 150 mM NaCl; 2 mM MgCl2; 0.5% Nonidet P−40; 10% Glycerol). Lysates were cleared via centrifugation at 10,000 × g for 10 minutes at 4°C, and then treated or not with RNAse A (15µL of RNAse A at 10 mg/mL for 1 mg of proteins; Thermo Scientific™, #EN0531). A fraction of the input (2%) was kept as control for the protein expression on SDS-PAGE. The Quick-RNA Midiprep kit was to purify crosslinked nucleic acids–RBP complexes. RNA concentration of the eluate was measured using NanoDrop (Thermo Scientific™), and 50 µg RNA was treated with RNAse I (500 U; Invitrogen™, #AM2295) for 40 min at 30°C. The samples were then mixed with 1X loading buffer for subsequent capillary western blot analysis.

CrossLinking and immunoprecipitation (CLIP)

Cells were cultured on a 15 cm dish until 70-80 % of confluence. The medium was removed, and the cells were washed with ice-cold PBS and irradiated with UV-C light at 254 nm. The cells were then lysed in 1 mL RIPA lysis buffer (50 mM Tris-HCl pH 7.4, 100 mM NaCl, 1% Nonidet P-40, 0.1% SDS, 0.5% Sodium deoxycholate), supplemented with RNAseOUT (40 U/mL; Invitrogen™, #10777019) and protease inhibitor cocktail (complete EDTA free; Roche, #11873580001). Lysates were cleared via centrifugation at 18,000 x g for 10 minutes at 4°C, and then treated or not with RNAse I (0.3 – 1 U) in combination with TURBO™ DNase I (4 U; Invitrogen, #AM2238) and incubated at 37°C for 3 minutes at 800 rpm. 1% of the lysate was used as input material to quantify total protein concentration in western blot analysis. The rest of the

lysate was incubated with the HK2 antibody-conjugated beads or GFP-Trap® Magnetic Agarose (ChromoTek, #gtma) overnight at 4°C while constantly rotating. For endogenous HK2 immunoprecipitation, 9 µg of HK2 antibody (Abcam, ab209847) or appropriate control IgG (rabbit; Cell Signaling, #2729S) were coupled overnight at 4°C to 90µl Dynabeads Protein G (Invitrogen™) while constantly rotating, and prior to cell harvesting. Conversely, GFP-Trap® Magnetic Agarose was used for the immunoprecipitation of HK2 mutants conjugated with GFP. The immunocomplexes were washed twice with RIPA-S buffer (50 mM Tris- HCl pH 7.4, 1 M NaCl, 1 mM EDTA, 1% Nonidet P-40, 0.1% SDS, 0.5% Sodium deoxycholate) and twice with PNK buffer (20 mM Tris-HCl pH 7.4, 10 mM $MgCl_2$, 0.2% Tween 20). After washes, 10% of the immunocomplexes was used to validate the correct immunoprecipitation by western blot analysis. Then, crosslinked nucleic acids were radiolabeled with ATP, [γ-32P] (PerkinElmer) by T4 polynucleotide kinase (PNK; New England Biolabs, #M0201S) for 30 minutes at 37°C. After two washes with RIPA-S buffer and one wash with PNK buffer, protein-RNA complexes were eluted in 1X loading buffer at 75°C for 10 minutes and separated by SDS-PAGE. Then the gel was dried, and complexes were exposed to a phosphorimaging screen and scanned with Amersham™ Typhoon™ Biomolecular Imager (CYTIVA). The files were processed with ImageJ software.

Sucrose density gradient ultracentrifugation and fractionation

For the sucrose density gradient ultracentrifugation and fractionation assay, previously published protocols were used as a basis (Huppertz *et al*, 2022; Caudron-Herger *et al*, 2019). A375 cells were cultured on a 15 cm dish and lysed in 300 µl lysis buffer (25 mM Tris-HCl pH 7.4, 2 mM EDTA, 150 mM KCl, 1 mM NaF, 0.5 mM DTT, 0.5% Nonidet P-40), supplemented with protease inhibitor cocktail (complete EDTA free; Roche, #11873580001). As control, lysis buffer was also supplemented with RNAseOUT (40 U/mL; Invitrogen™, #10777019). Lysates were pre-cleared via centrifugation at 10,000 × g for 10 minutes at 4°C. The lysates were then treated with a combination of RNase I (150 U; Invitrogen™, #AM2295) and RNase A/T1 (50 U / 125 U; Thermo Scientific™, #EN0551) and incubated at 37°C for 15 minutes. For the control sample, RNaseOUT was added to the lysate and the sample was incubated for 15 min at 4°C. For the fractionation, sucrose gradients were prepared from 5% (w/v) to 25% (w/v) sucrose (in 150 mM KCl, 25 mM Tris-HCl pH 7.4 and 2 mM EDTA) using Isco Model

160 Gradient Former. Lysates were then separated by centrifugation at 30,000 rpm and 4°C in an SW41Ti rotor (Beckman) for 18 hours. After ultracentrifugation, the lysate fractions were monitored and carefully collected using a gradient fractionation system (Isco) (20 fractions were collected of approximately 1000 µl) and transferred into fresh 1.5 mL tubes. For the protein precipitation, 150 µl of cold 100% Trichloroacetic acid (TCA; Sigma-Aldrich, #T6399) was added, and the samples were incubated on ice for 30 minutes. The fractions were centrifuged at 18,000 x g for 20 minutes at 4°C. The TCA supernatant was carefully removed, and the pellets were washed once with 1 ml cold acetone (stored at −20°C). The fractions were vortexed, and an additional centrifugation step was performed at 18,000 x g for 30 minutes at 4°C. The supernatant was carefully removed, and the pellet air-dried. Finally, the pellets were resuspended in 20 µl 1X loading buffer, incubated at 95°C for 5 minutes, and used for SDS-PAGE and immunoblotting.

RNA immunoprecipitation (RIP) assay

Prior to harvesting cells, 9 µg of antibody anti-HK2 (Abcam, ab209847) were coupled overnight at 4°C to 90µl Dynabeads Protein G (Invitrogen™) while constantly rotating. A375 and A2058 cells were cultured on a 15 cm dish and lysed in 500 µl Co-IP buffer (50 mM Tris-HCl pH 7.4, 1 mM EDTA, 150 mM NaCl, 0.1% Nonidet P-40), supplemented with protease inhibitor cocktail (complete EDTA free; Roche, #11873580001) and RNAseOUT (40 U/mL; Invitrogen™, #10777019) for 30 minutes at 4°C. Lysates were cleared via centrifugation at 18,000 x g for 10 minutes at 4°C. After lysis, 1% and 10% of the lysate was used as input material to confirm total protein and RNA levels, respectively. The rest of the lysate was incubated with the HK2 antibody-conjugated beads overnight at 4°C while constantly rotating. The immunocomplexes were washed five times with ice-cold CO-IP buffer supplemented with protease inhibitor cocktail and RNAseOUT. After washes, 10% of the immunocomplexes was used to validate the correct immunoprecipitation by western blot analysis. The rest of the beads were eluted with 100 µl Protein-RNA elution buffer (100 mM Tris-HCl pH 8, 10 mM EDTA, 1% SDS) at 80°C for 5 minutes, followed by another 5 minutes incubation at room temperature. To recover the RNA bound by HK2, the beads were resuspended in TRIzol (Invitrogen™, #15596018), as well as the input RNA, and RNA extraction was followed according to manufacturer's procedure. The extracted RNA was then used for subsequent RT-qPCR experiments.

In silico binding prediction

The catRAPID algorithm (Armaos *et al*, 2021) was used to estimate the potential binding sites of HK2 on *SOX10* mRNA. The highest-raking site at RNA position 206-321 bp was used for subsequent analysis.

Seahorse metabolic flux assay

Oxygen consumption rates (OCR) and extracellular acidification rates (ECAR) were analysed on a XF96 Extracellular Flux Analyzer (Seahorse Bioscience). A375 cells were plated in non-buffered DMEM medium supplemented with 25 mM glucose (Sigma-Aldrich, #D9434) or galactose (Sigma-Aldrich, #G5388). Measurements were obtained under basal conditions (no treatment) and after the addition of mitochondrial inhibitors (oligomycin, 1µM; FCCP, 0.5µM; rotenone/antimycin A, 0.5µM), or glycolysis inhibitor (2-DG, 16mM) (MedChemExpress, #HY-13966).

Colony formation assay

Cells transfected with 25nM siRNA (Dharmacon) were seeded in triplicates in six-well plates. After 10 days of incubation, cells were washed with PBS 1X (Gibco™, #70011044) and stained with 0.5% of crystal violet (Sigma Aldrich, #C0775) for 15 min. Plates were washed with water and dried before imaging. Colony area was quantified using ImageJ-plugin “ColonyArea”(Guzmán *et al*, 2014).

Luciferase assay

A375 cells were transiently transfected with Firefly and Renilla luciferase reporters using Lipofectamine 2000 Reagent (Invitrogen™, #11668019). Renilla vectors containing the full-length (FL) *SOX10* 3’UTR or 5′UTR, as well as six *SOX10* 5’UTR mutants (Δ1-Δ6) harboring deletions of ~50 nucleotides, were transfected in the cells. An empty Renilla vector (without *SOX10* 5’ or 3’UTR) was used as control for the experiment. After 48h, part of the transfected cells was harvested for RNA extraction to measure the vectors’ RNA expression by qPCR, while the rest of the cells were used to measure the luciferase activity using the Dual-Luciferase Reporter Assay System (Promega). Data was presented as the ratio between Renilla and Firefly luciferase RNA expression or luminescence activities, respectively.

Proliferation assay

Cells transfected with 25nM siRNA (Dharmacon) were seeded in triplicates in six-well plates. The cell growth was analyzed for percent plate coverage with IncuCyte S3 Live Cell Analysis System (Sartorius). Pictures of each well were acquired every 3 hours for 7 days.

Protein extracts, SDS-PAGE and Western blot

Whole cell lysates were prepared using RIPA buffer supplemented with RNaseOUT (40 U/mL; Invitrogen™, #10777019) and protease inhibitor cocktail (complete EDTA free; Roche, #11873580001). Lysates were cleared via centrifugation at 18,000 x g for 10 minutes at 4°C. Cell lysates were quantified for protein concentration using a bicinchoninic acid (BCA) protein assay kit (Thermo Scientific™, #23225). Protein samples were resolved on NuPAGE 4–12% Bis-Tris gels with MOPS buffer or 3–8% Tris-acetate gels with Tris-acetate buffer (Life Technologies, #LA0041) and then transferred to 0.45 µm nitrocellulose membrane (Amersham). After saturation in Tris-buffered saline buffer containing 0.01% Tween-20 (TBST) and supplemented with 5% powdered milk, the membranes were incubated with primary antibodies either for 1 hour at room temperature or overnight at 4 °C with agitations, followed by 3 X TBST washes of 15 minutes each, and incubation of the membranes with peroxidase (HRP)-conjugated secondary antibodies diluted in 5% milk TBST for one hour at room temperature. After 3 X TBST washes of 5 minutes each, the membranes were incubated in ECL solution for development.

The following antibodies were used for assays: anti-HK2 (Abcam, #ab209847; 1:1,000 dilution), anti-SOX10 (Santa Cruz Biotechnology, #sc365692; 1:1,000 dilution), anti-GFP (Roche, #11814460001; 1:1,000 dilution), anti-HUR (Santa Cruz Biotechnology, #sc-5261; 1:1,000 dilution), anti-H3 (Abcam, #ab1791; 1:500 dilution), anti-GAPDH (Sigma-Aldrich, #G9545; 1:5,000), anti-PKM2 (Cell Signaling, #4053S; 1:1,000 dilution), anti-LDHB (Santa Cruz Biotechnology, #sc100775; 1:1,000 dilution), anti-S6 ribosomal protein (Cell Signaling, #2317; 1:1,000 dilution), anti-VCL (Abcam, #ab129002; 1:3,000 dilution), anti-alpha Tubulin antibody (GeneTex, # GTX628802; 1:1000 dilution), anti-HSC70 antibody (Santa Cruz Biotechnology, #sc-7298; 1:1,000 dilution), anti-ACOT1/2 (Santa Cruz Biotechnology, #sc-373917; 1:1000 dilution), goat anti-rabbit (Sigma-Aldrich, Thermo Fisher Scientific, 1:2,000 dilution) and goat anti-mouse (Sigma-Aldrich, Thermo Fisher Scientific, 1:5,000 dilution) antibodies.

RNA extraction and RT-qPCR

RNA was isolated using the TRIzol-chloroform method and treated with DNase I (TURBO DNA-free; Invitrogen™, #AM1907) according to the manufacturer's instructions. After DNase treatment, RNA was quantified using a Nanodrop 2000 spectrophotometer (Thermo Scientific™), and 1 µg total RNA was used to synthesize cDNA using SuperScript III Reverse Transcriptase (200 U/µL; Invitrogen™, #18080044) and random hexamer primers (Invitrogen™, #SO142), according to the manufacturer's instructions. Quantitative PCR (qPCR) was performed using the Power SYBR Green PCR Master Mix (Thermo Scientific™, #4367559) on a CFX96 Real-Time PCR Detection System (Bio-Rad Laboratories Inc). Primer sequences are given in Table S3. Gene expression values were determined relative to VCL and are shown as a relative fold change to the value of control samples. All experiments were performed in biological triplicates and error bars indicate ± standard deviation as assayed by the ΔΔCt method.

For RT-qPCR analysis of polysome fractions, RNA of each fraction (250 µL), comprising both monosome fractions and polysome fractions, was extracted using TRIzol LS (Invitrogen™, #10296028). The extracted RNA was diluted in 30 µL RNase-free water (Invitrogen™, #10977035). For each fraction, the same volume of RNA was retrotranscribed into cDNA using SuperScript IV Reverse Transcriptase (Invitrogen™, #18090010) and random hexamer primers (Invitrogen™, #SO142), according to the manufacturer's instructions. Following the reverse transcription, mRNA abundance was determined by qPCR using Power SYBR Green PCR Master Mix (Thermo Scientific™, #4367559). Data were analyzed by the threshold cycle (Ct) comparative method and quantified as percentage of the total RNA considering the whole fractions stand for 100%. HPRT gene was used as a control.

RNA Proximity Ligation Assay (RNA-PLA)

Interactions between HK2 and SOX10 mRNA were monitored *in cellulo* by RNA-PLA (Zhang *et al*, 2016). The experiment was performed using Duolink In situ Detection Reagents FarRed according to the manufacturer's instructions (Sigma-Aldrich, #DUO92013). A375 cells were seeded on coverslips 45mn 24 h before transfection with siRNAs targeting HK2 (siHK2), SOX10 (siSOX10) or control (siCTRL). After 48 h, cells were fixed with 4% PFA in PBS for 30 minutes at room temperature. Next,

coverslips were washed with PBS and permeabilized with Tween 0.2% in PBS for 10 minutes at room temperature. Cells were then washed with PBS and blocked using a blocking buffer (10% goat serum and 0.1% Triton X-100 in PBS supplemented with 10 ug of salmon sperm) for 1 h at room temperature. Cells were once again washed with PBS and incubated in blocking buffer containing 100 nM of an anti-sense PLUS probe in a wet chamber at 4°C overnight. Salmon sperm was boiled for 3 minutes at 70°C prior to addition. Of note, this probe was composed of a 20mer of DNA complementary to the SOX10 5'UTR, a polyA linker and a sequence complementary to the PLA MINUS probe:
GCGGTCCAGCTCGGGGCTGGGAGGTGACGCTGGTGGGCTGGGAGGGAAAAA AAAAAAAAAAAAAAAATATGACAGAACTAGACACTCTT.
Subsequently, cells were washed with PBS and incubated in blocking buffer for 1 h at room temperature. Then, HK2 primary antibody (Abcam, # ab209847) was diluted in blocking buffer (1.1000) and incubated for 1 h at 37°C. Next, the Duolink® PLA® probes anti-Rabbit MINUS (5X) containing secondary antibodies conjugated to oligonucleotides were added, and the mixture was incubated for 1 hour at 37°C. A ligation solution is then added to ligate the complementary oligonucleotides of the two probes (PLUS and MINUS) if in proximity (< 40 nm) to form a closed circle by incubating the coverslips 45mn at 37°C. This DNA was subsequently amplified by rolling circle replication: Duolink polymerase and its buffer are spread on the coverslips, then incubated for 2 hours at 37°C. The coverslips were finally mounted in ProLong™ Diamond Antifade Mountant with DAPI (Invitrogen™, #P36935) to visualize the nuclei and the amplicons were detected by far-red fluorescent probes. Images of each coverslip were acquired using Leica 3D SIM (Structured Illumination Microscopy) microscope at the PICT-IBiSA Imaging Facility in Orsay, and PLA spots were analyzed using the semi-automatic macro *Mic-Maq* on *Fiji* software.

Immunohistochemistry on patient biopsies

All patients signed an informed consent form that authorized tumor biopsies and molecular studies in the context of the institutional CRB-approved protocol MSN-08-027 CPP Ile de France (registration number: 2008-A00373-52).

Quantification and statistical analysis

Statistical analyses were performed on GraphPad Prism (Version 10.3.0) and statistical significance defined as a P value < 0.05 was determined by two-tailed unpaired Student's t test. Comparisons in multiple groups were analyzed with one-way or two-way ANOVA, as indicated in the figure legends. All data in this study are presented as the mean standard deviation or mean standard error.

ACKNOWLEDGEMENTS

This work was supported by grants from Institut Curie, Gustave Roussy, INSERM, CNRS, Equipe labellisée Ligue Nationale Contre le Cancer (LNCC) (to SV), La fondation Carrefour, la Fondation du Crédit Mutuel, et Sébastien Bazin (to CR). This project has received funding from the European Union's Horizon 2020 research and innovation program under the Marie Skłodowska-Curie grant agreement No 847718. High-throughput sequencing was performed by the ICGex NGS platform of the Institut Curie supported by the grants ANR-10-EQPX-03 (Equipex) and ANR-10-INBS-09-08 (France Génomique Consortium) from the Agence Nationale de la Recherche ("Investissements d'Avenir" program), by the ITMO-Cancer Aviesan (Plan Cancer III) and by the SiRIC-Curie program (SiRIC Grant INCa-DGOS-465 and INCa-DGOS-Inserm_12554). Data management, quality control and primary analysis were performed by the Bioinformatics platform of the Institut Curie. ALD was successively supported by pre-doctoral fellowships from the Marie Skłodowska-Curie grant agreement No 847718 and FRM (Fondation pour la Recherche Medicale). GC was supported by the Marie Sklodowska-Curie Campus France Fellowship PRESTIGE-2017-3-0017.

AUTHOR INFORMATION

ALD performed CLIP, RIP, WB, RT-qPCR, luciferase, proliferation and clonogenic assays. AMP and GC performed polysome profiling experiments. GC and VQ performed the 2C experiment. CML performed bioinformatic analysis. DB performed the RNA-PLA experiment. RNA sequencing was performed by VR and SB. ALD, AMP, GC, CR and SV conceived the experiments and analyzed data. SV and CR coordinated the whole study. ALD and SV wrote the manuscript with the help of CR and AMP. Funding acquisition: SV, CR

COMPETING INTERESTS

Authors declare that they have no competing interest.

DATA AVAILABILITY

All data are available in the main text or the supplementary materials.

The datasets generated in this study have been deposited in the Gene Expression Omnibus repository (GEO) under the accession number GSE274146 (token: **qpkhimgaffylzsd**).

SUPPLEMENTARY INFORMATION

Suppementary Figures S1-S7

Suppementary Table S1

Suppementary Table S2 and S3

REFERENCES

Armaos A, Colantoni A, Proietti G, Rupert J & Tartaglia GG (2021) catRAPID omics v2.0: going deeper and wider in the prediction of protein–RNA interactions. *Nucleic Acids Research* 49: W72–W79

Asencio C, Chatterjee A & Hentze MW (2018) Silica-based solid-phase extraction of cross-linked nucleic acid–bound proteins. *Life Science Alliance* 1

AZOULAY-ZOHAR H, ISRAELSON A, ABU-HAMAD S & SHOSHAN-BARMATZ V (2004) In self-defence: hexokinase promotes voltage-dependent anion channel closure and prevents mitochondria-mediated apoptotic cell death. *Biochemical Journal* 377: 347–355

Backlund M, Stein F, Rettel M, Schwarzl T, Perez-Perri JI, Brosig A, Zhou Y, Neu-Yilik G, Hentze MW & Kulozik AE (2020) Plasticity of nuclear and cytoplasmic stress responses of RNA-binding proteins. *Nucleic Acids Research* 48: 4725–4740

Blaha CS, Ramakrishnan G, Jeon S-M, Nogueira V, Rho H, Kang S, Bhaskar P, Terry AR, Aissa AF, Frolov MV, *et al* (2022) A non-catalytic scaffolding activity of hexokinase 2 contributes to EMT and metastasis. *Nat Commun* 13: 899

Bonafé N, Gilmore-Hebert M, Folk NL, Azodi M, Zhou Y & Chambers SK (2005) Glyceraldehyde-3-Phosphate Dehydrogenase Binds to the AU-Rich 3′ Untranslated Region of Colony-Stimulating Factor–1 (CSF-1) Messenger RNA in Human Ovarian Cancer Cells: Possible Role in CSF-1 Posttranscriptional Regulation and Tumor Phenotype. *Cancer Research* 65: 3762–3771

Boussemart L, Malka-Mahieu H, Girault I, Allard D, Hemmingsson O, Tomasic G, Thomas M, Basmadjian C, Ribeiro N, Thuaud F, *et al* (2014) eIF4F is a nexus of resistance to anti-BRAF and anti-MEK cancer therapies. *Nature* 513: 105–109

Busk M, Horsman MR, Kristjansen PEG, van der Kogel AJ, Bussink J & Overgaard J (2008) Aerobic glycolysis in cancers: Implications for the usability of oxygen-responsive genes and fluorodeoxyglucose-PET as markers of tissue hypoxia. *International Journal of Cancer* 122: 2726–2734

Castello A, Fischer B, Frese CK, Horos R, Alleaume A-M, Foehr S, Curk T, Krijgsveld J & Hentze MW (2016) Comprehensive Identification of RNA-Binding Domains in Human Cells. *Molecular Cell* 63: 696–710

Castello A, Hentze MW & Preiss T (2015) Metabolic Enzymes Enjoying New Partnerships as RNA-Binding Proteins. *Trends Endocrinol Metab* 26: 746–757

Caudron-Herger M, Rusin SF, Adamo ME, Seiler J, Schmid VK, Barreau E, Kettenbach AN & Diederichs S (2019) R-DeeP: Proteome-wide and Quantitative Identification of RNA-Dependent Proteins by Density Gradient Ultracentrifugation. *Molecular Cell* 75: 184-199.e10

Chang C-H, Curtis JD, Maggi LB, Faubert B, Villarino AV, O'Sullivan D, Huang SC-C, van der Windt GJW, Blagih J, Qiu J, *et al* (2013) Posttranscriptional control of T cell effector function by aerobic glycolysis. *Cell* 153: 1239–1251

Cronin JC, Loftus SK, Baxter LL, Swatkoski S, Gucek M & Pavan WJ (2018) Identification and functional analysis of SOX10 phosphorylation sites in melanoma. *PLoS One* 13: e0190834

DeBerardinis RJ & Chandel NS (2020) We need to talk about the Warburg effect. *Nat Metab* 2: 127–129

Fabbri L, Chakraborty A, Robert C & Vagner S (2021) The plasticity of mRNA translation during cancer progression and therapy resistance. *Nat Rev Cancer* 21: 558–577

Graf SA, Busch C, Bosserhoff A-K, Besch R & Berking C (2014) SOX10 promotes melanoma cell invasion by regulating melanoma inhibitory activity. *J Invest Dermatol* 134: 2212–2220

Guo D, Tong Y, Jiang X, Meng Y, Jiang H, Du L, Wu Q, Li S, Luo S, Li M, *et al* (2022) Aerobic glycolysis promotes tumor immune evasion by hexokinase2-mediated phosphorylation of IκBα. *Cell Metabolism* 34: 1312-1324.e6

Guzmán C, Bagga M, Kaur A, Westermarck J & Abankwa D (2014) ColonyArea: An ImageJ Plugin to Automatically Quantify Colony Formation in Clonogenic Assays. *PLOS ONE* 9: e92444

Hafner M, Katsantoni M, Köster T, Marks J, Mukherjee J, Staiger D, Ule J & Zavolan M (2021) CLIP and complementary methods. *Nat Rev Methods Primers* 1: 1–23

Han S, Ren Y, He W, Liu H, Zhi Z, Zhu X, Yang T, Rong Y, Ma B, Purwin TJ, *et al* (2018) ERK-mediated phosphorylation regulates SOX10 sumoylation and targets expression in mutant BRAF melanoma. *Nat Commun* 9: 28

Huppertz I, Perez-Perri JI, Mantas P, Sekaran T, Schwarzl T, Russo F, Ferring-Appel D, Koskova Z, Dimitrova-Paternoga L, Kafkia E, *et al* (2022) Riboregulation of Enolase 1 activity controls glycolysis and embryonic stem cell differentiation. *Molecular Cell* 82: 2666-2680.e11

Ikeda Y, Yamaji R, Irie K, Kioka N & Murakami A (2012) Glyceraldehyde-3-phosphate dehydrogenase regulates cyclooxygenase-2 expression by targeting mRNA stability. *Archives of Biochemistry and Biophysics* 528: 141–147

Kejiou NS, Ilan L, Aigner S, Luo E, Tonn T, Ozadam H, Lee M, Cole GB, Rabano I, Rajakulendran N, *et al* (2023) Pyruvate Kinase M (PKM) binds ribosomes in a poly-ADP ribosylation dependent manner to induce translational stalling. *Nucleic Acids Research* 51: 6461–6478

Kondo S, Kubota S, Mukudai Y, Nishida T, Yoshihama Y, Shirota T, Shintani S & Takigawa M (2011) Binding of glyceraldehyde-3-phosphate dehydrogenase to the *cis*-acting element of structure-anchored repression in *ccn2* mRNA. *Biochemical and Biophysical Research Communications* 405: 382–387

Kudryavtseva AV, Fedorova MS, Zhavoronkov A, Moskalev AA, Zasedatelev AS, Dmitriev AA, Sadritdinova AF, Karpova IY, Nyushko KM, Kalinin DV, *et al* (2016) Effect of lentivirus-mediated shRNA inactivation of HK1, HK2, and HK3 genes in colorectal cancer and melanoma cells. *BMC Genet* 17: 156

Lee FCY & Ule J (2018) Advances in CLIP Technologies for Studies of Protein-RNA Interactions. *Mol Cell* 69: 354–369

Liu Z, Jia X, Duan Y, Xiao H, Sundqvist K-G, Permert J & Wang F (2013) Excess glucose induces hypoxia-inducible factor-1α in pancreatic cancer cells and stimulates glucose metabolism and cell migration. *Cancer Biol Ther* 14: 428–435

Love MI, Huber W & Anders S (2014) Moderated estimation of fold change and dispersion for RNA-seq data with DESeq2. *Genome Biology* 15: 550

Lunt SY & Vander Heiden MG (2011) Aerobic glycolysis: meeting the metabolic requirements of cell proliferation. *Annu Rev Cell Dev Biol* 27: 441–464

Miao W, Porter DF, Lopez-Pajares V, Siprashvili Z, Meyers RM, Bai Y, Nguyen DT, Ko LA, Zarnegar BJ, Ferguson ID, *et al* (2023) Glucose dissociates DDX21 dimers to regulate mRNA splicing and tissue differentiation. *Cell* 186: 80-97.e26

Nagy E & Rigby WFC (1995) Glyceraldehyde-3-phosphate Dehydrogenase Selectively Binds AU-rich RNA in the NAD+-binding Region (Rossmann Fold) (∗). *Journal of Biological Chemistry* 270: 2755–2763

Nawaz MH, Ferreira JC, Nedyalkova L, Zhu H, Carrasco-López C, Kirmizialtin S & Rabeh WM (2018) The catalytic inactivation of the N-half of human hexokinase 2

and structural and biochemical characterization of its mitochondrial conformation. *Biosci Rep* 38: BSR20171666

Parmenter TJ, Kleinschmidt M, Kinross KM, Bond ST, Li J, Kaadige MR, Rao A, Sheppard KE, Hugo W, Pupo GM, *et al* (2014) Response of BRAF-mutant melanoma to BRAF inhibition is mediated by a network of transcriptional regulators of glycolysis. *Cancer Discov* 4: 423–433

Patra KC, Wang Q, Bhaskar PT, Miller L, Wang Z, Wheaton W, Chandel N, Laakso M, Muller WJ, Allen EL, *et al* (2013) Hexokinase 2 is required for tumor initiation and maintenance and its systemic deletion is therapeutic in mouse models of cancer. *Cancer Cell* 24: 213–228

Qin J-Z, Xin H & Nickoloff BJ (2010) Targeting glutamine metabolism sensitizes melanoma cells to TRAIL-induced death. *Biochemical and Biophysical Research Communications* 398: 146–152

Queiroz RML, Smith T, Villanueva E, Marti-Solano M, Monti M, Pizzinga M, Mirea D-M, Ramakrishna M, Harvey RF, Dezi V, *et al* (2019) Comprehensive identification of RNA–protein interactions in any organism using orthogonal organic phase separation (OOPS). *Nat Biotechnol* 37: 169–178

Rosenbaum SR, Caksa S, Stefanski CD, Trachtenberg IV, Wilson HP, Wilski NA, Ott CA, Purwin TJ, Haj JI, Pomante D, *et al* (2024) SOX10 Loss Sensitizes Melanoma Cells to Cytokine-Mediated Inflammatory Cell Death. *Molecular Cancer Research* 22: 209–220

Rossman MG, Liljas A, Brändén C-I & Banaszak LJ (1975) 2 Evolutionary and Structural Relationships among Dehydrogenases. In *The Enzymes*, Boyer PD (ed) pp 61–102. Academic Press

Scott DA, Richardson AD, Filipp FV, Knutzen CA, Chiang GG, Ronai ZA, Osterman AL & Smith JW (2011) Comparative metabolic flux profiling of melanoma cell lines: beyond the Warburg effect. *J Biol Chem* 286: 42626–42634

Servant N, Philippe LR, phupe & Allain F (2023) bioinfo-pf-curie/RNA-seq: v4.0.0.

Shan W, Zhou Y & Tam KY (2022) The development of small-molecule inhibitors targeting hexokinase 2. *Drug Discovery Today* 27: 2574–2585

Shen S, Faouzi S, Bastide A, Martineau S, Malka-Mahieu H, Fu Y, Sun X, Mateus C, Routier E, Roy S, *et al* (2019) An epitranscriptomic mechanism underlies selective mRNA translation remodelling in melanoma persister cells. *Nat Commun* 10: 5713

Simsek D, Tiu GC, Flynn RA, Byeon GW, Leppek K, Xu AF, Chang HY & Barna M (2017) The Mammalian Ribo-interactome Reveals Ribosome Functional Diversity and Heterogeneity. *Cell* 169: 1051-1065.e18

Song P, Yang F, Jin H & Wang X (2021) The regulation of protein translation and its implications for cancer. *Sig Transduct Target Ther* 6: 1–9

Trendel J, Schwarzl T, Horos R, Prakash A, Bateman A, Hentze MW & Krijgsveld J (2019) The Human RNA-Binding Proteome and Its Dynamics during Translational Arrest. *Cell* 176: 391-403.e19

Urdaneta EC, Vieira-Vieira CH, Hick T, Wessels H-H, Figini D, Moschall R, Medenbach J, Ohler U, Granneman S, Selbach M, *et al* (2019) Purification of cross-linked RNA-protein complexes by phenol-toluol extraction. *Nat Commun* 10: 990

Vander Heiden MG, Cantley LC & Thompson CB (2009) Understanding the Warburg Effect: The Metabolic Requirements of Cell Proliferation. *Science* 324: 1029–1033

Wang F, Zhang S, Vuckovic I, Jeon R, Lerman A, Folmes CD, Dzeja PP & Herrmann J (2018) Glycolytic Stimulation Is Not a Requirement for M2 Macrophage Differentiation. *Cell Metabolism* 28: 463-475.e4

Wang W, Liu Z, Zhao L, Sun J, He Q, Yan W, Lu Z & Wang A (2017) Hexokinase 2 enhances the metastatic potential of tongue squamous cell carcinoma via the SOD2-H2O2 pathway. *Oncotarget* 8: 3344–3354

Warburg O (1956) On Respiratory Impairment in Cancer Cells. *Science* 124: 269–270

Weinberg F, Hamanaka R, Wheaton WW, Weinberg S, Joseph J, Lopez M, Kalyanaraman B, Mutlu GM, Budinger GRS & Chandel NS (2010) Mitochondrial metabolism and ROS generation are essential for Kras-mediated tumorigenicity. *Proceedings of the National Academy of Sciences* 107: 8788–8793

Wickham H (2009) ggplot2: Elegant Graphics for Data Analysis New York, NY: Springer

Wolf A, Agnihotri S, Micallef J, Mukherjee J, Sabha N, Cairns R, Hawkins C & Guha A (2011) Hexokinase 2 is a key mediator of aerobic glycolysis and promotes tumor growth in human glioblastoma multiforme. *J Exp Med* 208: 313–326

Wolf AJ, Reyes CN, Liang W, Becker C, Shimada K, Wheeler ML, Cho HC, Popescu NI, Coggeshall KM, Arditi M, *et al* (2016) Hexokinase Is an Innate Immune Receptor for the Detection of Bacterial Peptidoglycan. *Cell* 166: 624–636

Xiao Z, Zou Q, Liu Y & Yang X (2016) Genome-wide assessment of differential translations with ribosome profiling data. *Nat Commun* 7

Zhang C, Liu J, Liang Y, Wu R, Zhao Y, Hong X, Lin M, Yu H, Liu L, Levine AJ, *et al* (2013) Tumour-associated mutant p53 drives the Warburg effect. *Nat Commun* 4: 2935

Zhang W, Xie M, Shu M-D, Steitz JA & DiMaio D (2016) A proximity-dependent assay for specific RNA–protein interactions in intact cells. *RNA* 22: 1785–1792

Zheng Y, Zhan Y, Zhang Y, Zhang Y, Liu Y, Xie Y, Sun Y, Qian J, Ding Y, Ding Y, *et al* (2023) Hexokinase 2 confers radio-resistance in hepatocellular carcinoma by promoting autophagy-dependent degradation of AIMP2. *Cell Death Dis* 14: 1–13

Zhou Y, Yi X, Stoffer JB, Bonafe N, Gilmore-Hebert M, McAlpine J & Chambers SK (2008) The Multifunctional Protein Glyceraldehyde-3-Phosphate Dehydrogenase Is Both Regulated and Controls Colony-Stimulating Factor-1 Messenger RNA Stability in Ovarian Cancer. *Molecular Cancer Research* 6: 1375–1384

Figure 1

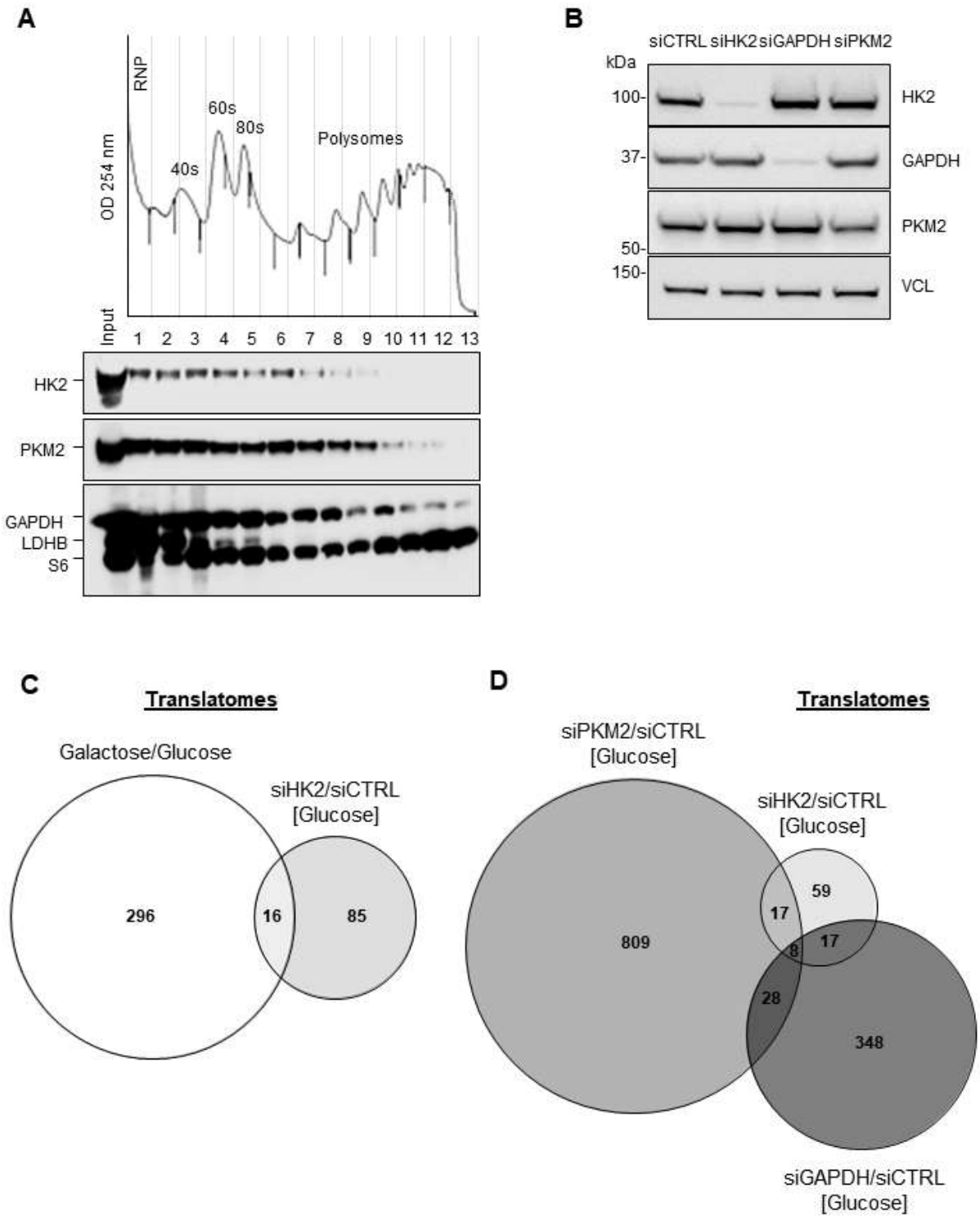
A
RNP
60s
80s
Polysomes
40s
OD 254 nm
Input
1 2 3 4 5 6 7 8 9 10 11 12 13
HK2
PKM2
GAPDH
LDHB
S6
B
siCTRL siHK2 siGAPDH siPKM2
kDa
100-
37-
50-
150-
HK2
GAPDH
PKM2
VCL
C
Translatomes
Galactose/Glucose
siHK2/siCTRL
[Glucose]
296
16
85
D
Translatomes
siPKM2/siCTRL
[Glucose]
siHK2/siCTRL
[Glucose]
809
59
17
8
17
28
348
siGAPDH/siCTRL
[Glucose]

Figure 1. HK2 regulates mRNA translation in melanoma cells.

(A) Western blot analysis of HK2, PKM2, GAPDH, LDHB and the ribosomal protein S6 in fractions (horizontal axes) obtained by sucrose-gradient (10-50%) ultracentrifugation of lysates from A375 cells. The cells were treated with 100 µg/ml Cycloheximide for 10 min prior to lysis to stabilize polysomes. Nucleic acids were monitored by OD254 nm, and proteins were monitored in each fraction by western blot. **(B)** Western blot analysis of HK2, GAPDH and PKM2 protein levels in A375 melanoma cells upon siRNA-mediated depletion of the enzymes (siHK2, siGAPDH and siPKM2, respectively) or control (siCTRL). VCL was used as loading control. **(C)** Comparison of translatomes between A375 cells cultured in galactose-containing medium relative to glucose (312 deregulated mRNAs, 214 being upregulated and 98 downregulated) and siRNA-mediated depletion of HK2 in cells cultured in glucose-containing medium relative to control (siHK2/siCTRL; 101 deregulated mRNAs, being 52 upregulated and 49 downregulated) (n = 3 biological replicates). **(D)** Comparison of translatomes between A375 cells upon siRNA-mediated depletion of key glycolytic enzymes (HK2, GAPDH, PKM2) in A375 cells relative to control. 401 mRNA candidates (269 upregulated and 132 downregulated) were found deregulated upon siRNA-mediated depletion of GAPDH relative to control (siGAPDH/siCTRL), and 862 mRNA candidates (554 upregulated and 308 downregulated) were found deregulated upon siRNA-mediated depletion of PKM2 (siPKM2/siCTRL). P-value ≤ 0.05 with fold change > 0.7 (DESeq2).

Figure 2

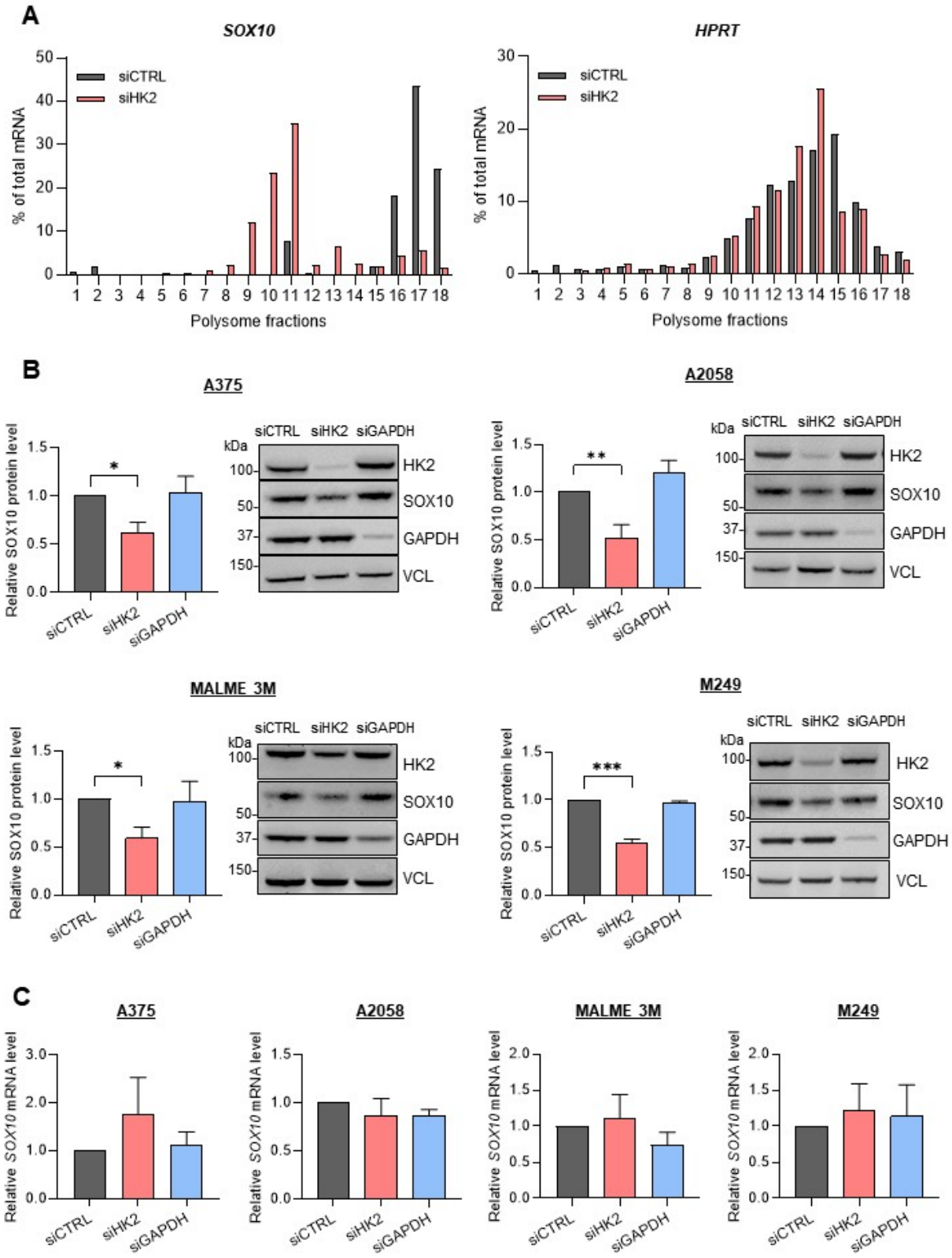
A
SOX10
HPRT
siCTRL
siHK2
% of total mRNA
Polysome fractions
B
A375
A2058
MALME_3M
M249
Relative SOX10 protein level
siCTRL siHK2 siGAPDH
kDa
HK2
SOX10
GAPDH
VCL
C
Relative SOX10 mRNA level

Figure 2. HK2 regulates the translation of the *SOX10* mRNA.

(A) RT-qPCR quantification representing the % of *SOX10* mRNA (left panel) or *HPRT* mRNA (right panel) in fractions (horizontal axes) obtained by sucrose-gradient (10-50%) ultracentrifugation of lysates from A375 cells transfected with siRNAs targeting HK2 (siHK2, light red) or control (siCTRL, grey) (n = 2 biological replicates). **(B)** Western blot analysis of the SOX10 protein level in distinct melanoma cell lines transfected with siRNAs targeting HK2 (siHK2, light red), GAPDH (siGAPDH, light blue) or control (siCTRL, grey). The SOX10 protein quantification is normalized to VCL expression. *p*-values were calculated by two-tailed unpaired *t*-test (SD, n = 3 biological replicates) and only significant comparisons are shown (* $p \leq 0.05$, ** $p \leq 0.01$, *** $p \leq 0.001$). **(C)** RT-qPCR quantification of the *SOX10* mRNA in different melanoma cell lines transfected with siRNAs targeting HK2 (siHK2, light red), GAPDH (siGAPDH, light blue) or control (siCTRL, grey). p-values were calculated by ordinary one-way ANOVA (SD, n = 3 biological replicates).

Figure 3

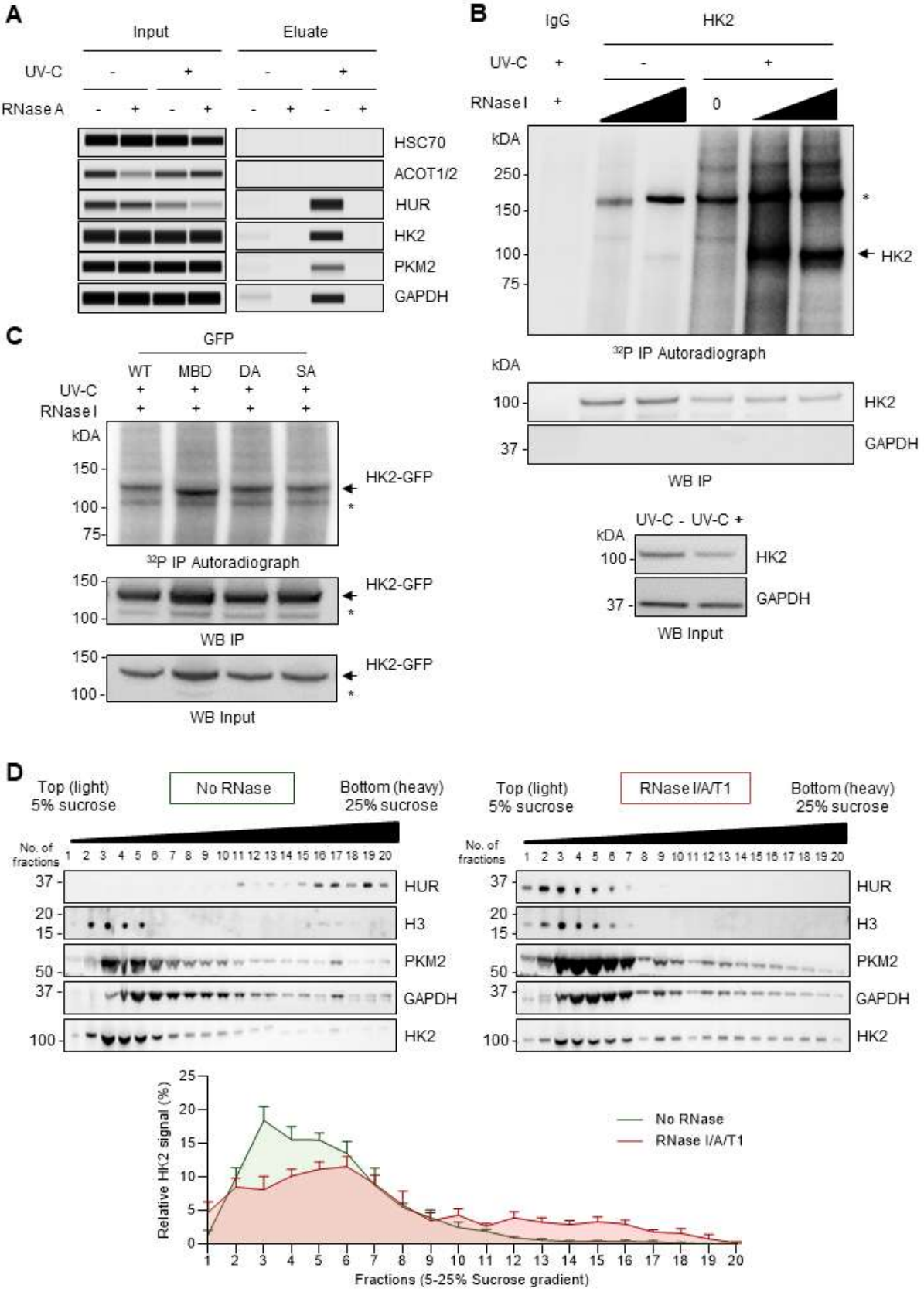
A
Input
Eluate
UV-C
RNase A
HSC70
ACOT1/2
HUR
HK2
PKM2
GAPDH
B
IgG
HK2
UV-C
RNase I
0
kDA
250
150
100
75
*
HK2
32P IP Autoradiograph
GAPDH
WB IP
UV-C - UV-C +
WB Input
C
GFP
WT
MBD
DA
SA
HK2-GFP
WB Input
D
Top (light) 5% sucrose
No RNase
Bottom (heavy) 25% sucrose
RNase I/A/T1
No. of fractions
Relative HK2 signal (%)
Fractions (5-25% Sucrose gradient)

Figure 3. HK2 binds directly to RNA.

(A) RNA-dependent retention of HK2 in silica matrix columns assessed by automated capillary western blot (Protein Simple ®) (n = 3 biological replicates). Specific HK2 signal was detected around the expected molecular mass in lysates of UV-C irradiated A375 cells not treated with RNase A prior to loading to the silica column. HUR, GAPDH and PKM2 were used as positive controls, and HSC70 and ACOT1/2 as negative controls. **(B)** CLIP from endogenous HK2 in A375 cells (n = 3 biological replicates). Upper panel: Autoradiography of HK2-RNA complexes in UV-C treated (+) or untreated (-) A375 cells. One major band is observed in the expected molecular mass of HK2, as indicated by a black arrow, and the asterisk (*) indicates a non-specific band. Middle and lower panel: western blots of HK2 and IgG immunoprecipitation, and HK2 and GAPDH (normalization control) input, respectively. Same conditions as the upper panel. **(C)** CLIP from GFP-HK2 transfected HEK293T cells (n=3 biological replicates). Upper panel: autoradiography of HK2-GFP-RNA complexes in UV-C treated (+) cells. Middle and lower panel: western blots of GFP and GFP immunoprecipitation, respectively. Same conditions as the upper panel. The arrow indicates the expected HK2-GFP molecular mass, and the asterisk (*) indicates a non-specific band. FL: full length; MBD: mitochondrial-binding deficient; DA: non-glucose-binding mutant; SA: catalytically inactive mutant. **(D)** Sucrose density gradient (5-25%) centrifugation and fractionation of A375 cell lysates treated with RNase I/A/T1 or left untreated (SD, n = 5 biological replicates). Upper panel: western blot of the sucrose-gradient fractions (horizontal axes) obtained after ultracentrifugation of lysates. HUR was used as a positive control, and H3 as a negative control. Lower panel: western blot quantification representing the % of HK2 in each sucrose fraction.

bioRxiv preprint doi: https://doi.org/10.1101/2024.08.13.607712

Figure 4

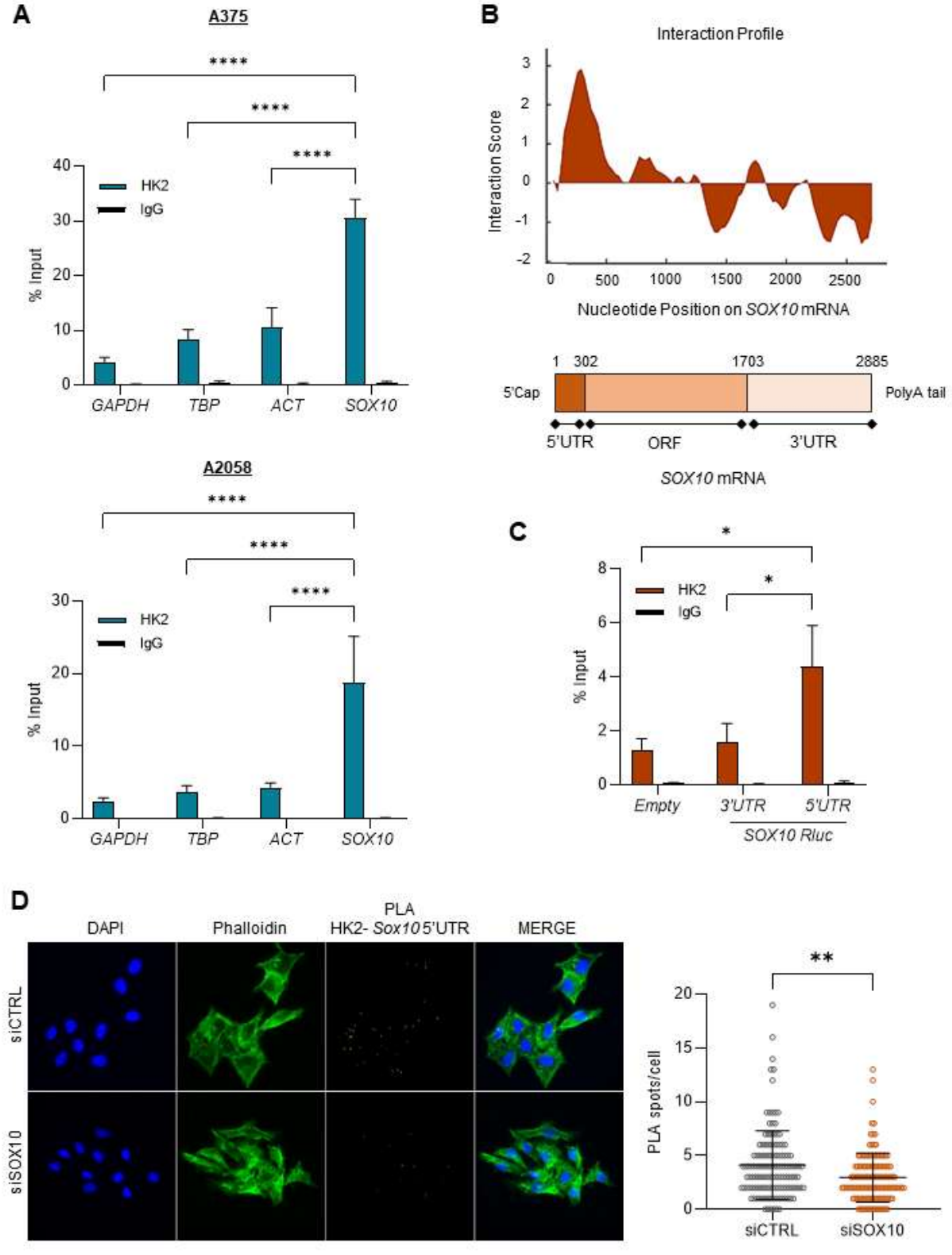
A
A375
****
****
****
40
30
20
10
0
% Input
HK2
IgG
GAPDH
TBP
ACT
SOX10
A2058
****
****
****
30
20
10
0
% Input
HK2
IgG
GAPDH
TBP
ACT
SOX10
B
Interaction Profile
Interaction Score
3
2
1
0
-1
-2
0
500
1000
1500
2000
2500
Nucleotide Position on SOX10 mRNA
1
302
1703
2885
5'Cap
PolyA tail
5'UTR
ORF
3'UTR
SOX10 mRNA
C
*
*
8
6
4
2
0
% Input
HK2
IgG
Empty
3'UTR
5'UTR
SOX10 Rluc
D
DAPI
Phalloidin
PLA
HK2- Sox10 5'UTR
MERGE
siCTRL
siSOX10
**
20
15
10
5
0
PLA spots/cell
siCTRL
siSOX10

Figure 4. HK2 associates with the 5'UTR of the *SOX10* mRNA.

(A) RIP experiment performed on A375 and A2058 melanoma cell lines (SD, n = 3 biological replicates). *SOX10* mRNA was analysed in IgG and HK2 immunoprecipitated samples and expressed as percentage of the mRNA present in the input. *GAPDH*, *TBP* and *ACT* mRNAs were used as negative controls. *p*-values were calculated by ordinary two-way ANOVA with Dunnett's multiple comparisons test (SD, n = 3 biological replicates) (**** $p \leq 0.0001$). **(B)** *In silico* prediction of HK2-*SOX10* mRNA interaction propensities using the *CatRAPID* algorithm. The highest interaction score observed between HK2 and the *SOX10* mRNA is at the *SOX10* 5'UTR. Upper panel: HK2-*SOX10* mRNA interaction profile. Lower panel: schematic representation of the *SOX10* mRNA. **(C)** RIP experiment performed on A375 cells transfected with luciferase reporters containing the *SOX10* 5'UTR and 3'UTR sequences upstream of the *Renilla* reporter gene. An Empty reporter was used as control. *Renilla* mRNA was analyzed in IgG and HK2 immunoprecipitated samples and expressed as percentage of the mRNA present in the input. *p*-values were calculated by ordinary two-way ANOVA with Dunnett's multiple comparisons test (SEM, n = 6 biological replicates) (* $p \leq 0.05$). **(D)** Representative fluorescence images and quantification of RNA-proximity ligation assays (PLA) of HK2 protein and *SOX10* mRNA in A375 cells transfected with siRNAs targeting SOX10 (siSOX10, orange) or control (siCTRL, grey) (n = 3 biological replicates). After 48h, cells were fixed, permeabilized, and incubated with anti-sense *SOX10* 5'UTR oligonucleotide probes and anti-HK2 antibody. Scale bar, 10 µm. HK2-*SOX10* mRNA PLA signal (yellow), Phalloidin staining (green), and DAPI staining (blue). The significance for PLA values was derived from the Mann-Whitney statistical test (SD, ** $p \leq 0.01$).

Figure 5

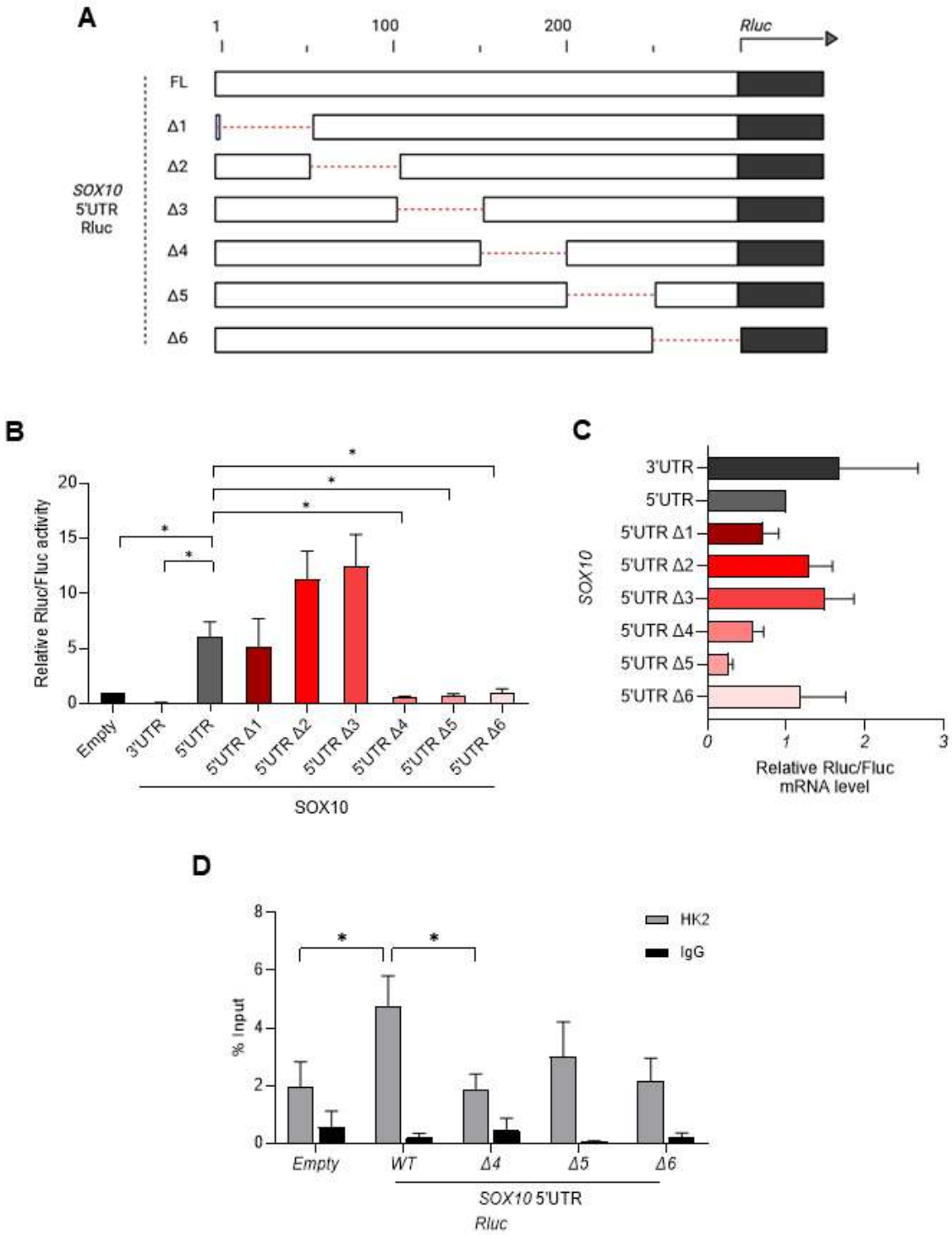
A
1
100
200
Rluc
FL
Δ1
Δ2
Δ3
Δ4
Δ5
Δ6
SOX10 5'UTR Rluc
B
Relative Rluc/Fluc activity
Empty
3'UTR
5'UTR
5'UTR Δ1
5'UTR Δ2
5'UTR Δ3
5'UTR Δ4
5'UTR Δ5
5'UTR Δ6
SOX10
C
SOX10
3'UTR
5'UTR
5'UTR Δ1
5'UTR Δ2
5'UTR Δ3
5'UTR Δ4
5'UTR Δ5
5'UTR Δ6
Relative Rluc/Fluc mRNA level
D
HK2
IgG
% Input
Empty
WT
Δ4
Δ5
Δ6
SOX10 5'UTR Rluc

Figure 5. The 3' half of the *SOX10* 5'UTR is essential for HK2 association and *SOX10* 5'UTR-driven translation.

(A) Schematic of full-length (FL) and mutated *SOX10* 5'UTR (Δ1-6) reporters cloned upstream of the Renilla reporter. The deleted regions of ~50nts are represented as red dashed lines. **(B)** Luciferase assay performed in A375 cells co-transfected with a Firefly reporter and the Renilla reporters in (A). An empty Renilla vector and the *SOX10* 3'UTR Renilla reporter were used as controls. The activity of the Firefly and Renilla reporters was measured 48h after transfection. The Renilla activity was normalized by the Firefly activity, and the data shown is relative to the Empty vector. *p*-values were calculated by Mann-Whitney statistical test (SEM, n = 4 biological replicates) (∗ $p < 0.05$). **(C)** RT-qPCR quantification of the *Renilla* mRNA from the same transfected cells in (B). The *Renilla* expression was normalized by the *Firefly* expression, and the data shown is relative to the expression of the Empty vector. *p*-values were calculated by Mann-Whitney statistical test (SEM, n = 4 biological replicates). **(D)** RIP experiment performed on A375 cells transfected with Renilla luciferase reporters containing the *SOX10* 5'UTR FL and Δ4, Δ5 and Δ6. *Renilla* mRNA was analyzed in IgG and HK2 immunoprecipitated samples and expressed as percentage of the mRNA present in the input. *p*-values were calculated by ordinary two-way ANOVA with Dunnett's multiple comparisons test (SEM, n = 3 biological replicates) (* $p \leq 0.05$).

Figure 6

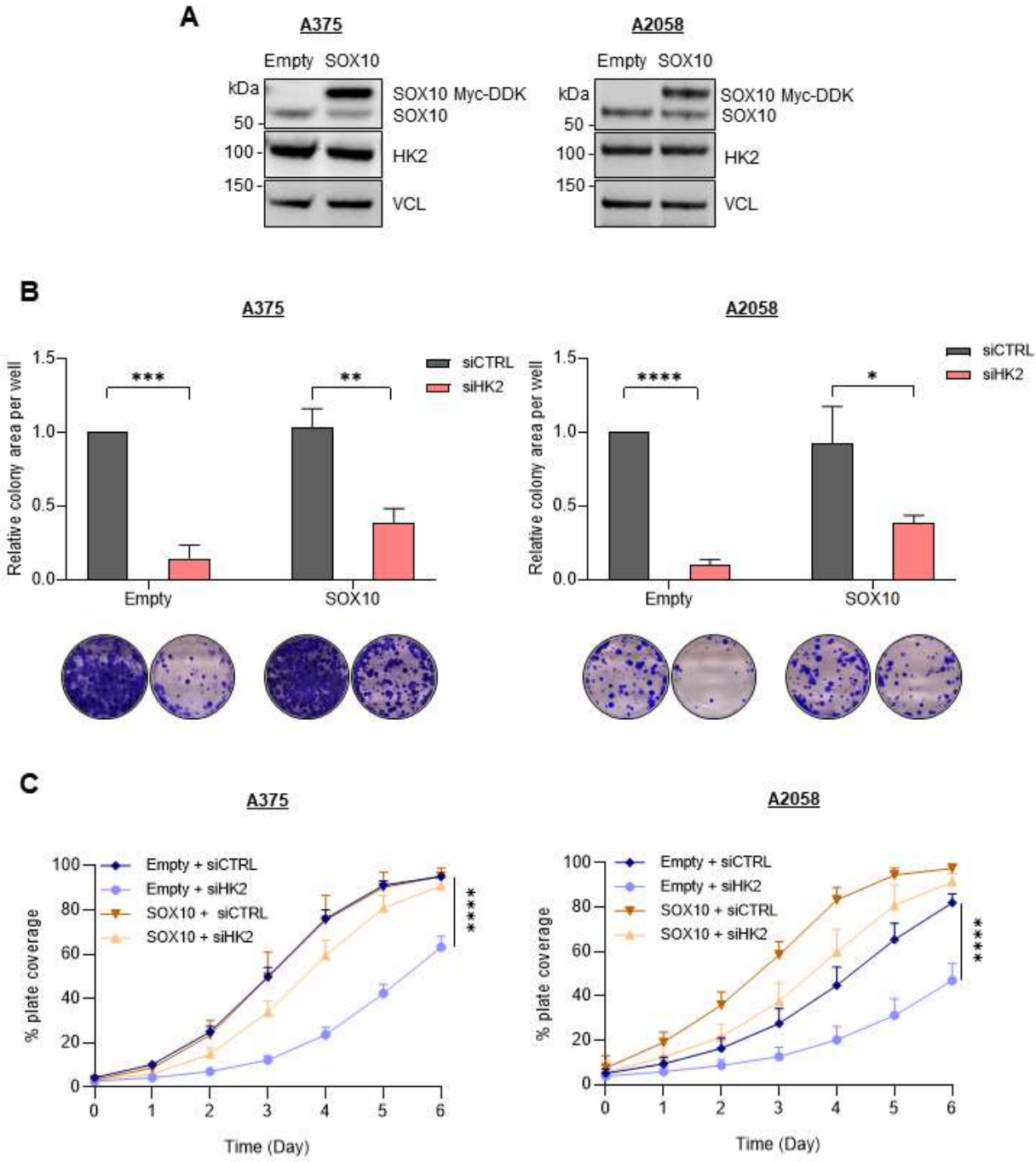
A
A375
Empty SOX10
kDa
50
100
150
SOX10 Myc-DDK
SOX10
HK2
VCL
A2058
Empty SOX10
kDa
50
100
150
SOX10 Myc-DDK
SOX10
HK2
VCL
B
A375
Relative colony area per well
1.5
1.0
0.5
0.0
***
**
siCTRL
siHK2
Empty
SOX10
A2058
Relative colony area per well
1.5
1.0
0.5
0.0
****
*
siCTRL
siHK2
Empty
SOX10
C
A375
% plate coverage
100
80
60
40
20
0
Empty + siCTRL
Empty + siHK2
SOX10 + siCTRL
SOX10 + siHK2
****
0 1 2 3 4 5 6
Time (Day)
A2058
% plate coverage
100
80
60
40
20
0
Empty + siCTRL
Empty + siHK2
SOX10 + siCTRL
SOX10 + siHK2
****
0 1 2 3 4 5 6
Time (Day)

Figure 6. HK2-dependent SOX10 translational regulation is involved in clonogenicity and proliferation properties of melanoma cells.

(A) Western blot analysis of the ectopic SOX10 Myc-DDK expression in A375 and A2058 melanoma cells. VCL was used as loading control (n = 3 biological replicates). **(B)** A375 and A2058 cells from (A) were plated 24h after transfection with siRNAs targeting HK2 (siHK2, light red) or control (siCTRL, grey). The colonies were stained with crystal violet after 10 days, and the clonogenic cell growth was measured. Upper panel: percentage of area covered by crystal violet stained cell colonies. Lower panel: representative images of three independent experiments. *p*-values were calculated by ordinary two-way ANOVA with Turkey's multiple comparison test (SD, n = 3 biological replicates), and only significant differences within the same cell line are shown (* $p \leq 0.05$, **** $p \leq 0.0001$). **(C)** Cell proliferation assay performed in A375 and A2058 cells from (A). Cells were plated 24h after transfection with siRNAs targeting HK2 (Empty, light blue; SOX10, light orange) or control (Empty, dark blue; SOX10 dark orange). *p*-values were calculated by ordinary two-way ANOVA with Turkey's multiple comparison test (SD, n = 3 biological replicates), and only significant differences within the same cell line are shown (**** $p \leq 0.0001$).

SUPPLEMENTARY INFORMATION

Figures S1-S7

An extra-glycolytic function for hexokinase 2 as an RNA-binding protein regulating *SOX10* mRNA translation in melanoma

Ana Luisa Dian, Antoine Moya-Plana, Giuseppina Claps, Céline M. Labbé, Virginie Quidville, Dorothée Baille, Virginie Raynal, Sylvain Baulande, Caroline Robert, Stéphan Vagner

bioRxiv preprint doi: https://doi.org/10.1101/2024.08.13.607712

Figure S1

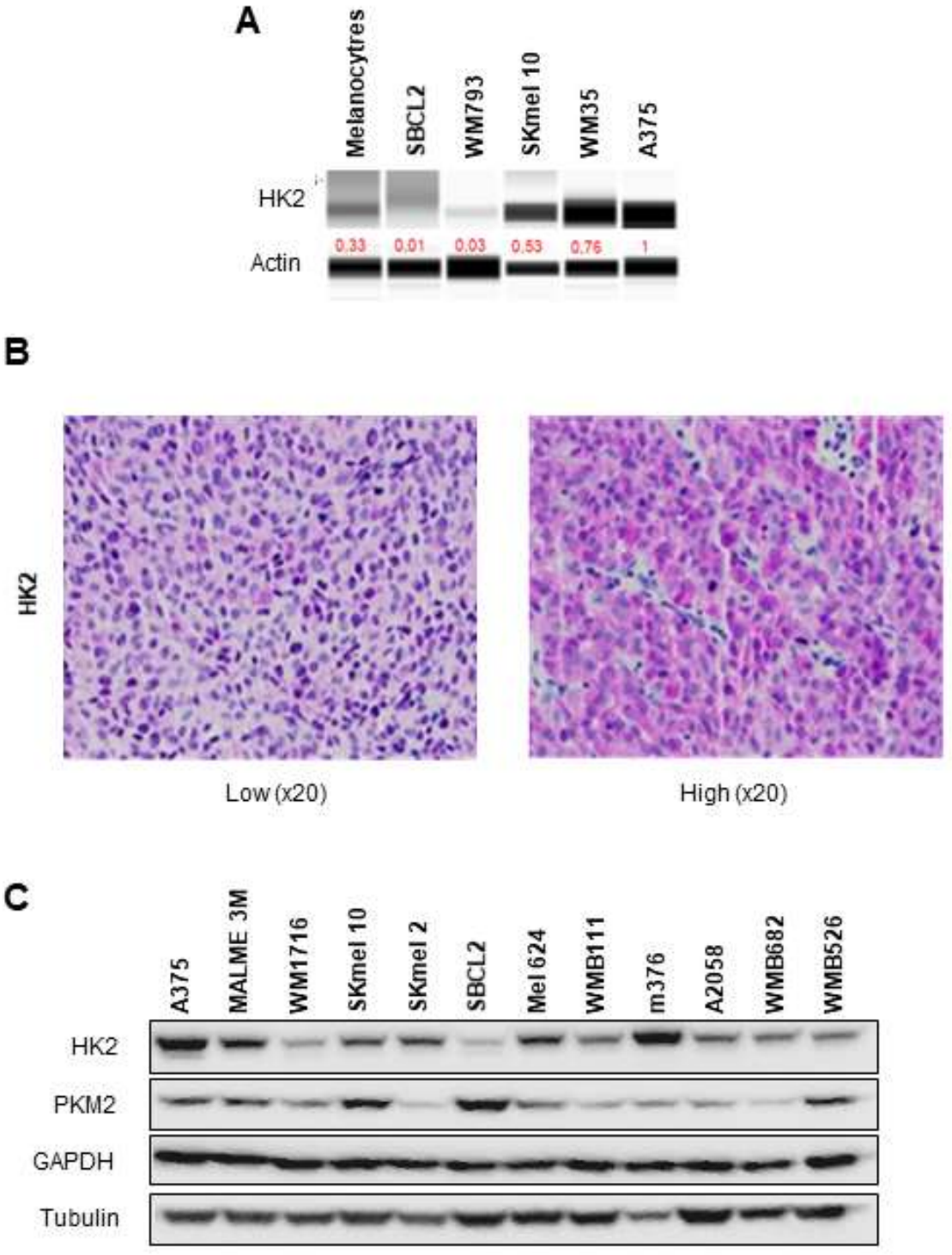
A
Melanocytes
SBCL2
WM793
SKmel 10
WM35
A375
HK2
Actin
0.33
0.01
0.03
0.53
0.76
1
B
HK2
Low (x20)
High (x20)
C
A375
MALME 3M
WM1716
SKmel 10
SKmel 2
SBCL2
Mel 624
WMB111
m376
A2058
WMB682
WMB526
HK2
PKM2
GAPDH
Tubulin

Figure S1. HK2 expression in melanoma cell lines and tumours.

(A) HK2 expression level assessed by automated capillary western blot (Protein Simple ®) analysis of normal melanocytes, early superficial melanoma with radial growth (RGP, SBCL2), early invasive melanoma (VGP, WM793), low invasive (SKMel10) and high invasive (A375) metastatic melanoma cell lines. Actin was used as loading control. **(B)** Immunohistochemical analysis of HK2 expression in two representative samples from a cohort of 31 patients with cutaneous melanoma. **(C)** Western blot analysis of key glycolytic enzymes (HK2, PKM2 and GAPDH) in a variety of melanoma cell lines. Tubulin was used as loading control.

Figure S2

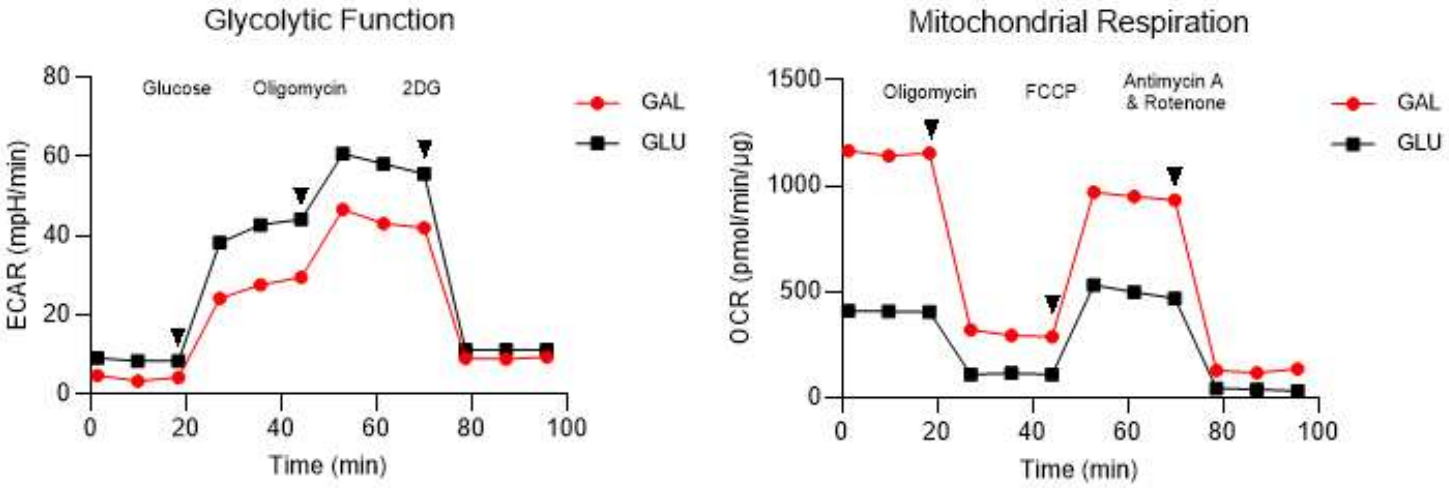

Metabolic profile of A375 cells analysed on a XF96 Extracellular Flux Analyzer.

Left panel: the extra-cellular acidification rate (ECAR), an indicator of aerobic glycolysis, was measured in A375 cells grown in either glucose or galactose-containing medium followed by consecutive treatments of Glucose, oligomycin, and 2-DG. Right panel: the oxygen consumption rate (OCR) was measured in A375 cells cultured either in glucose or galactose-containing medium followed by consecutive treatments of oligomycin, FCCP, and antimycin A & rotenone.

Figure S3

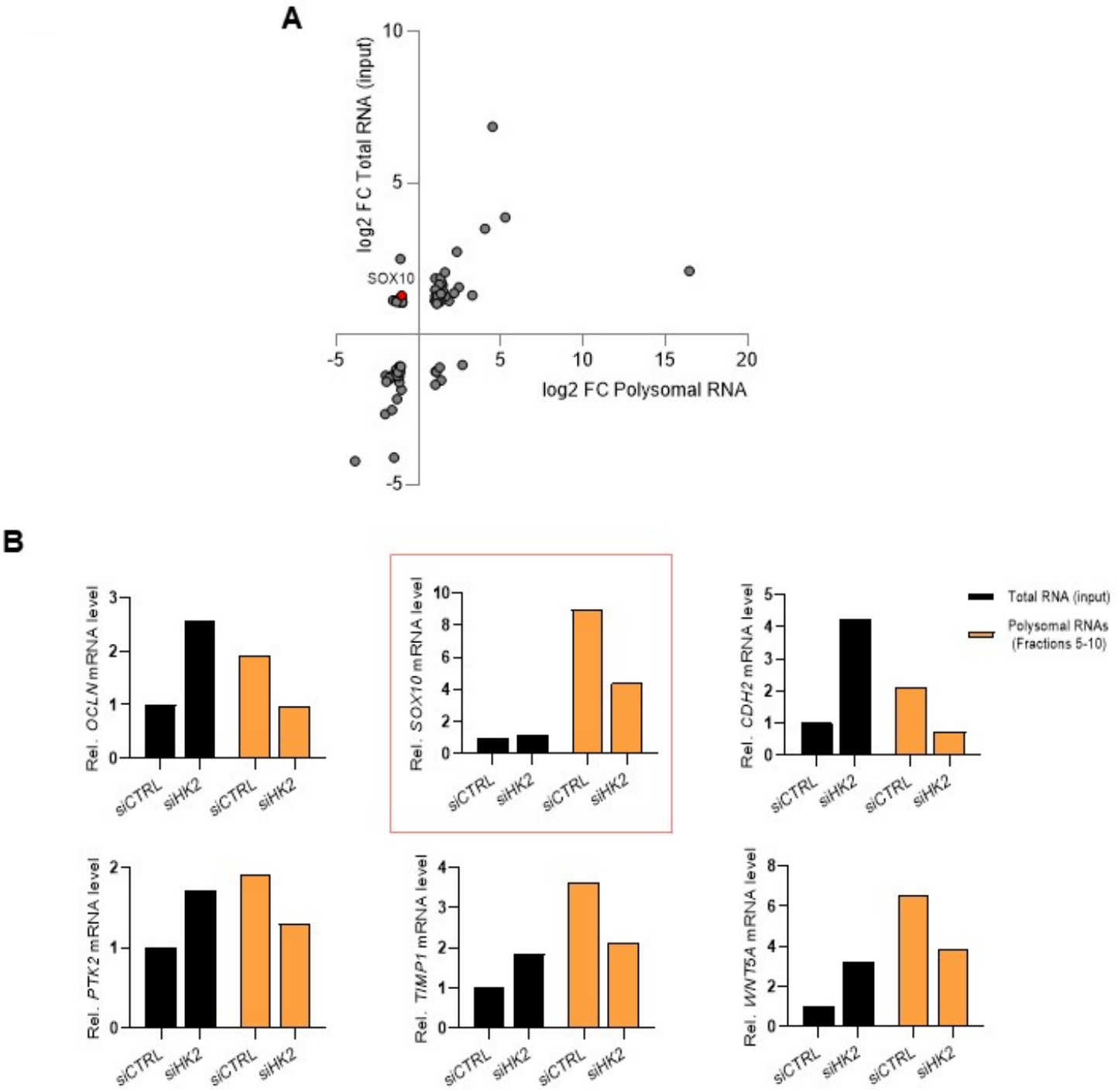
A
log2 FC Total RNA (input)
log2 FC Polysomal RNA
SOX10
10
5
-5
5
10
15
20
-5
B
Rel. OCLN mRNA level
Rel. SOX10 mRNA level
Rel. CDH2 mRNA level
Rel. PTK2 mRNA level
Rel. TIMP1 mRNA level
Rel. WNT5A mRNA level
siCTRL
siHK2
siCTRL
siHK2
Total RNA (input)
Polysomal RNAs (Fractions 5-10)

Figure S3. HK2 regulates the expression of cancer-related genes.

(A) RT-qPCR quantification of 84 EMT-associates genes. Transcriptional (total RNA) and translational (polysomal RNA) levels of each gene were obtained from polysome profiling of A375 cells transfected with siRNAs targeting HK2 (siHK2) or control (siCTR) and measured using RT^2 Profiler PCR Array. **(B)** RT-qPCR analysis of potential key genes of EMT (*OCLN*, *SOX10*, *CDH2*, *PTK2*, *TIMP1*, and *WNT5A*) whose expression could be translationally regulated by HK2. Transcriptional (total RNA; black) and translational (polysomal RNA; orange) levels of each gene were obtained from polysome profiling of A375 cells transfected with siRNAs targeting HK2 (siHK2) or control (siCTR) and measured using RT^2 Profiler PCR Array.

Figure S4

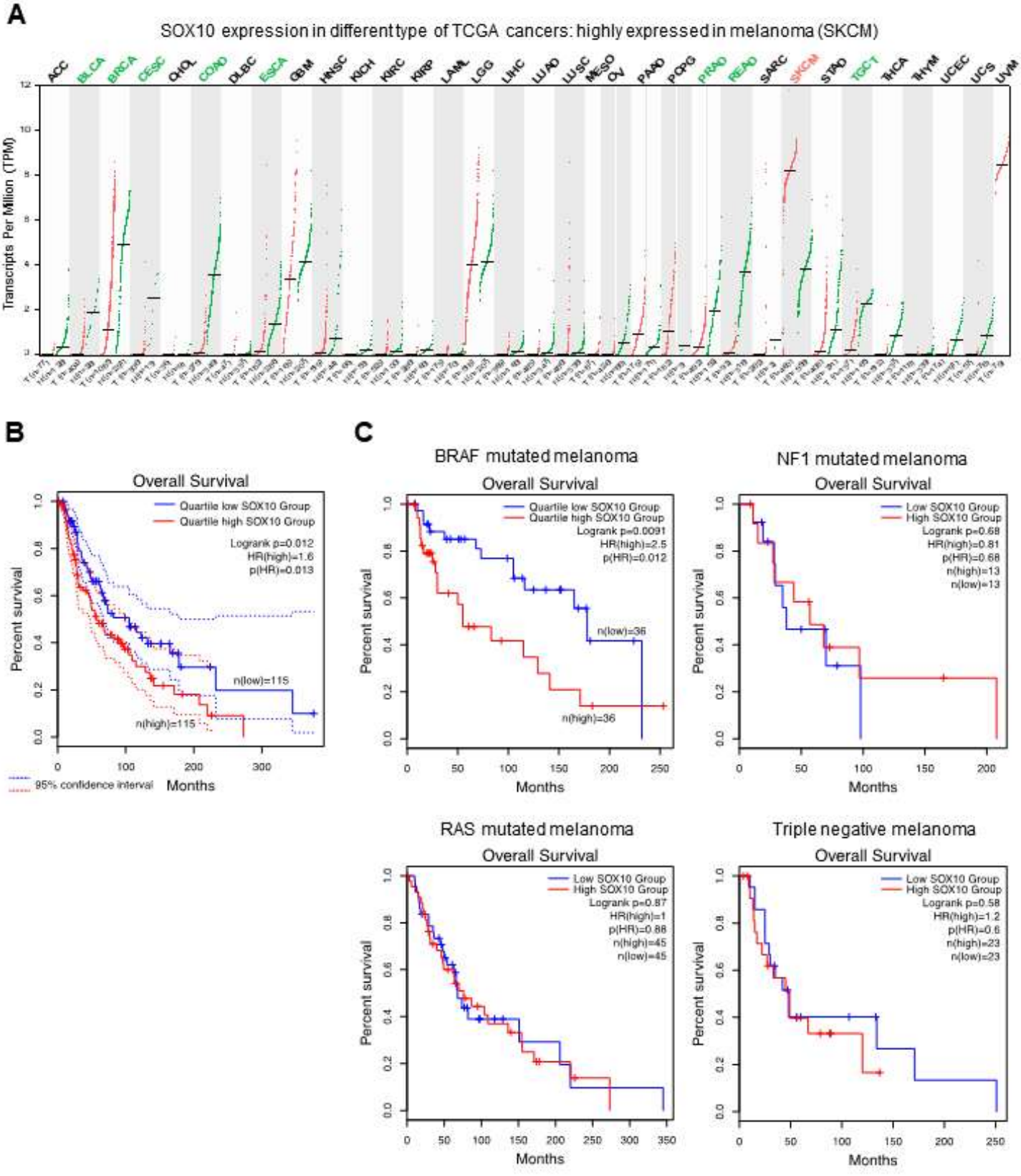

Figure S4. SOX10 expression is associated with prognosis in patients with cutaneous melanoma.

(A) SOX10 expression in different type of solid cancers from TGCA database. **(B)** Analysis of the impact of SOX10 expression in overall survival of patients with cutaneous melanoma. **(C)** Analysis of the impact of SOX10 expression in overall survival according to molecular profile of the tumour. T: tumour (red dots); N: normal tissue (green dots).

bioRxiv preprint doi: https://doi.org/10.1101/2024.08.13.607712

Figure S5

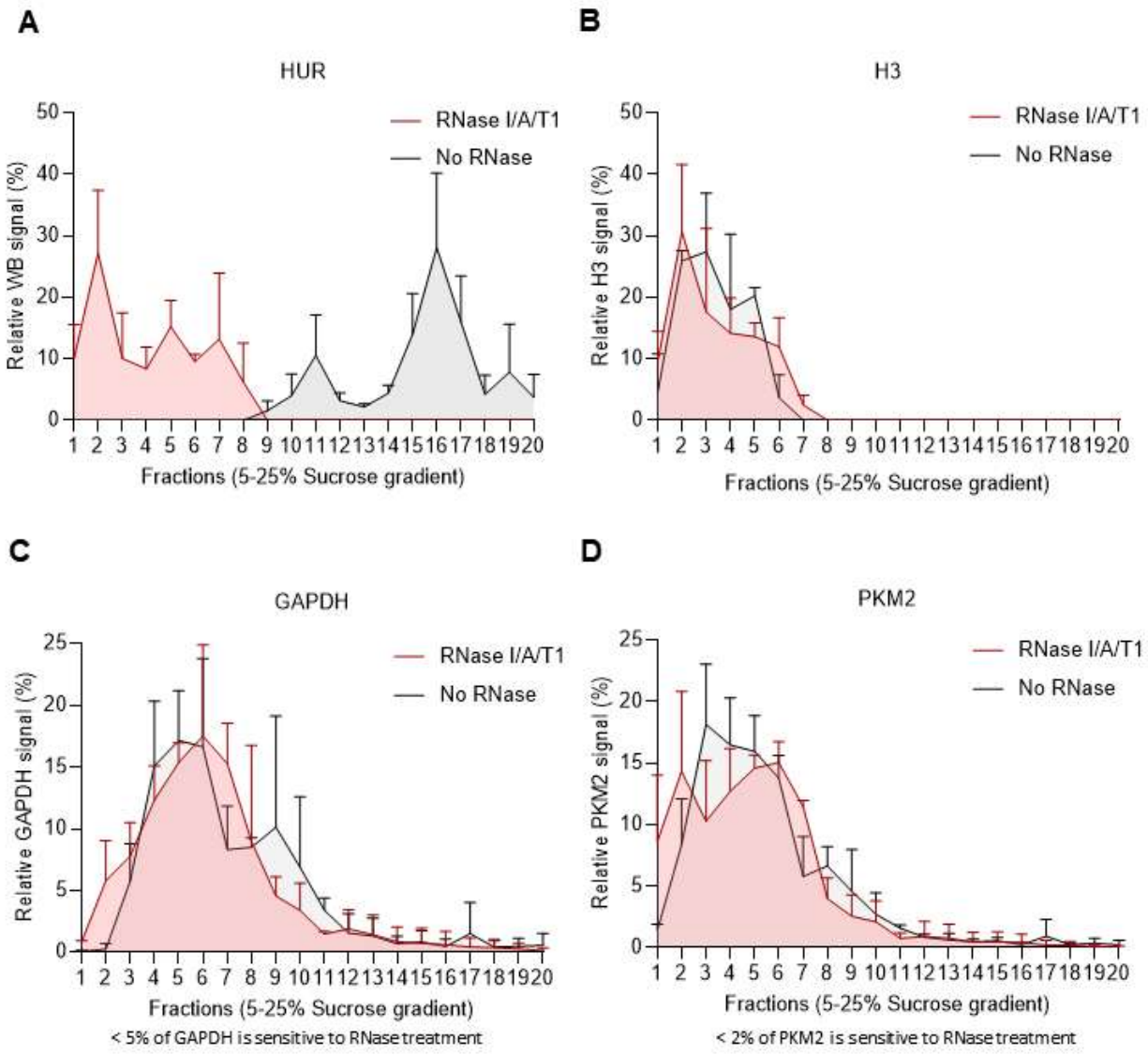

Sucrose density gradient centrifugation and fractionation of A375 cell lysates. Western blot quantification representing the % of **(A)** HUR, **(B)** H3, **(C)** GAPDH and **(D)** PKM2 in each sucrose fraction of lysates treated with RNase I/A/T1 or left untreated (SD, n = 3 biological replicates).

Figure S6

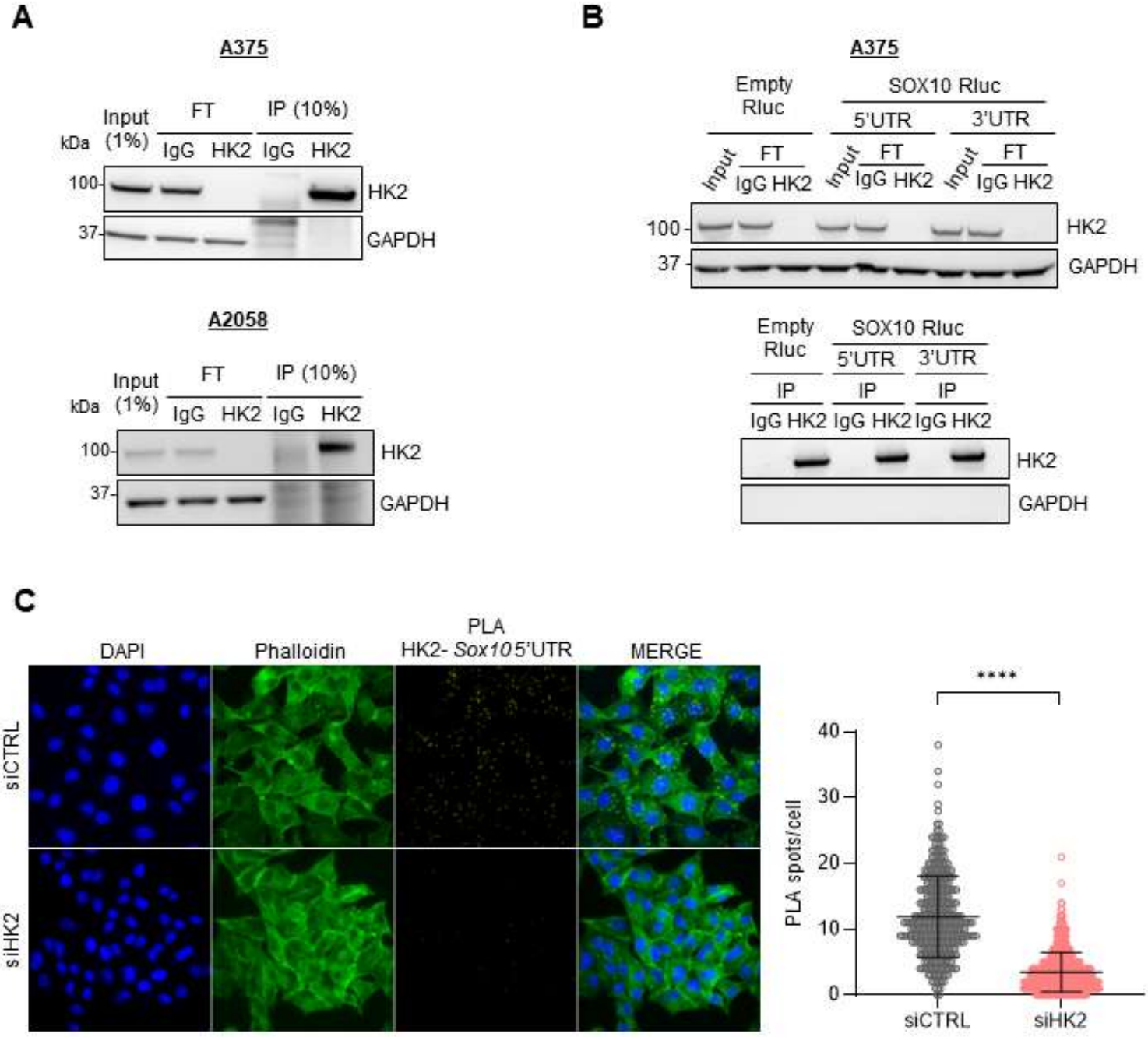
A
A375
Input (1%)
FT
IP (10%)
kDa
IgG
HK2
IgG
HK2
100
HK2
37
GAPDH
A2058
Input (1%)
FT
IP (10%)
kDa
IgG
HK2
IgG
HK2
100
HK2
37
GAPDH
B
A375
Empty Rluc
SOX10 Rluc
5'UTR
3'UTR
Input
FT
IgG
HK2
100
HK2
37
GAPDH
Empty Rluc
SOX10 Rluc
5'UTR
3'UTR
IP
IgG
HK2
HK2
GAPDH
C
DAPI
Phalloidin
PLA
HK2- Sox10 5'UTR
MERGE
siCTRL
siHK2
****
PLA spots/cell
40
30
20
10
0
siCTRL
siHK2

Figure S6. Analysis of HK2-*SOX10* mRNA interaction.

(A) Western blot of HK2 and GAPDH (normalization control) from RIP experiment performed on A375 and A2058 melanoma cell lines (representative images, n = 3 biological replicates). **(B)** Western blot of HK2 and GAPDH (normalization control) from RIP experiment performed on A375 cells transfected with luciferase reporters containing the *SOX10* 5'UTR and 3'UTR sequences upstream of the Renilla luciferase reporter gene. An empty reporter was used as control (representative images, n = 3 biological replicates). **(C)** Representative fluorescence images and quantification of RNA-proximity ligation assays (PLA) of HK2 protein and *SOX10* mRNA in A375 cells transfected with siRNAs targeting HK2 (siHK2, light red) or control (siCTRL, grey) (n = 3 biological replicates). After 48h, cells were fixed, permeabilized, and incubated with anti-sense *SOX10* 5'UTR oligonucleotide probes and anti-HK2 antibody. Scale bar, 10 µm. HK2-*SOX10* mRNA PLA signal (yellow), Phalloidin staining (green), and DAPI staining (blue). The significance for PLA values was derived from the Mann-Whitney statistical test (SD, **** $p \leq 0.0001$).

Figure S7

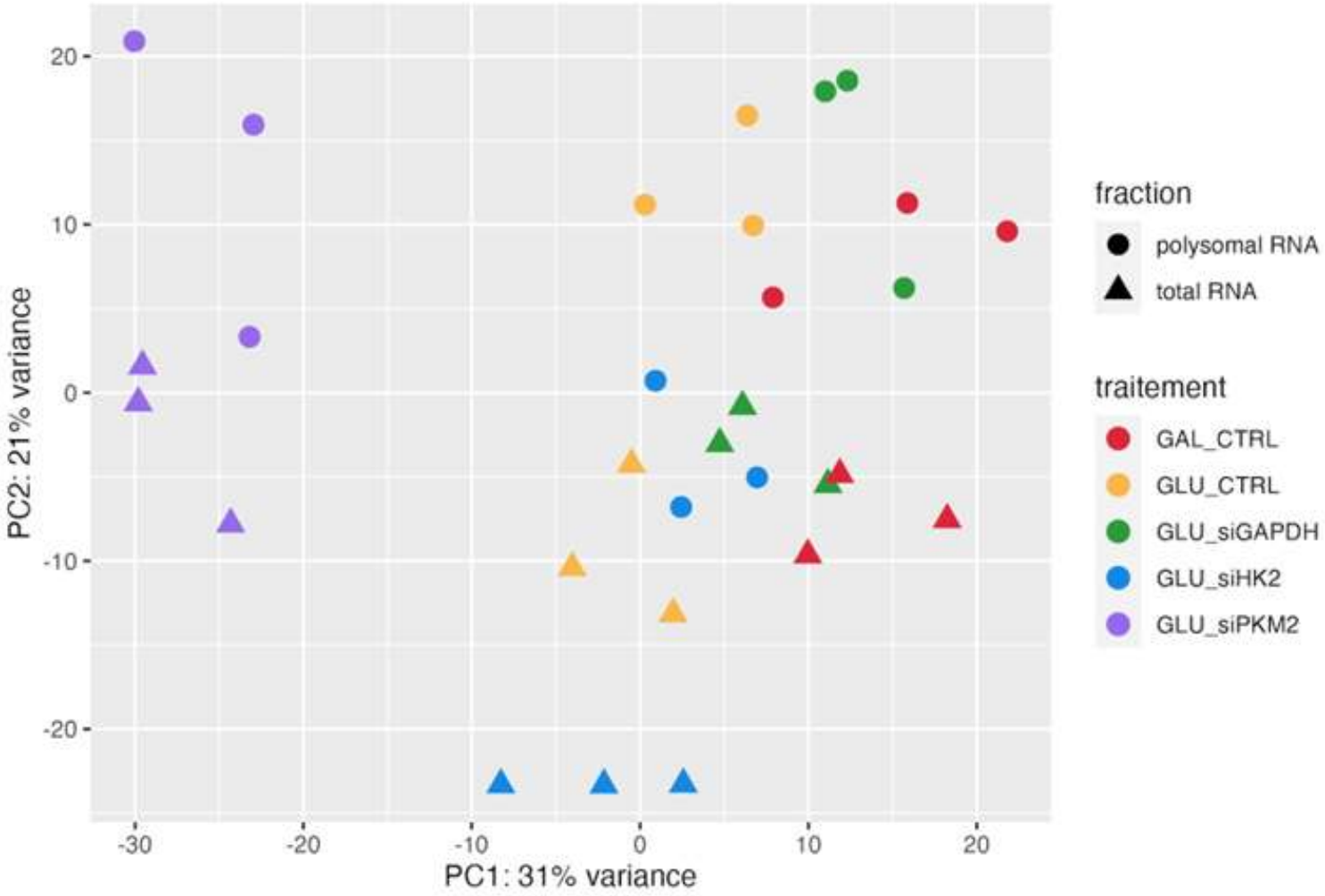

PCA plot using the VST data.

The variance stabilizing transformation (VST) offered by DESeq2 was used on the raw count data to stabilize the variance across the mean. The principal components analysis (PCA) plot was built using the ggplot2 package.

SUPPLEMENTARY INFORMATION

Table S1

https://www.biorxiv.org/content/10.1101/2024.08.13.607712v1.supplementary-material

Tables S2 and S3

An extra-glycolytic function for hexokinase 2 as an RNA-binding protein regulating *SOX10* mRNA translation in melanoma

Ana Luisa Dian, Antoine Moya-Plana, Giuseppina Claps, Céline M. Labbé, Virginie Quidville, Dorothée Baille, Séverine Roy, Virginie Raynal, Sylvain Baulande, Caroline Robert, Stéphan Vagner

Table S2. Transcriptome and translatoma analyses on RT² Profiler™ PCR Array. Transcriptional (total RNA, "Input") and translational (polysomal RNA, "HP") levels of each gene were obtained from polysome profiling of A375 cells transfected with siRNAs targeting HK2 (siHK2) or control (siCTR) and measured using RT² Profiler PCR Array (n = 1). HP, heavy polysomes.

Gene Name	**Input siHK2 vs Input siCTRL** log2(fold change)	**HP siHK2 vs HP siCTRL** log2(fold change)
AHNAK	1.06	-1.35
AKT1	-1.08	-1.09
BMP1	1.33	1.34
BMP2	2.04	1.59
BMP7	-1.68	1
CALD1	1	1.1
CAMK2N1	-1.27	-1.28
CAV2	-1.28	-1.16
CDH1	1.05	-1.01
CDH2	1.09	-1.38
COL1A2	2.48	-1.12
COL3A1	2.08	16.46
COL5A2	1.24	1.13
CTNNB1	-1.38	-1.33
DESI1	1.42	1.47
DSC2	-1.41	-1.2
DSP	1.08	1.02
EGFR	-1.58	-1.97
ERBB3	1.24	1
ESR1	-2.16	-1.32
F11R	-1.46	-1.81
FGFBP1	1.46	1.01
FN1	1.64	1.25
FOXC2	3.86	5.25
FZD7	1.49	1.14
GEMIN2	-1.61	-1.19
GNG11	1.15	-1.2
GSC	1.21	-1.07
GSK3B	1.15	-1.08
IGFBP4	-1.11	-1.14
IL1RN	1.09	1.01
ILK	-1.4	-1.52
ITGA5	1.3	1.11
ITGAV	1.08	1.17
ITGB1	1.37	1.3
JAG1	1.36	1.14
KRT14	-2.52	-1.63
KRT19	1.09	1.05

KRT7	1.09	1.01
MAP1B	1.84	1.31
MMP2	1.31	1.36
MMP3	-1.54	1.36
MMP9	1.03	-1.05
MSN	1.69	1.39
MST1R	-1.03	2.66
NODAL	1.35	2.14
NOTCH1	1.45	1.03
NUDT13	1.04	-1.02
OCLN	1.11	-1.57
PDGFRB	2.72	2.31
PLEK2	1.28	3.26
PTK2	1.15	-1.17
PTP4A1	-1.08	-1.18
RAC1	1.09	1.33
RGS2	3.48	4.03
SERPINE1	6.86	4.49
SMAD2	1.06	1.23
SNAI1	1.61	1.44
SNAI2	-2.66	-2.05
SNAI3	1.54	2.43
SOX10	1.27	-1.04
SPARC	1.15	1.1
SPP1	1.24	1.64
STAT3	-1.48	-1.73
STEAP1	-1.11	1.26
TCF3	1.05	-1.12
TCF4	-1.85	-1.06
TFP12	1.09	1.83
TGFB1	1.44	1.41
TGFB2	1.84	1.01
TGFB3	1.02	1.09
TIMP1	1.2	-1.03
TMEFF1	-1.26	1.06
TMEM132A	1.11	1.05
TSPAN13	-1.25	1.02
TWIST1	-1.34	-1.3
VCAN	-4.22	-3.89
VIM	1.04	1.17
VPS13A	-1.38	-1.67
WNT11	-1.38	-2.01
WNT5A	1.04	-1.03
WNT5B	-4.1	-1.51
ZEB1	-1.18	-1.38
ZEB2	-1.25	-1.17

Table S3. Relevant oligonucleotides.

NAME OF THE OLIGONUCLEOTIDE	SEQUENCE
RTqPCR primers	
VCL Forward	TGATGATTAGAGACATCACCGCT
VCL Reverse	AACAAAGGAGAAACCTGACCT
GAPDH Forward	TCCCATCACCATCTTCCAGG
GAPDH Reverse	TCCATGGTGGTGAAGACGC
TBP Forward	GGAAGGGGCATTATTTGTG
TBP Reverse	GCCCAGATAGCAGCACGGTA
ACT Forward	CCGTGTTTCCTTCCATCGTC
ACT Reverse	ACGATGCCATGCTCAATGGG
Renilla Forward	ACGGATGATAACTGGTCCGC
Renilla Reverse	CGCGCTACTGGCTCAATATG
Firefly Forward	GAAATGTCCGTTCGGTTGGC
Firefly Reverse	TCCGATAAATAACGCGCCCA
OCLN Forward	GGTCGGGCCCAGTTGC
OCLN Reverse	ATGATTCGGTTTGAATTCATCAGG
CDH2 Forward	ACTCCAGGGGACCTTTTCCT
CDH2 Reverse	TGCCCTCAAATGAAACCGGG
PTK2 Forward	TTGGGCGGAAAGAAATCCTG
PTK2 Reverse	GTCCAGGTTGGCAGTAGGAG
TMP1 Forward	GACACCAGAGAACCCACCAT
TMP1 Reverse	CACGAACTTGGCCCTGATGA
WNT5A Forward	GCTCGCATCCTCATGAACCT
WNT5A Reverse	GCCACATCAGCCAGGTTGTA
SOX10 5'UTR Forward	CACTTCCTAAGGACGAGCCC
SOX10 5'UTR Reverse	TCCTCGCAAAGAGTCCAACG
SOX10 CDS Forward	GGCTGCTGAACGAAAGTGA
SOX10 CDS Reverse	TCTTGTAGTGGGCCTGGATG
SOX10 POLYSOME Forward	CCAGGCCCACTACAAGAGC
SOX10 POLYSOME Reverse	CTCTGTCTTCGGGGTGGTTG

3.2 ADDITIONAL RESULTS

Investigation of HK2-RNA interactions

Since we observed that HK2 associates with the *SOX10* mRNA in melanoma cells, we asked whether this association was sensitive to changes in glycolysis, as both canonical and uncanonical functions of glycolytic enzymes are often shown to be regulated by metabolites. We, therefore, cultured A375 cells in medium containing galactose instead of glucose for 24 h. The metabolism of galactose eventually converges with the glucose metabolism through the Leloir pathway. However, because this conversion occurs at a much slower rate than glucose entry into glycolysis, it inhibits glycolysis and favours oxidative phosphorylation (OXPHOS)[323–325]. We found that the replacement of glucose with galactose decreased the association of HK2 to the *SOX10* mRNA (Figure 1A). Likewise, the glucose analogue 2-deoxyglucose (2-DG) also decreased this association in comparison to cells cultured in glucose-containing medium (Figure 1B). Although 2-DG can be phosphorylated to 2-deoxyglucose-6-phosphate (2-DG6P) by the hexokinase, it cannot be metabolized in glycolysis, which results in its rapid accumulation in the cells and glycolysis inhibition. Interestingly, replacement of glucose with either galactose or 2-DG reduced SOX10 protein expression, which was not accompanied by reduction in the mRNA level (Figure 1C and D). Taken together, these results suggest that glycolysis inhibition may decrease *SOX10* mRNA translation by impairing the association between HK2 and the SOX10 mRNA. Further experiments (e.g., polysome profiling) are required for further investigation.

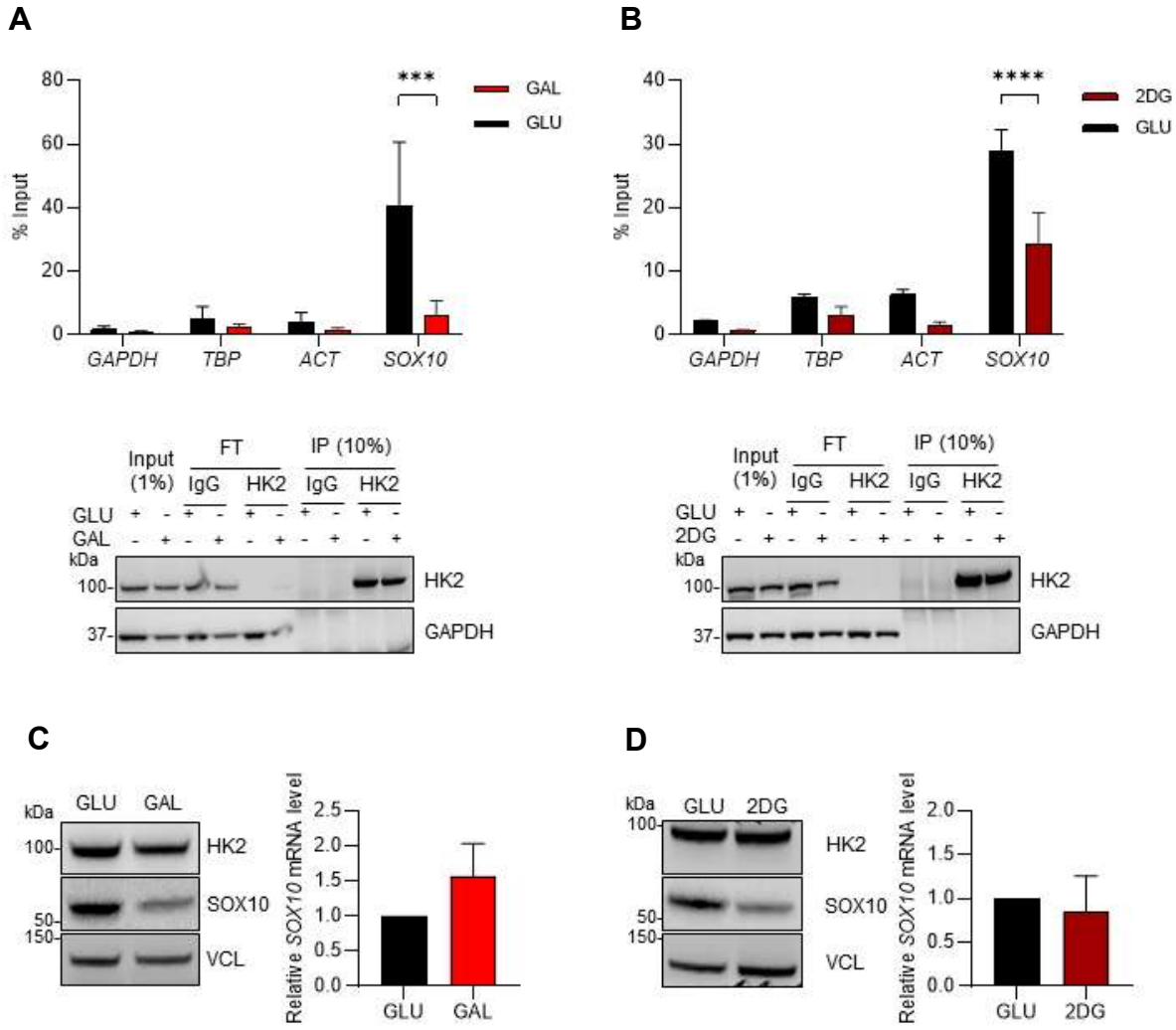

Figure 4. Replacement of glucose with galactose or 2-DG decrease HK2-*SOX10* mRNA interaction. (**A**) RIP experiment performed on A375 cells (SD, n = 3 biological replicates) incubated in glucose-free medium either in the presence of 5 g/L glucose (GLU) or 5 g/L galactose (GAL) for 24 h. *SOX10* mRNA was analysed in IgG and HK2 immunoprecipitated samples and expressed as percentage of the mRNA present in the input. *GAPDH*, *TBP* and *ACT* mRNAs were used as negative controls. *p*-values were calculated by ordinary two-way ANOVA with Dunnett's multiple comparisons test (SD, n = 3 biological replicates) (*** $p \leq 0.001$). (**B**) RIP experiment performed on A375 cells (SD, n = 3 biological replicates) incubated in glucose-free medium either in the presence of 16mM glucose (GLU) or 16mM 2-DG for 24 h. *SOX10* mRNA was analysed in IgG and HK2 immunoprecipitated samples and expressed as percentage of the mRNA present in the input. *GAPDH*, *TBP* and *ACT* mRNAs were used as negative controls. *p*-values were calculated by ordinary two-way ANOVA with Dunnett's multiple comparisons test (SD, n = 3 biological replicates) (**** $p \leq 0.0001$). (**C**) Western blot analysis and RT-qPCR quantification of *SOX10* mRNA (SD, n = 3 biological replicates) of A375 cells incubated in glucose-free medium either in the presence of 5 g/L glucose (GLU) or 5 g/L galactose (GAL) for 24 h. VCL was used as loading control. (**D**) Western blot analysis and RT-qPCR quantification of *SOX10* mRNA (SD, n = 3 biological replicates) of A375 cells incubated in glucose-free medium either in the presence of 16mM glucose (GLU) or 16mM 2-DG for 24 h. VCL was used as loading control.

We observed that HK2 associates with the *SOX10* mRNA in melanoma cells, and that this association is sensitive to changes in glycolysis. We, therefore, investigated whether the metabolic switch from glycolysis to mitochondrial respiration could impact the composition of HK2-containing complexes in an RNA-dependent manner. To this end, we cultured A375 cells in medium containing either glucose or galactose for 24 h. Next, we subjected RNase-treated or untreated lysates of these cells to sucrose density gradient (5% - 25%) ultracentrifugation and fractionation. By these means, we identified that the total cellular HK2 in both glucose and galactose conditions changed their distribution in the sucrose gradient following RNase treatment; however, the changes observed were less pronounced when cells were cultured in galactose- than glucose-containing medium (19,70% and 28,55%, respectively) (Figure 2). This result indicates that the composition of HK2-containing complexes is slightly less dependent on RNA in galactose.

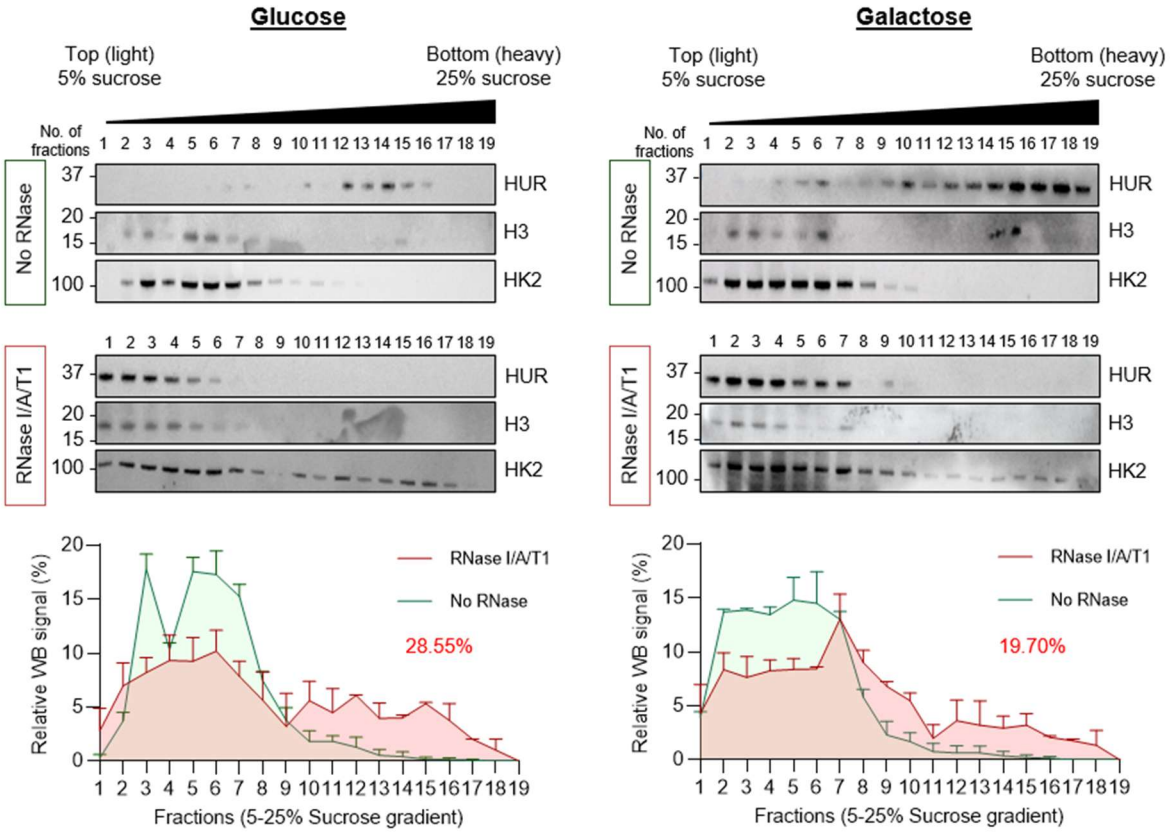

Figure 2. Sucrose density gradient (5-25%) centrifugation and fractionation of A375 cell cultured in glucose- (left panel) or galactose- (right panel) containing medium. The cells were lysed, and lysates were treated with RNase I/A/T1 or left untreated (SD, n = 2 biological replicates). Upper panel: western blot analysis of the sucrose-gradient fractions (horizontal axes) obtained after ultracentrifugation of the lysates. HUR was used as a positive control, and H3 as a negative control. Lower panel: western blot quantification representing the % of HK2 in each sucrose fraction.

Besides moonlighting as a non-canonical RBP, HK2 has been recently shown to act as a scaffold that forms a complex with the glycogen synthase kinase 3 (GSK3β) and the

regulatory subunit α of protein kinase A (PRKAR1a). This scaffolding activity was proposed to facilitate the phosphorylation and inhibition of GSK3β by PKA, contributing to EMT and breast cancer metastasis[317]. In this scenario, HK2 acts as an A-kinase anchoring protein (AKAP) in the presence of glucose. Indeed, AKAPs have been shown to facilitate the activity of PKA by anchoring this kinase near to its targets, frequently by tethering PKA to organelles and membranes[326]. By these means, PKA emerges as a key mediator in cyclic adenosine monophosphate (cAMP)-dependent signalling pathways. Intriguingly, PKA has been shown to stimulate the binding of the AKAP121, a mitochondrial AKAP mouse protein, to RNA by phosphorylating the KH domain of AKAP121[327]. This binding was proposed to tether mRNAs that encode mitochondrial proteins to the outer mitochondrial membrane (OMM) to facilitate localized translation and import of the newly synthesized proteins into the mitochondria. Although HK2 does not harbour a KH domain, this kinase moonlight as (1) an RBP, (2) an AKAP[317], and (3) it can bind to OMM through VDAC1[328]. Therefore, we next investigated whether HK2 could bind to the *SOX10* mRNA in a PRKAR1a-dependent manner.

PKA exists as a tetramer consisting of two regulatory and two catalytic subunits. Binding of cAMP to the regulatory subunits is required to activate PKA by promoting its dissociation from the catalytic subunits. Then, the catalytic subunits are activated via ATP-binding[329]. Therefore, to test the hypothesis that PKA mediates the RNA-binding activity of HK2, we examined the effect of inhibiting this catalytic activation on the ability of HK2 to bind to the *SOX10* mRNA. To this end, we used a reversible ATP-competitive inhibitor of PKA (H89), and we found that H89 treatment reduced HK2-*SOX10* mRNA association (Figure 3A). This finding suggests that the activation of the catalytic subunits of PKA may play a role in this interaction. Next, to further investigate the involvement of PKA activity on HK2-SOX10 interaction, we decided to modulate cAMP-dependent signalling pathways by inhibiting or promoting the cAMP synthesis. First, we explored whether the use of a non-competitive adenylyl cyclase inhibitor (2’5’-Dideoxyadenosine) would impact this interaction (Figure 3B). Of note, adenylyl cyclase is an enzyme that synthesizes cAMP from ATP, which, in turn, binds to the regulatory subunits of PKA and activates the kinase[329]. Second, we explored the effect of enhancing intracellular cAMP formation and accumulation (Figure 2C). To this end, we induced the formation of cAMP through increased adenylyl cyclase activation (Forskolin, FSK), and cAMP accumulation by inhibiting its break down into 5’AMP by phosphodiesterase (PDE) using a broad-spectrum PDE inhibitor (IBMX, 3-Isobutyl-1-methylxanthine). However, neither the inhibition of intracellular cAMP formation nor cAMP induction and accumulation impacted HK2 association with the *SOX10* mRNA. Finally, to directly verify whether PKA was required for this association, we performed a siRNA-mediated depletion of PRKAR1a. However, we found that depletion of PRKAR1a did not affect HK2-*SOX10* interaction (Figure 3D). Together, these results indicate that HK2’s binding to the *SOX10* mRNA does not require PKA nor the

interaction with its regulatory subunit α, and that the decrease observed upon H89 treatment is potentially due to nonspecific effects of this inhibitor.

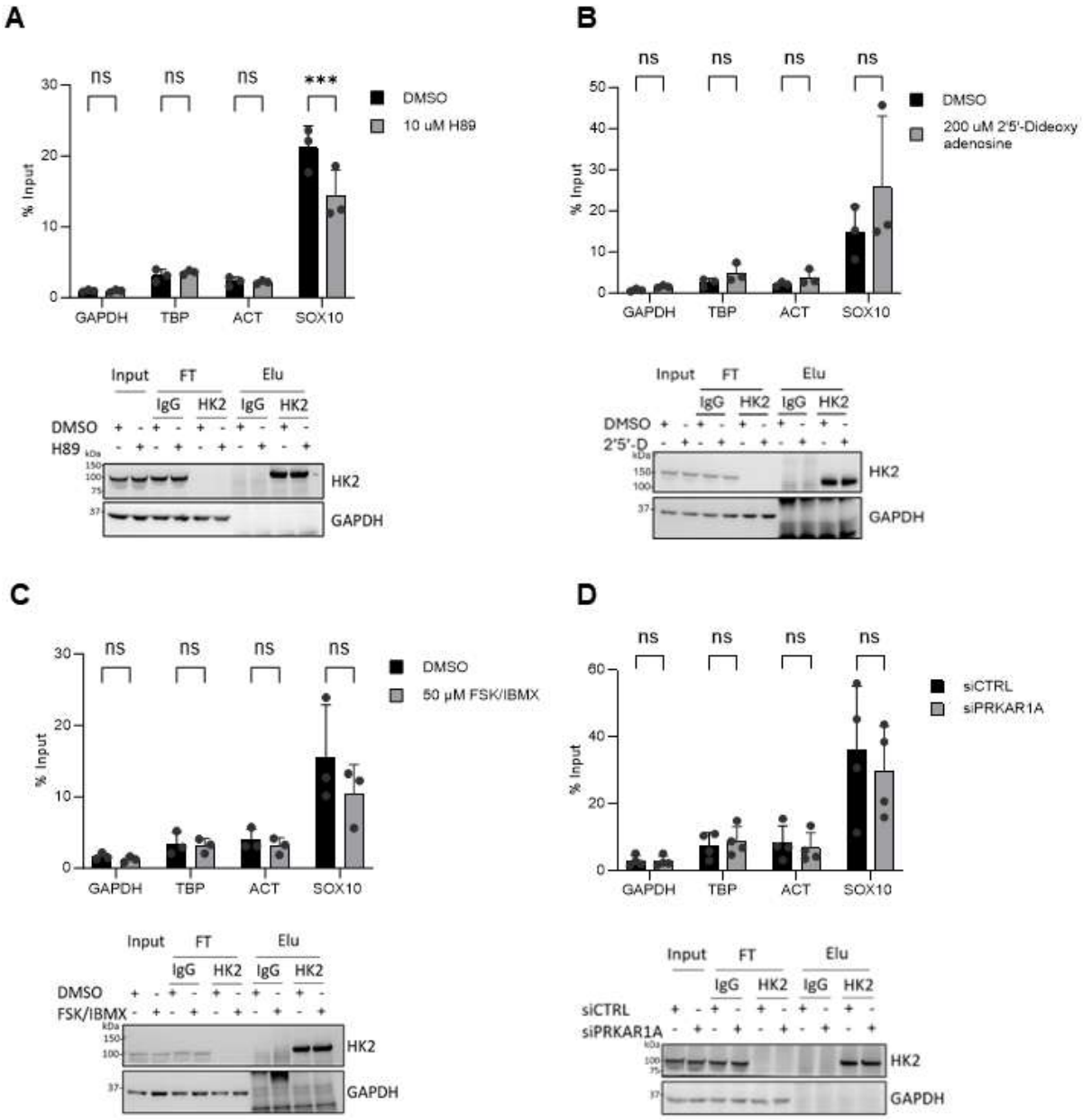

Figure 3. HK2 interacts with *SOX10* mRNA in a PKA-independent manner. RIP experiments were performed on A375 cells. (**A**) Cells were incubated either in the presence of 10 µM H89 (N-(2-(4-bromocinnamylamino) ethyl)-5-isoquinolinesulfonamide) or DMSO for 2 h. (**B**) Cells were incubated either in 200 µM 2'5'-Dideoxyadenosine or DMSO for 6 h. (**C**) Cells were incubated in 50 µM Forskolin (FSK) and 50 µM IBMX (3-Isobutyl-1-methylxanthine) or DMSO for 2 h. (**D**) Cells were transfected with siRNAs targeting the regulatory subunit α of protein kinase A (siPRKAR1a) or control (siCTRL) and incubated for 48 h. *SOX10* mRNA was analysed in IgG and HK2 immunoprecipitated samples and expressed as percentage of the mRNA present in the input. *GAPDH*, *TBP* and *ACT* mRNAs were used as negative controls. *p*-values were calculated by ordinary two-way ANOVA with Dunnett's multiple comparisons test (SD, n = 3 biological replicates in A, B and C; and n = 4 in D) (*** $p \leq 0.001$; ns = non-significant).

Investigation of the translational regulation of SOX10 mRNA mediated by HK2

Moya-Plana (2020), a former PhD student at Caroline Robert's group at Institut Gustave Roussy, showed by polysome profiling in A375 melanoma cells that HK2 depletion decreases the translation of the *SOX10* mRNA by shifting the association of the mRNA from heavy polysomes fractions to lighter polysome fractions[318]. To further examine the translational control of HK2 on *SOX10* mRNA in melanoma cells, we employed another technique, termed AHA-mediated ribosome isolation (AHAribo)[330], on A2058 and M249 melanoma cells upon siRNA-mediated depletion of HK2. This technique allows for the co-purification of RNAs and translating ribosomes via nascent peptide chains that incorporated the non-canonical amino acid L-azidohomoalanine (AHA)[330]. Briefly, the AHAribo protocol (RNA module) was performed following 5 main steps (Figure 4A): (1) cell treatment, when cells were incubated in methionine-depleted medium and treated with the methionine analogue AHA and sBlock (which was used to stabilize AHA-peptides on ribosomes and polysomes); (2) cell lysis and AHA 'copper-free click reaction'[331]; (3) active polysome capture using magnetic beads; and (4) translatome capture followed by (5) RT-qPCR for mRNA quantification and analysis. As expected, we observed that HK2 depletion decreased the interaction between *SOX10* mRNA and translating ribosomes, thereby indicating that *SOX10* mRNA is less actively translated upon HK2 KD (Figure 4B).

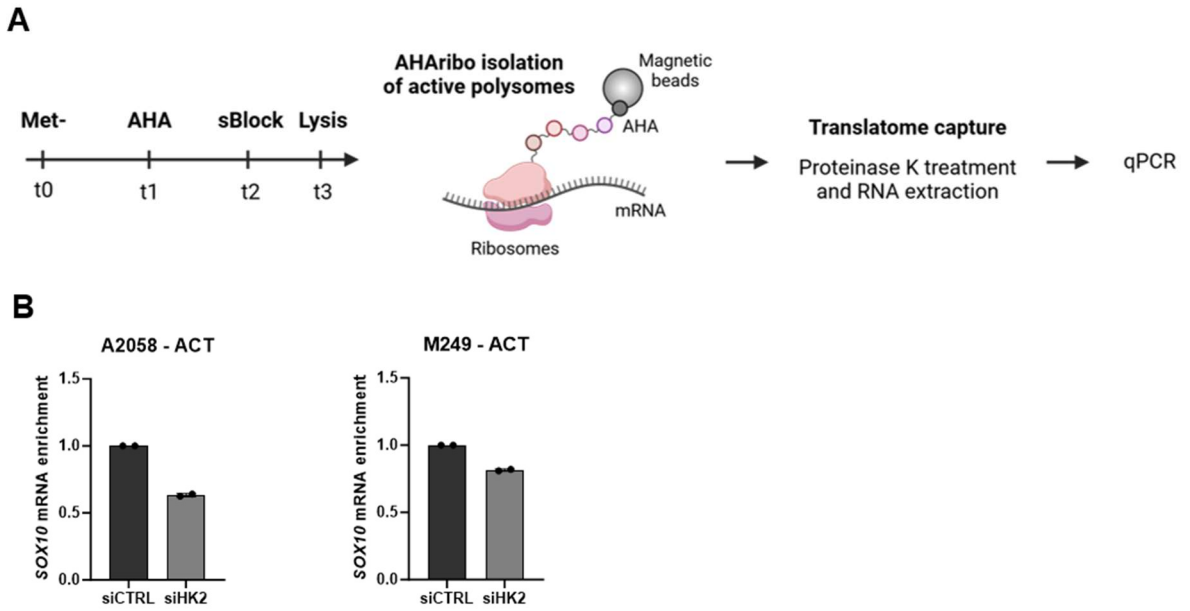

Figure 4. HK2 regulates *SOX10* mRNA translation in melanoma cells using AHAribo. (**A**) Schematic representation of the AHAribo workflow. After methionine depletion, AHA and sBlock incubation, cell lysates were processed for isolation of translational complexes via AHA incorporation in nascent peptides. (**B**) A2058 and M249 melanoma cell lines were transfected with siRNAs targeting HK2 (siHK2,

grey) or control (siCTRL, black). *SOX10* mRNA enrichment is normalized to *β-actin* (*ACT*) and presented as relative to the siCTRL condition (SD, n = 2 biological replicates).

Evaluation of HK2-*SOX10* interaction in cancer-related phenotypes

To investigate the involvement of HK2 in cancer-related phenotypes, we assessed the migration and invasion of A375 cells upon siRNA-mediated inhibition of HK2 in wound healing and transwell assays. Moya-Plana (2020) found that migration and invasion potential of melanoma cells were dependent on HK2 expression[318], as previously demonstrated in other cancer types[332–336]. To specifically address the role of aerobic glycolysis and HK2 in melanoma cell aggressive behaviour, he performed transwell experiments in cells cultured in either glucose- or galactose-containing media. He observed that both migration and invasion properties of melanoma cells decreased significantly in galactose media[318]. However, depletion of HK2 also led to an important inhibition of both phenotypes, even when compared to the blockage of aerobic glycolysis upon galactose[318]. Strinkingly, depletion of HK2 in galactose exhibited an even greater impact in both cell invasion and migration[318]. Thus, we hypothesized that HK2 may have an extra-metabolic function involved in the regulation of melanoma aggressiveness.

Since we demonstrate that HK2 is a non-canonical RBP that binds and regulates the translation of the *SOX10* mRNA in melanoma, we further investigated whether the effects observed by depleting HK2 were mediated through SOX10. Of note, SOX10 has been shown to play key roles in melanoma initiation, proliferation, invasion, survival and drug resistance against current melanoma targeted therapies (BRAF and MEK inhibitors, BRAFi and MEKi)[319–321]. Using 2D IncuCyte scratch-wound healing assays, we conducted migration assays in A375 cells upon HK2 depletion. This assay was simultaneously performed in A375 cells that ectopically expressed SOX10, which were generated through the transduction of lentivirus particles carrying the *SOX10* CDS (therefore without the 5'UTR). We observed that cells upon HK2 knock down travelled significantly less than controls (Figure 5), in accordance with our findings that the migration potential of A375 cells is dependent on HK2 expression. However, ectopic expression of SOX10 did not reduce the effect observed upon HK2 depletion. Conversely, depletion of HK2 in SOX10 transduced cells showed an even further decrease in the migratory capacity of the cells when compared to control cells.

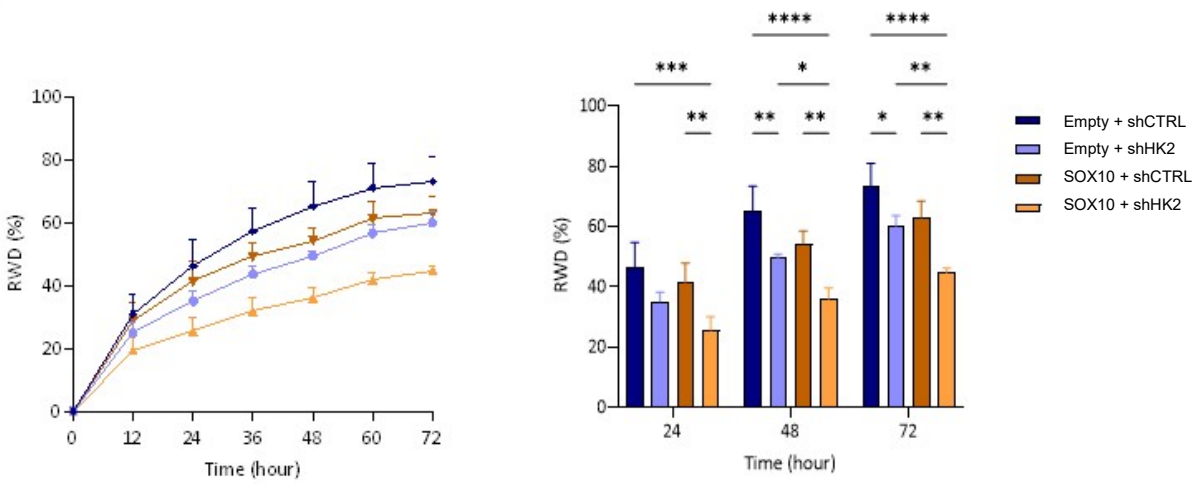

Figure 5. Depletion of HK2 leads to a decrease in A375 cell migration. Scratch-wound assay comparing the migratory capacity of A375 cells ectopically expressing SOX10 (SOX10) cells to parental cells (Empty). Both cell lines were plated 24h after transfection with siRNAs targeting HK2 (Empty, light blue; SOX10, light orange) or control (Empty, dark blue; SOX10 dark orange). p-values were calculated by ordinary two-way ANOVA with Turkey's multiple comparison test (SD, n = 3 biological replicates), and only significant differences within the same cell line are shown (*p ≤ 0.05; ** p ≤ 0.01; *** p ≤ 0.001; **** p ≤ 0.0001).

To confirm the results obtained by transiently inhibiting HK2, we stably knocked down HK2 in A375 cells (both parental and SOX10) by transducing small hairpin RNAs (shRNA) targeting HK2 expression (shHK2) or control (shCTRL). We observed by western blot and RT-qPCR that HK2 was efficiently depleted in both cell lines (Figures 6A and B). The stable HK2 KD decreased endogenous SOX10 protein levels, as observed in western blot analyses. This decrease, however, was not observed in the ectopically expressed SOX10, in which only SOX10 CDS was transduced. Additionally, the *SOX10* mRNA level, which was evaluated by RT-qPCR experiments, remained unchanged upon HK2 KD. Using 2D IncuCyte scratch-wound healing assays, we con ducted migration and invasion assays in A375 cells (parental and SOX10) upon shRNA-mediated HK2 KD. In accordance with our previous results, we found that the migration and invasive potential of A375 cells dependent on HK2 expression (Figure 6C). Besides, ectopic expression of SOX10 did not reduce the effect observed upon HK2 KD. In the migration assay, in particular, SOX10 expression in cells upon HK2 depletion seems to further decrease the migratory capacity of the cells.

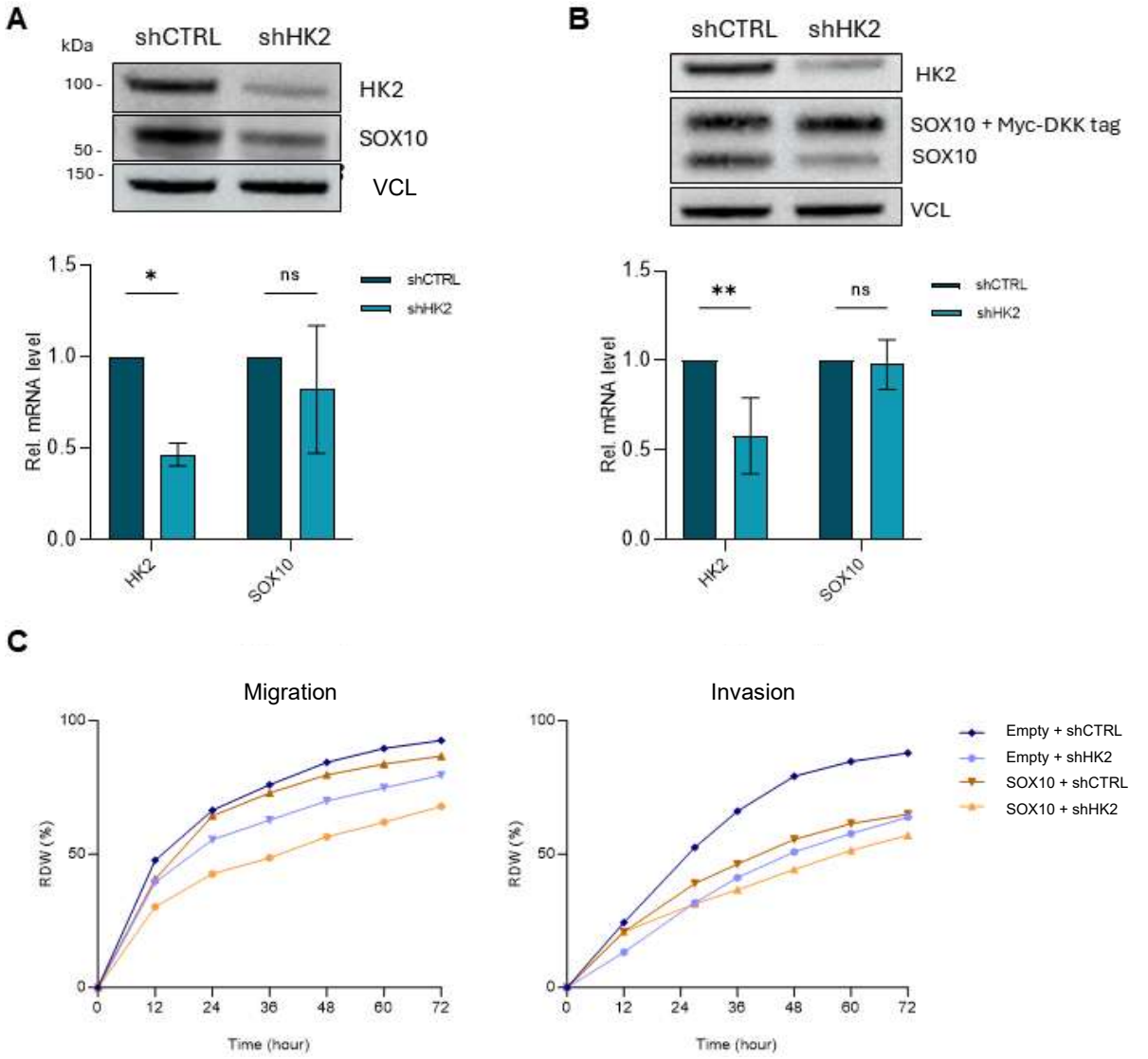

Figure 6. Depletion of HK2 leads to a decrease in melanoma cell migration and invasion independently of SOX10. Upper panel: western blot analyses of the shRNA-mediated HK2 knock down in (**A**) A375 melanoma cells and (**B**) A375 cells ectopically expressing SOX10. VCL was used as loading control. Lower panel: RT-qPCR quantification of the *SOX10* mRNA in both HK2 KD and parental cell lines. p-values were calculated by ordinary one-way ANOVA (SD, n = 3 biological replicates). (**C**) Scratch-wound assay comparing the migratory capacity of A375 cells ectopically expressing SOX10 (SOX10) cells to parental cells (Empty) (n = 1). Both cell lines were transduced with shRNAs targeting HK2 (Empty, light blue; SOX10, light orange) or control (Empty, dark blue; SOX10 dark orange).

We next explored another strategy to study the involvement of HK2-SOX10 interaction in migration; however, this strategy is also a wound healing-based method. In this assay, an ibidi Culture-Insert containing two cell culture reservoirs was placed on a cell culture surface. A375 or A2058 cells were seeded in both reservoirs and reverse transfected with siHK2 or siCTRL. After 48h of incubation, the insert was removed, the wound healing process was evaluated for 10 h, and the free-cell gap was measured. In accordance with our previous results, HK2 KD in both A375 and A2058 cells displayed

decreased migration, which was not rescued by SOX10 expression (Figure 7). Together, these results suggest that the role of HK2 in migration and invasion of A375 and A2058 melanoma cells may not involve SOX10.

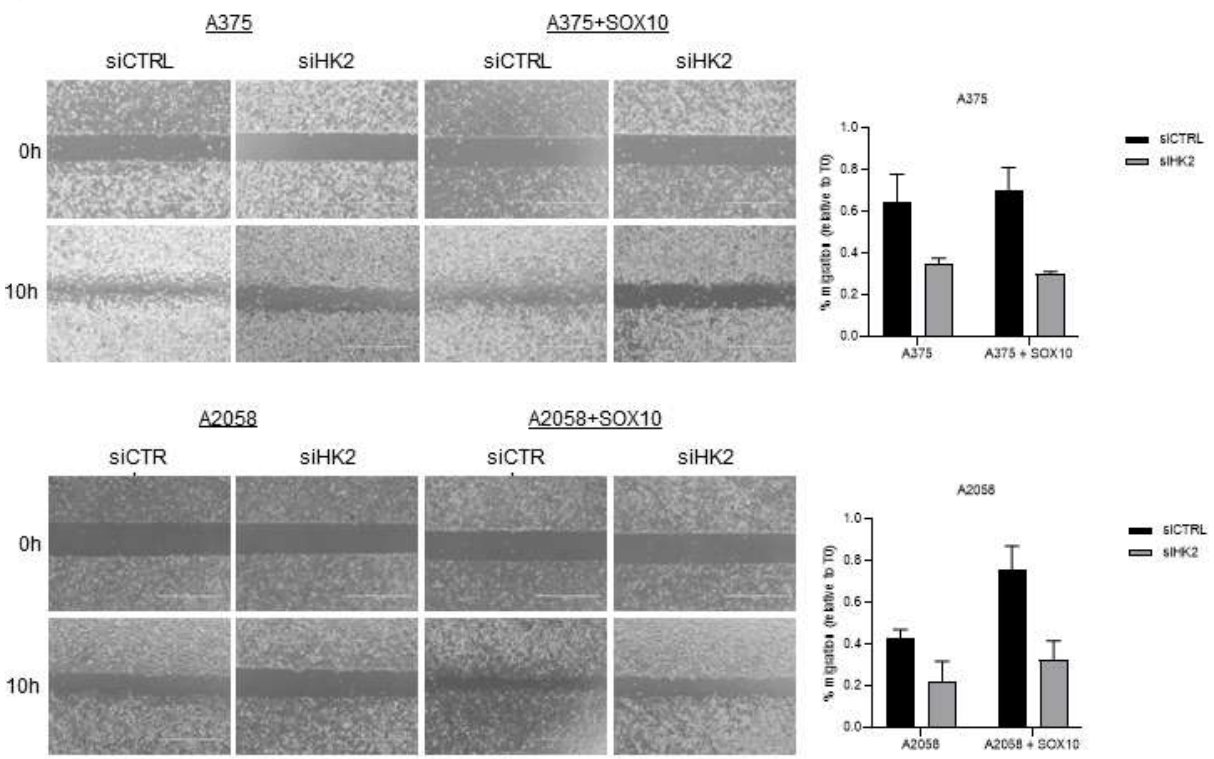

Figure 7. Wound healing assay using the ibidi Culture-Insert 2 Well. HK2 depletion decreases melanoma cell migration and invasion independently of SOX10 (SD, n = 2 biological replicates).

We also investigated the possibility that the HK2-*SOX10* mRNA interaction is involved in drug resistance of melanoma cells against BRAF and MEK inhibitors in clonogenic and invasion assays. We found that HK2 KD or incubation of the cells with BRAFi (vemurafenib) and MEKi (cobimetinib) impaired colony formation (Figure 8A) and invasion of A375 cells (Figure 8B). In fact, incubation of Empty A375 cells with BRAFi/MEKi impaired clonogenicity and invasion in the same or in a greater extent than HK2 KD cells incubated in DMSO. Curiously, while the area covered by the cells upon HK2 depletion and control cells under drug treatment are not significantly different, we can observe that HK2 depletion reduced the number of colonies, while drug treatment seemed to reduce the size (growth) of the colonies regardless of HK2 expression. Indeed, the effect of drug treatment in both cell lines (A375 Empty and SOX10) seems to be independent of HK2 expression, since HK2 depletion did not affect the cell phenotypes. Intriguingly, ectopic expression of SOX10 upon drug treatment strongly inhibited colony formation regardless and it seemed to further decrease the ability of the cells to invade the wound area covered with matrigel (extracellular matrix,

ECM). These results suggest that HK2 is not involved in drug resistance, while SOX10 expression appears to render cells more sensitive to BRAF and MEK inhibition.

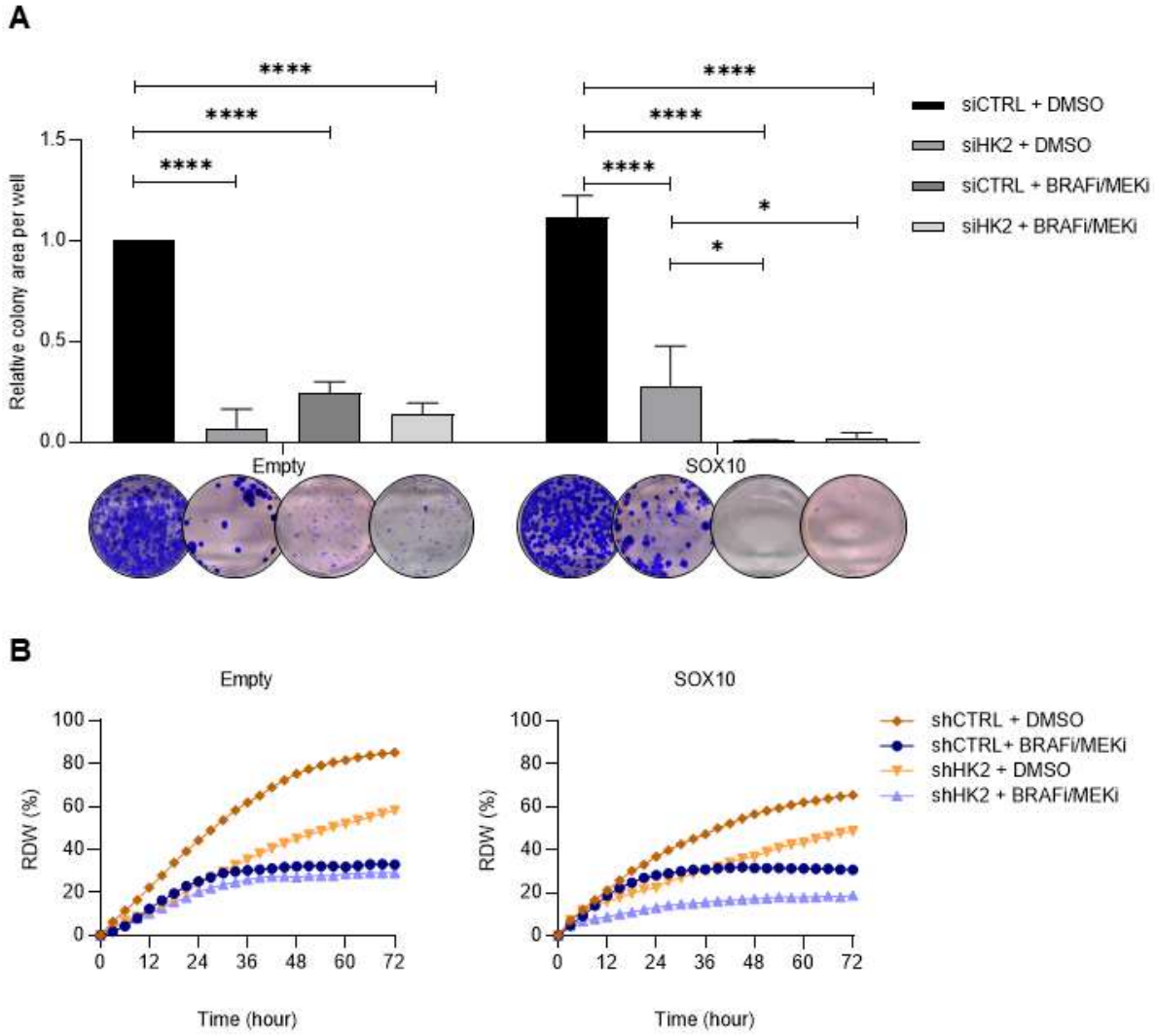

Figure 8. Depletion of HK2 decreases melanoma cell invasion and clonogenicity. (**A**) A375 cells were plated 24h after transfection with siRNAs targeting HK2 (siHK2) or control (siCTRL). The cells were treated with Cobimetinib (0.01 µM) and Vemurafenib (0.1 µM) or DMSO every 3 days. The colonies were stained with crystal violet after 10 days, and the clonogenic cell growth was measured. Upper panel: percentage of area covered by crystal violet stained cell colonies. *p*-values were calculated by ordinary two-way ANOVA with Turkey's multiple comparison test (SD, n = 3 biological replicates), and only significant differences within the same cell line are shown (* $p \leq 0.05$, ** $p \leq 0.01$, **** $p \leq 0.0001$). Lower panel: representative images of three independent experiments. (**B**) Scratch-wound assay comparing the invasion capacity of A375 cells (Empty or SOX10) incubated with 0.4 µM of Vemurafenib/Cobimetinib to DMSO treated cells (control) (n = 1). Both cell lines were transduced with shRNAs targeting HK2 (Empty, light blue; SOX10, light orange) or control (Empty, dark blue; SOX10 dark orange). Martigel was prepared with BRAFi/MEKi-containing medium.

4 DISCUSSION AND PERSPECTIVES

The Hexokinase II (HK2), the first enzyme in the glucose metabolism, is highly expressed in cancer cells. Although HK2's role in tumorigenesis has been attributed to its glycolytic activity, this enzyme has been shown to execute non-canonical functions that often regulate processes that are highly relevant for cell transformation and cancer development. For example, HK2 has been shown to interact with nuclear proteins and regulate essential processes including DNA-damage response and chromatin accessibility in acute myeloid leukaemia, thereby controlling stem cell function and differentiation through the regulation of gene expression[337]. Other examples include a non-catalytic scaffolding activity of HK2 involved in SNAIL-mediated epithelial-to-mesenchymal transition (EMT) and breast cancer metastasis[317], and protein kinase activity involved in PD-L1-dependent tumour immune evasion[338]. Recently, HK2 has been also proposed to transcriptionally regulate the expression of SLUG, pERK, and vimentin via the SOD2-H2O2 pathway in oral squamous cell carcinoma[336].

In collaboration with Caroline Robert's laboratory at Institut Gustave Roussy, we found that HK2 is a novel glycolytic enzyme that associates with polysomes in A375 melanoma cells. We wondered whether this interaction characterized a non-canonical and yet non-described role of HK2 in regulating mRNA translation in cancer. Indeed, other glycolytic enzymes have been found to regulate mRNA translation either by direct binding to RNAs (including tRNAs[98,157–160]) and/or by interacting with ribosomes[114,164]. Both isoforms of the Pyruvate Kinase M (PKM), for example, were found to interact with endoplasmic reticulum (ER)-associated ribosomes, functioning as RNA-binding proteins to activate the translation of ER-destined mRNAs[164]. Conversely, PKM recruitment to cytosolic polysomes (ER-excluded) combined with its moonlighting RNA-binding activity was shown to induce translational stalling[114]. We therefore evaluated the influence of HK2 on the translation of cancer-relevant mRNAs in melanoma, and we found that this enzyme specifically regulates the translation of the *SOX10* mRNA, which encodes an important transcriptional factor involved in melanoma initiation, proliferation, invasion, survival and drug resistance against current melanoma targeted therapies (BRAF and MEK inhibitors)[319–321].

We thus investigated the possibility that HK2 regulates SOX10 mRNA translation through an as-yet undescribed RNA-binding activity. Although HK2 does not harbour any recognisable RNA-binding domain, this enzyme has been recurrently proposed to bind poly(A) and non-poly(A) RNAs in human cells in large-scale RNA interactome studies[77–79,83]. Besides, yeast hexokinases have already been shown to directly bind nucleic acids[64]. In agreement with these studies, we showed in this thesis that HK2 directly binds RNA *in vivo*. With the use of HK2 mutants, we also demonstrated that this RNA-binding activity does not dependent on the enzyme's catalytic activity or localization at the outer mitochondrial membrane (OMM). Curiously, sucrose gradient

experiments suggest that HK2-containing complexes exhibit a greater dependence on RNA than complexes containing other known RNA-binding glycolytic enzymes, such as PKM2 and the glyceraldehyde-3-phosphate dehydrogenase (GAPDH). Hence, our results strongly suggest that HK2 is a novel *bona fide* RNA-binding protein, whose previously unidentified moonlighting function needs to be characterized.

Next, we found that HK2 binds and affects *SOX10* mRNA translation in a 5'UTR-dependent manner. Given the importance of 5'UTRs for translation initiation, together with previous observations that specific RNA-binding glycolytic enzymes are polysome interactors that modulate mRNA translation, it is conceivable that HK2 may facilitate *SOX10* mRNA translation initiation by promoting ribosome association with the mRNA. Accordingly, we do observe that HK2 depletion decreases *SOX10* mRNA association with translationally active polysomes in melanoma cells. However, further studies are required to test whether HK2 facilitates ribosomal assembly, for example, through the recruitment of eIF4F factors to the *SOX10* 5'UTR. Besides, our study does not exclude the possibility that the regulation of *SOX10* mRNA translation occurs by indirect binding of HK2. Therefore, other assays are also required to confirm the potential direct binding between HK2 and the *SOX10* mRNA, besides helping in the identification of the structural basis involved in this interaction.

Several reports demonstrated that the translational control exerted through the RNA-binding activity of glycolytic enzymes can be regulated by glycolytic substrates, metabolites, or cellular metabolic states[20,96–98,130,131,168]. Accordingly, inhibition of glycolysis diminished HK2 interaction and, as suggested by western blot and RT-qPCR experiments, potentially *SOX10* mRNA translation even though the RNA-binding activity of HK2 does not necessarily require its catalytic activity, as observed in CLIP experiments. However, our experiments also suggest that the composition of HK2-containing complexes may be less dependent on RNA in cells fed with galactose instead of glucose. Therefore, approaches to study *in vivo* and *in vitro* mRNA translation and RNA-protein interactions are necessary to further investigate how glycolytic substrates and metabolites are involved in the control of mRNA translation mediated by HK2's RNA-binding activity. In addition, further studies are required to explore whether HK2 globally loses its ability to bind RNA in the absence of glucose or whether the enzyme selectively binds distinct mRNAs depending on the metabolic status of the cell. Nevertheless, our data suggest the existence of a sophisticated link between metabolism and gene regulation to directly control gene expression.

In an attempt to identify the key elements involved in the *SOX10* mRNA translational regulation mediated by HK2, we tested whether the RNA-binding activity of this glycolytic enzyme is dependent on its interaction with the protein kinase A (PKA). Of note, HK2 has been recently shown to interact with the regulatory subunit α of PKA (PRKAR1a) and act as an A-kinase anchoring protein (AKAP) in the presence of glucose[317]. Besides, PKA has been shown to stimulate the RNA-binding activity of another mitochondrial AKAP (AKAP121)[327]. Although our results indicate that HK2's

binding to the *SOX10* mRNA does not require PKA nor the interaction with its regulatory subunit α, we found that a reversible ATP-competitive inhibitor of PKA, H89, impaired this association. We hypothesize that the observed effect of H89 treatment is due to its action on nonspecific targets. Indeed, H89 has been shown to directly and indirectly affect the activity of protein kinases other than PKA, particularly basophilic kinases such as AKT (also known as protein kinase B, PKB)[339,340]. Although studies differ whether H89 activity sustains[339] or inhibit[340] the activity (phosphorylation) of AKT, this kinase has been shown to directly impact HK2's localization and function. For example, AKT activation was shown to phosphorylate HK2 and induce HK2-mitochondrial association, thereby increasing glucose uptake and cell survival[341]. However, its inhibition in HeLa cells, for example, was shown to promote HK2 dissociation from the mitochondria and nuclear accumulation[342]. Therefore, the involvement of AKT in the RNA-binding activity of HK2 needs to be further investigated. Furthermore, recent studies have also revealed that HK2 possesses protein kinase activities in glioblastoma cells[338], suggesting that it may also function as a basophilic kinase in certain cellular contexts. This makes HK2 a potential target of H89. Given that this inhibitor reduces HK2-*SOX10* mRNA interaction, the effect of H89 on *SOX10* translation also needs to be investigated.

Translation regulation is an essential mechanism for gene expression, dynamically controlling protein synthesis and thereby contributing to the determination of the cellular phenotype[193,194]. In recent years, increasing evidence has shown that abnormal mRNA translation is crucial for the development and progression of various cancers[193,208]. The glycolytic enzyme HK2 has previously been shown as involved in melanoma cell migration and invasion, potentially through extra-metabolic functions[318]. Indeed, Moya-Plana (2020) demonstrated that depletion of HK2 in cells upon glycolysis inhibition (by culturing cells in galactose) exhibited a greater negative impact in both phenotypes when compared to cells cultured in the presence of glucose. We therefore wondered whether HK2-mediated regulation of SOX10 could be involved in these findings. However, in contrast to this hypothesis, we later found that HK2's interaction with *SOX10* mRNA dramatically decreases upon galactose. Additionally, we found that ectopic expression of SOX10 did not reduce the effect of HK2 depletion on migration and, potentially, in invasion. Together, these findings suggest that HK2-*SOX10* mRNA interaction do not play a role in promoting cell invasion and migration. Our results are in accordance with different reports demonstrating that SOX10 expression inversely correlates with cell migration and invasion[343,344]. Although we do not observe an increase in these phenotypes upon SOX10 downregulation due to HK2 knock down (probably because the impact of HK2 depletion in glycolysis is stronger than the subsequent effect of SOX10 downregulation), our results suggest that SOX10 ectopic expression upon HK2 depletion may further decrease melanoma cell migration, still in accordance with previous findings[343,344]. And while SOX10 knock down has been shown to promote cell migration and invasion[343,344], it has also been demonstrated to decrease melanoma

cell proliferation and clonogenicity[319,321]. Indeed, in contrast to our previous findings from cell migration and invasion assays, we found that HK2-dependent SOX10 translational regulation is (at least in part) involved in the ability of melanoma cells to proliferate and form colonies.

Recently, SOX10 knocked down was also proposed to convert melanocytic and intermediate melanoma cells into a mesenchymal-like cell state[343–345]. Indeed, melanoma cells exhibit three main states: (1) a more proliferative, melanocytic state, in which cells express high levels of SOX10 (and other additional melanocyte-specific markers, such as MITF and TYR); (2) a more migratory and invasive mesenchymal state, that exhibits high levels of SOX9 and related EMT genes; and (3) a moderately invasive, intermediate cell state, in which cells co-express melanocytic and mesenchymal genes[345]. A375 melanoma cells, for example, have been shown to exhibit mixed melanocytic and mesenchymal signatures, thereby an intermediary phenotype[345]. Importantly, this intermediate state has also been shown to occur in melanoma biopsies and in multiple patient cohorts[344]. Therefore, we hypothesize that HK2 may regulate the expression of key genes involved in the promotion of cell migration and invasion, while simultaneously regulating *SOX10* mRNA translation to support cell proliferation. Hence, a deeper understanding of the cellular processes influenced by HK2's non-canonical activities and their underlying molecular mechanisms represent promising directions for future research. Such studies could lead to the development of novel therapeutics that specifically target cancer cells while sparing non-malignant counterparts, thereby offering new perspectives in cancer treatment.

While MAPK-targeted therapeutic response of patients with $BRAF^{V600E}$ melanoma is usually high, these patients frequently acquired drug resistance due to genetic mutations and non-genetic adaptation mechanisms[308]. In fact, translational reprogramming is one of the many strategies used by cancer cells to adapt during therapy and overcome drug efficacy[194]. Therefore, we briefly investigated the involvement of HK2-dependent SOX10 translational control in melanoma resistance against BRAF and MEK inhibitors in clonogenic and invasion assays. Our results suggest that HK2 is not involved in drug resistance, while ectopic expression of SOX10 render cells more sensitive to BRAF and MEK inhibition. Accordingly, $BRAF^{V600E}$-mutated melanoma cells that are tolerant (persistent) to anti- MAPK-targeted therapy have been shown to switch their metabolism from glycolysis to mitochondrial respiration[311,346]. Indeed, $BRAF^{V600E}$ melanoma cells under targeted therapy were recently shown to rewire their proteome by favouring the translation of valine codon-enriched mRNAs, thus enhancing mitochondria respiration over glycolysis[311]. However, the metabolic switch observed in tolerant and resistant cells was also demonstrated to be mediated by other mechanisms besides translation, such as by the transcriptional downregulation of key glycolytic enzymes (e.g., HK2) and glycolysis-related pathways[346,347].

We indeed observed that treatment with BRAF and MEK inhibitors strongly reduced HK2 expression (data not shown), possibly explaining why siRNA-depletion of HK2 does not impact the clonogenicity of cells under drug treatment. Although SOX10 expression in these cells remains to be evaluated, we would expect that this transcriptional factor is less translated upon HK2 inhibition. In fact, reduced SOX10 expression has been previously detected in the surviving A375 cell population following 14 days of treatment with BRAF and MEK inhibitors[343]. Accordingly, two independent studies proposed that cells with low SOX10 expression preferentially survive upon treatment[321,343]. They also demonstrated that SOX10-deficient melanoma cells were significantly less sensitive to MEK and/or BRAF inhibitors in both short-term and long-term assays[321,343]. This is in agreement with our results demonstrating that SOX10 ectopic expression upon drug treatment inhibits clonogenicity and potentially decreases cell invasion even further. Nonetheless, previous studies have also demonstrated synergistic effects of combining BRAF and MEK inhibitors with cIAP1/2 inhibitors (Birinapant) in $BRAF^{V600E}$ melanoma cells to selectively target SOX10-deficient cells[343]. Therefore, investigation of the potential effects of combining cIAP1/2 inhibitors with HK2 (or HK2-SOX10 interaction) inhibitors in $BRAF^{V600E}$ melanoma cells may provide valuable insights in cancer treatment. Besides, the investigation of extra-metabolic activities of mitochondrial enzymes expressed upon drug treatment may also reveal novel therapeutic targets. The 3-Hydroxyacyl-CoA Dehydrogenase (HADH), for example, is a key enzyme in fatty acid oxidation whose translation is favoured under MAPK-targeted therapy. As GAPDH, this enzyme is a dehydrogenase that harbour a di-nucleotide binding domain, also known as Rossmann fold, which has been extensively proposed to mediate RNA-binding[93,96–99].

Our findings underscore a non-metabolic function of the glycolytic enzyme HK2, indicating that cancer cells may enhance glycolysis for purposes beyond simple anabolism. While aerobic glycolysis provides significant advantages for rapidly growing and proliferating cells, contributing to 60% of total cellular ATP production in cancer[109] and supplying glycolytic intermediates necessary for the biosynthesis of nucleic acids, lipids, and amino acids[106], its role extends further. Given that many metabolic enzymes also serve as RNA-binding proteins engaged in post-transcriptional RNA-processing reactions and considering that aberrant mRNA translation is a hallmark of tumours, it is crucial to investigate the significance of HK2's interactions with RNA beyond SOX10. We believe that HK2 might regulate the translation of numerous other key mRNAs involved in cancer-relevant signalling pathways. On the other hand, a potential riboregulation of HK2, as demonstrated in other glycolytic enzymes[20,120,122], should also be investigated. Therefore, understanding the cellular processes influenced by HK2's RNA-binding activity and uncovering their underlying molecular mechanisms represent promising directions for future research. Such studies could lead to the development of novel therapeutics that specifically target cancer cells while sparing non-malignant counterparts, offering new perspectives in cancer treatment.

REFERENCES

1. Corley, M., Burns, M. C. & Yeo, G. W. How RNA-Binding Proteins Interact with RNA: Molecules and Mechanisms. *Molecular Cell* **78**, 9–29 (2020).

2. Mitchell, S. F. & Parker, R. Principles and Properties of Eukaryotic mRNPs. *Molecular Cell* **54**, 547–558 (2014).

3. Castello, A. *et al.* Insights into RNA Biology from an Atlas of Mammalian mRNA-Binding Proteins. *Cell* **149**, 1393–1406 (2012).

4. Hentze, M. W., Castello, A., Schwarzl, T. & Preiss, T. A brave new world of RNA-binding proteins. *Nature Reviews Molecular Cell Biology* **19**, 327–341 (2018).

5. Glisovic, T., Bachorik, J. L., Yong, J. & Dreyfuss, G. RNA-binding proteins and post-transcriptional gene regulation. *FEBS Letters* **582**, 1977–1986 (2008).

6. Choi, Y. *et al.* Time-resolved profiling of RNA binding proteins throughout the mRNA life cycle. *Molecular Cell* (2024) doi:10.1016/j.molcel.2024.03.012.

7. Gebauer, F., Schwarzl, T., Valcárcel, J. & Hentze, M. W. RNA-binding proteins in human genetic disease. *Nat Rev Genet* **22**, 185–198 (2021).

8. Gerstberger, S., Hafner, M. & Tuschl, T. A census of human RNA-binding proteins. *Nat Rev Genet* **15**, 829–845 (2014).

9. Zhou, B. *et al.* Translation of noncoding RNAs and cancer. *Cancer Lett* **497**, 89–99 (2021).

10. Zhou, Y. *et al.* Systematic analysis of RNA-binding proteins identifies targetable therapeutic vulnerabilities in osteosarcoma. *Nat Commun* **15**, 2810 (2024).

11. Antal, C. E. *et al.* A super-enhancer-regulated RNA-binding protein cascade drives pancreatic cancer. *Nat Commun* **14**, 5195 (2023).

12. Maurin, M. *et al.* RBFOX2 deregulation promotes pancreatic cancer progression and metastasis through alternative splicing. *Nat Commun* **14**, 8444 (2023).

13. Mestre-Farràs, N. *et al.* Melanoma RBPome identification reveals PDIA6 as an unconventional RNA-binding protein involved in metastasis. *Nucleic Acids Research* **50**, 8207–8225 (2022).

14. Fernandopulle, M. S., Lippincott-Schwartz, J. & Ward, M. E. RNA transport and local translation in neurodevelopmental and neurodegenerative disease. *Nat Neurosci* **24**, 622–632 (2021).

15. Völkers, M., Preiss, T. & Hentze, M. W. RNA-binding proteins in cardiovascular biology and disease: the beat goes on. *Nat Rev Cardiol* 1–18 (2024) doi:10.1038/s41569-023-00958-z.

16. De Boulle, K. *et al.* A point mutation in the FMR-1 gene associated with fragile X mental retardation. *Nat Genet* **3**, 31–35 (1993).

17. Siomi, H., Choi, M., Siomi, M. C., Nussbaum, R. L. & Dreyfuss, G. Essential role for KH domains in RNA binding: impaired RNA binding by a mutation in the KH domain of FMR1 that causes fragile X syndrome. *Cell* **77**, 33–39 (1994).

18. Bertoldo, J. B., Müller, S. & Hüttelmaier, S. RNA-binding proteins in cancer drug discovery. *Drug Discovery Today* **28**, 103580 (2023).

19. Tan, X. *et al.* LncRNA SNHG1 and RNA binding protein hnRNPL form a complex and coregulate CDH1 to boost the growth and metastasis of prostate cancer. *Cell Death Dis* **12**, 1–14 (2021).

20. Huppertz, I. *et al.* Riboregulation of Enolase 1 activity controls glycolysis and embryonic stem cell differentiation. *Molecular Cell* **82**, 2666-2680.e11 (2022).

21. Yu, S. *et al.* A novel lncRNA, TCONS_00006195, represses hepatocellular carcinoma progression by inhibiting enzymatic activity of ENO1. *Cell Death Dis* **9**, 1–13 (2018).

22. Cook, K. B., Kazan, H., Zuberi, K., Morris, Q. & Hughes, T. R. RBPDB: a database of RNA-binding specificities. *Nucleic Acids Research* **39**, D301–D308 (2011).

23. Caudron-Herger, M., Jansen, R. E., Wassmer, E. & Diederichs, S. RBP2GO: a comprehensive pan-species database on RNA-binding proteins, their interactions and functions. *Nucleic Acids Research* **49**, D425–D436 (2021).

24. Ramanathan, M., Porter, D. F. & Khavari, P. A. Methods to study RNA–protein interactions. *Nat Methods* **16**, 225–234 (2019).

25. Hafner, M. *et al.* CLIP and complementary methods. *Nat Rev Methods Primers* **1**, 1–23 (2021).

26. Gräwe, C., Stelloo, S., Hout, F. A. H. van & Vermeulen, M. RNA-Centric Methods: Toward the Interactome of Specific RNA Transcripts. *Trends in Biotechnology* **39**, 890–900 (2021).

27. Detecting RNA-Protein Interaction Using End-Labeled Biotinylated RNA Oligonucleotides and Immunoblotting - PubMed. https://pubmed.ncbi.nlm.nih.gov/26965255/.

28. Leppek, K. & Stoecklin, G. An optimized streptavidin-binding RNA aptamer for purification of ribonucleoprotein complexes identifies novel ARE-binding proteins. *Nucleic Acids Research* **42**, e13 (2014).

29. Lee, H. Y. *et al.* RNA–protein analysis using a conditional CRISPR nuclease. *Proceedings of the National Academy of Sciences* **110**, 5416–5421 (2013).

30. Siprashvili, Z. *et al.* The noncoding RNAs SNORD50A and SNORD50B bind K-Ras and are recurrently deleted in human cancer. *Nat Genet* **48**, 53–58 (2016).

31. Yap, K., Chung, T. H. & Makeyev, E. V. Analysis of RNA-containing compartments by hybridization and proximity labeling in cultured human cells. *STAR Protocols* **3**, 101139 (2022).

32. Yap, K., Chung, T. H. & Makeyev, E. V. Hybridization-proximity labeling reveals spatially ordered interactions of nuclear RNA compartments. *Molecular Cell* **82**, 463-478.e11 (2022).

33. Akaki, K., Mino, T. & Takeuchi, O. DSP-crosslinking and Immunoprecipitation to Isolate Weak Protein Complex. *Bio Protoc* **12**, e4478 (2022).

34. Xiang, C. C. *et al.* Using DSP, a reversible cross-linker, to fix tissue sections for immunostaining, microdissection and expression profiling. *Nucleic Acids Research* **32**, e185 (2004).

35. Weissinger, R., Heinold, L., Akram, S., Jansen, R.-P. & Hermesh, O. RNA Proximity Labeling: A New Detection Tool for RNA–Protein Interactions. *Molecules* **26**, 2270 (2021).

36. Dumrongprechachan, V. *et al.* Cell-type and subcellular compartment-specific APEX2 proximity labeling reveals activity-dependent nuclear proteome dynamics in the striatum. *Nat Commun* **12**, 4855 (2021).

37. Mukherjee, J. *et al.* β-Actin mRNA interactome mapping by proximity biotinylation. *Proceedings of the National Academy of Sciences* **116**, 12863–12872 (2019).

38. Yi, W. *et al.* CRISPR-assisted detection of RNA–protein interactions in living cells. *Nat Methods* **17**, 685–688 (2020).

39. Han, Y. *et al.* Directed Evolution of Split APEX2 Peroxidase. *ACS Chem. Biol.* **14**, 619–635 (2019).

40. MILI, S. & STEITZ, J. A. Evidence for reassociation of RNA-binding proteins after cell lysis: Implications for the interpretation of immunoprecipitation analyses. *RNA* **10**, 1692–1694 (2004).

41. Simon, M. D. *et al.* The genomic binding sites of a noncoding RNA. *Proc Natl Acad Sci U S A* **108**, 20497–20502 (2011).

42. Chu, C. *et al.* Systematic Discovery of Xist RNA Binding Proteins. *Cell* **161**, 404–416 (2015).

43. McHugh, C. A. & Guttman, M. RAP-MS: A Method to Identify Proteins that Interact Directly with a Specific RNA Molecule in Cells. *Methods Mol Biol* **1649**, 473–488 (2018).

44. Matia-González, A. M., Iadevaia, V. & Gerber, A. P. A versatile tandem RNA isolation procedure to capture in vivo formed mRNA-protein complexes. *Methods* **118–119**, 93–100 (2017).

45. Tsai, B. P., Wang, X., Huang, L. & Waterman, M. L. Quantitative profiling of in vivo-assembled RNA-protein complexes using a novel integrated proteomic approach. *Mol Cell Proteomics* **10**, M110.007385 (2011).

46. Zeng, F. *et al.* A protocol for PAIR: PNA-assisted identification of RNA binding proteins in living cells. *Nat Protoc* **1**, 920–927 (2006).

47. Sutherland, B. W., Toews, J. & Kast, J. Utility of formaldehyde cross-linking and mass spectrometry in the study of protein-protein interactions. *J Mass Spectrom* **43**, 699–715 (2008).

48. Greenberg, J. R. Ultraviolet light-induced crosslinking of mRNA to proteins. *Nucleic Acids Res* **6**, 715–732 (1979).

49. Pashev, I. G., Dimitrov, S. I. & Angelov, D. Crosslinking proteins to nucleic acids by ultraviolet laser irradiation. *Trends Biochem Sci* **16**, 323–326 (1991).

50. Hockensmith, J. W., Kubasek, W. L., Vorachek, W. R. & von Hippel, P. H. Laser cross-linking of proteins to nucleic acids. I. Examining physical parameters of protein-nucleic acid complexes. *J Biol Chem* **268**, 15712–15720 (1993).

51. da Rocha, S. T. & Heard, E. Novel players in X inactivation: insights into Xist-mediated gene silencing and chromosome conformation. *Nat Struct Mol Biol* **24**, 197–204 (2017).

52. Lee, F. C. Y. & Ule, J. Advances in CLIP Technologies for Studies of Protein-RNA Interactions. *Mol Cell* **69**, 354–369 (2018).

53. Lerner, M. R. & Steitz, J. A. Antibodies to small nuclear RNAs complexed with proteins are produced by patients with systemic lupus erythematosus. *Proceedings of the National Academy of Sciences* **76**, 5495–5499 (1979).

54. Niranjanakumari, S., Lasda, E., Brazas, R. & Garcia-Blanco, M. A. Reversible cross-linking combined with immunoprecipitation to study RNA–protein interactions in vivo. *Methods* **26**, 182–190 (2002).

55. Keene, J. D., Komisarow, J. M. & Friedersdorf, M. B. RIP-Chip: the isolation and identification of mRNAs, microRNAs and protein components of ribonucleoprotein complexes from cell extracts. *Nat Protoc* **1**, 302–307 (2006).

56. Tenenbaum, S. A., Carson, C. C., Lager, P. J. & Keene, J. D. Identifying mRNA subsets in messenger ribonucleoprotein complexes by using cDNA arrays. *Proceedings of the National Academy of Sciences* **97**, 14085–14090 (2000).

57. Zhao, J. *et al.* Genome-wide Identification of Polycomb-Associated RNAs by RIP-seq. *Molecular Cell* **40**, 939–953 (2010).

58. Singh, G. *et al.* The Cellular EJC Interactome Reveals Higher-Order mRNP Structure and an EJC-SR Protein Nexus. *Cell* **151**, 750–764 (2012).

59. Kurosaki, T., Mitsutomi, S., Hewko, A., Akimitsu, N. & Maquat, L. E. Integrative omics indicate FMRP sequesters mRNA from translation and deadenylation in human neuronal cells. *Molecular Cell* **82**, 4564-4581.e11 (2022).

60. Kurosaki, T. *et al.* Loss of the fragile X syndrome protein FMRP results in misregulation of nonsense-mediated mRNA decay. *Nat Cell Biol* **23**, 40–48 (2021).

61. Kurosaki, T. *et al.* A post-translational regulatory switch on UPF1 controls targeted mRNA degradation. *Genes Dev* **28**, 1900–1916 (2014).

62. Singh, G., Ricci, E. P. & Moore, M. J. RIPiT-Seq: A high-throughput approach for footprinting RNA:protein complexes. *Methods* **65**, 320–332 (2014).

63. Bono, F. & Gehring, N. H. Assembly, disassembly and recycling. *RNA Biology* (2011) doi:10.4161/rna.8.1.13618.

64. Asencio, C., Chatterjee, A. & Hentze, M. W. Silica-based solid-phase extraction of cross-linked nucleic acid–bound proteins. *Life Science Alliance* **1**, (2018).

65. Licatalosi, D. D. *et al.* HITS-CLIP yields genome-wide insights into brain alternative RNA processing. *Nature* **456**, 464–469 (2008).

66. Ule, J., Jensen, K., Mele, A. & Darnell, R. B. CLIP: a method for identifying protein-RNA interaction sites in living cells. *Methods* **37**, 376–386 (2005).

67. Hafner, M. *et al.* Transcriptome-wide identification of RNA-binding protein and microRNA target sites by PAR-CLIP. *Cell* **141**, 129–141 (2010).

68. Scheibe, M., Butter, F., Hafner, M., Tuschl, T. & Mann, M. Quantitative mass spectrometry and PAR-CLIP to identify RNA-protein interactions. *Nucleic Acids Research* **40**, 9897–9902 (2012).

69. König, J. *et al.* iCLIP reveals the function of hnRNP particles in splicing at individual nucleotide resolution. *Nat Struct Mol Biol* **17**, 909–915 (2010).

70. N, H. *et al.* Insights into the design and interpretation of iCLIP experiments. *Genome Biol* **18**, 7–7 (2017).

71. Chakrabarti, A. M., Haberman, N., Praznik, A., Luscombe, N. M. & Ule, J. Data Science Issues in Studying Protein–RNA Interactions with CLIP Technologies. *Annu Rev Biomed Data Sci* **1**, 235–261 (2018).

72. Schwarzl, T. *et al.* Improved discovery of RNA-binding protein binding sites in eCLIP data using DEWSeq. *Nucleic Acids Res* **52**, e1 (2024).

73. Van Nostrand, E. L. *et al.* Robust transcriptome-wide discovery of RNA-binding protein binding sites with enhanced CLIP (eCLIP). *Nat Methods* **13**, 508–514 (2016).

74. Brannan, K. W. *et al.* Robust single-cell discovery of RNA targets of RNA-binding proteins and ribosomes. *Nat Methods* **18**, 507–519 (2021).

75. McMahon, A. C. *et al.* TRIBE: Hijacking an RNA-Editing Enzyme to Identify Cell-Specific Targets of RNA-Binding Proteins. *Cell* **165**, 742–753 (2016).

76. Xu, W., Rahman, R. & Rosbash, M. Mechanistic implications of enhanced editing by a HyperTRIBE RNA-binding protein. *RNA* **24**, 173–182 (2018).

77. Trendel, J. *et al.* The Human RNA-Binding Proteome and Its Dynamics during Translational Arrest. *Cell* **176**, 391-403.e19 (2019).

78. Queiroz, R. M. L. *et al.* Comprehensive identification of RNA–protein interactions in any organism using orthogonal organic phase separation (OOPS). *Nat Biotechnol* **37**, 169–178 (2019).

79. Urdaneta, E. C. *et al.* Purification of cross-linked RNA-protein complexes by phenol-toluol extraction. *Nat Commun* **10**, 990 (2019).

80. Baltz, A. G. *et al.* The mRNA-Bound Proteome and Its Global Occupancy Profile on Protein-Coding Transcripts. *Molecular Cell* **46**, 674–690 (2012).

81. Beckmann, B. M. *et al.* The RNA-binding proteomes from yeast to man harbour conserved enigmRBPs. *Nat Commun* **6**, 1–9 (2015).

82. Perez-Perri, J. I. *et al.* Discovery of RNA-binding proteins and characterization of their dynamic responses by enhanced RNA interactome capture. *Nat Commun* **9**, 1–13 (2018).

83. Backlund, M. *et al.* Plasticity of nuclear and cytoplasmic stress responses of RNA-binding proteins. *Nucleic Acids Research* **48**, 4725–4740 (2020).

84. Sun, H., Fu, B., Qian, X., Xu, P. & Qin, W. Nuclear and cytoplasmic specific RNA binding proteome enrichment and its changes upon ferroptosis induction. *Nat Commun* **15**, 852 (2024).

85. Perez-Perri, J. I. *et al.* The RNA-binding protein landscapes differ between mammalian organs and cultured cells. *Nat Commun* **14**, 2074 (2023).

86. Shchepachev, V. *et al.* Defining the RNA interactome by total RNA-associated protein purification. *Molecular Systems Biology* **15**, e8689 (2019).

87. Villanueva, E. *et al.* Efficient recovery of the RNA-bound proteome and protein-bound transcriptome using phase separation (OOPS). *Nat Protoc* **15**, 2568–2588 (2020).

88. Castello, A. *et al.* System-wide identification of RNA-binding proteins by interactome capture. *Nat Protoc* **8**, 491–500 (2013).

89. Castello, A., Fischer, B., Hentze, M. W. & Preiss, T. RNA-binding proteins in Mendelian disease. *Trends in Genetics* **29**, 318–327 (2013).

90. Perez-Perri, J. I. *et al.* Global analysis of RNA-binding protein dynamics by comparative and enhanced RNA interactome capture. *Nat Protoc* **16**, 27–60 (2021).

91. Lunde, B. M., Moore, C. & Varani, G. RNA-binding proteins: modular design for efficient function. *Nat Rev Mol Cell Biol* **8**, 479–490 (2007).

92. Ray, D. *et al.* A compendium of RNA-binding motifs for decoding gene regulation. *Nature* **499**, 172–177 (2013).

93. Castello, A. *et al.* Identification of RNA-binding domains of RNA-binding proteins in cultured cells on a system-wide scale with RBDmap. *Nat Protoc* **12**, 2447–2464 (2017).

94. Castello, A. *et al.* Comprehensive Identification of RNA-Binding Domains in Human Cells. *Molecular Cell* **63**, 696–710 (2016).

95. Rossman, M. G., Liljas, A., Brändén, C.-I. & Banaszak, L. J. 2 Evolutionary and Structural Relationships among Dehydrogenases. in *The Enzymes* (ed. Boyer, P. D.) vol. 11 61–102 (Academic Press, 1975).

96. Ikeda, Y., Yamaji, R., Irie, K., Kioka, N. & Murakami, A. Glyceraldehyde-3-phosphate dehydrogenase regulates cyclooxygenase-2 expression by targeting mRNA stability. *Archives of Biochemistry and Biophysics* **528**, 141–147 (2012).

97. Nagy, E. & Rigby, W. F. C. Glyceraldehyde-3-phosphate Dehydrogenase Selectively Binds AU-rich RNA in the NAD+-binding Region (Rossmann Fold) (∗). *Journal of Biological Chemistry* **270**, 2755–2763 (1995).

98. Singh, R. & Green, M. R. Sequence-specific binding of transfer RNA by glyceraldehyde-3-phosphate dehydrogenase. *Science* **259**, 365–368 (1993).

99. White, M. R. *et al.* A Dimer Interface Mutation in Glyceraldehyde-3-Phosphate Dehydrogenase Regulates Its Binding to AU-rich RNA *. *Journal of Biological Chemistry* **290**, 1770–1785 (2015).

100. Heindel, A. J. *et al.* Chemoproteomic capture of RNA binding activity in living cells. *Nat Commun* **14**, 6282 (2023).

101. Hentze, M. W., Muckenthaler, M. U., Galy, B. & Camaschella, C. Two to Tango: Regulation of Mammalian Iron Metabolism. *Cell* **142**, 24–38 (2010).

102. Chang, C.-H. *et al.* Posttranscriptional control of T cell effector function by aerobic glycolysis. *Cell* **153**, 1239–1251 (2013).

103. Zheng, L., Roeder, R. G. & Luo, Y. S Phase Activation of the Histone H2B Promoter by OCA-S, a Coactivator Complex that Contains GAPDH as a Key Component. *Cell* **114**, 255–266 (2003).

104. Wegener, M. & Dietz, K.-J. The mutual interaction of glycolytic enzymes and RNA in post-transcriptional regulation. *RNA* **28**, 1446–1468 (2022).

105. Hentze, M. W. & Preiss, T. The REM phase of gene regulation. *Trends in Biochemical Sciences* **35**, 423–426 (2010).

106. Vander Heiden, M. G., Cantley, L. C. & Thompson, C. B. Understanding the Warburg Effect: The Metabolic Requirements of Cell Proliferation. *Science* **324**, 1029–1033 (2009).

107. Shiratori, R. *et al.* Glycolytic suppression dramatically changes the intracellular metabolic profile of multiple cancer cell lines in a mitochondrial metabolism-dependent manner. *Scientific Reports* **9**, 18699 (2019).

108. Warburg, O. On respiratory impairment in cancer cells. *Science* **124**, 269–270 (1956).

109. Busk, M. *et al.* Aerobic glycolysis in cancers: Implications for the usability of oxygen-responsive genes and fluorodeoxyglucose-PET as markers of tissue hypoxia. *International Journal of Cancer* **122**, 2726–2734 (2008).

110. Kumar, P. R., Moore, J. A., Bowles, K. M., Rushworth, S. A. & Moncrieff, M. D. Mitochondrial oxidative phosphorylation in cutaneous melanoma. *Br J Cancer* **124**, 115–123 (2021).

111. Seki, S. M. & Gaultier, A. Exploring Non-Metabolic Functions of Glycolytic Enzymes in Immunity. *Front Immunol* **8**, 1549 (2017).

112. Cañete-Soler, R., Reddy, K. S., Tolan, D. R. & Zhai, J. Aldolases A and C Are Ribonucleolytic Components of a Neuronal Complex That Regulates the Stability of the Light-Neurofilament mRNA. *J Neurosci* **25**, 4353–4364 (2005).

113. Shetty, S., Muniyappa, H., Halady, P. K. S. & Idell, S. Regulation of Urokinase Receptor Expression by Phosphoglycerate Kinase. *Am J Respir Cell Mol Biol* **31**, 100–106 (2004).

114. Kejiou, N. S. *et al.* Pyruvate Kinase M (PKM) binds ribosomes in a poly-ADP ribosylation dependent manner to induce translational stalling. *Nucleic Acids Research* **51**, 6461–6478 (2023).

115. Miao, W. *et al.* Glucose dissociates DDX21 dimers to regulate mRNA splicing and tissue differentiation. *Cell* **186**, 80-97.e26 (2023).

116. Courteau, L. *et al.* Hexokinase 2 controls cellular stress response through localization of an RNA-binding protein. *Cell Death Dis* **6**, e1837 (2015).

117. Hall, D. A. *et al.* Regulation of Gene Expression by a Metabolic Enzyme. *Science* **306**, 482–484 (2004).

118. Scherrer, T., Mittal, N., Janga, S. C. & Gerber, A. P. A Screen for RNA-Binding Proteins in Yeast Indicates Dual Functions for Many Enzymes. *PLOS ONE* **5**, e15499 (2010).

119. Matia-González, A. M., Laing, E. E. & Gerber, A. P. Conserved mRNA-binding proteomes in eukaryotic organisms. *Nat Struct Mol Biol* **22**, 1027–1033 (2015).

120. Fuller, G. G. *et al.* RNA promotes phase separation of glycolysis enzymes into yeast G bodies in hypoxia. *eLife* https://elifesciences.org/articles/48480/figures (2020) doi:10.7554/eLife.48480.

121. Hogan, D. J., Riordan, D. P., Gerber, A. P., Herschlag, D. & Brown, P. O. Diverse RNA-Binding Proteins Interact with Functionally Related Sets of RNAs, Suggesting an Extensive Regulatory System. *PLOS Biology* **6**, e255 (2008).

122. Jin, M. *et al.* Glycolytic Enzymes Coalesce in G Bodies under Hypoxic Stress. *Cell Reports* **20**, 895–908 (2017).

123. Jang, S. *et al.* Phosphofructokinase relocalizes into subcellular compartments with liquid-like properties in vivo. *Biophysical Journal* **120**, 1170–1186 (2021).

124. Tien, C.-F. *et al.* Inhibition of aldolase A blocks biogenesis of ATP and attenuates Japanese encephalitis virus production. *Biochemical and Biophysical Research Communications* **443**, 464–469 (2014).

125. Maines, T. R., Young, M., Dinh, N. N.-N. & Brinton, M. A. Two cellular proteins that interact with a stem loop in the simian hemorrhagic fever virus 3'(+)NCR RNA. *Virus Research* **109**, 109–124 (2005).

126. Kiri, A. & Goldspink, G. RNA-protein interactions of the 3' untranslated regions of myosin heavy chain transcripts. *J Muscle Res Cell Motil* **23**, 119–129 (2002).

127. Milhaud, P., Blanchard, J.-M. & Jeanteur, P. Hela cytosolic protein isolated by poly (A)-sepharose chromatography is glyceraldehyde-3-P-dehydrogenase. *Biochimie* **60**, 1343–1346 (1979).

128. Bonafé, N. *et al.* Glyceraldehyde-3-Phosphate Dehydrogenase Binds to the AU-Rich 3' Untranslated Region of Colony-Stimulating Factor–1 (CSF-1) Messenger RNA in Human Ovarian Cancer Cells: Possible Role in CSF-1 Posttranscriptional Regulation and Tumor Phenotype. *Cancer Research* **65**, 3762–3771 (2005).

129. Zhou, Y. *et al.* The Multifunctional Protein Glyceraldehyde-3-Phosphate Dehydrogenase Is Both Regulated and Controls Colony-Stimulating Factor-1 Messenger RNA Stability in Ovarian Cancer. *Molecular Cancer Research* **6**, 1375–1384 (2008).

130. Rodríguez-Pascual, F. *et al.* Glyceraldehyde-3-Phosphate Dehydrogenase Regulates Endothelin-1 Expression by a Novel, Redox-Sensitive Mechanism Involving mRNA Stability. *Mol Cell Biol* **28**, 7139–7155 (2008).

131. Kondo, S. *et al.* Binding of glyceraldehyde-3-phosphate dehydrogenase to the *cis*-acting element of structure-anchored repression in *ccn2* mRNA. *Biochemical and Biophysical Research Communications* **405**, 382–387 (2011).

132. Zeng, T. *et al.* A novel variant in the 3' UTR of human SCN1A gene from a patient with Dravet syndrome decreases mRNA stability mediated by GAPDH's binding. *Hum Genet* **133**, 801–811 (2014).

133. Lin, G.-W. *et al.* GAPDH-mediated posttranscriptional regulations of sodium channel *Scn1a* and *Scn3a* genes under seizure and ketogenic diet conditions. *Neuropharmacology* **113**, 480–489 (2017).

134. Millet, P., Vachharajani, V., McPhail, L., Yoza, B. & McCall, C. E. GAPDH Binding to TNF-α mRNA Contributes to Posttranscriptional Repression in Monocytes: A Novel Mechanism of Communication between Inflammation and Metabolism. *The Journal of Immunology* **196**, 2541–2551 (2016).

135. Xu, Y. *et al.* Glycolysis determines dichotomous regulation of T cell subsets in hypoxia. *J Clin Invest* **126**, 2678–2688 (2016).

136. Backlund, M. *et al.* Posttranscriptional regulation of angiotensin II type 1 receptor expression by glyceraldehyde 3-phosphate dehydrogenase. *Nucleic Acids Research* **37**, 2346–2358 (2009).

137. McGowan, K. & Pekala, P. H. Dehydrogenase binding to the 3'-untranslated region of GLUT1 mRNA. *Biochem Biophys Res Commun* **221**, 42–45 (1996).

138. Nicholls, C. *et al.* Glyceraldehyde-3-phosphate dehydrogenase (GAPDH) induces cancer cell senescence by interacting with telomerase RNA component. *Proc Natl Acad Sci U S A* **109**, 13308–13313 (2012).

139. Petrik, J., Parker, H. & Alexander, G. J. M. Human hepatic glyceraldehyde-3-phosphate dehydrogenase binds to the poly(U) tract of the 3' non-coding region of hepatitis C virus genomic RNA. *Journal of General Virology* **80**, 3109–3113 (1999).

140. Zang, W.-Q., Fieno, A. M., Grant, R. A. & Yen, T. S. B. Identification of Glyceraldehyde-3-phosphate Dehydrogenase as a Cellular Protein that Binds to the Hepatitis B Virus Posttranscriptional Regulatory Element. *Virology* **248**, 46–52 (1998).

141. Dollenmaier, G. & Weitz, M. Interaction of glyceraldehyde-3-phosphate dehydrogenase with secondary and tertiary RNA structural elements of the hepatitis A virus 3' translated and non-translated regions. *Journal of General Virology* **84**, 403–414 (2003).

142. De, B. P., Gupta, S., Zhao, H., Drazba, J. A. & Banerjee, A. K. Specific interaction in vitro and in vivo of glyceraldehyde-3-phosphate dehydrogenase and LA protein with cis-acting RNAs of human parainfluenza virus type 3. *J Biol Chem* **271**, 24728–24735 (1996).

143. Lin, S.-S., Chang, S. C., Wang, Y.-H., Sun, C.-Y. & Chang, M.-F. Specific Interaction between the Hepatitis Delta Virus RNA and Glyceraldehyde 3-Phosphate Dehydrogenase: An Enhancement on Ribozyme Catalysis. *Virology* **271**, 46–57 (2000).

144. Garcin, E. D. GAPDH as a model non-canonical AU-rich RNA binding protein. *Seminars in Cell & Developmental Biology* **86**, 162–173 (2019).

145. Yi, M., Schultz, D. E. & Lemon, S. M. Functional Significance of the Interaction of Hepatitis A Virus RNA with Glyceraldehyde 3-Phosphate Dehydrogenase (GAPDH): Opposing Effects of GAPDH and Polypyrimidine Tract Binding Protein on Internal Ribosome Entry Site Function. *J Virol* **74**, 6459–6468 (2000).

146. Ogino, T. *et al.* Involvement of a Cellular Glycolytic Enzyme, Phosphoglycerate Kinase, in Sendai Virus Transcription*. *Journal of Biological Chemistry* **274**, 35999–36008 (1999).

147. Cheng, S.-F., Huang, Y.-P., Chen, L.-H., Hsu, Y.-H. & Tsai, C.-H. Chloroplast Phosphoglycerate Kinase Is Involved in the Targeting of Bamboo mosaic virus to Chloroplasts in Nicotiana benthamiana Plants. *Plant Physiology* **163**, 1598–1608 (2013).

148. Lin, J.-W., Ding, M.-P., Hsu, Y.-H. & Tsai, C.-H. Chloroplast phosphoglycerate kinase, a gluconeogenetic enzyme, is required for efficient accumulation of Bamboo mosaic virus. *Nucleic Acids Research* **35**, 424–432 (2007).

149. Shetty, S. & Idell, S. Urokinase receptor mRNA stability involves tyrosine phosphorylation in lung epithelial cells. *Am J Respir Cell Mol Biol* **30**, 69–75 (2004).

150. Ho, M.-Y. *et al.* Nucleotide-binding domain of phosphoglycerate kinase 1 reduces tumor growth by suppressing COX-2 expression. *Cancer Science* **101**, 2411–2416 (2010).

151. Ogino, T., Yamadera, T., Nonaka, T., Imajoh-Ohmi, S. & Mizumoto, K. Enolase, a Cellular Glycolytic Enzyme, Is Required for Efficient Transcription of Sendai Virus Genome. *Biochemical and Biophysical Research Communications* **285**, 447–455 (2001).

152. Py, B., Higgins, C. F., Krisch, H. M. & Carpousis, A. J. A DEAD-box RNA helicase in the Escherichia coli RNA degradosome. *Nature* **381**, 169–172 (1996).

153. Miczak, A., Kaberdin, V. R., Wei, C. L. & Lin-Chao, S. Proteins associated with RNase E in a multicomponent ribonucleolytic complex. *Proceedings of the National Academy of Sciences* **93**, 3865–3869 (1996).

154. Kühnel, K. & Luisi, B. F. Crystal structure of the *Escherichia coli* RNA degradosome component enolase1. *Journal of Molecular Biology* **313**, 583–592 (2001).

155. Chandran, V. & Luisi, B. F. Recognition of Enolase in the *Escherichia coli* RNA Degradosome. *Journal of Molecular Biology* **358**, 8–15 (2006).

156. Morita, T., Kawamoto, H., Mizota, T., Inada, T. & Aiba, H. Enolase in the RNA degradosome plays a crucial role in the rapid decay of glucose transporter mRNA in the response to phosphosugar stress in Escherichia coli. *Molecular Microbiology* **54**, 1063–1075 (2004).

157. Baleva, M. V. *et al.* Factors beyond enolase 2 and mitochondrial lysyl-tRNA synthetase precursor are required for tRNA import into yeast mitochondria. *Biochemistry Moscow* **82**, 1324–1335 (2017).

158. Entelis, N. *et al.* A glycolytic enzyme, enolase, is recruited as a cofactor of tRNA targeting toward mitochondria in Saccharomyces cerevisiae. *Genes Dev* **20**, 1609–1620 (2006).

159. Baleva, M. *et al.* A Moonlighting Human Protein Is Involved in Mitochondrial Import of tRNA. *International Journal of Molecular Sciences* **16**, 9354–9367 (2015).

160. Sy, B. *et al.* High-Resolution, High-Throughput Analysis of Hfq-Binding Sites Using UV Crosslinking and Analysis of cDNA (CRAC). in *Bacterial Regulatory RNA: Methods and Protocols* (eds. Arluison, V. & Valverde, C.) 251–272 (Springer, New York, NY, 2018). doi:10.1007/978-1-4939-7634-8_15.

161. Hernández-Pérez, L. *et al.* α-Enolase binds to RNA. *Biochimie* **93**, 1520–1528 (2011).

162. Zhang, T. *et al.* ENO1 suppresses cancer cell ferroptosis by degrading the mRNA of iron regulatory protein 1. *Nat Cancer* **3**, 75–89 (2022).

163. Zahra, K., Dey, T., Ashish, Mishra, S. P. & Pandey, U. Pyruvate Kinase M2 and Cancer: The Role of PKM2 in Promoting Tumorigenesis. *Front Oncol* **10**, 159 (2020).

164. Simsek, D. *et al.* The Mammalian Ribo-interactome Reveals Ribosome Functional Diversity and Heterogeneity. *Cell* **169**, 1051-1065.e18 (2017).

165. Bian, Z. *et al.* LncRNA–FEZF1-AS1 Promotes Tumor Proliferation and Metastasis in Colorectal Cancer by Regulating PKM2 Signaling. *Clinical Cancer Research* **24**, 4808–4819 (2018).

166. Xie, Z. *et al.* Exosomal lncRNA HOTAIR induces PDL1+ B cells to impede anti-tumor immunity in colorectal cancer. *Biochemical and Biophysical Research Communications* **644**, 112–121 (2023).

167. Dai, T. *et al.* Long non-coding RNA VAL facilitates PKM2 enzymatic activity to promote glycolysis and malignancy of gastric cancer. *Clinical and Translational Medicine* **12**, e1088 (2022).

168. Pioli, P. A., Hamilton, B. J., Connolly, J. E., Brewer, G. & Rigby, W. F. C. Lactate Dehydrogenase Is an AU-rich Element-binding Protein That Directly Interacts with AUF1*. *Journal of Biological Chemistry* **277**, 35738–35745 (2002).

169. Zhu, Y. *et al.* The long noncoding RNA glycoLINC assembles a lower glycolytic metabolon to promote glycolysis. *Molecular Cell* **82**, 542-554.e6 (2022).

170. Cieśla, J. Metabolic enzymes that bind RNA: yet another level of cellular regulatory network? *Acta Biochim Pol* **53**, 11–32 (2006).

171. Sang, L. *et al.* Mitochondrial long non-coding RNA GAS5 tunes TCA metabolism in response to nutrient stress. *Nat Metab* **3**, 90–106 (2021).

172. Xu, F. *et al.* LncRNA AC020978 facilitates non-small cell lung cancer progression by interacting with malate dehydrogenase 2 and activating the AKT pathway. *Cancer Sci* **112**, 4501–4514 (2021).

173. Muckenthaler, M. U., Rivella, S., Hentze, M. W. & Galy, B. A Red Carpet for Iron Metabolism. *Cell* **168**, 344–361 (2017).

174. Castello, A., Hentze, M. W. & Preiss, T. Metabolic Enzymes Enjoying New Partnerships as RNA-Binding Proteins. *Trends Endocrinol Metab* **26**, 746–757 (2015).

175. Hentze, M. W. *et al.* Identification of the iron-responsive element for the translational regulation of human ferritin mRNA. *Science* **238**, 1570–1573 (1987).

176. Muckenthaler, M., Gray, N. K. & Hentze, M. W. IRP-1 binding to ferritin mRNA prevents the recruitment of the small ribosomal subunit by the cap-binding complex eIF4F. *Mol Cell* **2**, 383–388 (1998).

177. Casey, J. L. *et al.* Iron-responsive elements: regulatory RNA sequences that control mRNA levels and translation. *Science* **240**, 924–928 (1988).

178. Müllner, E. W. & Kühn, L. C. A stem-loop in the 3' untranslated region mediates iron-dependent regulation of transferrin receptor mRNA stability in the cytoplasm. *Cell* **53**, 815–825 (1988).

179. Hentze, M. W. & Kühn, L. C. Molecular control of vertebrate iron metabolism: mRNA-based regulatory circuits operated by iron, nitric oxide, and oxidative stress. *Proc Natl Acad Sci U S A* **93**, 8175–8182 (1996).

180. Wallander, M. L., Leibold, E. A. & Eisenstein, R. S. Molecular control of vertebrate iron homeostasis by iron regulatory proteins. *Biochimica et Biophysica Acta (BBA) - Molecular Cell Research* **1763**, 668–689 (2006).

181. Walden, W. E. *et al.* Structure of dual function iron regulatory protein 1 complexed with ferritin IRE-RNA. *Science* **314**, 1903–1908 (2006).

182. Noble, M., Chatterjee, A., Sekaran, T., Schwarzl, T. & Hentze, M. W. Cytosolic RNA binding of the mitochondrial TCA cycle enzyme malate dehydrogenase (MDH2). *RNA* rna.079925.123 (2024) doi:10.1261/rna.079925.123.

183. Chen, Y.-H. *et al.* MDH2 is an RNA binding protein involved in downregulation of sodium channel *Scn1a* expression under seizure condition. *Biochimica et Biophysica Acta (BBA) - Molecular Basis of Disease* **1863**, 1492–1499 (2017).

184. Asencio, C., Schwarzl, T., Sahadevan, S. & Hentze, M. W. Small noncoding RNA interactome capture reveals pervasive, carbon source-dependent tRNA engagement of yeast glycolytic enzymes. *RNA* **29**, 330–345 (2023).

185. Yang, S.-Y. *et al.* Roles of 17β-hydroxysteroid dehydrogenase type 10 in neurodegenerative disorders. *J Steroid Biochem Mol Biol* **143**, 460–472 (2014).

186. Holzmann, J. *et al.* RNase P without RNA: identification and functional reconstitution of the human mitochondrial tRNA processing enzyme. *Cell* **135**, 462–474 (2008).

187. Rauschenberger, K. *et al.* A non-enzymatic function of 17beta-hydroxysteroid dehydrogenase type 10 is required for mitochondrial integrity and cell survival. *EMBO Mol Med* **2**, 51–62 (2010).

188. Liu, X., Reig, B., Nasrallah, I. M. & Stover, P. J. Human Cytoplasmic Serine Hydroxymethyltransferase Is an mRNA Binding Protein. *Biochemistry* **39**, 11523–11531 (2000).

189. Guiducci, G. *et al.* The moonlighting RNA-binding activity of cytosolic serine hydroxymethyltransferase contributes to control compartmentalization of serine metabolism. *Nucleic Acids Res* **47**, 4240–4254 (2019).

190. Sonneveld, S., Verhagen, B. M. P. & Tanenbaum, M. E. Heterogeneity in mRNA Translation. *Trends in Cell Biology* **30**, 606–618 (2020).

191. Schwanhäusser, B. *et al*. Global quantification of mammalian gene expression control. *Nature* **473**, 337–342 (2011).

192. Liu, Y., Beyer, A. & Aebersold, R. On the Dependency of Cellular Protein Levels on mRNA Abundance. *Cell* **165**, 535–550 (2016).

193. Song, P., Yang, F., Jin, H. & Wang, X. The regulation of protein translation and its implications for cancer. *Sig Transduct Target Ther* **6**, 1–9 (2021).

194. Fabbri, L., Chakraborty, A., Robert, C. & Vagner, S. The plasticity of mRNA translation during cancer progression and therapy resistance. *Nat Rev Cancer* **21**, 558–577 (2021).

195. de la Parra, C., Walters, B. A., Geter, P. & Schneider, R. J. Translation initiation factors and their relevance in cancer. *Curr Opin Genet Dev* **48**, 82–88 (2018).

196. Lane, N. & Martin, W. The energetics of genome complexity. *Nature* **467**, 929–934 (2010).

197. Wang, S. & Sun, S. Translation dysregulation in neurodegenerative diseases: a focus on ALS. *Molecular Neurodegeneration* **18**, 58 (2023).

198. Hershey, J. W. B., Sonenberg, N. & Mathews, M. B. Principles of Translational Control. *Cold Spring Harb Perspect Biol* **11**, a032607 (2019).

199. Merrick, W. C. Cap-dependent and cap-independent translation in eukaryotic systems. *Gene* **332**, 1–11 (2004).

200. Shatsky, I. N., Terenin, I. M., Smirnova, V. V. & Andreev, D. E. Cap-Independent Translation: What's in a Name? *Trends in Biochemical Sciences* **43**, 882–895 (2018).

201. Wang, Z., Gerstein, M. & Snyder, M. RNA-Seq: a revolutionary tool for transcriptomics. *Nat Rev Genet* **10**, 57–63 (2009).

202. Aebersold, R. & Mann, M. Mass-spectrometric exploration of proteome structure and function. *Nature* **537**, 347–355 (2016).

203. Bartish, M. *et al*. The role of eIF4F-driven mRNA translation in regulating the tumour microenvironment. *Nat Rev Cancer* **23**, 408–425 (2023).

204. Zhang, D., Gao, Y., Zhu, L., Wang, Y. & Li, P. Advances and opportunities in methods to study protein translation - A review. *International Journal of Biological Macromolecules* **259**, 129150 (2024).

205. Chassé, H., Boulben, S., Costache, V., Cormier, P. & Morales, J. Analysis of translation using polysome profiling. *Nucleic Acids Research* **45**, e15 (2017).

206. Fremin, B. J., Nicolaou, C. & Bhatt, A. S. Simultaneous ribosome profiling of hundreds of microbes from the human microbiome. *Nat Protoc* **16**, 4676–4691 (2021).

207. Ingolia, N. T. Ribosome Footprint Profiling of Translation throughout the Genome. *Cell* **165**, 22–33 (2016).

208. Jia, X. *et al.* Protein translation: biological processes and therapeutic strategies for human diseases. *Sig Transduct Target Ther* **9**, 1–17 (2024).

209. Braselmann, E., Rathbun, C., Richards, E. M. & Palmer, A. E. Illuminating RNA Biology: Tools for Imaging RNA in Live Mammalian Cells. *Cell Chemical Biology* **27**, 891–903 (2020).

210. Wang, D., Shalamberidze, A., Arguello, A. E., Purse, B. W. & Kleiner, R. E. Live-Cell RNA Imaging with Metabolically Incorporated Fluorescent Nucleosides. *J. Am. Chem. Soc.* **144**, 14647–14656 (2022).

211. Enam, S. U. *et al.* Puromycin reactivity does not accurately localize translation at the subcellular level. *eLife* **9**, e60303 (2020).

212. Aviner, R. The science of puromycin: From studies of ribosome function to applications in biotechnology. *Computational and Structural Biotechnology Journal* **18**, 1074–1083 (2020).

213. Chin, A. & Lécuyer, E. Puromycin Labeling Coupled with Proximity Ligation Assays to Define Sites of mRNA Translation in Drosophila Embryos and Human Cells. in *Mapping Genetic Interactions* (eds. Vizeacoumar, F. J. & Freywald, A.) 267–284 (Springer US, New York, NY, 2021). doi:10.1007/978-1-0716-1740-3_15.

214. Shirokikh, N. E., Archer, S. K., Beilharz, T. H., Powell, D. & Preiss, T. Translation complex profile sequencing to study the in vivo dynamics of mRNA–ribosome interactions during translation initiation, elongation and termination. *Nat Protoc* **12**, 697–731 (2017).

215. Jobava, R. *et al.* Adaptive translational pausing is a hallmark of the cellular response to severe environmental stress. *Molecular Cell* **81**, 4191-4208.e8 (2021).

216. Ivanov, I. P. *et al.* Evolutionarily conserved inhibitory uORFs sensitize Hox mRNA translation to start codon selection stringency. *Proceedings of the National Academy of Sciences* **119**, e2117226119 (2022).

217. Li, Q., Yang, H., Stroup, E. K., Wang, H. & Ji, Z. Low-input RNase footprinting for simultaneous quantification of cytosolic and mitochondrial translation. *Genome Res.* **32**, 545–557 (2022).

218. Santos, D. A., Shi, L., Tu, B. P. & Weissman, J. S. Cycloheximide can distort measurements of mRNA levels and translation efficiency. *Nucleic Acids Research* **47**, 4974–4985 (2019).

219. Garreau de Loubresse, N. *et al.* Structural basis for the inhibition of the eukaryotic ribosome. *Nature* **513**, 517–522 (2014).

220. Williams, C. C., Jan, C. H. & Weissman, J. S. Targeting and plasticity of mitochondrial proteins revealed by proximity-specific ribosome profiling. *Science* **346**, 748–751 (2014).

221. David, A. *et al.* Nuclear translation visualized by ribosome-bound nascent chain puromycylation. *Journal of Cell Biology* **197**, 45–57 (2012).

222. Costa, E. A., Subramanian, K., Nunnari, J. & Weissman, J. S. Defining the physiological role of SRP in protein-targeting efficiency and specificity. *Science* **359**, 689–692 (2018).

223. Fairhead, M. & Howarth, M. Site-specific biotinylation of purified proteins using BirA. *Methods Mol Biol* **1266**, 171–184 (2015).

224. Lautier, O. *et al.* Co-translational assembly and localized translation of nucleoporins in nuclear pore complex biogenesis. *Molecular Cell* **81**, 2417-2427.e5 (2021).

225. Soto, I. *et al.* Balanced mitochondrial and cytosolic translatomes underlie the biogenesis of human respiratory complexes. *Genome Biology* **23**, 170 (2022).

226. Remes, C. *et al.* Translation initiation of leaderless and polycistronic transcripts in mammalian mitochondria. *Nucleic Acids Research* **51**, 891–907 (2023).

227. Soto, I., Couvillion, M. & Stirling Churchman, L. Human Mitoribosome Profiling: A Re-engineered Approach Tailored to Study Mitochondrial Translation. in *The Mitoribosome: Methods and Protocols* (eds. Barrientos, A. & Fontanesi, F.) 257–280 (Springer US, New York, NY, 2023). doi:10.1007/978-1-0716-3171-3_15.

228. Becher, I. *et al.* Pervasive Protein Thermal Stability Variation during the Cell Cycle. *Cell* **173**, 1495-1507.e18 (2018).

229. Beller, N. C., Lukowski, J. K., Ludwig, K. R. & Hummon, A. B. Spatial Stable Isotopic Labeling by Amino Acids in Cell Culture: Pulse-Chase Labeling of Three-Dimensional Multicellular Spheroids for Global Proteome Analysis. *Anal. Chem.* **93**, 15990–15999 (2021).

230. Gebauer, F. & Hentze, M. W. Molecular mechanisms of translational control. *Nat Rev Mol Cell Biol* **5**, 827–835 (2004).

231. Wang, X., Hou, J., Quedenau, C. & Chen, W. Pervasive isoform-specific translational regulation via alternative transcription start sites in mammals. *Molecular Systems Biology* **12**, 875 (2016).

232. Floor, S. N. & Doudna, J. A. Tunable protein synthesis by transcript isoforms in human cells. *eLife* **5**, e10921 (2016).

233. Mayr, C. Evolution and Biological Roles of Alternative 3'UTRs. *Trends in Cell Biology* **26**, 227–237 (2016).

234. Weingarten-Gabbay, S. *et al.* Systematic discovery of cap-independent translation sequences in human and viral genomes. *Science* **351**, aad4939 (2016).

235. Woods, C. T. *et al.* Comparative Visualization of the RNA Suboptimal Conformational Ensemble In Vivo. *Biophysical Journal* **113**, 290–301 (2017).

236. Beaudoin, J.-D. *et al.* Analyses of mRNA structure dynamics identify embryonic gene regulatory programs. *Nat Struct Mol Biol* **25**, 677–686 (2018).

237. Adivarahan, S. *et al.* Spatial Organization of Single mRNPs at Different Stages of the Gene Expression Pathway. *Molecular Cell* **72**, 727-738.e5 (2018).

238. Mustoe, A. M. *et al.* Pervasive Regulatory Functions of mRNA Structure Revealed by High-Resolution SHAPE Probing. *Cell* **173**, 181-195.e18 (2018).

239. Mizrahi, O. *et al.* Virus-Induced Changes in mRNA Secondary Structure Uncover *cis*-Regulatory Elements that Directly Control Gene Expression. *Molecular Cell* **72**, 862-874.e5 (2018).

240. Wiener, D. & Schwartz, S. The epitranscriptome beyond m6A. *Nat Rev Genet* **22**, 119–131 (2021).

241. Jiang, X. *et al.* The role of m6A modification in the biological functions and diseases. *Sig Transduct Target Ther* **6**, 1–16 (2021).

242. Meyer, K. D. *et al.* 5' UTR m(6)A Promotes Cap-Independent Translation. *Cell* **163**, 999–1010 (2015).

243. Choe, J. *et al.* mRNA circularization by METTL3-eIF3h enhances translation and promotes oncogenesis. *Nature* **561**, 556–560 (2018).

244. Shi, H. *et al.* m6A facilitates hippocampus-dependent learning and memory through YTHDF1. *Nature* **563**, 249–253 (2018).

245. Choi, J. *et al.* N6-methyladenosine in mRNA disrupts tRNA selection and translation-elongation dynamics. *Nat Struct Mol Biol* **23**, 110–115 (2016).

246. Humphreys, D. T., Westman, B. J., Martin, D. I. K. & Preiss, T. MicroRNAs control translation initiation by inhibiting eukaryotic initiation factor 4E/cap and poly(A) tail function. *Proc Natl Acad Sci U S A* **102**, 16961–16966 (2005).

247. Duchaine, T. F. & Fabian, M. R. Mechanistic Insights into MicroRNA-Mediated Gene Silencing. *Cold Spring Harb Perspect Biol* **11**, a032771 (2019).

248. Ma, L., Teruya-Feldstein, J. & Weinberg, R. A. Tumour invasion and metastasis initiated by microRNA-10b in breast cancer. *Nature* **449**, 682–688 (2007).

249. Ørom, U. A., Nielsen, F. C. & Lund, A. H. MicroRNA-10a binds the 5'UTR of ribosomal protein mRNAs and enhances their translation. *Mol Cell* **30**, 460–471 (2008).

250. Mubaid, S. *et al.* HuR counteracts miR-330 to promote STAT3 translation during inflammation-induced muscle wasting. *Proc Natl Acad Sci U S A* **116**, 17261–17270 (2019).

251. Miao, H. *et al.* A long noncoding RNA distributed in both nucleus and cytoplasm operates in the PYCARD-regulated apoptosis by coordinating the epigenetic and translational regulation. *PLOS Genetics* **15**, e1008144 (2019).

252. Liu, P. Y. *et al.* The long noncoding RNA lncNB1 promotes tumorigenesis by interacting with ribosomal protein RPL35. *Nat Commun* **10**, 5026 (2019).

253. Lian, Y. *et al.* A Novel lncRNA, LINC00460, Affects Cell Proliferation and Apoptosis by Regulating KLF2 and CUL4A Expression in Colorectal Cancer. *Mol Ther Nucleic Acids* **12**, 684–697 (2018).

254. Yang, Y. *et al.* Novel Role of FBXW7 Circular RNA in Repressing Glioma Tumorigenesis. *J Natl Cancer Inst* **110**, 304–315 (2018).

255. Wu, N. *et al.* Translation of yes-associated protein (YAP) was antagonized by its circular RNA via suppressing the assembly of the translation initiation machinery. *Cell Death Differ* **26**, 2758–2773 (2019).

256. Abdelmohsen, K. *et al.* Identification of HuR target circular RNAs uncovers suppression of PABPN1 translation by CircPABPN1. *RNA Biology* **14**, 361–369 (2017).

257. Napoli, I. *et al.* The fragile X syndrome protein represses activity-dependent translation through CYFIP1, a new 4E-BP. *Cell* **134**, 1042–1054 (2008).

258. Dugré-Brisson, S. *et al.* Interaction of Staufen1 with the 5' end of mRNA facilitates translation of these RNAs. *Nucleic Acids Res* **33**, 4797–4812 (2005).

259. Ramos, H. *et al.* The double-stranded RNA-binding protein, Staufen1, is an IRES-transacting factor regulating HIV-1 cap-independent translation initiation. *Nucleic Acids Research* **50**, 411–429 (2022).

260. Piecyk, M. *et al.* TIA-1 is a translational silencer that selectively regulates the expression of TNF-α. *The EMBO Journal* **19**, 4154–4163 (2000).

261. Grosset, C. *et al. In Vivo* Studies of Translational Repression Mediated by the Granulocyte-Macrophage Colony-stimulating Factor AU-rich Element*. *Journal of Biological Chemistry* **279**, 13354–13362 (2004).

262. Dixon, D. A. *et al.* Regulation of Cyclooxygenase-2 Expression by the Translational Silencer TIA-1. *Journal of Experimental Medicine* **198**, 475–481 (2003).

263. Vyas, K. *et al.* Genome-Wide Polysome Profiling Reveals an Inflammation-Responsive Posttranscriptional Operon in Gamma Interferon-Activated Monocytes. *Molecular and Cellular Biology* **29**, 458–470 (2009).

264. Moore, M. J. *et al.* ZFP36 RNA-binding proteins restrain T cell activation and anti-viral immunity. *eLife* **7**, e33057 (2018).

265. Liepelt, A. *et al.* Translation control of TAK1 mRNA by hnRNP K modulates LPS-induced macrophage activation. *RNA* **20**, 899–911 (2014).

266. Bell, S. E. *et al.* The RNA binding protein Zfp36l1 is required for normal vascularisation and post-transcriptionally regulates VEGF expression. *Developmental Dynamics* **235**, 3144–3155 (2006).

267. Ray, P. S. & Fox, P. L. A post-transcriptional pathway represses monocyte VEGF-A expression and angiogenic activity. *The EMBO Journal* **26**, 3360–3372 (2007).

268. Ray, P. S. *et al.* A stress-responsive RNA switch regulates VEGFA expression. *Nature* **457**, 915–919 (2009).

269. Gao, J. *et al.* CLUH regulates mitochondrial biogenesis by binding mRNAs of nuclear-encoded mitochondrial proteins. *Journal of Cell Biology* **207**, 213–223 (2014).

270. Schatton, D. *et al.* CLUH regulates mitochondrial metabolism by controlling translation and decay of target mRNAs. *Journal of Cell Biology* **216**, 675–693 (2017).

271. Vardi-Oknin, D. & Arava, Y. Characterization of Factors Involved in Localized Translation Near Mitochondria by Ribosome-Proximity Labeling. *Front. Cell Dev. Biol.* **7**, (2019).

272. Dobbyn, H. C. *et al.* Regulation of BAG-1 IRES-mediated translation following chemotoxic stress. *Oncogene* **27**, 1167–1174 (2008).

273. Winkler, C. *et al.* Attenuation of the ELAV1-like protein HuR sensitizes adenocarcinoma cells to the intrinsic apoptotic pathway by increasing the translation of caspase-2L. *Cell Death Dis* **5**, e1321–e1321 (2014).

274. Tcherkezian, J. *et al.* Proteomic analysis of cap-dependent translation identifies LARP1 as a key regulator of 5'TOP mRNA translation. *Genes Dev.* **28**, 357–371 (2014).

275. Fonseca, B. D. *et al.* La-related Protein 1 (LARP1) Represses Terminal Oligopyrimidine (TOP) mRNA Translation Downstream of mTOR Complex 1 (mTORC1)*. *Journal of Biological Chemistry* **290**, 15996–16020 (2015).

276. Lahr, R. M. *et al.* La-related protein 1 (LARP1) binds the mRNA cap, blocking eIF4F assembly on TOP mRNAs. *eLife* **6**, e24146 (2017).

277. Kudinov, A. E., Karanicolas, J., Golemis, E. A. & Boumber, Y. Musashi RNA-Binding Proteins as Cancer Drivers and Novel Therapeutic Targets. *Clinical Cancer Research* **23**, 2143–2153 (2017).

278. Ho, J. J. D. *et al.* A network of RNA-binding proteins controls translation efficiency to activate anaerobic metabolism. *Nat Commun* **11**, 2677 (2020).

279. Vattem, K. M. & Wek, R. C. Reinitiation involving upstream ORFs regulates ATF4 mRNA translation in mammalian cells. *Proceedings of the National Academy of Sciences* **101**, 11269–11274 (2004).

280. Vagner, S. *et al.* Translation of CUG- but not AUG-initiated forms of human fibroblast growth factor 2 is activated in transformed and stressed cells. *Journal of Cell Biology* **135**, 1391–1402 (1996).

281. Meiron, M., Anunu, R., Scheinman, E. J., Hashmueli, S. & Levi, B.-Z. New Isoforms of VEGF Are Translated from Alternative Initiation CUG Codons Located in Its 5'UTR. *Biochemical and Biophysical Research Communications* **282**, 1053–1060 (2001).

282. Ingolia, N. T., Ghaemmaghami, S., Newman, J. R. S. & Weissman, J. S. Genome-Wide Analysis in Vivo of Translation with Nucleotide Resolution Using Ribosome Profiling. *Science* **324**, 218–223 (2009).

283. Lee, S. *et al.* Global mapping of translation initiation sites in mammalian cells at single-nucleotide resolution. *Proceedings of the National Academy of Sciences* **109**, E2424–E2432 (2012).

284. Meyer, K. D. *et al.* 5' UTR m6A Promotes Cap-Independent Translation. *Cell* **163**, 999–1010 (2015).

285. Chen, T.-M. *et al.* Overexpression of FGF9 in colon cancer cells is mediated by hypoxia-induced translational activation. *Nucleic Acids Res* **42**, 2932–2944 (2014).

286. Chen, T.-M. *et al.* hnRNPM induces translation switch under hypoxia to promote colon cancer development. *EBioMedicine* **41**, 299–309 (2019).

287. Leprivier, G. *et al.* The eEF2 Kinase Confers Resistance to Nutrient Deprivation by Blocking Translation Elongation. *Cell* **153**, 1064–1079 (2013).

288. Shalgi, R. *et al.* Widespread Regulation of Translation by Elongation Pausing in Heat Shock. *Molecular Cell* **49**, 439–452 (2013).

289. Endres, L. *et al.* Alkbh8 Regulates Selenocysteine-Protein Expression to Protect against Reactive Oxygen Species Damage. *PLOS ONE* **10**, e0131335 (2015).

290. Kochavi, A., Lovecchio, D., Faller, W. J. & Agami, R. Proteome diversification by mRNA translation in cancer. *Molecular Cell* **83**, 469–480 (2023).

291. Mounir, Z. *et al.* Tumor Suppression by PTEN Requires the Activation of the PKR-eIF2α Phosphorylation Pathway. *Science Signaling* **2**, ra85–ra85 (2009).

292. Zhu, K., Chan, W., Heymach, J., Wilkinson, M. & McConkey, D. J. Control of HIF-1α Expression by eIF2α Phosphorylation–Mediated Translational Repression. *Cancer Research* **69**, 1836–1843 (2009).

293. Boussemart, L. *et al.* eIF4F is a nexus of resistance to anti-BRAF and anti-MEK cancer therapies. *Nature* **513**, 105–109 (2014).

294. Xu, Y. *et al.* Translation control of the immune checkpoint in cancer and its therapeutic targeting. *Nat Med* **25**, 301–311 (2019).

295. Pavon-Eternod, M. *et al.* tRNA over-expression in breast cancer and functional consequences. *Nucleic Acids Research* **37**, 7268–7280 (2009).

296. Rapino, F. *et al.* Codon-specific translation reprogramming promotes resistance to targeted therapy. *Nature* **558**, 605–609 (2018).

297. Robichaud, N. *et al.* Phosphorylation of eIF4E promotes EMT and metastasis via translational control of SNAIL and MMP-3. *Oncogene* **34**, 2032–2042 (2015).

298. Feng, Y. *et al.* Epithelial-to-Mesenchymal Transition Activates PERK–eIF2α and Sensitizes Cells to Endoplasmic Reticulum Stress. *Cancer Discovery* **4**, 702–715 (2014).

299. Nagelkerke, A. *et al.* Hypoxia stimulates migration of breast cancer cells via the PERK/ATF4/LAMP3-arm of the unfolded protein response. *Breast Cancer Res* **15**, R2 (2013).

300. Chaudhury, A. *et al.* CELF1 is a central node in post-transcriptional regulatory programmes underlying EMT. *Nat Commun* **7**, 13362 (2016).

301. Wurth, L. *et al.* UNR/CSDE1 Drives a Post-transcriptional Program to Promote Melanoma Invasion and Metastasis. *Cancer Cell* **30**, 694–707 (2016).

302. Zismanov, V. *et al.* Phosphorylation of eIF2α Is a Translational Control Mechanism Regulating Muscle Stem Cell Quiescence and Self-Renewal. *Cell Stem Cell* **18**, 79–90 (2016).

303. Signer, R. A. J. *et al.* The rate of protein synthesis in hematopoietic stem cells is limited partly by 4E-BPs. *Genes Dev.* **30**, 1698–1703 (2016).

304. Samanta, S. *et al.* IMP3 promotes stem-like properties in triple-negative breast cancer by regulating SLUG. *Oncogene* **35**, 1111–1121 (2016).

305. Huang, H. *et al.* Recognition of RNA N6-methyladenosine by IGF2BP proteins enhances mRNA stability and translation. *Nat Cell Biol* **20**, 285–295 (2018).

306. Zhang, C. *et al.* YTHDF2 promotes the liver cancer stem cell phenotype and cancer metastasis by regulating OCT4 expression via m6A RNA methylation. *Oncogene* **39**, 4507–4518 (2020).

307. Weng, H. *et al.* METTL14 Inhibits Hematopoietic Stem/Progenitor Differentiation and Promotes Leukemogenesis via mRNA m6A Modification. *Cell Stem Cell* **22**, 191-205.e9 (2018).

308. Rambow, F., Marine, J.-C. & Goding, C. R. Melanoma plasticity and phenotypic diversity: therapeutic barriers and opportunities. *Genes Dev.* **33**, 1295–1318 (2019).

309. Phung, B. *et al.* The X-Linked DDX3X RNA Helicase Dictates Translation Reprogramming and Metastasis in Melanoma. *Cell Reports* **27**, 3573-3586.e7 (2019).

310. Falletta, P. *et al.* Translation reprogramming is an evolutionarily conserved driver of phenotypic plasticity and therapeutic resistance in melanoma. *Genes Dev.* **31**, 18–33 (2017).

311. El-Hachem, N. *et al.* Valine aminoacyl-tRNA synthetase promotes therapy resistance in melanoma. *Nat Cell Biol* 1–11 (2024) doi:10.1038/s41556-024-01439-2.

312. Guo, Q. *et al.* The MNK1/2–eIF4E Axis Supports Immune Suppression and Metastasis in Postpartum Breast Cancer. *Cancer Research* **81**, 3876–3889 (2021).

313. Suo, J. *et al.* Int6 reduction activates stromal fibroblasts to enhance transforming activity in breast epithelial cells. *Cell Biosci* **5**, 10 (2015).

314. Lugano, R., Ramachandran, M. & Dimberg, A. Tumor angiogenesis: causes, consequences, challenges and opportunities. *Cell. Mol. Life Sci.* **77**, 1745–1770 (2020).

315. Morfoisse, F. *et al.* Hypoxia Induces VEGF-C Expression in Metastatic Tumor Cells via a HIF-1α-Independent Translation-Mediated Mechanism. *Cell Reports* **6**, 155–167 (2014).

316. Han, D. *et al.* Anti-tumour immunity controlled through mRNA m6A methylation and YTHDF1 in dendritic cells. *Nature* **566**, 270–274 (2019).

317. Blaha, C. S. *et al.* A non-catalytic scaffolding activity of hexokinase 2 contributes to EMT and metastasis. *Nat Commun* **13**, 899 (2022).

318. Moya Plana, A. Recherche de biomarqueurs pronostiques dans le mélanome muqueux non opérable et/ou métastatique : Régulation traductionnelle de SOX10 par l'hexokinase 2 et modulation de l'agressivité tumorale dans le mélanome cutané. (université Paris-Saclay, 2020).

319. Han, S. *et al.* ERK-mediated phosphorylation regulates SOX10 sumoylation and targets expression in mutant BRAF melanoma. *Nat Commun* **9**, 28 (2018).

320. Yu, L. *et al.* Sex-Determining Region Y Chromosome-Related High-Mobility-Group Box 10 in Cancer: A Potential Therapeutic Target. *Front Cell Dev Biol* **8**, 564740 (2020).

321. Sun, C. *et al.* Reversible and adaptive resistance to BRAF(V600E) inhibition in melanoma. *Nature* **508**, 118–122 (2014).

322. Zhang, W., Xie, M., Shu, M.-D., Steitz, J. A. & DiMaio, D. A proximity-dependent assay for specific RNA–protein interactions in intact cells. *RNA* **22**, 1785–1792 (2016).

323. Zhang, C. *et al.* Tumour-associated mutant p53 drives the Warburg effect. *Nat Commun* **4**, 2935 (2013).

324. Wang, F. *et al.* Glycolytic Stimulation Is Not a Requirement for M2 Macrophage Differentiation. *Cell Metabolism* **28**, 463-475.e4 (2018).

325. Weinberg, F. *et al.* Mitochondrial metabolism and ROS generation are essential for Kras-mediated tumorigenicity. *Proceedings of the National Academy of Sciences* **107**, 8788–8793 (2010).

326. Beene, D. L. & Scott, J. D. A-kinase anchoring proteins take shape. *Current Opinion in Cell Biology* **19**, 192–198 (2007).

327. Ginsberg, M. D., Feliciello, A., Jones, J. K., Avvedimento, E. V. & Gottesman, M. E. PKA-dependent Binding of mRNA to the Mitochondrial AKAP121 Protein. *Journal of Molecular Biology* **327**, 885–897 (2003).

328. Haloi, N. *et al.* Structural basis of complex formation between mitochondrial anion channel VDAC1 and Hexokinase-II. *Commun Biol* **4**, 1–12 (2021).

329. Murray, A. J. Pharmacological PKA Inhibition: All May Not Be What It Seems. *Science Signaling* **1**, re4–re4 (2008).

330. Minati, L. *et al.* One-shot analysis of translated mammalian lncRNAs with AHARIBO. *eLife* **10**, e59303 (2021).

331. Jewett, J. C. & Bertozzi, C. R. Cu-free click cycloaddition reactions in chemical biology. *Chem. Soc. Rev.* **39**, 1272–1279 (2010).

332. Liu, Z. *et al.* Excess glucose induces hypoxia-inducible factor-1α in pancreatic cancer cells and stimulates glucose metabolism and cell migration. *Cancer Biol Ther* **14**, 428–435 (2013).

333. Wolf, A. *et al.* Hexokinase 2 is a key mediator of aerobic glycolysis and promotes tumor growth in human glioblastoma multiforme. *J Exp Med* **208**, 313–326 (2011).

334. Kudryavtseva, A. V. *et al.* Effect of lentivirus-mediated shRNA inactivation of HK1, HK2, and HK3 genes in colorectal cancer and melanoma cells. *BMC Genet* **17**, 156 (2016).

335. Patra, K. C. *et al.* Hexokinase 2 is required for tumor initiation and maintenance and its systemic deletion is therapeutic in mouse models of cancer. *Cancer Cell* **24**, 213–228 (2013).

336. Wang, W. *et al.* Hexokinase 2 enhances the metastatic potential of tongue squamous cell carcinoma via the SOD2-H2O2 pathway. *Oncotarget* **8**, 3344–3354 (2017).

337. Thomas, G. E. *et al.* The metabolic enzyme hexokinase 2 localizes to the nucleus in AML and normal haematopoietic stem and progenitor cells to maintain stemness. *Nat Cell Biol* **24**, 872–884 (2022).

338. Guo, D. *et al*. Aerobic glycolysis promotes tumor immune evasion by hexokinase2-mediated phosphorylation of IκBα. *Cell Metabolism* **34**, 1312-1324.e6 (2022).

339. Melick, C. H. & Jewell, J. L. Small molecule H89 renders the phosphorylation of S6K1 and AKT resistant to mTOR inhibitors. *Biochem J* **477**, 1847–1863 (2020).

340. Limbutara, K., Kelleher, A., Yang, C.-R., Raghuram, V. & Knepper, M. A. Phosphorylation Changes in Response to Kinase Inhibitor H89 in PKA-Null Cells. *Sci Rep* **9**, 2814 (2019).

341. Hoxhaj, G. & Manning, B. D. The PI3K–AKT network at the interface of oncogenic signalling and cancer metabolism. *Nat Rev Cancer* **20**, 74–88 (2020).

342. Neary, C. L. & Pastorino, J. G. Akt inhibition promotes hexokinase 2 redistribution and glucose uptake in cancer cells. *Journal of Cellular Physiology* **228**, 1943–1948 (2013).

343. Capparelli, C. *et al*. Targeting SOX10-deficient cells to reduce the dormant-invasive phenotype state in melanoma. *Nat Commun* **13**, 1381 (2022).

344. Wouters, J. *et al*. Robust gene expression programs underlie recurrent cell states and phenotype switching in melanoma. *Nature Cell Biology* **22**, 986–998 (2020).

345. Aiello-Couzo, N. M. & Kang, Y. A bridge between melanoma cell states. *Nat Cell Biol* **22**, 913–914 (2020).

346. Shen, S. *et al*. Melanoma Persister Cells Are Tolerant to BRAF/MEK Inhibitors via ACOX1-Mediated Fatty Acid Oxidation. *Cell Reports* **33**, (2020).

347. Shen, S., Vagner, S. & Robert, C. Persistent Cancer Cells: The Deadly Survivors. *Cell* **183**, 860–874 (2020).

PUBLICATION ANNEXES

Bull Cancer 2022; 109: 728-735

en ligne sur / *on line on*
www.em-consulte.com/revue/bulcan
www.sciencedirect.com

At the crossroads of RNA biology, genome integrity and cancer

Summary

This article is the synthesis of the scientific presentations that took place during two international courses at Institute Curie, one on post-transcriptional gene regulation and the other on genome instability and human disease, that were joined together in their 2021 edition. This joined course brought together the knowledge on RNA metabolism and the maintenance of genome stability.

Keywords RNA; Post-transcriptional regulation; Genome instability; DNA damage; DNA repair; R-loops

Abbreviations

mRNAs	messenger RNAs
mNET-seq	mammalian Native Elongating Transcript sequencing
POINT-seq	Polymerase Intact Nascent Transcript sequencing
RNAPII	RNA Polymerase II
poly(A) tail	polyadenylate tail
CPA	Cleavage and Polyadenylation
CPF	Cleavage and Polyadenylation Factor
RBPs	RNA Binding Proteins
EJC	Exon Junction Complex
NMD	Nonsense mediated decay
NIN	Ninein
ROS	Reactive oxygen species
OOPs	Orthogonal Organic Phase separation
SG	Stress Granules
RNP	ribonucleoprotein
tRNAs	transfer RNAs
rRNAs	ribosomal RNAs
DDR	DNA damage response
PARPi	poly-ADP ribose polymerase 1 inhibitor
QIBC	quantitative imaging based cytometry
MiDAS	Mitotic DNA synthesis
OK-seq	Okazaki fragments sequencing
DSB	DNA double strand break
HR	Homologous recombination
NHEJ	Non-homologous end joining
ssDNA	Single stranded DNA
TAD	Topologically associated domain
IPA	intronic polyadenylation
UV-C	ultraviolet C
dilncRNAs	Damage-induced long non coding RNAs
DRIP	DNA-RNA immunoprecipitation

The mutual interactions between RNA metabolism and the DNA damage response have gained particular interest over the recent years and entail important clinical implications. This has led the organizers of two international courses at Institut Curie ("5th Course on Post transcriptional gene regulation" and "3rd Course on Genome integrity and human diseases") to exceptionally join their efforts. On the one hand, the "post transcriptional gene regulation" course focuses on the study of post transcriptional regulations, from molecular mechanisms to genome wide networks. On the other, the "genome integrity and human disease" course aims to introduce basic mechanisms contributing to the maintenance of genome stability from molecular mechanisms up to omics approaches. Here, we discuss some of the highlights of this 7 day course, sponsored by Institut Curie and Société Française du Cancer, that took place in real time virtual format in April 12–20 2021.

Post-transcriptional gene regulation

Post-transcriptional regulation plays an important role in controlling gene expression by subjecting precursor of messenger RNAs (mRNAs) called pre-mRNAs to a host of maturation events (*i.e.* splicing and polyadenylation) before being exported to the cytoplasm. Pre-mRNA splicing mainly occurs co transcriptionally. The lab of Maria Carmo Fonseca (Instituto de Medicina Molecular João Lobo Antunes, PT) has contributed to determining splicing kinetics in Metazoans by using several technologies. Live cell imaging of stable transgenes showed a transcription rate of about 4 kilobases per minute and a splicing reaction lasting only for a few seconds [1]. More recently, through genome wide analyses of nascent transcripts in human cells with the mNET-seq (mammalian native elongating transcript sequencing) and POINT-seq (polymerase intact nascent transcript sequencing) techniques, her team showed that for most introns, splicing takes place co transcriptionally, immediately after the 3′ splice site is transcribed by RNA polymerase II (RNAPII) [2,3]. However, for some introns splicing is delayed. These data raise questions about the molecular mechanisms underlying such different splicing kinetics, and their consequences on gene expression, alternative splicing regulation and, potentially, DNA-RNA hybrid formation and genome stability (which are discussed below).
Besides splicing, another key step of pre-mRNA maturation is 3′ end processing, which generally consists in-RNA cleavage at the polyadenylation site and in the addition of a polyadenylate tail (poly[A]) tail), that is not encoded in DNA. This cleavage and polyadenylation (CPA) process is coupled to transcription termination. In addition, the poly(A) tail promotes the nucleo-cytoplasmic export, translation and stability of the mRNA, and is the substrate of deadenylases that trigger mRNA degradation. The lab of Lori Passmore (MRC Laboratory of Molecular Biology, Cambridge, UK) determined the molecular structure of a key multiprotein component of the yeast CPA machinery, Cleavage and Polyadenylation Factor (CPF), by using *in vitro* reconstitution

experiments, cryo–electron microscopy and X-ray crystallography [4,5]. They also determined the structural determinants of poly(A) tail recognition by two deadenylases [6]. These studies provided insights into the molecular mechanisms of CPA and deadenylation processes in yeast, with implications for human cells since most protein components of these machineries are highly conserved in humans. Moreover, both polyadenylation (e.g., FIP1L1, CPSF3/CPSF73, NUDT21/CFIm25) and deadenylation factors (*e.g.*, CCR4–NOT complex components) have been involved in cancer [7,8]. In this context, recent work from Lori Passmore and collaborators showed that CPSF3 is a druggable node in acute myeloid leukemia and Ewing sarcoma [9].

During co–transcriptional RNA processing, RNA–binding proteins (RBPs) are deposited on transcripts, and some of them follow mRNAs into the cytoplasm and impact their fate. This is the case of the exon junction complex (EJC), a protein complex that is deposited on transcripts during splicing and promotes their nucleo-cytoplasmic export and translation. The EJC is best known for its role in triggering nonsense mediated decay (NMD) of mRNAs that have a premature stop codon located upstream of the last exon junction, which is the case of many aberrant transcripts that are produced by mutated genes or upon splicing factor mutations in diseases like cancer. About twenty years ago, Hervé Le Hir (now at Institut de Biologie of ENS, Paris, FR) discovered the EJC and its role in various processes, including NMD, mRNA export, translation and specific localization within the cytoplasm [10]. More recently, his lab showed that the EJC is localized at basal bodies during ciliogenesis in mouse neural stem cells and mediates the localization of the NIN (ninein) mRNA to centrioles, that form basal bodies and where the NIN protein plays a key function. Furthermore, EJC down-regulation impairs ciliogenesis [11]. These findings may explain the involvement of the EJC in neural stem cell division and human neurodevelopmental disorders.

Once in the cytoplasm, mRNAs are subjected to translational regulation. Alterations in the mRNA translation machinery can impact diverse cellular aspects, such as cell proliferation and metabolism. Davide Ruggero (UCSF Helen Diller Family Comprehensive Cancer Center, US) presented the activity of a general translation initiation factor, eIF4E, that binds to the "cap" structure located at the 5′ end of all mRNAs. His lab showed that eIF4E is essential for translating a subset of mRNAs implicated in the regulation of intracellular ROS levels, which is critical for tumour cell survival. Interestingly, recently they demonstrated that eIF4E heterozygous mice are resistant to diet-induced obesity, suggesting that diminished eIF4E levels can promote enhanced metabolic fitness [12].

Anne Willis (MRC Toxicology Unit, University of Cambridge, UK) provided evidence that mRNA translation of ribosomal proteins and nuclear encoded mitochondrial factors is altered in malignant mesothelioma [13]. In an effort to identify RBPs involved in the cellular response to toxic injury and external stress, Anne Willis also presented the development of experimental approaches such as Orthogonal Organic Phase Separation (OOPs) that allows to discriminate RNA-bound proteins [14]. mRNA translation is also modified upon stress induction within stress induced membrane-less organelles, so called stress granules (SG). Jeffrey A Chao (Friedrich Miescher Institute for Biomedical Research, Basel, CH) presented an elegant technique based on single molecule imaging to analyse mRNA translation in living cells. In contrast to the current model that postulates mRNA translation is inhibited in SG, he showed that translation in SG is not a rare event, and that the SG environment does not directly inhibit translation [15].

The link between cytoplasmic membrane-less ribonucleoprotein (RNP) granules and mRNA fate was presented by Dominique Weil (Institute of Biology Paris Seine, Paris, FR) who focuses on P-bodies. Her contribution in the development of a method to purify these granules enabled the characterization of RNA and protein content present in P-bodies using RNA-Seq and mass spectrometry, respectively. The comparison of the transcriptome of P-bodies before or after silencing mRNA decay or other repression factors revealed that GC content shapes mRNA storage and decay. Indeed, AU-rich and GC-rich mRNAs globally follow different decay pathways and the global GC content of mRNAs in P-bodies are closely linked to mRNA stability, translation rate, RBP and miRNA binding [16]. This study proposes an integrated view of the post transcriptional control of mRNA translation and mRNA stability.

More than just an mRNA storage compartment, P-bodies have been discovered to be implicated in a variety of polarized and non-polarized cells to compartmentalize protein synthesis. Florence Besse (Institut de Biologie Valrose, FR) has evidence that the targeting of the transcripts to their destination is operated by RNP granules which contain RNA cargo and regulatory proteins [17]. Using high resolution live imaging techniques, she showed that the targeting of mRNAs in neuronal RNP granules is a dynamic and reversible mechanism [18]. She has also found that defects in this process are linked to neurodegenerative diseases.

More than 150 chemical modifications of RNAs have recently been identified [19], which includes N6 methyladenosine (m6A), the most widespread modification on mammalian mRNAs, pseudouridine (X), ribose methylations (Nm), N1-methyladenosine (m1A), 5-methylcytidine (m5 C), N-7 methylguanosine (m7G) and N-4 acetylcytidine (ac4 C) among many others. These modifications harbor the potential of regulating the properties of RNAs and have emerged as critical regulators of gene expression, highlighting the importance of understanding their nature and role in biology and disease [20]. Although N4 acetylcytidine (ac4 C) is possibly one of the most highly conserved mechanisms of enzymatic modification of RNA, especially in tRNAs and rRNAs, the function of this cytidine acetylation, as well as its role in biology and disease, have yet to be

elucidated [21]. Shraga Schwartz (Weizmann Institute of Science, Rehovot, IL) presented a novel chemical approach for quantitative mapping of ac4 C at single nucleotide resolution in order to study hyperthermophiles archaea. With this new insight, ac4 C appeared as an essential modification for these microorganisms to resist extreme temperatures [21].

Recent advances in the DNA damage response

Many chemotherapeutic drugs used in combination with radiotherapy kill cancer cells by damaging DNA, and many of them, target DNA replication based processes given the highly replicative nature of cancer cells. Moreover, the DNA damage response (DDR) factors and the pathways themselves are potential targets to improve anti cancer therapies. Such strategy is beautifully illustrated by the clinical use of PARP inhibitors (PARPi) that target the DNA damage sensors poly-ADP-ribose polymerase 1 and 2 (PARP1/2). Dr Matthias Altmeyer (Department of Molecular Mechanisms of Disease, University of Zurich, CH) uses quantitative imaging based cytometry (QIBC), a high-content microscopy approach to quantify the chromatin association of DDR factors and relevant parameters such as cytotoxicity according to cell cycle progression in single cells. Applying QIBC to investigate the cell response to PARPi, Dr Altmeyer revealed that these drugs have an impact outside S-phase specific DNA damage response. By testing a panel of cell lines, it was possible to predict PARPi resistance or hypersensitivity and to delineate distinct cell responses to different PARPi in a quantitative manner [22]. One deleterious consequence of failures in S-phase progression is unfinished DNA replication resulting in under-replicated regions, also known as fragile sites, when cells enter mitosis. To overcome unfinished DNA replication, a process named MiDAS (Mitotic DNA synthesis) is active in mitosis to replicate under- replicated regions using a form of break nduced-replication [23]. Briefly, under-replicated DNA is cleaved by various endonucleases, generating a break from which DNA synthesis is initiated in a conservative mode, as opposed to the canonical semi conservative DNA synthesis. If MiDAS fails, 53BP1 nuclear bodies shield inherited genomic lesions from repair or degradation in G1. As a consequence of the inherited genomic lesions, the innate immune response can be activated through cGAS-TING pathway. Overall, the use of single cell experiments combined with technologies to map fragile sites and their behavior in a cell cycle specific manner provides a better description and understanding of the DDR.

Dr Chunlong Chen (Institut Curie, FR) has presented how genome-wide studies help to understand the dynamics of DNA replication in normal and challenged conditions. His lab focuses on understanding the spatio-temporal program of the human genome aiming to better understand how this program is deregulated in cancer cells or can be targeted to improve anti-cancer therapies. Deregulation of the DNA replication program threatens genome stability and is often observed in cancer cells. Chen's team has pioneered the development of deep sequencing of Okazaki fragments (OK Seq), that mark the synthesis of the lagging strand, thus providing crucial information about replication fork directionality genome-wide [24]. His team has also developed the Repli-Seq approach that allows the timing and replication dynamics of any specific locus to be investigated [25]. Combining these approaches, Dr Chen has presented how gene transcription landscape impact on DNA replication dynamics with the emerging concept that transcription during S-phase is a source of replication stress leading to recurrent genome instability when transcription replication conflicts are not dealt with properly [26]. For example, his results have confirmed the concept that large genes embedding long-transcription units strongly delay replication completion resulting in fragile sites at which DNA synthesis is not completed before cells enter mitosis.

The most toxic DNA lesions induced by anticancer therapies are DNA double strand breaks (DSB) which are repaired either by the non-homologous end-joining (NHEJ) or homologous recombination (HR) pathway. This last pathway has been the focus of intense research since inactivation of HR (caused by BRCA1 or BRCA2 mutations for example) leads to predisposition to breast and ovarian cancers. Repair pathway choice between NHEJ and HR is under the control of several factors that prevent or favor the resection of a DSB in which single stranded DNA (ssDNA) is generated, a process essential for HR-dependent repair. The presentation of Dr Dipanjan Chowdhury (Division of Radiation and Genome Stability, Dana Farber Cancer Institute, Boston, US) highlighted a novel factor involved in the resection of DSBs, identified in a loss of function CRISPR screen. This screen was focused on the identification of factors causing PARPi resistance or platinum-based therapy in BRCA mutated cell lines. This screen led to the discovery of DYNLL1 as a novel inhibitor of DSB end-resection [27]. Mechanistically, DYNLL1 interacts with the nuclease MRE11 (which mutations cause Ataxia Telangiectasia like disorder) to impair its activity. Moreover, decrease in DYNLL1 expression in carcinomas with low BRCA1 expression reduced genomic alterations. Together, this work highlights an important new factor in DSB-repair influencing responses to cancer therapies.

The substrate of the DDR is not the naked DNA but the chromatin, which plays a pivotal role in the signalling of DSB and their repair. The team of Gaëlle Legube (CBI, Toulouse, FR) has a particular interest in understanding how chromatin folding and modifications trigger the DDR. To do so, the team has developed unique tools to induce □100 DSBs (DIvA) in cells and to analyse their signalling and repair according to the chromatin landscape [28]. The research of Legube's team previously reported that DSB within transcriptionally active regions are preferentially repaired by the HR pathway and that DSB mobility, clustering and nuclear positioning are key determinants of repair pathway choice [29–31]. More recently, her team has revealed how

chromatin folding impacts early sensing of DSBs. One of the first events at DSB sites is the phosphorylation of the histone variant H2AX by the sensor kinase ATM (mutations of which cause Ataxia Telangiectasia disorder), a histone modification known as γH2AX. γH2AX is visible in the form of sub-nuclear foci since this modification can spread up to 50 kb around the site of the DSB. The mechanistic insight into the rapid spreading of γH2AX around DSB sites was missing. Gaëlle Legube presented her most recent research explaining that topologically associated domains (TAD), that are self-interacting genomic regions, are pivotal to establish the early steps of the DDR. TAD boundaries assist in the establishment of γH2AX via one-sided cohesin-mediated loop extrusion on both sides of the DSB [32]. Taken together, she proposes that TADs are functional units of the DDR to establish γH2AX chromatin domains that promote DSB signalling and repair foci.

The links between DNA damage and RNA biology

It is now well established that DNA damage widely impacts gene expression at the level of transcription, but also at multiple post-transcriptional levels [33]. In particular, Martin Dutertre (Institut Curie, FR) showed that alternative splicing is widely regulated in cancer cell response and resistance to genotoxic anticancer agents, such as topoisomerase inhibitors [34–36]. In recent years, many genes have been found to contain alternative polyadenylation sites within annotated introns, and their use generates so-called intronic polyadenylation (IPA) isoforms with alternative last exons. Martin Dutertre showed that IPA isoforms are widely regulated by camptothecin and doxorubicin (topoisomerase I and II inhibitors, respectively) but with different genome-wide patterns: mainly, down-regulation events in the case of doxorubicin, and equal proportions of up-and down-regulation events in the case of camptothecin [35]. He also presented data showing the widespread regulation of IPA isoforms by cisplatin, another genotoxic anticancer agent. IPA isoform regulation is enriched in genes related to the DDR, cell cycle and cell death, and he identified IPA isoforms that impact cell sensitivity to genotoxic agents. In addition, while the regulation of IPA isoforms has been mainly studied at the level of transcript synthesis, splicing and polyadenylation, he presented unpublished genome-wide analyses of their cytoplasmic regulation and of their translation status, by using 3-′ seq (RNA-seq focused on the 3′ end of polyA+ RNA) on subcellular compartments and polysome fractions. These analyses reveal diverse fates and translational outcomes of IPA isoforms. Finally, he discussed the increasing evidence for reciprocal links between pre-mRNA 3′ end processing (cleavage and polyadenylation) and genome stability [37].

The regulation of gene expression at multiple levels by DNA-damaging agents has been particularly characterized in the case of ultraviolet C (UV-C) irradiation. Jesper Svejstrup (University of Copenhagen, DK) showed, by using genome-wide GRO-seq analyses, that UV-C cell irradiation causes an inhibition of transcription elongation within 45 min. This is followed by an inhibition of transcription initiation within 2 to 4 hours due to RNAPII degradation. Finally, transcription restarts between 12 and 24 hours after irradiation thanks to RNAPII recovery, which is compromised in Cockayne syndrome B cells [38]. His lab also showed by RNA-seq analysis that elongation inhibition by UV-C irradiation is accompanied by an increase in the relative levels of IPA versus full-length mRNA isoforms in many long genes. In the *ASCC3* gene, IPA generates a transcript isoform with a non-coding function that antagonizes the function of the *ASCC3* protein-encoded by the full-length mRNA in transcription recovery following UV-C irradiation [39]. Jesper Svejstrup and his collaborators found that the *ASCC3* protein is also involved in the management of translational stress due to ribosome collisions [40]. Recently, they discovered that collided ribosomes are coactivators of cGAS, a sensor of cytosolic DNA that activates interferon- stimulated genes and thereby the innate immune response [41]. This finding may be relevant to understand inflammation caused by viral infections.

The links between genome stability and RNA biology are not limited to post transcriptional gene regulation by DNA damage. Indeed, in the last decade, non-coding RNAs have emerged as pivotal players in the maintenance of genome stability in response to DNA damage (see also next section). Dr Fabrizio d'Adda di Fagagna (IFOM, Milano, IT) has made major discoveries in this field by establishing that DSBs are actively transcribed by RNAPII although some details of this mechanism remain to be elucidated [42]. His team has proposed that RNAPII is recruited to DSB to generate ncRNAs named damage induced long non-coding RNAs (dilncRNAs) that are important to foster DSB signaling and DDR foci by a liquid phase-separation process [43]. The inhibition of dilncRNAs using antisense oligonucleotides (called AOS) lead to site-specific inhibition of the DDR, affecting DSB repair by NHEJ and HR. These results bring about the concept that DSB-induced transcription is essential to fully activate the DDR. Moreover, the use of telomere specific AOS to inhibit the DDR induced by telomere shortening restored tissue homeostasis in animal models, providing a potential clinical option to treat diseases associated to accelerated aging [44,45]. Finally, Dr Fabrizio d'Adda di Fagagna presented his recent work on the mechanism of recruitment of RNAPII to DSBs: he showed that RNAPII recruitment requires the MRN complex which cleaves the dsDNA providing an entry point for RNAPII binding and transcription initiation [46]. Monika Gullerova (University of Oxford, UK) has also contributed to describe how ncRNAs are generated at DSBs. Her lab showed that in human and mouse cells, a fraction of the endoribonuclease Dicer–which is best known for its cytoplasmic role in microRNA processing–is present in the nucleus, phosphorylated upon DNA damage, recruited to DSBs, and processes damage induced dsRNA

[47,48]. Furthermore, she showed that Dicer depletion delays the DDR by impaired recruitment of repair factors MDC1 and 53BP1 [48]. She presented novel work pertaining to a novel noncanonical pathway of ncRNA processing by Dicer.

RNA-containing structures such DNA-RNA hybrids or ribonucleotide insertions have recently emerged as essential players in the maintenance of genome integrity. RNA in the form of R-loops is the subject of study of Fred Chédin lab (UC Davis, US). These 3-stranded nucleic acid structures are composed of a DNA-RNA hybrid and a displaced ssDNA strand which form co transcriptionally. R–loops have physiological roles such as transcription regulation but may also impose pathological consequences for the cell. The Chedin lab has pioneered several high-throughput technologies based on DRIP (DNA-RNA immunoprecipitation) such as DRIP-seq and DRIPc-seq to map R-loops at the single molecule level in the mammalian genome using the RNA-DNA hybrid specific antibody S9.6. Using these technologies, they have found that there are around 300 R-loops/per cell and that R-loops are on average □300 bp in size. Chedin focused his talk on the physiological role of R-loops: these functions include helping to pause the RNA pol II as well as transcription termination. Interestingly, he introduced the concept that these structures can transiently absorb or relax negative super-coiling which in turn may impact promoter activation and/or replication origin firing. Super helicity also drives R-loop formation; thus, the dynamic formation and resolution of R-loops may contribute to the regulation of gene expression genome wide acting as an epigenetic mark [49,50].

R-loops can be a source of genome instability in particular in the context of replication, the focus of Karlene Cimprich team (Standford University, USA). In their lab, they recently developed a technique based on DRIPseq called qDRIP which allows not only strand specific mapping of DNA-RNA hybrids as DRIPc-seq but facilitates the comparison of the DNA-RNA hybrid content between different biological conditions using synthetic DNA-RNA hybrids as internal standards [51]. Although most laboratories have studied R-loops in the nuclear compartment, one of Cimprich's lab most surprising recent findings is the presence of

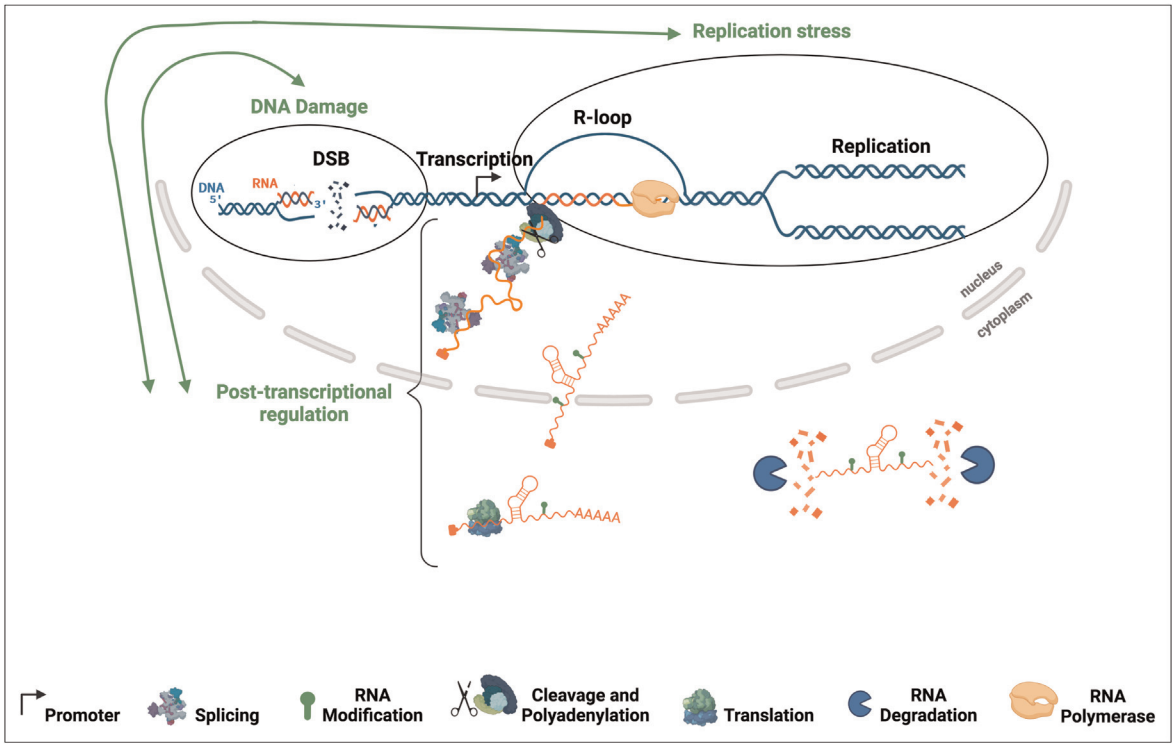

FIGURE 1

Reciprocal links between RNA biology and genome integrity. Some RNA molecules are produced at sites of double–strand DNA breaks and promote the recruitment of repair factors. R–loops, which are made of DNA-RNA hybrids and a displaced DNA strand, are involved in transcription–replication conflicts, leading to replication stress and DNA damage. Defects in pre messenger RNA splicing and cleavage/polyadenylation, which are generally coupled to transcription, can favor DNA damage. DNA damage signaling widely impacts post–transcriptional steps of gene expression, including RNA splicing, cleavage/polyadenylation, modification, export, localization, translation and degradation, all of which contribute to the regulation of genes involved in the DNA damage response (DDR). DNA is depicted in blue and RNA in orange. DSB, double–strand DNA break (Created with BioRender.com).

R-loops also in the cytoplasm. The role of these R-loops, how they form and why is currently under investigation.

Contributing to the question of the origin of R-loops tackled by Chedin and Cimprich labs; Benoit Palancade (Institut Jacques Monod, FR) described a series of elegant experiments performed in the yeast *S. cerevisiae* model system to demonstrate that R-loops form preferentially in intron-less genes and reciprocally, intronic sequences protect from R loop formation [52]. These findings have led his team to hypothesize that introns protect from genome instability. In his talk, Benoit Palancade also brought up one of the conundrums in the field that is whether DNA-RNA hybrids are an obstacle or a necessary intermediate for DSB repair: He discussed that nascent RNA at DSBs may serve as a template for repair by HR in a process he describes as transcription associated recombination (TAR); whereas other labs have shown that the accumulation of DNA RNA hybrids during transcription can have deleterious consequences for genetic integrity, as mentioned above. This conundrum was further discussed by Aura Carreira (Institut Curie, FR). Her lab recently focused on the RNA helicase DDX5, a novel partner of the breast cancer susceptibility protein BRCA2. Her team found that BRCA2 and DDX5 localize at DNA RNA hybrids at induced DSBs of actively transcribed regions. Using a missense variant of BRCA2 detected in breast cancer patients that reduces the association between the two proteins, they could show that BRCA2 and DDX5 cooperate to resolve DNA-RNA hybrids at DSBs whereas in cells bearing the variant repair by HR is delayed [53]. Thus, in this scenario, DNA-RNA hybrids appear to be deleterious for repair by HR.

In conclusion, this course has underscored the multiple and reciprocal links between RNA biology and genome integrity (*figure 1*). Indeed, DNA damage and replication stress widely impact gene expression and RNA metabolism at multiple post-transcriptional levels. Conversely, post transcriptional regulation of DDR genes impacts genome integrity; moreover, RNA processing-which is extensively coupled to transcription and chromatin-is involved in both the generation and repair of DNA damage. The study of these links is a recently expanding field that enhances our understanding of genome biology (by integrating genome expression, replication and integrity) and sheds new light on the molecular mechanisms of cancer development and therapy.

Disclosure of interest: the authors declare that they have no competing interest.

References

[1] Martin RM, Rino J, Carvalho C, Kirchhausen T, Carmo Fonseca M. Live cell visualization of pre mrna splicing with single molecule sensitivity. Cell Rep 2013;4:1144–55. http://dx.doi.org/10.1016/j.celrep.2013.08.013.

[2] Nojima T, Gomes T, Grosso ARF, Kimura H, Dye MJ, Dhir S, et al. Mammalian net seq reveals genome wide nascent transcription coupled to rna processing. Cell 2015;161:526–40. http://dx.doi.org/10.1016/j.cell.2015.03.027.

[3] Sousa Luís R, Dujardin G, Zukher I, Kimura H, Weldon C, Carmo Fonseca M, et al. Point technology illuminates the processing of polymerase associated intact nascent transcripts. Mol Cell 2021;81:1935–50. http://dx.doi.org/10.1016/j.molcel.2021.02.034.

[4] Casañal A, Kumar A, Hill CH, Easter AD, Emsley P, Degliesposti G, et al. Architecture of eukaryotic mRNA 3′ end processing machinery. Science 2017;358:1056–9. http://dx.doi.org/10.1126/science.aao6535.

[5] Hill CH, Boreikait□ V, Kumar A, Casañal A, Kubík P, Degliesposti G, et al. Activation of the endonuclease that defines mrna 3′ ends requires incorporation into an 8 subunit core cleavage and polyadenylation factor complex. Mol Cell 2019;73:1217–31. http://dx.doi.org/10.1016/j.molcel.2018.12.023.

[6] Tang TTL, Stowell JAW, Hill CH, Passmore LA. The intrinsic structure of poly (A) RNA determines the specificity of Pan2 and Caf1 deadenylases. Nat Struct Mol Biol 2019;26:433–42. http://dx.doi.org/10.1038/s4159401902279.

[7] Nourse J, Spada S, Danckwardt S. Emerging roles of rna 3′ end cleavage and polyadenylation in pathogenesis, diagnosis and therapy of human disorders. Biomolecules 2020;10:915. http://dx.doi.org/10.3390/biom10060915.

[8] Chalabi Hagkarim N, Grand RJ. The regulatory properties of the Ccr4–not complex. Cells 2020;9:2379. http://dx.doi.org/10.3390/cells9112379.

[9] Ross NT, Lohmann F, Carbonneau S, Fazal A, Weihofen WA, Gleim S, et al. CPSF3 dependent pre-mRNA processing as a druggable node in AML and Ewing's sarcoma. Nat Chem Biol 2020;16:50–9. http://dx.doi.org/10.1038/s4158901904241.

[10] Hir HL, Saulière J, Wang Z. The exon junction complex as a node of post transcriptional networks. Nat Rev Mol Cell Biol 2016;17:41–54. http://dx.doi.org/10.1038/nrm.2015.7.

[11] Kwon OS, Mishra R, Safieddine A, Coleno E, Alasseur Q, Faucourt M, et al. Exon junction complex dependent mRNA localization is linked to centrosome organization during ciliogenesis. Nat Commun 2021;12:1351. http://dx.doi.org/10.1038/s4146702121590w.

[12] Conn CS, Yang H, Tom HJ, Ikeda K, Oses Prieto JA, Vu H, et al. The major cap binding protein eIF4E regulates lipid homeostasis and diet induced obesity. Nat Metab 2021;3:244–57. http://dx.doi.org/10.1038/s4225502100349z.

[13] Grosso S, Marini A, Gyuraszova K, Voorde JV, Sfakianos A, Garland GD, et al. The pathogenesis of mesothelioma is driven by a dysregulated translatome. Nat Commun 2021;12:4920. http://dx.doi.org/10.1038/s41467021251737.

[14] Villanueva E, Smith T, Queiroz RML, Monti M, Pizzinga M, Elzek M, et al. Efficient recovery of the RNA bound proteome and protein bound transcriptome using phase separation (OOPS). Nat Protoc 2020;15:2568–88. http://dx.doi.org/10.1038/s4159602003442.

[15] Mateju D, Chao JA. Stress granules: regulators or by-products? FEBS J 2021;15821. http://dx.doi.org/10.1111/febs.15821.

[16] Courel M, Clément Y, Bossevain C, Foretek D, Vidal Cruchez O, Yi Z, et al. GC content shapes mRNA storage and decay in human cells. ELife 2019;8:e49708. http://dx.doi.org/10.7554/eLife.49708.

[17] Pushpalatha KV, Besse F. Local translation in axons: when membraneless rnp granules meet membrane bound organelles. Front Mol Biosci 2019;6:129. http://dx.doi.org/10.3389/fmolb.2019.00129.

[18] Formicola N, Heim M, Dufourt J, Lancelot AS, Nakamura A, Lagha M, et al. Correction: tyramine induces dynamic RNP granule remodeling and translation activation in the Drosophila brain. ELife 2021;10:e70755. http://dx.doi.org/10.7554/eLife.70755.

[19] Boccaletto P, Machnicka MA, Purta E, Pi□tkowski P, Bagi□ski B, Wirecki TK, et al. Modomics: a database of RNA modification pathways. 2017 update. Nucleic Acids Res 2018;46:D303–7. http://dx.doi.org/10.1093/nar/gkx1030.

[20] Schwartz S. Cracking the epitranscriptome. RNA 2016;22:169–74. http://dx.doi.org/10.1261/rna.054502.115.

[21] Sas Chen A, Thomas JM, Matzov D, Taoka M, Nance KD, Nir R, et al. Dynamic RNA acetylation revealed by quantitative cross evolutionary mapping. Nature 2020;583:638–43. http://dx.doi.org/10.1038/s4158602024182.

[22] Michelena J, Lezaja A, Teloni F, Schmid T, Imhof R, Altmeyer M. Analysis of PARP inhibitor toxicity by multidimensional fluorescence microscopy reveals mechanisms of sensitivity and resistance. Nat Commun 2018;9:2678. http://dx.doi.org/10.1038/s41467018050319.

[23] Lezaja A, Altmeyer M. Dealing with DNA lesions: when one cell cycle is not enough. Curr Opin Cell Biol 2021;70:27–36. http://dx.doi.org/10.1016/j.ceb.2020.11.001.

[24] Petryk N, Kahli M, d'Aubenton Carafa Y, Jaszczyszyn Y, Shen Y, Silvain M, et al. Replication landscape of the human genome. Nat Commun 2016;7:10208. http://dx.doi.org/10.1038/ncomms10208.

[25] Brison O, El Hilali S, Azar D, Koundrioukoff S, Schmidt M, Nähse V, et al. Transcription mediated organization of the replication initiation program across large genes sets common fragile sites genome-wide. Nat Commun 2019;10:5693. http://dx.doi.org/10.1038/s41467019136745.

[26] Promonet A, Padioleau I, Liu Y, Sanz L, Biernacka A, Schmitz AL, et al. Topoisomerase 1 prevents replication stress at R loop enriched transcription termination sites. Nat Commun 2020;11:3940. http://dx.doi.org/10.1038/s41467020178582.

[27] He YJ, Meghani K, Caron MC, Yang C, Ronato DA, Bian J, et al. DYNLL1 binds to MRE11 to limit DNA end resection in BRCA1 deficient cells. Nature 2018;563:522–6. http://dx.doi.org/10.1038/s41586-018-06705.

[28] Clouaire T, Rocher V, Lashgari A, Arnould C, Aguirrebengoa M, Biernacka A, et al. Comprehensive mapping of histone modifications at dna double strand breaks deciphers repair pathway chromatin signatures. Mol Cell 2018;72:250–262.e6. http://dx.doi.org/10.1016/j.molcel.2018.08.020.

[29] Aymard F, Aguirrebengoa M, Guillou E, Javierre BM, Bugler B, Arnould C, et al. Genome wide mapping of long range contacts unveils clustering of DNA double strand breaks at damaged active genes. Nat Struct Mol Biol 2017;24:353–61. http://dx.doi.org/10.1038/nsmb.3387.

[30] Marnef A, Cohen S, Legube G. Transcription coupled DNA double strand break repair: active genes need special care. J Mol Biol 2017;429:1277–88. http://dx.doi.org/10.1016/j.jmb.2017.03.024.

[31] Marnef A, Finoux AL, Arnould C, Guillou E, Daburon V, Rocher V, et al. A cohesin/HUSH and LINC-dependent pathway controls ribosomal DNA double strand break repair. Genes Dev 2019;33:1175–90. http://dx.doi.org/10.1101/gad.324012.119.

[32] Arnould C, Rocher V, Finoux AL, Clouaire T, Li K, Zhou F, et al. Loop extrusion as a mechanism for formation of DNA damage repair foci. Nature 2021;590:660–5. http://dx.doi.org/10.1038/s4158602103193z.

[33] Dutertre M, Lambert S, Carreira A, Amor Guéret M, Vagner S. DNA damage: RNA binding proteins protect from near and far. Trends Biochem Sci 2014;39:141–9. http://dx.doi.org/10.1016/j.tibs.2014.01.003.

[34] Dutertre M, Sanchez G, De Cian MC, Barbier J, Dardenne E, Gratadou L, et al. Cotranscriptional exon skipping in the genotoxic stress response. Nat Struct Mol Biol 2010;17:1358–66. http://dx.doi.org/10.1038/nsmb.1912.

[35] Dutertre M, Chakrama FZ, Combe E, Desmet FO, Mortada H, Polay Espinoza M, et al. A recently evolved class of alternative 3′ terminal exons involved in cell cycle regulation by topoisomerase inhibitors. Nat Commun 2014;5:3395. http://dx.doi.org/10.1038/ncomms4395.

[36] Tanaka I, Chakraborty A, Saulnier O, Benoit Pilven C, Vacher S, Labiod D, et al. ZRANB2 and SYF2-mediated splicing programs converging on ECT2 are involved in breast cancer cell resistance to doxorubicin. Nucleic Acids Res 2020;48:2676–93. http://dx.doi.org/10.1093/nar/qkz1213.

[37] Dutertre M, Sfaxi R, Vagner S. Reciprocal links between pre messenger RNA 3′ end processing and genome stability. Trends Biochem Sci 2021;46:579–94. http://dx.doi.org/10.1016/j.tibs.2021.01.009.

[38] Tufegd□ić Vidaković A, Mitter R, Kelly GP, Neumann M, Harreman M, Rodríguez Martínez M, et al. Regulation of the RNAPII pool is integral to the DNA damage response. Cell 2020;180:1245–61. http://dx.doi.org/10.1016/j.cell.2020.02.009.

[39] Williamson L, Saponaro M, Boeing S, East P, Mitter R, Kantidakis T, et al. UV irradiation induces a non-coding RNA that functionally opposes the protein encoded by the same gene. Cell 2017;168:843–55. http://dx.doi.org/10.1016/j.cell.2017.01.019.

[40] Juszkiewicz S, Speldewinde SH, Wan L, Svejstrup JQ, Hegde RS. The ASC 1 complex disassembles collided ribosomes. Mol Cell 2020;79:603–614.e8. http://dx.doi.org/10.1016/j.molcel.2020.06.006.

[41] Wan L, Juszkiewicz S, Blears D, Bajpe PK, Han Z, Faull P, et al. Translation stress and collided ribosomes are co activators of cGAS. Mol Cell 2021;81:2808–22. http://dx.doi.org/10.1016/j.molcel.2021.05.018.

[42] Michelini F, Pitchiaya S, Vitelli V, Sharma S, Gioia U, Pessina F, et al. Damage induced lncRNAs control the DNA damage response through interaction with DDRNAs at individual double strand breaks. Nat Cell Biol 2017;19:1400–11. http://dx.doi.org/10.1038/ncb3643.

[43] Pessina F, Giavazzi F, Yin Y, Gioia U, Vitelli V, Galbiati A, et al. Functional transcription promoters at DNA double strand breaks mediate RNA driven phase separation of damage response factors. Nat Cell Biol 2019;21:1286–99. http://dx.doi.org/10.1038/s4155601903924.

[44] Aguado J, Sola Carvajal A, Cancila V, Revêchon G, Ong PF, Jones Weinert CW, et al. Inhibition of DNA damage response at telomeres improves the detrimental phenotypes of Hutchinson–Gilford Progeria syndrome. Nat Commun 2019;10:4990. http://dx.doi.org/10.1038/s41467019130183.

[45] Di Micco R, Krizhanovsky V, Baker D, d'Adda di Fagagna F. Cellular senescence in ageing: from mechanisms to therapeutic opportunities. Nat Rev Mol Cell Biol 2021;22:75–95. http://dx.doi.org/10.1038/s4158002000314w.

[46] Sharma S, Anand R, Zhang X, Francia S, Michelini F, Galbiati A, et al. MRE11 RAD50 NBS1 complex is sufficient to promote transcription by rna polymerase II at double strand breaks by melting DNA ends. Cell Rep 2021;34:108565. http://dx.doi.org/10.1016/j.celrep.2020.108565.

[47] Burger K, Gullerova M. Nuclear re localization of Dicer in primary mouse embryonic fibroblast nuclei following DNA damage. PLoS Genet 2018;14:e1007151. http://dx.doi.org/10.1371/journal.pgen.1007151.

[48] Burger K, Schlackow M, Potts M, Hester S, Mohammed S, Gullerova M. Nuclear phosphorylated Dicer processes double stranded RNA in response to DNA damage. J Cell Biol 2017;216:2373–89. http://dx.doi.org/10.1083/jcb.201612131.

[49] Chedin F, Benham CJ. Emerging roles for R loop structures in the management of topological stress. J Biol Chem 2020;295:4684–95. http://dx.doi.org/10.1074/jbc.REV119.006364.

[50] Ginno PA, Lott PL, Christensen HC, Korf I, Chédin F. R Loop formation is a distinctive characteristic of unmethylated human cpg island promoters. Mol Cell 2012;45:814–25. http://dx.doi.org/10.1016/j.molcel.2012.01.017.

[51] Crossley MP, Bocek MJ, Hamperl S, Swigut T, Cimprich KA. qDRIP: a method to quantitatively assess RNA–DNA hybrid formation genome wide. Nucleic Acids Res 2020;48:e84. http://dx.doi.org/10.1093/nar/gkaa500.

[52] Bonnet A, Grosso AR, Elkaoutari A, Coleno E, Presle A, Sridhara SC, et al. Introns protect eukaryotic genomes from transcription associated genetic instability. Mol Cell 2017;67:608–621.e6. http://dx.doi.org/10.1016/j.molcel.2017.07.002.

[53] Sessa G, Gómez González B, Silva S, Pérez Calero C, Beaurepere R, Barroso S, et al. BRCA2 promotes DNA RNA hybrid resolution by DDX5 helicase at DNA breaks to facilitate their repair. EMBO J 2021;40. http://dx.doi.org/10.15252/embj.2020106018.

Biswendu Biswas[1], Rady Chaaban[1], Shrena Chakraborty[1], Alexandre Devaux[1], Ana Luisa Dian[1], Anna Minello[1], Jenny Kaur Singh[1], Stephan Vagner, Patricia Uguen, Sarah Lambert, Martin Dutertre, Aura Carreira

CNRS UMR 3348 Genome integrity, RNA and Cancer, Institut Curie, University Paris-Saclay, 91401 Orsay, France

Correspondence: Patricia Uguen, CNRS UMR 3348 Genome integrity, RNA and Cancer, Institut Curie, University Paris-Saclay, 91401 Orsay, France

patricia.uguen@curie.fr

[1]Equal contribution.

Received 20 December 2021
Accepted 21 February 2022
Available online: 18 May 2022

https://doi.org/10.1016/j.bulcan.2022.02.014

Bull Cancer 2024; xx: xxx

en ligne sur / *on line on*
www.em-consulte.com/revue/bulcan
www.sciencedirect.com

Post-transcriptional gene regulation: From mechanisms to RNA chemistry and therapeutics

Summary

A better understanding of the RNA biology and chemistry is necessary to then develop new RNA therapeutic strategies. This review is the synthesis of a series of conferences that took place during the 6th international course on post-transcriptional gene regulation at Institut Curie. This year, the course made a special focus on RNA chemistry.

Keywords RNA; Post-transcriptional regulation; RNA therapeutics

Abbreviations ASOantisense Oligonucleotide; dsRNAdouble-stranded RNA; EJCexon-junction complex; EMTepithelial-to-mesenchymal transition; FDAFood and Drug Administration; G4G4-quadruplex; m^6AN6-methylAdenosine; mRNAmessenger RNA; miRNAmicroRNA; NMDnonsense-mediated decay; PTBpolypyrimidine tract-binding protein; PTCpremature termination codon; RNAPIIRNA polymerase II; RBPRNA-Binding protein; RNAiRNA interference; RNPRiboNucleoProtein; SELEXsystematic evolution of ligands by exponential enrichment; siRNAsmall interfering RNA; tRNAtransfer RNA; UTRuntranslated region; vRNAviral RNA; 5BrdU5-Bromo deoxyUridine

Introduction

Among the different layers regulating gene expression, the post-transcriptional gene regulation is an essential biological process that has gained interest in recent years because of its implication in many diseases. The aim of this review is to summarize the scientific presentations that took place during the 6th course on post-transcriptional gene regulation at Institut Curie. This course was focused on various aspects of RNA biology (chemistry and therapeutics). Here, we discuss some of the highlights of this five-day course, sponsored by the Institut Curie, the Graduate School Life Science and Health of the Université Paris-Saclay, the École normale supérieure, and that took place at the Institut Curie in Orsay and Paris, in April 24–28, 2023.

RNA splicing

One of the major gene regulatory processes used by the cell to acquire new phenotypic traits and gain protein diversity is pre-messenger RNA (pre-mRNA) alternative splicing, which generates different mature mRNAs from the same transcribed gene. It is performed by the splicing machinery, called the spliceosome, and targets the genomic regions that must be excised or kept in the final mRNA via two alternative mechanisms, so-called exon or intron definition [1]. However, the choice between one and the other mechanism is not fully understood yet. The team of Gil Ast (Department of Human Molecular Genetics Medical School, Tel Aviv, IL) has been studying the impact of gene architecture and its 3D genomic organization in alternative splicing regulation and the choice of exon or intron definition. Compilations of genomic and transcriptomic datasets showed the appearance of two distinct exon-intron architectures during evolution of warm-blooded organisms from a common ancestor with a differential GC content between the exons and short introns [2]. One architecture, termed leveled architecture, is defined by short introns with overall higher GC content in the exons and flanking introns. Whereas the second one, named differential architecture, is preserving the differential exon-intron GC content, but with longer introns. His team has now identified a 3D spatial organization of the genome based on this GC content gradient that would impact the choice of exon or intron definition and thus the final splicing outcome [3]. They found that genes with high GC content and leveled architecture are located in the inner part of the nucleus where they are usually defined at the intron level, leading to more frequent intron retention, while low GC content genes with differential architecture are more in the nuclear periphery and associated with exon definition and thus exon skipping. Moreover, this spatial organization creates two distinct environments with specific sub-networks of splicing factors favoring one splicing definition or the other, depending on the given architecture of the gene and thus determining the final splicing outcome.

Delving deeper into the role of chromatin organization in splicing, the team of Reini Luco (Institut Curie, Orsay, FR) found that chromatin modifications, such as H3K36me3 and H3K27me3, can also deeply impact cell-specific alternative splicing by favoring the recruitment of the splicing factors, such as PTB (polypyrimidine tract-binding protein), to the pre-mRNA via direct interaction with specific chromatin-adaptor complexes [4,5]. To explore further the biological relevance of these splicing-associated histone marks, the team moved into a dynamic cell reprogramming system dependent on well-known changes in splicing essential for early development and tumor metastasis, called the epithelial-to-mesenchymal transition (EMT). They found that at several genes essential for EMT, such as *FGFR2* and *CTNND1,* well-defined changes in specific histone marks right at the regulated exon are essential for the dynamic splicing changes responsible for EMT's phenotype [6]. Looking at how these exon-specific histone marks are regulated, the Luco team

To cite this article: Bonnet C, et al. Post-transcriptional gene regulation: From mechanisms to RNA chemistry and therapeutics. Bull Cancer (2024), https://doi.org/10.1016/j.bulcan.2024.04.005

has uncovered a role for 3D chromatin organization in which alternatively spliced exons physically interact with long distant regulatory regions important for EMT's splicing regulation.

Finally, upon splicing, a group of proteins are recruited at the exon-exon-junctions for stabilization of the mRNA and its transport to the cytoplasm for translation, called the Exon-Junction Complex (EJC) [7]. This protein complex is first assembled at the exon-junction by the spliceosome during splicing, and then is transported into the cytoplasm. Hervé Le Hir's team (Institut of biologie of the école normale supérieure, Paris, FR) has identified the 4 proteins composing its core structure, and their 3D organization [8,9]. One of these core proteins is eIF4AIII, a helicase that binds to the RNA, more specifically to its sugar backbone, independently of its sequence. This complex can only be assembled on RNA. First, the EJC can regulate pre-mRNA splicing by changing RNA polymerase II elongation rate [10]. It can also modulate mRNA nonsense-mediated decay (NMD) that degrades transcripts containing a premature termination codon (PTC) or regulates gene expression levels. If a PTC is a few base pairs upstream of a splice site, the EJC can help recruit the proteins needed to trigger the NMD [11]. On the other hand, the EJC can mask mRNA post-transcriptional modifications that destabilize the mRNA [12]. Finally, they recently showed that EJC is present around centrosomes which allow an active transport of the messenger ribonucleoprotein (mRNP) to accumulate transcripts at a specific location where they are translated [13]. Interestingly, most functions of the EJC appear to be indirectly or directly linked to translational control. Future studies will undoubtedly reveal new mechanisms by which the EJC, in association with other proteins, activates or represses translation.

RNA translation

Throughout the course of evolution, species undergo adaptive transformations in response to their environment yielding, among various outcomes, the de novo emergence of translated open reading frames (ORFs) [14]. This discovery was facilitated by the use of ribosome profiling (Ribo-seq), enabling the monitoring of actively translated regions of mRNAs in vivo. This technique has revealed thousands of translated short ORFs (sORFs) that result in the production of microproteins, found in both coding and non-coding regions of the genome [15]. The research group led by Norbert Hübner (Max Delbrück Center for Molecular Medicine, Berlin, DE) has significantly advanced our understanding of micropeptides in humans. They identified many microproteins (< 100 amino acids) including 221 novel translated sORFs that are shorter than 16 amino acids in five human tissues (brain, heart, liver, kidney and testis) [16]. Most of these human microproteins recently emerged during evolution and show only limited sequence conservation, restricted to primates. The team investigated these microproteins in terms of their sequence (e.g. presence of a transmembrane domain), cellular localization (e.g. nucleus, mitochondria) and interactions with other partners. They conducted a high-throughput protein interaction screen on peptide matrix (PRISMA) and discovered that small peptides interact with proteins involved in several cellular mechanisms such as mRNA splicing, translational regulation and endocytosis. For instance, they characterized a 5 amino acid-long peptide translated from an upstream ORF within the myotubularin related protein 3 (*MTMR3*) gene, which is associated with all four clathrins, the phosphatidylinositol binding clathrin assembly protein (PICALM) and the clathrin interactor 1 (CLINT1). Hence, their research not only offers insights for exploring evolutionary novel human microproteins but also provides tools to understand their cellular functions [16].

Furthermore, over the past few years, the translation of these non-canonical ORFs has been associated with tumorigenic mechanisms [17–19]. More broadly, perturbations in global translation can represent a major event that contributes to the development of cancer. Indeed, cancer cells often remodel post-transcriptional regulatory networks as they progress toward metastasis [20,21]. However, the identification of key post-transcriptional regulators that drive pathologic gene expression remains a challenge. Aiming to identify these regulators, Albertas Navickas (Institut Curie, Orsay, FR) and collaborators have identified oncogenic RNA-binding proteins (RBPs) through the detection of coordinated changes in their target regulons [22]. For example, they revealed that the RNA-binding motif single-strand interacting protein 1 (RBMS1) acts as a suppressor of colon cancer metastasis and as a post-transcriptional regulator of RNA stability by directly binding to its target mRNAs [22]. Moreover, in cell lines and patient-derived xenograft models of breast cancer metastasis, the Small Nuclear Ribonucleoprotein Polypeptide A' (SNRPA1) was revealed to mediate aberrant alternative splicing in highly metastatic breast cancer through direct interactions with the SNRPA1-associated structural splicing enhancers (S3Es) [21]. In the scope of translational regulation, ribosome profiling and alternative polyadenylation data of poorly and highly metastatic breast cancer cells and patient-derived xenografts revealed the Heterogeneous Nuclear RiboNucleoProtein C (HNRNPC) as a translational controller [20]. In highly metastatic cells, HNRNPC is downregulated which causes its target mRNAs to undergo 3'UTR lengthening via alternative polyadenylation site selection and, subsequently, translation repression. Altogether, these results uncover previously unknown gene regulatory programs mediated by key RBPs involved in cancer metastasis. Thus, these RBPs, together with their target mRNAs, provide more knowledge to identify points of vulnerability to design new targets and to better determine the prognosis.

In line with the objective of enhancing therapeutic approaches, the laboratory of Reuven Agami (The Netherlands Cancer Institute NKI, Amsterdam, NL) has used the Ribo-seq technology to

study events regulated at the mRNA translation level, and consequently discovered a novel point of vulnerability in cancers. The mRNA translation is disrupted by oncogenes to facilitate cancer development, and his team found that this disruption affects the quality of proteins, and that cancer cells exhibit deficiencies in amino acids [23]. Indeed, in order to survive, tumors adapt to their abnormal growth by hijacking the pathways of amino acid production. An example of such metabolic alteration is the tryptophan shortage. Reuven Agami and his collaborators demonstrated that in melanoma, interferon-γ (INF-γ) released from T cells triggers the upregulation of the indoleamine 2,3-dioxygenase 1 (IDO1) enzyme, that catabolizes the tryptophan into kynurenine [24]. They found that the deprivation of this amino acid results in the synthesis of aberrant proteins by ribosomal frameshifting and substituants (tryptophan-to-phenylalanine), an event they referred to as "sloppiness in mRNA translation" [25,26]. Additionally, the tryptophan deficiency in melanoma cells is associated with the hyperactivation of the MAPK pathway. The sloppiness can therefore be eliminated through the pharmacological inhibition of the oncogenic MAPK signaling [26]. However, in cells resistant to these drugs, the sloppiness is restored, which can activate the response of T lymphocytes. Indeed, the sloppiness results in the presentation of aberrant peptides on the cell surface, targeted by T cells, and thereby expanding the antigen landscape. These abnormal neoepitopes thus represent a vulnerability that can be explored to improve anti-cancer strategies [26].

RNA degradation

Targeting RNA processing mechanisms and associated RBPs thus opens new therapeutic pathways for better treating human diseases. In addition to cancer, pathogenic viruses represent a threat to public health and therefore pose significant socio-economic challenges. In RNA viruses, the RNA has a central role serving both as the viral genome and mRNA for protein synthesis [27,28]. However, viral genome-encoded proteins are not sufficient to enable viral infection. To address this limitation, it is therefore unsurprising that these obligatory intracellular parasites heavily rely on host cell proteins for their life cycle [27,28]. Using novel multi-omics strategies, Alfredo Castello's team (MRC University of Glasgow Centre for Virus Research, Glasgow, UK) showed that RNA viruses hijack cellular RBPs to regulate their life cycle [27,28]. Through the development and use of the comparative RNA Interactome Capture (cRIC) approach, they identified RBPs that displayed differential interaction with RNA and altered localization upon sindbis virus (SINV) infection [29,30]. Those RBPs with enhanced activity were found to accumulate in the viral factories together with the viral RNA (vRNA), thereby regulating the viral fitness and infection capacity. For example, the 5'-3' exoribonuclease 1 (XRN1) was detected near viral replication factories and its knockdown induced cell resistance to SINV infection [29]. Accordingly, infection with severe acute respiratory syndrome coronavirus 2 (SARS-CoV-2) in human lung cancer epithelial cells led to remodeling of the cellular RNA-bound proteome [31]. Interestingly, the development and employment of a new technology, named vRNA Interactome Capture (vRIC), revealed shared host-virus interactions between SARS-CoV-2 and SINV, despite the absence of sequence homology between the two vRNAs [30,31]. Collectively, these findings uncover the existence of key RBPs involved in virus infection regulation, and therefore a new universe of host-virus interactions emerges, harboring the potential for the development of antiviral treatments. Indeed, experiments with available inhibitors revealed that cellular RBPs are promising targets for broad-spectrum antiviral therapies [30].

In mammalian cells, early resistance against viral replication relies on the rapid activation of innate immune responses that trigger interferon (IFN) production. However, the inducible protection conferred by these cytokines is much more pronounced in differentiated cells than in embryonic or adult stem cells [32]. In organisms in which the IFN system is absent (e.g. invertebrates and plants), the protection against virus infection is conferred by means of RNA interference (RNAi). This process is initiated by the protein Dicer, which recognizes and cleaves viral double-strand RNA (dsRNA) [33]. Using in vitro models and brain organoids, the laboratory of Enzo Poirier (Institut Curie, Paris, FR) demonstrated in an innovative way a new pathway in which mammalian stem cells protect themselves from RNA viruses, such as Zika virus (ZIKV) and SARS-CoV-2 [34]. These cells were shown to preferentially express an alternatively spliced isoform of Dicer, termed antiviral Dicer (aviD), which enhances antiviral RNAi by processing long double-strand viral RNAs into small interfering RNAs (siRNAs). These siRNAs guide a sequence-specific degradation of corresponding vRNAs through the RNA-induced silencing (RISC) complex. Notably, in cases where a viral suppressor of RNAi (VSR) is used in the context of aviD, the viral dsRNA is shielded from Dicer cleavage resulting in increased viral production [34]. Thus, this indicates that the degradation of viral dsRNA in mammalian stem cells relies on the RISC complex, shedding light on the molecular regulation of antiviral RNAi in mammalian innate immunity.

Beyond its importance in combating vRNA, the RISC complex is crucial in gene regulation by controlling the fate of the RNA at the post-transcriptional level. However, the timing and molecular mechanism involved in this control are not yet fully understood. These are the questions that Stefan Ameres' group (Max Perutz Labs, Vienna, AT) is trying to answer, and their research has contributed to a deeper understanding of the RNA silencing biology. By combining the technique of thiol (SH)-linked alkylation for the metabolic sequencing of RNA (SLAMseq) with bioinformatics approaches [35], they found that the identity of the Argonaute (Ago) protein, which is a core protein of the RISC complex in double-stranded microRNA (miRNA)

maturation, determines the stability and function of small RNAs [36]. For instance, in Drosophila, the Ago2-bound miRNA duplexes are approximately two times more stable than those bound to Ago1. Additionally, the Ago1-dependent pathway generates single-stranded miRNAs, whereas the Ago2-mediated pathway produces siRNAs. The balance between these two pathways thereby reflects specific developmental requirements. Indeed, Ago1 facilitates the selective and rapid renewal of miRNAs in response to environmental changes and cellular differentiation, while Ago2 plays a pivotal role in antiviral defense. Furthermore, their investigations have revealed that the Ago-mediated processing is a fast process, occurring in less than 5 minutes, which can be disrupted by the uridylation of pre-miRNAs. Indeed, Stefan Ameres and his collaborators have shown that 3' uridylation of RNA is a modification that helps to control the RNA quality and thus contributes to the regulation of the fate of RNA [37,38]. This RNA modification therefore represents a novel layer of gene regulation.

RNA modifications

RNA can be post-transcriptionally modified by more than a hundred distinct chemical modifications [39]. These post-transcriptional modifications play important roles in various biological processes [40]. Pierre Close's laboratory (GIGA Institute, Liège, BE) found that the RNA modification landscape has important functional consequences in cell physiology through its work on transfer RNA (tRNA) modification. Indeed, they have shown the importance of tRNA modifications and their control of protein synthesis in the growth, invasion, and therapeutic resistance of cancers. During tumorigenesis, oncogenic signalling can change the expression of tRNAs, and this is correlated with changes in mRNA translation of genes with specific codon usage. Specifically, enzymes regulating wobble uridine tRNA (U34-tRNA) modification are upregulated in melanoma. U34-tRNA modifications are required for specific codon decoding during translation to promote the expression of selected genes like HIF1A, which drives glycolysis and therapeutic resistance in melanoma [41,42]. Curiously, it has been discovered that gene codon content is necessary but not sufficient to predict protein fate. Indeed, most genes can escape regulation by U34-tRNA modifications whereas for several genes, these modifications are essential to maintain translation speed and protein output. It appears that the presence of specific hydrophilic motifs causes protein aggregation and degradation upon codon-dependent translation elongation defects [43]. Therefore, it is the combination of codon content and the presence of hydrophilic motifs that defines the proteome. Together, these results provide a better understanding of the impact of translation regulation by tRNA modification on proteome homeostasis. This highlights the importance of codon-specific mRNA translation and tRNA modifications as possible therapeutic targets in cancer.

Because of their cellular abundance, RNA post-transcriptional modifications were first identified in rRNA and tRNA. However, it is now clear that all species of RNA undergo dynamic modification, including mRNAs [44]. Considering all cellular RNA, pseudouridylation (the conversion of uridine into pseudouridine) is one of the most abundant post-transcriptional modifications, but its biological role remains poorly understood [45]. Marianne Farnebo's Group (Karolinska Institute, Stockholm, SE) has highlighted that pseudouridine is deposited onto mRNAs during their transcription through the action of the pseudouridine synthase dyskerin. Indeed, in cells depleted in dyskerin, the amount of pseudouridine in mRNAs is significantly reduced, suggesting that dyskerin is responsible for the majority of mRNA pseudouridylation. Moreover, by performing ChIP-seq and co-immunoprecipitation experiments, they have shown that dyskerin is associated with RNAPII and enriched in genes transcribed by RNAPII throughout the genome [46]. The consequences of this co-transcriptional mRNA pseudouridylation by dyskerin are a repression of translation allowing controlled protein synthesis. However, when the function of dyskerin is impaired, it has different outcomes on translation depending on the duration of impairment; short-term depletion enhances translation due to reduced mRNA pseudouridylation whereas long-term depletion attenuates translation due to defective rRNA pseudouridylation and processing. In fact, pseudouridine can also affect the structure and function of various non-coding RNAs and not only mRNAs. Thus, pseudouridylation of mRNAs by dyskerin appears to be part of a general mechanism enabling communication between transcription and translation, with important implications for both normal development and disease. Going beyond RNA modification, Farnebo's group has evidence that RNA itself could be a "modification'' for the chromatin regulating its compactions. This effect on chromatin occurs only with single-stranded RNA and in a sequence-independent manner. Mechanistically, RNA binds histones and neutralizes their positively charged tails, which restricts histone self-association and interaction with DNA, thereby promoting an open chromatin state. Conversely, removal of the negatively charged RNA exposes the positive charges on histone tails, which stimulates electrostatic interactions with DNA, resulting in tighter packing of the chromatin [43]. This discovery provides a novel and conceptionally simple mechanism by which RNA is involved in the opening and closure of chromatin and establishes RNA as a key functional component of eukaryotic chromatin.

Another widespread RNA modification is N^6-methyladenosine (m^6A), a methyl modification of adenosine. Novel high-throughput m^6A mapping methods (e.g. MeRIP-seq, miCLIP) developed in Samie Jaffrey's team (Cornell University, New York, USA) have contributed to a significant progress in uncovering the landscape of m^6A modifications in mammalian mRNAs [44,45]. It is now known that m^6A modifications in mRNAs influence different

To cite this article: Bonnet C, et al. Post-transcriptional gene regulation: From mechanisms to RNA chemistry and therapeutics. Bull Cancer (2024), https://doi.org/10.1016/j.bulcan.2024.04.005

gene expression processes in both physiological and pathological conditions, such as RNA splicing, nuclear transport, mRNA stability and translation [46,47]. m^6A is installed co-transcriptionally in the nucleus by the m^6A writer complex and is removed by erasers. Importantly, m^6A functions in mRNAs are mediated by m^6A binding proteins, also called as "readers". The most well-established readers are the nuclear YTHDC1, responsible for nuclear RNA processing, and the cytosolic YTHDF1, 2, and 3. How distinct cytosolic readers, sharing high amino acid similarity, may mediate different fates of m^6A-modified mRNAs, such as decay or translational control, is a subject of debate. The aim of Jaffrey's lab is to elucidate this aspect. Starting from the observation that the amino acid sequence of the three YTHDF proteins contains low complexity domains, they found that the three readers, by preferentially interacting with mRNAs containing multiple m^6A sites, may associate and undergo phase separation into P-bodies and stress granules [48], where they predominantly function, in a redundant manner, in mediating degradation of m^6A-modified mRNA [49]. However, the mechanism by which m^6A modifications dictate the fate of distinct m^6A-modified mRNAs may be context-specific and influenced by the localization of m^6A within mRNA body. Further analysis to clarify this aspect is needed. In addition to chemical modifications installed on transcript body, the 5' end of mRNA is modified by a so-called m^7G cap structure that participates in different biological processes, including pre-mRNA processing and translation [50]. The mRNA cap structure can be additionally methylated. Depending on the presence of 2'-O-methylation on the first, or both the first and second transcribed nucleotide, mRNA caps exist in either the Cap1 or Cap2 form, respectively [51]. Although Cap1 methylation is present in all mRNAs, Cap2 methylation seems to be restricted to a subset of mRNAs [52]. Jaffrey's team latest work explored the molecular basis of Cap2 selectivity and functions. By developing novel methods (CLAM-Cap-Seq) to profile Cap2 transcriptome-wide as well as on specific mRNAs of interest, they found that Cap2 modification can be present in all mRNAs, but it increases throughout mRNAs lifetime, being thus more enriched as mRNAs age [53]. In addition, by performing experiments in cells with reduced level of Cap2, they found that this epitranscriptomic modification mainly functions in suppressing the activation of the innate immune response by inhibiting RIG-I binding to Cap1, thus providing a mechanism to distinguish self RNA from viral RNA.

Additionally, metabolite-derived cap structures have been discovered in both prokaryotes and eukaryotes. These caps originate from nucleotide-derived molecules, including nicotinamide adenine dinucleotide (NAD), flavin adenine dinucleotide (FAD) and dinucleoside polyphosphates [54]. The latter are small signalling molecules, also called as "alarmones", whose cellular concentrations increase during stress, hence the name. The molecular target of such "alarmones" was not known. By developing a liquid chromatography-mass spectrometry technique for the detection of dinucleoside polyphosphates, the group of Hana Cahová (Institute of Organic Chemistry and Biochemistry of the Czech Academy of Sciences, Prague, CZ) has discovered that alarmones are a non-canonical form of 5' RNA caps in bacteria [55]. They found that dinucleoside polyphosphate capped RNA can be cleaved by two types of enzymes, RppH and ApaH, and thus degraded. However, in stationary phase of growth, and thus under starvation, the dinucleoside polyphosphate RNA caps increase and undergo methylation, protecting RNA from cleavage and further degradation during stress. Thus, the presence of dinucleoside polyphosphate caps, which is strictly dependent on the environmental conditions, may represent a way to preserve specific species of mRNAs during stress.

RNA therapeutics

More than 150 different RNA chemical modifications have been identified so far, characterized by a wide variety of chemical diversities. However, the function of most of these modifications is still unknown. Therefore, the development of reliable chemoenzymatic methods allowing to produce chemically modified RNA may help to elucidate the function of these native modified RNAs and their putative use as RNA tools (such as siRNA, miRNA, antisense nucleotides (ASOs) or aptamers). Introduction of modified nucleotides is a common approach used to increase RNA stability. For example, RNA molecules used to silence genes are quickly degraded by nucleases after cellular uptake and thus modifications make them more resistant to the attack of these enzymes. Aptamers, which are single-stranded oligonucleotides, can act as antagonists or agonists for specific proteins by binding their targets with potentially high affinity. These structured nucleic acid ligands require modifications not only to increase their resistance to nucleases, but also to increase the number of putative targets. Thus, to obtain more stable oligonucleotides, non-native modifications are introduced either at the level of the base, the ribose or the sugar/phosphate backbone. Two major methods already exist to modify nucleic acid: (i) the automated solid-phase synthesis and (ii) the enzymatic synthesis [56]. Due to inherent limitations of both approaches, chemoenzymatic methods are under development in Marcel Hollenstein's group (Institut Pasteur, Paris, FR). Currently, his group is working on the polymerization of modified dNTPs and ligation of oligonucleotides with modified fragments. They equipped the nucleobase of a nucleoside triphosphate with a vancomycin moiety and showed the ability of DNA polymerase to incorporate the modified analogue during DNA synthesis [57]. This modified nucleotide was compatible with SELEX methodology (systematic evolution of ligands by exponential enrichment), and therefore, it was employed to select new aptamers to tackle antimicrobial resistance and restore drug effectiveness. Our global recent experience has shown that nucleic acid

therapeutics are an invaluable alternative to classical vaccine strategies, as it has been highlighted by the development of the mRNA vaccines against SARS-CoV-2.

Indeed, oligonucleotide-based therapies have the potential to treat a wide range of diseases by preventing, replacing, adding, or editing RNA and DNA. Besides aptamers, these novel intervention strategies also comprise the use of antisense oligonucleotides, RNAi and the CRISPR/Cas9 technology. In this context, Jørgen Kjems' group (Interdisciplinary nanoscience center, Aarhus, DK) works on RNA chemical modifications and the design of efficient delivery systems for RNA therapeutics. For example, his group reported a 2'-fluoro protected RNA aptamer which has the ability to bind with high affinity to the receptor-binding domain of SARS-CoV-2 spike protein and inhibits its interaction with the host receptor ACE2 [58]. Impressively, a trimer of this RNA aptamer was able to enhance the binding affinity in the low picomolar range. In addition, Kjems' team recent work focused on the use of aptamers as diagnostic and predictive biomarkers for bladder cancer patients. They developed an RNA aptamer-based strategy called APTASHAPE, which is based on serum-stable RNA oligonucleotides interacting with the proteome of plasma from bladder cancer or healthy control patients [59]. Thus, they were able to identify 33 aptamers that differentiate in abundance between plasma samples from patients with various stages of bladder cancer and controls. Differences in aptamer abundance reflected differences in global proteome of the plasma samples, highlighting how this aptamer-based strategy can be employed for the discovery of new disease biomarkers. Moreover, therapeutic targeting of highly expressed non-coding RNAs represents a novel approach for the treatment of diverse diseases such as cancer. The group of Maria Duca (Institute of Chemistry of Nice, FR) works on development of new RNA ligands able to target molecules such as miRNA. Ribosomal RNAs are well-established antibiotic targets; for example, aminoglycosides and tetracyclines have been already used for several decades. The importance and feasibility of RNA targeting by small molecules has been confirmed in 2021, when Risdiplam was approved by the FDA (Food and Drug Administration)

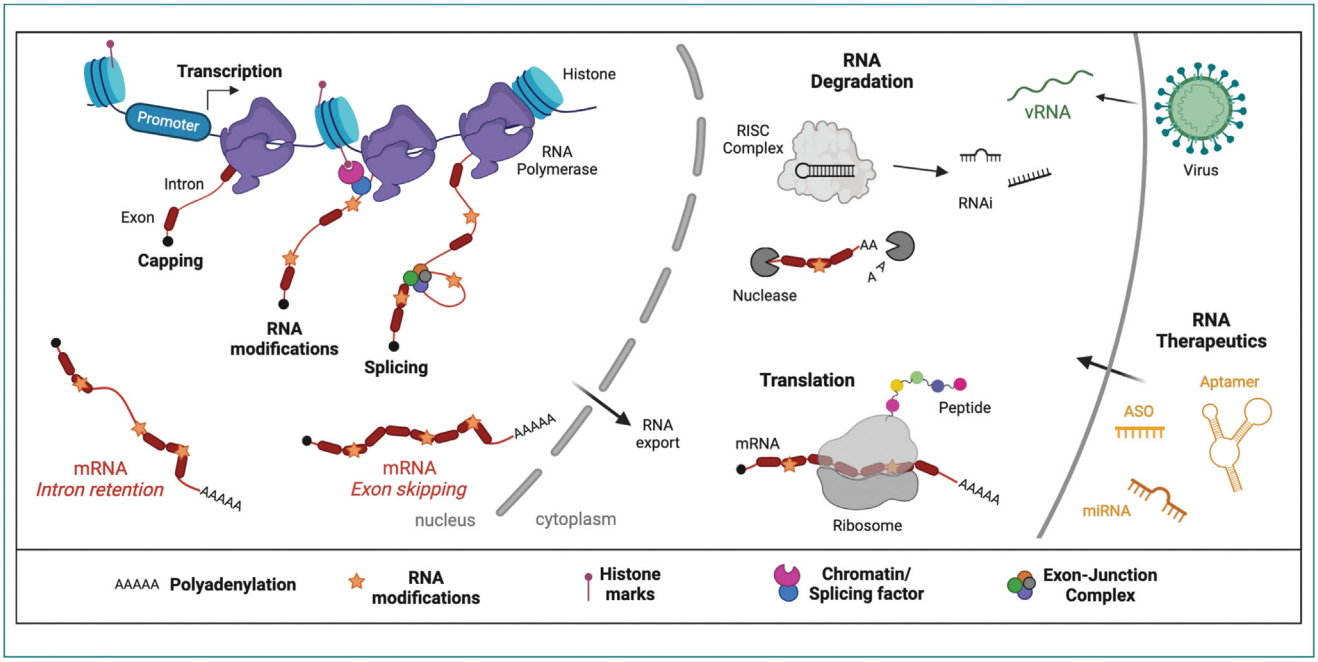

FIGURE 1

Copy of Curie Course. Illustration of the various aspects of the RNA biology and therapeutic aspects discussed in the course. During and after transcription, the molecule of RNA can undergo several regulatory processes important for gene expression that can be targeted with therapeutical purposes. There is (pre-)mRNA alternative splicing, which is the excision of intronic and/or exonic sequences and which is driven by the Exon-Junction Complex; RNA polyadenylation to mark the end of the transcript; RNA modification with the addition of post-transcriptional modifications along the RNA (marked by orange stars on the figure); mRNA export through nuclear pore complex to reach the cytoplasm to perform RNA translation in which the messenger RNA (mRNA) is translated into a peptide thanks to the ribosome complex; and RNA degradation either by nuclease or RISC complex (a ribonucleoprotein complex which forms RNA interference molecules (RNAi) to then target complementary mRNA). The study of these regulatory layers, combined with the chemistry of RNA, allow the design of new RNA therapeutic strategies, such as the use of sequence-specific antisense oligonucleotides (ASO), microRNAs (miRNA) or aptamers. RISC: RNA-induced silencing complex; vRNA: viral RNA. (created by BioRender.com)

for the treatment of the spinal muscular atrophy [60]. The drug modulates splicing and enables the SMN2 gene to produce a full-length SMN protein, which prevents the truncated protein-induced motor neuron deterioration and death. The Duca's lab developed a different approach for the discovery of new RNA ligands, in which they designed and synthesized multimodal RNA binders to increase affinity and selectivity toward the target. For example, her lab designed and synthesized new powerful RNA binders by conjugating the C-terminal lateral chain of bleomycin A5 to different chemical scaffolds known to be able to interact with RNA residues and inhibit the biogenesis of oncogenic pre-miRNAs [61]. In addition, her lab established several chemical library screenings to identify new potential bioactive compounds: they use approaches such as phenotypic screening, target-based screenings, Inforna strategy and RIBOTACS (Ribonuclease-targeted chimeras).

Likewise, emerging evidence has highlighted the involvement of non-canonical nucleic acid secondary structures called G-quadruplexes (G4s) in key cellular processes including translation regulation, 3'-end processing, alternative splicing, and mRNA localization. Importantly, specific G4 ligands not only stabilize G4s and may promote their formation but can modify RNA functions by increasing the lifetime of these structures and modulating their recognition by protein partners. This is why G4 ligands represent highly promising candidates for drug discovery able to act selectively at specific G-rich RNA loci. Daniela Verga (Institut Curie, Orsay, FR) works on the design, synthesis, biophysical and biochemical evaluation of G4 ligands. Her group exploited new methods to follow G4 ligand distribution in both metaphase chromosome spreads and in cells to associate ligand localization to specific cellular responses. For example, they functionalized a highly selective G4 ligand (PhenDC3) with a bromine and followed its distribution on metaphase chromosome spreads by using nanoscale secondary ion mass spectrometry (nanoSIMS) [62]. A more recent research has used other G4 ligands, belonging to the same family of PhenDC3, to develop a new immunofluorescence method allowing the detection of the compounds and, therefore, G4 structures in cells with increased resolution. The more promising compounds were functionalized in situ with 5BrdU (5-bromo deoxyuridine), a hapten which can be recognized by a commercially available antibody, by click reaction (CuAAC, copper catalyzed alkyne-azide cycloaddition reaction) [63].

Conclusion

In conclusion, this course has underscored the importance of post-transcriptional regulation of gene expression in both physiology and disease, such as cancer and viral infection. In particular, the course provided mechanistic insights into the many steps leading to the production of a mature RNA and the control of its translation, and highlighted how RNA chemistry plays a fundamental role in such processes and can be exploited for therapeutics (*figure 1*). Indeed, all the steps involved in RNA metabolism, including pre-mRNA splicing, mRNA editing, translation, and degradation, together with RNA intrinsic features and trans-acting factors participating in such processes, are key contributors of cancer progression, viral infections, as well as immunological responses. This indicates how the post-transcriptional regulation of gene expression, as well as the RNA molecule itself, represents promising target in many pathologies. Moreover, the RNA molecule and chemistry may be useful tools for therapeutic applications, highlighting how advances in RNA biology and chemistry can be fully integrated to pave the way to new therapeutic strategies.

Disclosure of interest: the authors declare that they have no competing interest.

References

[1] Ule J, Blencowe BJ. Alternative splicing regulatory networks: functions, mechanisms and evolution. Mol Cell 2019;76:329–45. http://dx.doi.org/10.1016/j.molcel.2019.09.017.

[2] Amit M, Donyo M, Hollander D, Goren A, Kim E, Gelfman S, et al. Content between exons and introns establishes distinct strategies of splice-site recognition. Cell Rep 2012;1:543–56. http://dx.doi.org/10.1016/j.celrep.2012.03.013.

[3] Tammer L, Hameiri O, Keydar I, Roy VR, Ashkenazy-Titelman A, Custódio N, et al. Gene architecture directs splicing outcome in separate nuclear spatial regions. Mol Cell 2022;82:1021–1034.e8. http://dx.doi.org/10.1016/j.molcel.2022.02.001.

[4] Luco RF, Pan Q, Tominaga K, Blencowe BJ, Pereira-Smith OM, Misteli T. Regulation of alternative splicing by histone modifications. Science 2010;327:996–1000. http://dx.doi.org/10.1126/science.1184208.

[5] Gonzalez I, Munita R, Agirre E, Dittmer TA, Gysling K, Misteli T, et al. A lncRNA regulates alternative splicing via establishment of a splicing-specific chromatin signature. Nat Struct Mol Biol 2015;22:370–6. http://dx.doi.org/10.1038/nsmb.3005.

[6] Segelle A, Núñez-Álvarez Y, Oldfield AJ, Webb KM, Voigt P, Luco RF. Histone marks regulate the epithelial-to-mesenchymal transition via alternative splicing. Cell Rep 2022;38:110357. http://dx.doi.org/10.1016/j.celrep.2022.110357.

[7] Hir H, Le Saulière J, Wang Z. The exon junction complex as a node of post-transcriptional networks. Nat Rev Mol Cell Biol 2016;17:41–54. http://dx.doi.org/10.1038/nrm.2015.7.

[8] Le Hir H, Izaurralde E, Maquat LE, Moore MJ. The spliceosome deposits multiple proteins 20–24 nucleotides upstream of mRNA exon–exon junctions. EMBO J 2000;19:6860–9. http://dx.doi.org/10.1093/emboj/19.24.6860.

[9] Buchwald G, Schüssler S, Basquin C, Le Hir H, Conti E. Crystal structure of the human eIF4AIII–CWC22 complex shows how a DEAD-box protein is inhibited by a MIF4G domain. Proc Natl Acad Sci 2013;110:E4611–18. http://dx.doi.org/10.1073/pnas.1314684110.

[10] Wang Z, Murigneux V, Le Hir H. Transcriptome-wide modulation of splicing by the exon junction complex. Genome Biol 2014;15:551. http://dx.doi.org/10.1186/s13059-014-0551-7.

[11] Le Hir H, Gatfield D, Izaurralde E, Moore MJ. The exon–exon junction complex provides a binding platform for factors involved in mRNA export and nonsense-mediated mRNA decay. EMBO J 2001;20:4987–97. http://dx.doi.org/10.1093/emboj/20.17.4987.

[12] Uzonyi A, Dierks D, Nir R, Kwon OS, Toth U, Barbosa I, et al. Exclusion of m6A from splice-site proximal regions by the exon junction complex

dictates m6A topologies and mRNA stability. Mol Cell 2023;83:237–251.e7. http://dx.doi.org/10.1016/j.molcel.2022.12.026.

[13] Kwon OS, Mishra R, Safieddine A, Coleno E, Alasseur Q, Faucourt M, et al. Exon junction complex dependent mRNA localization is linked to centrosome organization during ciliogenesis. Nat Commun 2021;12:1351. http://dx.doi.org/10.1038/s41467-021-21590-w.

[14] Broeils LA, Ruiz-Orera J, Snel B, Hubner N, van Heesch S. Evolution and implications of de novo genes in humans. Nat Ecol Evol 2023;7:804–15. http://dx.doi.org/10.1038/s41559-023-02014-y.

[15] Mudge JM, Ruiz-Orera J, Prensner JR, Brunet MA, Calvet F, Jungreis I, et al. Standardized annotation of translated open reading frames. Nat Biotechnol 2022;40:994–9. http://dx.doi.org/10.1038/s41587-022-01369-0.

[16] Sandmann C-L, Schulz JF, Ruiz-Orera J, Kirchner M, Ziehm M, Adami E, et al. Evolutionary origins and interactomes of human, young microproteins and small peptides translated from short open reading frames. Mol Cell 2023;83:994–1011.e18. http://dx.doi.org/10.1016/j.molcel.2023.01.023.

[17] Prensner JR, Enache OM, Luria V, Krug K, Clauser KR, Dempster JM, et al. Noncanonical open reading frames encode functional proteins essential for cancer cell survival. Nat Biotechnol 2021;39:697–704. http://dx.doi.org/10.1038/s41587-020-00806-2.

[18] Suenaga Y, Islam SMR, Alagu J, Kaneko Y, Kato M, Tanaka Y, et al. NCYM, a Cis-antisense gene of MYCN, encodes a de novo evolved protein that inhibits GSK3β resulting in the stabilization of MYCN in human neuroblastomas. PLoS Genet 2014;10:e1003996. http://dx.doi.org/10.1371/journal.pgen.1003996.

[19] Buhl AM, Jurlander J, Jørgensen FS, Ottesen AM, Cowland JB, Gjerdrum LM, et al. Identification of a gene on chromosome 12q22 uniquely overexpressed in chronic lymphocytic leukemia. Blood 2006;107:2904–11. http://dx.doi.org/10.1182/blood-2005-07-2615.

[20] Navickas A, Asgharian H, Winkler J, Fish L, Garcia K, Markett D, et al. An mRNA processing pathway suppresses metastasis by governing translational control from the nucleus. Nat Cell Biol 2023;25:892–903. http://dx.doi.org/10.1038/s41556-023-01141-9.

[21] Fish L, Khoroshkin M, Navickas A, Garcia K, Culbertson B, Hänisch B, et al. A prometastatic splicing program regulated by SNRPA1 interactions with structured RNA elements. Science 2021;372. http://dx.doi.org/10.1126/science.abc7531.

[22] Yu J, Navickas A, Asgharian H, Culbertson B, Fish L, Garcia K, et al. RBMS1 suppresses colon cancer metastasis through targeted stabilization of its mRNA regulon. Cancer Discov 2020;10:1410–23. http://dx.doi.org/10.1158/2159-8290.CD-19-1375.

[23] Loayza-Puch F, Rooijers K, Buil LCM, Zijlstra J, Oude Vrielink JF, Lopes R, et al. Tumour-specific proline vulnerability uncovered by differential ribosome codon reading. Nature 2016;530:490–4. http://dx.doi.org/10.1038/nature16982.

[24] Bartok O, Pataskar A, Nagel R, Laos M, Goldfarb E, Hayoun D, et al. Anti-tumour immunity induces aberrant peptide presentation in melanoma. Nature 2021;590:332–7. http://dx.doi.org/10.1038/s41586-020-03054-1.

[25] Pataskar A, Champagne J, Nagel R, Kenski J, Laos M, Michaux J, et al. Tryptophan depletion results in tryptophan-to-phenylalanine substitutants. Nature 2022;603:721–7. http://dx.doi.org/10.1038/s41586-022-04499-2.

[26] Champagne J, Pataskar A, Blommaert N, Nagel R, Wernaart D, Ramalho S, et al. Oncogene-dependent sloppiness in mRNA translation. Mol Cell 2021;81:4709–4721.e9. http://dx.doi.org/10.1016/j.molcel.2021.09.002.

[27] Dicker K, Järvelin AI, Garcia-Moreno M, Castello A. The importance of virion-incorporated cellular RNA-Binding Proteins in viral particle assembly and infectivity. Semin Cell Dev Biol 2021;111:108–18. http://dx.doi.org/10.1016/j.semcdb.2020.08.002.

[28] Iselin L, Palmalux N, Kamel W, Simmonds P, Mohammed S, Castello A. Uncovering viral RNA-host cell interactions on a proteome-wide scale. Trends Biochem Sci 2022;47:23–38. http://dx.doi.org/10.1016/j.tibs.2021.08.002.

[29] Garcia-Moreno M, Noerenberg M, Ni S, Järvelin AI, González-Almela E, Lenz CE, et al. System-wide Profiling of RNA-binding proteins uncovers key regulators of virus infection. Mol Cell 2019;74:196–211.e11. http://dx.doi.org/10.1016/j.molcel.2019.01.017.

[30] Kamel W, Ruscica V, Garcia-Moreno M, Palmalux N, Iselin L, Hannan M, et al. Compositional analysis of Sindbis virus ribonucleoproteins reveals an extensive co-opting of key nuclear RNA-binding proteins. BioRxiv 2021;2021. http://dx.doi.org/10.1101/2021.10.06.463336.

[31] Kamel W, Noerenberg M, Cerikan B, Chen H, Järvelin AI, Kammoun M, et al. Global analysis of protein-RNA interactions in SARS-CoV-2-infected cells reveals key regulators of infection. Mol Cell 2021;81:2851–2867.e7. http://dx.doi.org/10.1016/j.molcel.2021.05.023.

[32] D'Angelo W, Gurung C, Acharya D, Chen B, Ortolano N, Gama V, et al. The molecular basis for the lack of inflammatory responses in mouse embryonic stem cells and their differentiated cells. J Immunol 2017;198:2147–55. http://dx.doi.org/10.4049/jimmunol.1601068.

[33] Maillard PV, van der Veen AG, Poirier EZ, Reis e Sousa C. Slicing and dicing viruses: antiviral RNA interference in mammals. EMBO J 2019;38:e100941. http://dx.doi.org/10.15252/embj.2018100941.

[34] Poirier EZ, Buck MD, Chakravarty P, Carvalho J, Frederico B, Cardoso A, et al. An isoform of Dicer protects mammalian stem cells against multiple RNA viruses. Science 2021;373:231–6. http://dx.doi.org/10.1126/science.abq2264.

[35] Herzog VA, Reichholf B, Neumann T, Rescheneder P, Bhat P, Burkard TR, et al. Thiol-linked alkylation of RNA to assess expression dynamics. Nat Methods 2017;14:1198–204. http://dx.doi.org/10.1038/nmeth.4435.

[36] Reichholf B, Herzog VA, Fasching N, Manzenreither RA, Sowemimo I, Ameres SL. Time-resolved small RNA sequencing unravels the molecular principles of MicroRNA homeostasis. Mol Cell 2019;75:756–768.e7. http://dx.doi.org/10.1016/j.molcel.2019.06.018.

[37] Reimão-Pinto MM, Ignatova V, Burkard TR, Hung J-H, Manzenreither RA, Sowemimo I, et al. Uridylation of RNA hairpins by tailor confines the emergence of MicroRNAs in drosophila. Mol Cell 2015;59:203–16. http://dx.doi.org/10.1016/j.molcel.2015.05.033.

[38] Reimão-Pinto MM, Manzenreither RA, Burkard TR, Sledz P, Jinek M, Mechtler K, et al. Molecular basis for cytoplasmic RNA surveillance by uridylation-triggered decay in Drosophila. EMBO J 2016;35:2417–34. http://dx.doi.org/10.15252/embj.201695164.

[39] Rapino F, Delaunay S, Rambow F, Zhou Z, Tharun L, De Tullio P, et al. Codon-specific translation reprogramming promotes resistance to targeted therapy. Nature 2018;558:605–9. http://dx.doi.org/10.1038/s41586-018-0243-7.

[40] McMahon M, Ruggero D. A wobbly road to drug resistance in melanoma: tRNA-modifying enzymes in translation reprogramming. EMBO J 2018;37:e99978. http://dx.doi.org/10.15252/embj.201899978.

[41] Rapino F, Zhou Z, Roncero Sanchez AM, Joiret M, Seca C, El Hachem N, et al. Wobble tRNA modification and hydrophilic amino acid patterns dictate protein fate. Nat Commun 2021;12:2170. http://dx.doi.org/10.1038/s41467-021-22254-5.

[42] Pederiva C, Trevisan DM, Peirasmaki D, Chen S, Savage SA, Larsson O, et al. Control of protein synthesis through mRNA pseudouridylation by dyskerin. Sci Adv 2023;9:eadg1805. http://dx.doi.org/10.1126/sciadv.adq1805.

[43] Dueva R, Akopyan K, Pederiva C, Trevisan D, Dhanjal S, Lindqvist A, et al. Neutralization of the positive charges on histone tails by RNA promotes an open chromatin structure. Cell Chem Biol 2019;26:1436–1449.e5. http://dx.doi.org/10.1016/j.chembiol.2019.08.002.

[44] Meyer KD, Saletore Y, Zumbo P, Elemento O, Mason CE, Jaffrey SR. Comprehensive analysis of mRNA methylation reveals enrichment in 3' UTRs and near stop codons. Cell 2012;149:1635–46. http://dx.doi.org/10.1016/j.cell.2012.05.003.

[45] Linder B, Grozhik AV, Olarerin-George AO, Meydan C, Mason CE, Jaffrey SR. Single-nucleotide-resolution mapping of m6A and m6Am throughout

the transcriptome. Nat Methods 2015;12:767–72. http://dx.doi.org/10.1038/nmeth.3453.
[46] Zaccara S, Ries RJ, Jaffrey SR. Reading, writing and erasing mRNA methylation. Nat Rev Mol Cell Biol 2019;20:608–24. http://dx.doi.org/10.1038/s41580-019-0168-5.
[47] He PC, He C. m6A RNA methylation: from mechanisms to therapeutic potential. EMBO J 2021;40:e105977. http://dx.doi.org/10.15252/embj.2020105977.
[48] Ries RJ, Zaccara S, Klein P, Olarerin-George A, Namkoong S, Pickering BF, et al. m6A enhances the phase separation potential of Mrna. Nature 2019;571:424–8. http://dx.doi.org/10.1038/s41586-019-1374-1.
[49] Zaccara S, Jaffrey SR. A unified model for the function of YTHDF proteins in regulating m6A-modified mRNA. Cell 2020;181:1582–1595.e18. http://dx.doi.org/10.1016/j.cell.2020.05.012.
[50] Ramanathan A, Robb GB. Chan S-H. mRNA capping: biological functions and applications. Nucleic Acids Res 2016;44:7511–26. http://dx.doi.org/10.1093/nar/gkw551.
[51] Furuichi Y. Shatkin AJBT-A in VR. Viral and cellular mRNA capping: past and prospects. Academic Press 2000;55:135–84. http://dx.doi.org/10.1016/S0065-3527(00)55003-9.
[52] Furuichi Y, Morgan M, Shatkin AJ, Jelinek W, Salditt-Georgieff M, Darnell JE. Methylated, blocked 5 termini in HeLa cell Mrna. Proc Natl Acad Sci 1975;72:1904–8. http://dx.doi.org/10.1073/pnas.72.5.1904.
[53] Despic V, Jaffrey SR. mRNA ageing shapes the Cap2 methylome in mammalian mRNA. Nature 2023;614:358–66. http://dx.doi.org/10.1038/s41586-022-05668-z.
[54] Doamekpor SK, Sharma S, Kiledjian M, Tong L. Recent insights into noncanonical 5' capping and decapping of RNA. J Biol Chem 2022;298:102171. http://dx.doi.org/10.1016/j.jbc.2022.102171.
[55] Hude□ek O, Benoni R, Reyes-Gutierrez PE, Culka M, □anderová H, Hubálek M, et al. Dinucleoside polyphosphates act as 5-RNA caps in bacteria. Nat Commun 2020;11:1052. http://dx.doi.org/10.1038/s41467-020-14896-8.
[56] Flamme M, McKenzie LK, Sarac I, Hollenstein M. Chemical methods for the modification of RNA. Methods 2019;161:64–82. http://dx.doi.org/10.1016/j.ymeth.2019.03.018.
[57] Figazzolo C, Bonhomme F, Saidjalolov S, Ethève-Quelquejeu M, Hollenstein M. Enzymatic synthesis of vancomycin-modified DNA. Molecules 2022;27:8927. http://dx.doi.org/10.3390/molecules27248927.
[58] Valero J, Civit L, Dupont DM, Selnihhin D, Reinert LS, Idorn M, et al. A serum-stable RNA aptamer specific for SARS-CoV-2 neutralizes viral entry. Proc Natl Acad Sci USA 2021;118. http://dx.doi.org/10.1073/pnas.2112942118 [e2112942118].
[59] Fjelstrup S, Dupont DM, Bus C, Enghild JJ, Jensen JB, Birkenkamp-Demtröder K, et al. Differential RNA aptamer affinity profiling on plasma as a potential diagnostic tool for bladder cancer. NAR Cancer 2022;4:zcac025. http://dx.doi.org/10.1093/narcan/zcac025.
[60] Ratni H, Scalco RS, Stephan AH. Risdiplam, the first approved small molecule splicing modifier drug as a blueprint for future transformative medicines. ACS Med Chem Lett 2021;12:874–7. http://dx.doi.org/10.1021/acsmedchemlett.0c00659.
[61] Maucort C, Bonnet M, Ortuno J-C, Tucker G, Quissac E, Verreault M, et al. Synthesis of bleomycin-inspired RNA ligands targeting the biogenesis of oncogenic miRNAs. J Med Chem 2023;66:10639–57. http://dx.doi.org/10.1021/acs.jmedchem.3c00797.
[62] Verga D, Hamon F, Nicoleau C, Guetta C, Wu T, Guerquin-Kern J, et al. Chemical imaging by NanoSIMS provides high-resolution localization of the G-Quadruplex interactive drug (Br)-PhenDC3 on human chromosomes. J Mol Biol Mol Imaging 2017;4:1–6.
[63] Masson T, Landras Guetta C, Laigre E, Cucchiarini A, Duchambon P, Teulade-Fichou M-P, et al. BrdU immuno-tagged G-quadruplex ligands: a new ligand-guided immunofluorescence approach for tracking G-quadruplexes in cells. Nucleic Acids Res 2021;49:12644–60. http://dx.doi.org/10.1093/nar/gkab1166.

Clara Bonnet[1,3], Ana Luisa Dian[1,3], Tristan Espie-Caullet[1,3], Lucilla Fabbri[1,3], Lucie Lagadec[1,3], Thibaud Pivron[1,3], Martin Dutertre[1], Reini Luco[1], Albertas Navickas[1], Stephan Vagner[1], Daniela Verga[2], Patricia Uguen[1]

[1]CNRS UMR3348 Genome integrity, RNA and Cancer, Institut Curie, University Paris-Saclay, 91401 Orsay, France
[2]CNRS UMR9187, Inserm U1196, Chemistry and Modelling for the Biology of Cancer, Institut Curie, université Paris-Saclay, 91405 Orsay, France

Correspondence: Patricia Uguen, CNRS UMR3348 Genome integrity, RNA and Cancer, Institut Curie, University Paris-Saclay, 91401 Orsay, France
patricia.uguen@curie.fr
[3]Equal contribution.

Available online:

https://doi.org/10.1016/j.bulcan.2024.04.005

STAR Protocols

CellPress
OPEN ACCESS

Protocol

Protocol to study the direct binding of proteins to RNA:DNA hybrids or RNA-DNA chimeras in living cells using cross-linking immunoprecipitation

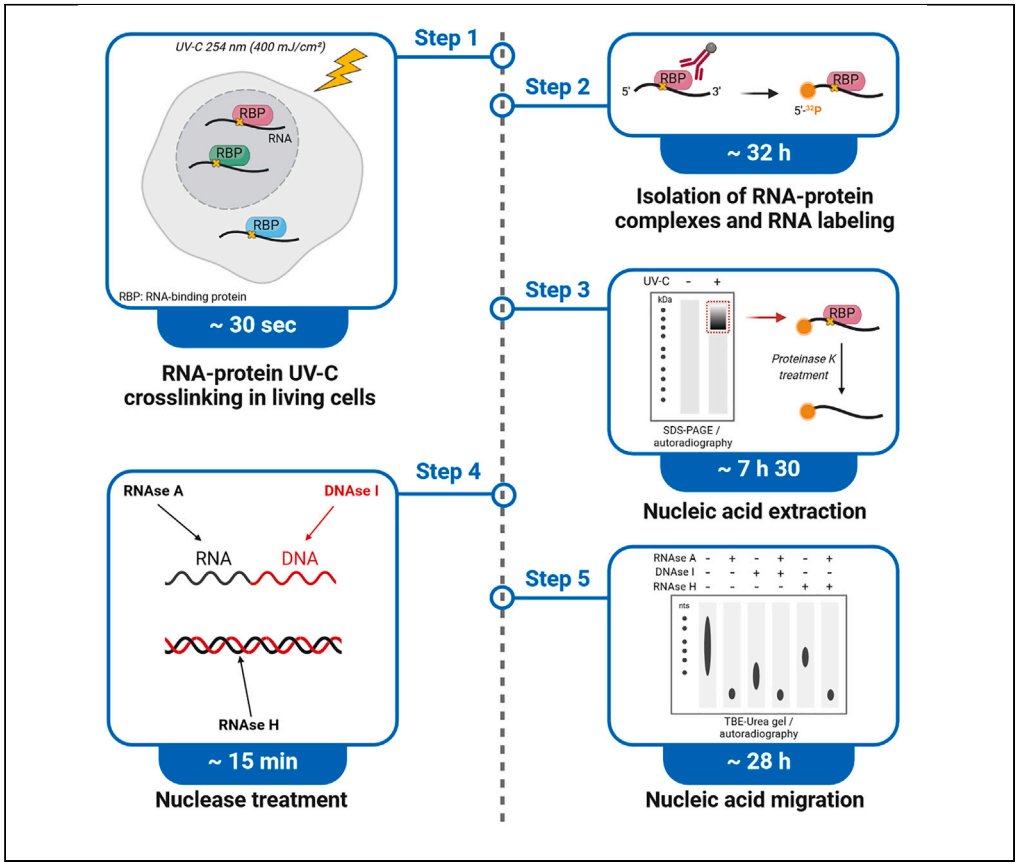

RNA-binding proteins (RBPs) are involved in many biological processes. The direct interaction between protein and RNA can be studied using cross-linking immunoprecipitation (CLIP) techniques in living cells. Here, we present a protocol to characterize the direct binding of proteins to RNA:DNA hybrids or RNA-DNA chimeras in living cells using CLIP. We describe steps for RNA-protein UV-C cross-linking in living cells, isolating RNA-protein complexes, RNA labeling, and extracting nucleic acid. We then detail procedures for nuclease treatment and nucleic acid migration.

Publisher's note: Undertaking any experimental protocol requires adherence to local institutional guidelines for laboratory safety and ethics.

Clara Bonnet, Ana Luisa Dian, Mélissa Leriche, Patricia Uguen, Stéphan Vagner

patricia.uguen@curie.fr (P.U.)
stephan.vagner@curie.fr (S.V.)

Highlights

Protocol to identify the direct interaction between protein and RNA in living cells

Steps to characterize the nature of nucleic acids bound to protein

Guide to characterize proteins interacting with RNA:DNA hybrids or RNA-DNA chimeras

Bonnet et al., STAR Protocols 5, 103292
September 20, 2024
https://doi.org/10.1016/j.xpro.2024.103292

STAR Protocols

CellPress
OPEN ACCESS

Protocol

Protocol to study the direct binding of proteins to RNA:DNA hybrids or RNA-DNA chimeras in living cells using cross-linking immunoprecipitation

Clara Bonnet,[1,2,3] Ana Luisa Dian,[1,2,3] Mélissa Leriche,[1,2,3] Patricia Uguen,[1,2,3,4,5,*] and Stéphan Vagner[1,2,3,*]

[1]Institut Curie, PSL Research University, CNRS UMR 3348, INSERM U1278, Orsay, France

[2]Université Paris-Saclay, CNRS UMR 3348, INSERM U1278, Orsay, France

[3]Equipe labellisée Ligue contre le Cancer, Orsay, France

[4]Technical contact

[5]Lead contact

*Correspondence: patricia.uguen@curie.fr (P.U.), stephan.vagner@curie.fr (S.V.)
https://doi.org/10.1016/j.xpro.2024.103292

SUMMARY

RNA-binding proteins (RBPs) are involved in many biological processes. The direct interaction between protein and RNA can be studied using cross-linking immunoprecipitation (CLIP) techniques in living cells. Here, we present a protocol to characterize the direct binding of proteins to RNA:DNA hybrids or RNA-DNA chimeras in living cells using CLIP. We describe steps for RNA-protein UV-C cross-linking in living cells, isolating RNA-protein complexes, RNA labeling, and extracting nucleic acid. We then detail procedures for nuclease treatment and nucleic acid migration.

BEFORE YOU BEGIN

Make sure the steps using radioactivity labeling are done in a designated and supervised radioactivity area. Prepare all the apparatus which are necessary to perform the experiments from radioactive labeling to extraction and purification of nucleic acids step. Of note, ($\gamma-^{32}$P)ATP is ordered a couple of days before labeling to ensure the highest specific activity. All the steps after cell lysis need to be performed in RNase-free conditions. All buffers are made with ultrapure RNAse-free water.

KEY RESOURCES TABLE

REAGENT or RESOURCE	SOURCE	IDENTIFIER
Antibodies		
Rabbit polyclonal anti-53BP1: for IP 1 μg/100 μg proteins and for WB 1:50,000	Bethyl Laboratories	Cat# A300-272A; RRID: AB_185520
Chemicals, peptides, and recombinant proteins		
PBS (10X), pH 7.4	Gibco	Cat# 70011044
UltraPure DNase/RNase-free distilled water	Invitrogen	Cat# 10977035
EDTA (0.5 M), pH 8.0, RNase-free	Invitrogen	Cat# AM9261
Trizma hydrochloride solution	Sigma-Aldrich	Cat# T2663
Sodium chloride solution	Sigma-Aldrich	Cat# S6546
IGEPAL CA-630	Sigma-Aldrich	Cat# I3021

(*Continued on next page*)

Continued

REAGENT or RESOURCE	SOURCE	IDENTIFIER
Sodium deoxycholate	Sigma-Aldrich	Cat# 30970
UltraPure SDS solution, 10%	Invitrogen	Cat# 15553027
Urea	Sigma-Aldrich	Cat# U6504
$MgCl_2$	Invitrogen	Cat# AM9530G
Tween 20	Sigma-Aldrich	Cat# P7949
cOmplete, EDTA-free protease inhibitor cocktail	Roche	Cat# 11873580001
RNaseOUT recombinant ribonuclease inhibitor	Invitrogen	Cat# 10777019
Bovine serum albumin solution	Sigma-Aldrich	Cat# A7284
ATP, [γ-^{32}P]- 3,000 Ci/mmol 10 mCi/mL EasyTide, 250 µCi	Revvity Health Sciences Inc	Cat# BLU502A250UC
T4 polynucleotide kinase (10 U/µL)	Thermo Scientific	Cat# EK0031
4X Bolt LDS sample buffer	Invitrogen	Cat# B0007
10X Bolt sample reducing agent	Invitrogen	Cat# B0009
NuPAGE 4%–12%, Bis-Tris, 1.0–1.5 mm, mini protein gels	Invitrogen	Cat# NP0321BOX
NuPAGE MOPS SDS running buffer (20X)	Invitrogen	Cat# NP0001
Precision Plus Protein dual color standards	Bio-Rad	Cat# 1610374
Ethanol absolute	VWR	Cat# 20821.310
NuPAGE transfer buffer (20X)	Invitrogen	Cat# NP00061
Proteinase K solution (20 mg/mL), RNA grade	Invitrogen	Cat# 25530049
Phenol:chloroform:iso-amyl alcohol (125:24:1)	Sigma-Aldrich	Cat# P1944
GlycoBlue coprecipitant (15 mg/mL)	Invitrogen	Cat# AM9515
Sodium acetate (3 M), pH 5.5, RNase-free	Invitrogen	Cat# AM9740
RNase A, DNase and protease-free (10 mg/mL)	Thermo Scientific	Cat# EN0531
RNase H (5,000 U/mL)	New England Biolabs	Cat# M0297L
RNase I (100 U/µL)	Invitrogen	Cat# AM2295
TURBO DNase	Invitrogen	Cat# AM1907
RNA loading dye, (2X)	New England Biolabs	Cat# B0363S
Novex TBE-urea gels, 6%	Invitrogen	Cat# EC6865BOX
TBE 10X solution 1 L	EUROMEDEX	Cat# ET020-A
DynaMarker prestain marker for small RNA plus	BioDynamics Laboratory Inc	Cat# DM253S
RNaseZap RNase decontamination solution	Invitrogen	Cat# AM9780
DMEM high glucose w/o L-glutamine w/o sodium pyruvate	Biowest	Cat# L0101-500
Fetal bovine serum	Gibco	Cat# A5256701
L-glutamine (200 mM) 100X CE	Eurobio Scientific	Cat# CSTGLU00-0U
Trypsin-EDTA 10X CE	Eurobio Scientific	Cat# CEZTDA01-0U
Critical commercial assays		
Pierce BCA protein assay kits	Thermo Scientific	Cat# 23225
Quick Start bovine serum albumin standard	Bio-Rad	Cat# 5000207
Experimental models: Cell lines		
Human: A2058 cells	ATCC	RRID: CVCL_1059
Human: U2OS cells	ATCC	RRID: CVCL_0042
Software and algorithms		
Amersham Typhoon scanner control software 2.0	Cytiva	
Other		
DynaMag-2 magnet	Invitrogen	Cat# 12321D
Dynabeads protein G for immunoprecipitation	Invitrogen	Cat# 10004D
Amersham Protran 0.45 NC 300 mm × 4 m	Cytiva	Cat# 10600002
Grade 3MM Chr blotting paper, sheet, 46 × 57 cm	Cytiva	Cat# 3030-917
5PRIME Phase Lock Gel – heavy	Quantabio, LLC	Cat# 2302830
Stratalinker UV crosslinker, model 1800	Stratagene	Cat# 53267-1
Amersham Typhoon biomolecular imager	Cytiva	Cat# 29187191
Molecular Devices Image Eraser model 810-UNV	Molecular Dynamics	Cat# 19170
Exposure cassette 20 × 25 cm	Cytiva	Cat# 29175523
DNA LoBind tubes 1.5 mL	Eppendorf SE	Cat# 0030108051
XCell SureLock mini-cell	Invitrogen	Cat# EI0001

(*Continued on next page*)

Continued

REAGENT or RESOURCE	SOURCE	IDENTIFIER
VWR gel dryer	VWR	Cat# MGD4534
Eppendorf ThermoMixer C	Eppendorf SE	Cat# EP5382000015
Disposable retractable scalpels no. 10	Swann-Morton	Cat# 3901
Mini-PROTEAN tetra vertical electrophoresis cell for mini precast gels, 4-gel	Bio-Rad	Cat# 1658004
Foam pads for Mini Trans-Blot cell	Bio-Rad	Cat# 1703933
Cell scraper M	TPP	Cat# 99003
Bioruptor standard sonicator	Diagenode	UCD-200

MATERIALS AND EQUIPMENT

DMEM Complete medium: DMEM High Glucose supplemented with 10% of Fetal Bovine Serum and 2 mM of L-Glutamine.

Coktail protease inhibitors 25X: Put 1 tablet of cOmplete, EDTA-free Protease Inhibitor Cocktail in 2 mL of Ultrapure RNAse/DNase-free water, and store for months at −20°C.

Lysis Buffer (RIPA) (500 mL)

Reagent	Final concentration	Amount
Tris-HCl pH 7.4 (1 M)	50 mM	25 mL
NaCl (5 M)	100 mM	10 mL
IGEPAL CA-630 (100%)	1%	5 mL
SDS (10%)	0.1%	5 mL
Sodium deoxycholate	0.5%	2.5 g
Ultrapure RNase/DNase-free water		455 mL

PK buffer (15 mL)

Reagent	Final concentration	Amount
Tris-HCl pH 7.4 (1 M)	100 mM	1.5 mL
NaCl (5 M)	50 mM	150 µL
EDTA (0.5 M)	10 mM	300 µL
Ultrapure RNase/DNase-free water		13.05 mL

PK-urea buffer (15 mL)

Reagent	Final concentration	Amount
Tris-HCl pH 7.4 (1 M)	100 mM	1.5 mL
NaCl (5 M)	50 mM	150 µL
EDTA (0.5 M)	10 mM	300 µL
Urea	7 M	6.3 g
Ultrapure RNase/DNase-free water		13.05 mL

Wash Buffer (PNK) (50 mL)

Reagent	Final concentration	Amount
Tris-HCl pH 7.4 (1 M)	20 mM	1 mL
MgCl2 (1 M)	10 mM	500 µL
Tween 20 (100%)	0.2%	100 µL
Ultrapure RNase/DNase-free water		48.4 mL

High Salt Buffer (RIPA-S) (50 mL)

Reagent	Final concentration	Amount
Tris-HCl pH 7.4 (1 M)	50 mM	2.5 mL
NaCl (5 M)	1 M	10 mL
EDTA (0.5 M)	1 mM	100 µL

(*Continued on next page*)

Continued		
Reagent	Final concentration	Amount
IGEPAL CA-630 (100%)	1%	500 μL
SDS (10%)	0.1%	500 μL
Sodium deoxycholate	0.5%	250 mg
Ultrapure RNase/DNase-free water		36.4 mL

T4 PNK mix (20 μL)		
Reagent	Final concentration	Amount
T4 PNK		1 μL
Buffer B		2 μL
(γ-^{32}P)ATP		0.5 μL
PNK buffer		16.5 μL

LDS mix (20 μL)		
Reagent	Final concentration	Amount
LDS 4X		5 μL
Reducing Reagent 10X		2 μL
PNK buffer		13 μL

⚠ CRITICAL: All buffers are filtrated and freshly prepared and kept at 4°C.

STEP-BY-STEP METHOD DETAILS

Cell culture

Timing: 3–4 days

1. Pre-warm DMEM Complete Medium at 37°C.
2. Thaw a cryovial containing frozen cells (protocol described here for the A2058 melanoma cell line) in a 37°C water bath for less than 1 min.
3. Transfer the cells (1 mL) into a T75 flask under a laminar flow hood (clean the hood with ethanol 70% and wear personal protective equipment).
4. Add 9 mL of pre-warmed DMEM Complete Medium into the T75 flask and incubate it for 24 h at 37°C with 5% of CO_2.
5. Once the cells are attached, aspirate the medium and add 10 mL of pre-warmed DMEM Complete Medium.
6. Maintain the cells until 90% of confluency before splitting them.

Note: The appropriate size of the flasks depends on the number of cells frozen in the cryovial.

Cells preparation

Timing: variable 48–72 h

7. Plate 1.5 × 10^6 A2058 cells in 100 mm dish to finally reach 80% of confluency. Use 4 dishes for UV-exposed condition and 2 dishes for non-exposed cells.

Note: The non-exposed UV-C cells serve as a critical control to verify that the signal obtained in CLIP at step 40 is indeed due to the covalent bond between proteins and RNA, induced by UV-C treatment.

8. Incubate cells for 48 h to 72 h at 37°C with 5% of CO_2.

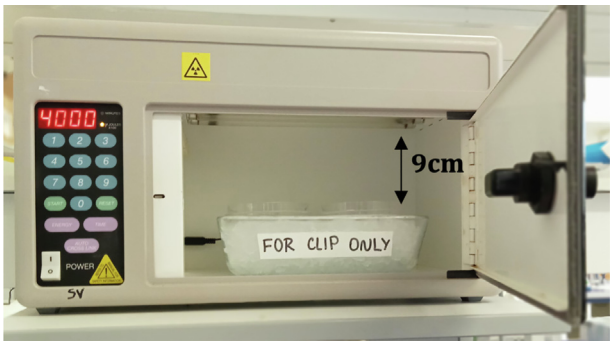

Figure 1. Stratalinker 1800 UV Crosslinker

A trail with ice is set in the middle of the box and plates without cover are placed on ice at 90 mm from the top of the box. The door is closed and 400 mJ/cm^2 is set up on the screen and then the UV is lighted on by pressing start button. After the UV-C exposure, the door is opened, and cells are scraped and lysed.

9. Remove cell culture medium and carefully wash cells with ice-cold 1X PBS to eliminate phenol red, which may interfere with UV-C, and place on ice.
10. Add 2 mL of ice-cold PBS to each dish.

Note: We estimate ≈5–7 million A2058 cells in one 100 mm diameter dish. The input for other cell lines requires optimization. The cells should be around 70%–80% confluent before the UV-C treatment since we are studying events that take place during the replication.

Note: It is possible to perform CLIP on transfected cells. In that case, seed cells and incubate them for 24 h at 37°C with 5% of CO_2. Then, transfect plasmids for protein expression using JetPEI transfection reagent, and incubate for 48 h at 37°C.

Note: Work on ice after removing dishes from the incubator to prevent RNA and protein degradation.

11. Remove dish lids and place the plate on an ice-filled tray in the Stratalinker 1800, or equivalent instrument, at 9 cm from the lights (Figure 1).
12. UV-C irradiate cells at 254 nm with a dose of 400 mJ/cm^2. This takes about 30 s.
13. Immediately scrape off cells with cell scrapers and transfer the cell suspension to a 50 mL Falcon tube.

Note: At the applied dose, UV-C creates covalent bonds between protein and RNA.

14. Centrifuge tubes for 5 min at 300 *g* at 4°C and discard the supernatant.

Note: At this stage, cell pellets can be stored at −80°C for future use.

⚠ CRITICAL: Ensure the use of sterile equipment throughout the CLIP procedure to prevent nucleic acid degradation.

Antibody fixation on magnetic beads

Timing: 5 h

Note: Use a magnetic tube rack to manipulate magnetic beads for an easy and more efficient isolation of proteins and nucleic acids. A few seconds are needed for the beads to stick to the

wall of the tube. Turning the magnetic rack over can help isolate the beads. A possible alternative to the magnetic rack is to centrifuge at 1,000 *g* for 5 min.

15. Gently wash the appropriate volume of Protein G magnetic beads with 10 volumes of ice-cold PBS supplemented by 0.02% of Tween (PBS-Tween 0.02%) 3 times.
16. Rotate beads in PBS-Tween 0.02% supplemented with BSA (100 μg/mL) to block the beads for 30 min at 4°C.
17. Wash 3 additional times with PBS-Tween 0.02% and resuspend in PBS-Tween 0.02%.
18. Add 5 μg of antibody to 50 μL of Protein G magnetics beads and rotate for at least 4 h at 4°C.
19. Wash 2 times with 1 mL of PBS-Tween 0.02%.
20. Resuspend with 1 mL of RIPA. The beads coupled with the antibody can be kept at 4°C for a couple of weeks. RIPA is kept at 4°C for several months.

Note: It is possible to perform the immunoprecipitation with GFP-Trap beads if the protein of interest is fused to GFP. The beads are washed 3 times with RIPA before incubation with lysate (1 mg for 30 μL of GFP-Trap beads).

Cell lysis and immunoprecipitation

Timing: 2 h for steps 21–25 and overnight for step 26

21. Resuspend in 10 times the packed cell volume (around 30–50 μL) in ice-cold RIPA supplemented with a cocktail of protease inhibitors 1X and RNase OUT at 0.1 mM final concentration and transfer to a 1.5 mL microtube.
22. Rotate the cell lysate at 4°C for 1 h.
23. Sonicate the samples using a water bath sonicator (with ice water) set as follows: 0.5′ OFF; 1′ ON; High intensity; 5 min.

Note: Sonication of the lysate facilitates complete lysis and breaks down aggregated chromatin in the sample.

24. Centrifuge at 15,000 *g* for 20 min at 4°C. Recover the supernatant in a 1.5 mL Eppendorf tube and proceed to protein quantification (using the Pierce BCA Protein Assay kit).
25. An optional RNA fragmentation step can be performed. When starting the characterization of a new RNA-binding protein it is necessary to perform the CLIP experiment with and without RNA fragmentation (mild RNase treatment: 0,004 U of RNAse I per μg of protein for 5 min at 37°C) before immunoprecipitation. The optimization of this step enables users to avoid the co-purification of proteins bound to the same RNA, especially for long RNAs.[1]
26. Add 0.5 mg of proteins (concentration at 1 mg/mL in lysis buffer) to the magnetic beads coupled to the antibody against the protein of interest in a final volume of 500 μL of RIPA and rotate overnight at 4°C.

Note: Save 1% of the lysate before adding to the beads. This will be used in the western blot to verify the quantity of starting proteins (input).

Radioactive labeling

Timing: 1 h

27. Put the tube on a magnetic rack and after few seconds, remove carefully the supernatant.

28. Resuspend the beads with 900 μL of ice-cold RIPA-S buffer supplemented with a cocktail of protease inhibitors 1X and RNase OUT at 0.1 mM final concentration. Put back the tube on the magnetic rack, remove the supernatant. Repeat this step. RIPA-S buffer is kept at 4°C for several months.
29. Wash, as described in step 28, twice with 900 μL of ice-cold PNK buffer supplemented with a cocktail of protease inhibitors 1X and RNase OUT at 0.1 mM final concentration. PNK buffer is kept at 4°C for several months.

Note: Save a few μL of the lysate (preferentially the same volume as the input) before washing the beads to verify by western blot the efficiency of immunoprecipitation. This fraction is named flow through.

Note: RIPA-S buffer, rich in salts, removes non-specific proteins bound to the beads without affecting the covalent link between the protein of interest and the RNA.

Note: After washing the beads, save 10% of beads + lysate to verify by western blot the quantity of proteins immunoprecipitated.

30. Prepare the T4 PNK (polynucleotide kinase) mix for the samples. Use 0.5 μL of fresh ($\gamma-^{32}$P)ATP (corresponding to 5 μCi) per sample.

Note: The following steps are performed in a radioactive area. Work behind a plexiglass screen and wear a ring and chest dosimeter.

Note: The T4 PNK transfers the γ-phosphate from radioactive ATP to the 5′OH end of single and double-strand RNA or DNA (forward reaction, buffer A). Buffer B contains ADP to perform an exchange reaction, that catalyzes the exchange of 5′-phosphate.

31. Resuspend the beads in 20 μL of the T4 PNK mix and incubate for 30 min at 37°C in a thermomixer at 800 rpm.
32. Wash the beads twice with 500 μL of ice-cold RIPA-S buffer and once with 500 μL of ice-cold PNK buffer.
33. Eluate the RNA-protein complexes with 20 μL of LDS mix freshly made.
34. Denature the samples for 10 min at 80°C in a thermomixer at 1,000 rpm.

Note: The simultaneous incubation of the beads at high temperature and with strong agitation allows an effective release of the protein-nucleic acid complexes from the beads for proper SDS-PAGE.

35. Recover the supernatant.

Note: Eluates can be stored at −20°C for future use.

SDS-PAGE and transfer

Timing: 5 h 30 min

36. Place the microtubes on the magnetic rack, collect the supernatant and load it on a 4%–12% Bis-Tris gradient gel. Use one well to load a pre-stained protein ladder.
37. Run the gel at 150 V in an XCell SureLock Mini-Cell filled with 1X MOPS SDS running buffer until the Coomassie blue (G250) dye reaches the bottom of the gel.

Note: Avoid the Coomassie blue (G250) dye front to leave the gel to prevent radioactive contamination of the running buffer, since it contains unincorporated radioactive ($\gamma-^{32}$P)ATP.

38. Transfer the protein-nucleic acid complexes from the gel to a nitrocellulose membrane using a liquid transfer device (Mini Trans-Blot Cell) at 100 V for 2 h in 1X Transfer buffer supplemented with 20% of absolute ethanol.

Note: Since 53BP1 is a high molecular weight protein (217 kDa), liquid transfer is preferred.

39. After transfer, place radioactive dots on the bands of the ladder for subsequent membrane cutting. Cover the membrane with Saran wrap and expose it on a radio-luminescent screen for a minimum of 2 h.
40. Read the screen using the Typhoon.

Note: The autoradiography is used as a mask for identifying and cutting out the region of the nitrocellulose membrane correspondent to the protein-nucleic acid complexes (at the expected size of the protein of interest). This process is facilitated by the proper placement of the radioactive dots on the ladder.

Extraction and purification of nucleic acid

Timing: 2 h

41. Cut the nitrocellulose membrane on a clean glass plate using a sterile scalpel. Place the membrane fragment into a 1.5 mL microtube. If there is a signal in the no UV-C condition, cut the membrane and perform the following steps to verify that the observed signal is not due to the presence of nucleic acids.
42. Add 200 μL of PK (proteinase K) buffer and 10 μL of proteinase K with the membrane. PK buffer is kept at 4°C for several months.
43. Incubate for 20 min at 45°C in a thermomixer at 1,000 rpm.

Note: Proteinase K is a protease that degrades proteins on the nitrocellulose membrane to release the bound nucleic acids. It cleaves peptide bonds on the carboxylic sides of aliphatic, aromatic or hydrophobic amino acids.

44. Add 200 μL of PK-urea buffer. PK-urea buffer is kept at 4°C for several months.
45. Incubate for 20 min at 45°C in a thermomixer at 1,000 rpm.

Note: Urea denatures protein substrates, increasing the efficiency of proteinase K digestion.

46. Transfer the 410 μL to a Phase Lock Gel Tube, without mixing, and add the same volume of phenol:chloroform:isoamyl alcohol.

Note: Phase Lock Gel tubes facilitate nucleic acid extraction and prevent interphase contamination.

Note: Handling phenol:chloroform:isoamyl alcohol requires the use of a chemical hood.

47. Incubate for 5 min at 30°C in a thermomixer at 1,100 rpm, then separate the phases by centrifuging for 5 min at 15,000 *g* at room temperature.
48. Collect the aqueous phase (top) and transfer it into a 1.5 mL microtube.
49. Precipitate the nucleic acids by adding a mix of 40 μL of sodium acetate (3M), 1 μL of glycoblue and 1 mL of 100% ethanol per sample.

50. Place the tube at −20°C overnight.
51. The next day, centrifuge for 20 min at 15,000 *g* at 4°C.
52. Remove the supernatant and wash the pellet with 1 mL of 80% ethanol.
53. Quickly dry the pellet and resuspend it in 24 μL of RNAse-free water.

Nuclease treatment

Timing: 15 min

54. Separate the 24 μL from the previous step into 6 tubes containing the same volume (i.e., 4 μL).
55. Add either 1 μL of water, or 1 μL of RNAse A at 10 mg/mL, or 1 μL of DNase I at 2 U/μL, or 1 μL of RNAse A + 1 μL of DNAse I, or 1 μL of RNAse H at 5,000 U/mL or 1 μL of RNAse A + 1 μL of RNAse H to each tube.
56. Incubate 10 min at 37°C in a thermomixer at 300 rpm.

Note: Enzymes are in excess here to maximize nucleic acid digestion. RNAse A degrades single-strand RNA specifically after C and U residues. RNAse H cleaves the RNA strand in a RNA:DNA hybrid. DNAse I cleaves single and double-stranded DNA.

Nucleic acid migration

Timing: 28 h

57. Add 5 μL of loading buffer (TBE-urea sample buffer 2X) and incubate for 5 min at 80°C in a thermomixer at 1,000 rpm.
58. Load the 10 μL sample onto a denaturing 6% TBE-urea gel in parallel with a DynaMarker Prestain Marker for Small RNA Plus ladder. Use 1X TBE as the migration buffer.
59. Run at 70 V and stop the migration once the bromophenol dye reaches $^{3}/_{4}$ of the gel.
60. After migration, place the gel on two sheets of Whatman paper, cover it with Saran wrap and vacuum-dry for 2 h 30 at 80°C.

Note: Proper vacuum should be maintained to prevent gel breakage.

61. Add radioactive dots on the ladder to locate the different RNA size. This will help to define the length of the nucleic acid fragments generated after enzymatic digestion after autoradiography.
62. Expose the dry gel on a radio-luminescent screen for a minimum of 24 h.
63. Read the screen using the Typhoon.

EXPECTED OUTCOMES

CLIP is commonly used to demonstrate direct interactions between RNA and proteins.[2] Several refinements of the initial CLIP protocol allow to address specific questions such as the identity of bound RNA or the definition of RNA-bound sites.[1] Here we propose a protocol to characterize interaction of proteins with RNA-DNA chimeras[3] or RNA:DNA hybrids. This should prove useful in the field of genome integrity.

Indeed, both DNA replication and the DNA damage response involve the intervention of RNA molecules.[4,5] During the discontinuous DNA replication of the lagging strand, the DNA primase first synthetizes RNA primers of 7–12 ribonucleotides (initially hybridized with the template DNA forming RNA:DNA hybrids) that are subsequently elongated by DNA POLδ, that synthesizes approximately 100 deoxyribonucleotides downstream the RNA primers (Okazaki fragments).[6] When POLδ reaches the downstream primer, it displaces the RNA sequence, generating a 5′-end ssRNA-DNA flap.[6–8] In addition to the short RNA:DNA hybrids formed by Okazaki fragments, longer RNA:DNA hybrids can be generated when nascent transcripts anneal to DNA template or other close homologous DNA

region. This physiological structure is called R-loop and is usually transient.[9] For example, transcription-replication-conflicts (TRC) favors the formation of R-loops and thus creating head-on TRC.[10] More recently, RNA:DNA hybrids have been also detected at DSB where they are important for proper DNA repair.[11] However, when R-loop are not properly removed or resolved, DNA replication or DSB repair pathway are affected and can lead to genome instability.[5]

We have developed a procedure to characterize direct interactions between RBPs and RNA:DNA hybrids or RNA-DNA chimeras. It is based on the CLIP method and allows the detection of RBP-bound RNA:DNA hybrids or RNA-DNA chimeras. Using different enzymatic treatments, we showed that 53BP1, typically described as involved in the DNA damage and replication stress response, directly interacts with Okazaki fragments through its RNA-binding activity at replication forks in the absence of external stress.[3] This protocol enables users to characterize *in vivo* the complexity of the nucleic acids bound to the protein of interest. Different enzymatic treatments can be applied to the nucleic acids extracted from radioactive labeled nucleic acids-RBP complexes to determine their composition, thereby identifying RBPs able to bind to ssRNAs, RNA-DNA chimeras or RNA:DNA hybrids. It can also be used on synchronized cells to only monitor RBPs during S-phase, as well as adapted to identify the RBP domain(s) involved in the interaction with nucleic acids of distinct natures.[3] In addition, this protocol enables one to roughly assess the size of the ribonucleotides and deoxyribonucleotides sequences bound to the protein of interest based on the radioactive signal emitted from the labeled nucleic acids that migrated on a denaturing TBE-urea gel alongside a pre-stained marker for RNA.

To characterize the complexity of the nucleic acids bound to 53BP1, we extracted nucleic acids from ^{32}P labeled nucleic acid-GFP-53BP1 complexes (Figure 2A). The extracted nucleic acids were then loaded on a denaturing TBE-urea gel, and the radioactive signal was revealed using autoradiography. We found that the nucleic acids bound to 53BP1 typically migrate as a smear ranging from 20 to 150 nt (Figure 2A; [3]). Treatment of the nucleic acids with RNase A, which cleaves single-stranded and double-stranded RNAs led to a collapsed smear well below 25 nt, therefore indicating the presence of ribonucleotides at the 5′ends of the nucleic acids bound to 53BP1. Strikingly, cleavage of single and double-stranded DNAs also affected the size of the smear. Indeed, following DNase I treatment, the size of the smear was also shortened, indicating that 53BP1 interact with nucleic acids composed of both ribonucleotides and deoxyribonucleotides. Moreover, digestion with a combination of RNAse A and DNase I led to a complete degradation of the remaining DNase I-resistant smear, confirming that it was composed of RNA. We therefore concluded that 53BP1 interacts with RNA-DNA chimeras composed of a small RNA sequence (less than 25 nt) at the 5′-end followed by a longer (up to 100 nt) DNA sequence at their 3′-ends.[3] This profile is characteristic of Okazaki fragments. To further determine the nature of the nucleic acids bound to 53BP1, we treated the extracted nucleic acids with RNase H (Figure 2B). RNase H is an endoribonuclease that specifically cleaves RNA hybridized to DNA. Strikingly, we observed that the nucleic acids bound to 53BP1 were weakly sensitive to RNase H treatment, thus indicating that 53BP1 also binds to RNA:DNA hybrids albeit to a small extent. The remaining smear was partially degraded following RNase A treatment, meaning that the remaining nucleic acids were composed of ssRNA at their 5′end (Figure 2B). Therefore, the combination of RNAse H and RNAse A treatments reveals that a small proportion of 53BP1 not only directly binds to RNA:DNA hybrids but also binds to other RNA species which could constitute the 5′ flap.

To gather more evidences that 53BP1 binds to RNA:DNA hybrids at replication forks in living cells, we performed a single-cell assay for *in situ* Protein Interaction with Nascent DNA Replication Forks (SIRF, [12]), as previously described.[3] This method uses *in situ* proximity ligation assays (PLA) combined with 5′-ethylene-2′-deoxyuridine (EdU)-biotin click-iT chemistry, allowing quantitative analyses of nascent DNA-protein interactions. Consistent with the hypotheses that 53BP1 binds to RNA:DNA hybrids, RNase H treatment decreased the recruitment of 53BP1 to the nascent DNA at the replication fork (Figure 3A). This decrease in the proximity between 53BP1 and nascent DNA was not due to

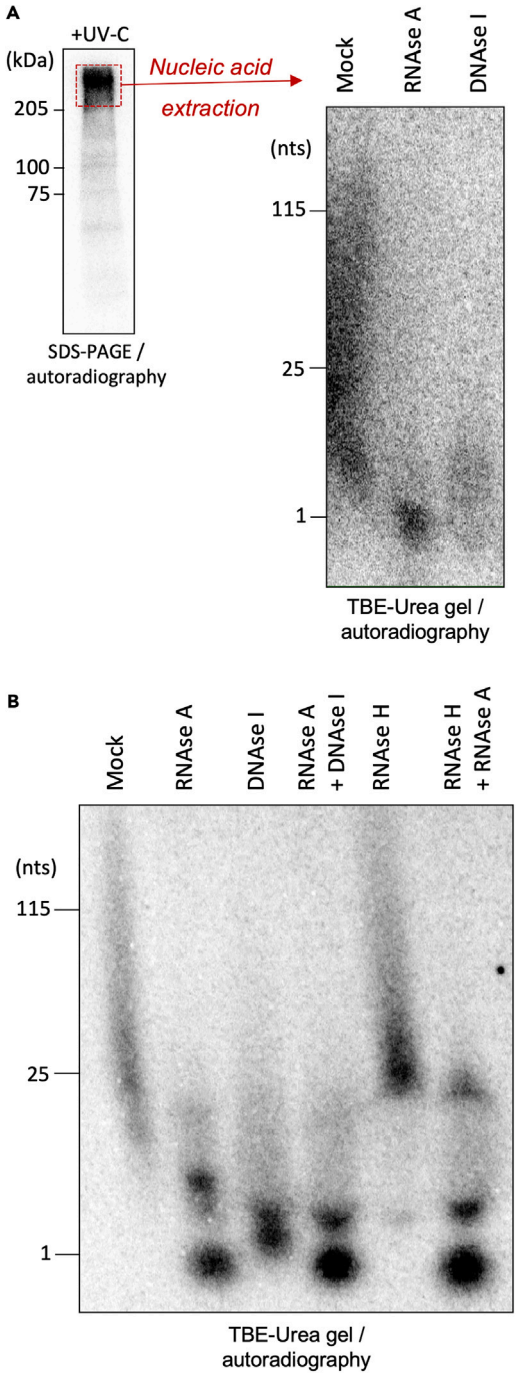

Figure 2. 53BP1 binds to RNA-embedded DNA

(A) CLIP (left panel) and nucleic acid extraction (right panel) from A2058 cells. The extracted nucleic acids are either non treated (mock) or treated for 10 min at 37°C with the indicated enzyme (either 1 μL RNAse A or 1 μL DNAse I). In this experiment, lysate was treated with 0,004 U of RNAse I per μg of protein for 5 min at 37°C before the immunoprecipitation step.

(B) Nucleic acid extraction from A2058 cells. The extracted nucleic acids are either non treated (mock) or treated for 10 min at 37°C with the indicated enzyme(s) as follow: lane "RNAse A" corresponds to 1 μL RNAse A at 10 mg/mL; lane "DNAse I" corresponds to 1 μL DNAse I at 2 U/μL; lane "RNase H" corresponds to 1 μL of RNAse H at 5,000 U/mL. The two other conditions correspond to treatment with two enzymes as indicated in the figure.

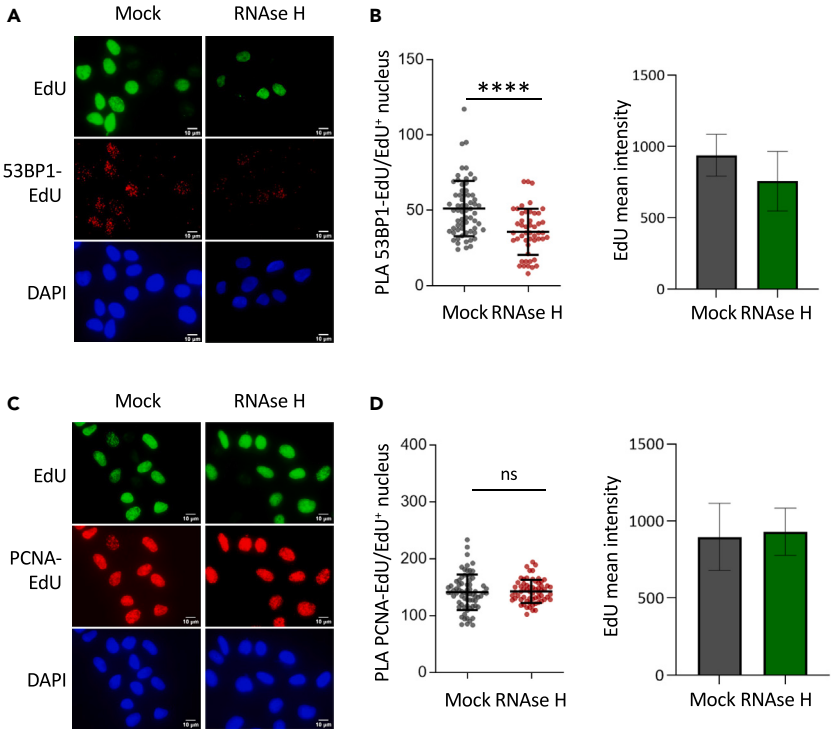

Figure 3. Interaction of 53BP1 with nascent DNA at replication fork is decreased upon RNAse H treatment

(A) Representative images of 53BP1-EdU SIRF in U2OS cells permeabilized and treated with RNAse H (60 U, 15 min at 37°C) or left untreated (Mock); PLA signal (red), Alexa Fluor 488–EdU staining (green), and DAPI staining (blue).

(B) The significance for 53BP1-EdU PLA values (shown as a scatter plot) was derived from the Mann-Whitney statistical test. Bars represent the mean ± SD ****$p < 0.0001$ ($n = 3$ biological replicates). EdU mean intensity of (A) is shown as a bar graph.

(C) Representative images of PCNA-EdU SIRF in U2OS cells permeabilized and treated with RNAse H (60 U, 15 min at 37°C) or left untreated (Mock); PLA signal (red), Alexa Fluor 488–EdU staining (green), and DAPI staining (blue).

(D) The significance for PCNA-EdU PLA values (shown as a scatter plot) was derived from the Mann-Whitney statistical test. Bars represent the mean ± SD ****$p < 0.0001$ ($n = 3$ biological replicates). EdU mean intensity of (C) is shown as a bar graph.

lower EdU incorporation (Figure 3B), since the EdU mean intensity was not impacted by the RNase H treatment. Moreover, the same effect of the RNAse H treatment was not observed on the recruitment of the PCNA protein (Proliferating Cell Nuclear Antigen), which is a component of the replisome and therefore a key factor in DNA replication, to the nascent DNA (Figures 3C and 3D). We therefore concluded that 53BP1 interacts with RNA:DNA hybrids at nascent DNA replication forks.

LIMITATIONS

CLIP is a qualitative approach to study RBP. Thus, CLIP is not appropriate to compare binding efficiencies between different RBPs or even between a wild-type protein and its variants. In addition, the efficiency of UV-C cross-linking is poor and is dependent on the mode of binding.[1] This could lead to false negative interpretations. UV-C preferentially cross-links RBPs to uridines and less to guanosines which can lead to a bias due to the ribonucleotide composition.[13]

The antibody specificity for the immunoprecipitation is critical although this can be overcome by the fusion of affinity tag to the protein of interest.

Some proteins are degraded after treatment with UV-C which decreases the efficiency of the CLIP detection.

This method needs radioactivity equipment and product which require authorization from IRSN (Institut de Radioprotection et de Sureté Nucléaire) or any governmental agency in charge of radiation safety rules.

TROUBLESHOOTING

Problem 1

Absence of signal on CLIP SDS-PAGE autoradiography (step 40).

Potential solution

Absence of signal on the ^{32}P autoradiograms could indicate several issues in different steps of the CLIP protocol. 1) Cross-linking conditions might need to be optimized (step 12). Poor cross-linking efficiencies might lead to loss of the RNA molecules associated to the protein of interest during the isolation of the complexes. 2) Ensure that the antibody is specific and efficient for the immunoprecipitation of the protein of interest (step 18). 3) Proteins localized to specific subcellular compartments may require the use of adapted cell lysis methods for protein extraction (steps 21 to 26). Additionally, low protein input may lead to an absence of signal. Therefore, ensure that enough protein is being used (step 26). 4) It might be necessary to optimize the radioactive labeling conditions (steps 30). Low levels of ^{32}P incorporation may lead to weak or undetectable signals on the autoradiograms. 5) RNA fragmentation may be necessary before immunoprecipitation for proper purification of the nucleic acid-protein complexes.

Problem 2

Presence of signal in UV- on CLIP SDS-PAGE autoradiography.

Potential solution

Phosphorylation of the protein by itself can give a radioactive band on the protein-nucleic acids gel. The nucleic acids extraction (steps 41 to 53) followed by enzymatic treatment by RNAse and/or DNAse (step 54 to the end) should precise whether in no UV-C condition there are RNA bound to the protein or whether it is due to protein phosphorylation.

Problem 3

There are several bands on CLIP SDS-PAGE autoradiography.

Potential solution

To define which band is indeed the band corresponding to the complex protein-nucleic acids, it is possible to perform an siRNA depletion against the protein of interest. The band corresponding to the studied RBP should decrease or even disappear. This is what we performed to precise which band what specific to 53BP1.[3] In addition, potential background can be removed by increasing the number of washes after immunoprecipitation step.

Problem 4

RNA degradation after extraction and purification of nucleic acids.

Potential solution

Unexpected RNA degradation could indicate contaminations or improper handling of samples and reagents. The experiment should be performed on a RNase-free environment, with the use of sterile materials.

RESOURCE AVAILABILITY

Lead contact

Further information and requests for resources and reagents should be directed to and will be fulfilled by the lead contacts, Patricia Uguen (patricia.uguen@curie.fr).

Technical contact

Technical questions on executing this protocol should be directed to the technical contact, Patricia Uguen (patricia.uguen@curie.fr).

Materials availability

This protocol did not generate new materials or reagent.

Data and code availability

This study did not create specific code or datasets.

ACKNOWLEDGMENTS

This work was supported by grants from Institut Curie, Gustave Roussy, INSERM, CNRS, and Equipe labellisée Ligue Nationale Contre le Cancer, the Association for Research against Cancer, Université Paris-Saclay. M.L. was supported by a pre-doctoral fellowship from Ligue Nationale Contre le Cancer, and C.B. by a pre-doctoral fellowship from the Ministère de l'Enseignement Supérieur et de la Recherche. A.L.D. received funding from the European Union's Horizon 2020 research and innovation program under the Marie Skłodowska-Curie grant agreement no. 847718.

AUTHOR CONTRIBUTIONS

Conceptualization, C.B., M.L, P.U., and S.V.; investigation, A.L.D., C.B., M.L., and P.U.; writing – original draft, A.L.D., C.B., P.U., and S.V.; writing – review and editing, A.L.D., C.B., P.U., and S.V.; funding acquisition, S.V.; supervision, P.U. and S.V.

DECLARATION OF INTERESTS

The authors declare no competing interests.

REFERENCES

1. Lee, F.C.Y., and Ule, J. (2018). Advances in CLIP Technologies for Studies of Protein-RNA Interactions. Mol. Cell *69*, 354–369. https://doi.org/10.1016/j.molcel.2018.01.005.

2. Ule, J., Jensen, K., Mele, A., and Darnell, R.B. (2005). CLIP: A method for identifying protein–RNA interaction sites in living cells. Methods *37*, 376–386. https://doi.org/10.1016/j.ymeth.2005.07.018.

3. Leriche, M., Bonnet, C., Jana, J., Chhetri, G., Mennour, S., Martineau, S., Pennaneach, V., Busso, D., Veaute, X., Bertrand, P., et al. (2023). 53BP1 interacts with the RNA primer from Okazaki fragments to support their processing during unperturbed DNA replication. Cell Rep. *42*, 113412. https://doi.org/10.1016/j.celrep.2023.113412.

4. Audoynaud, C., Vagner, S., and Lambert, S. (2021). Non-homologous end-joining at challenged replication forks: an RNA connection? Trends Genet. *37*, 973–985. https://doi.org/10.1016/j.tig.2021.06.010.

5. Brickner, J.R., Garzon, J.L., and Cimprich, K.A. (2022). Walking a tightrope: The complex balancing act of R-loops in genome stability. Mol. Cell *82*, 2267–2297. https://doi.org/10.1016/j.molcel.2022.04.014.

6. Burgers, P.M.J., and Kunkel, T.A. (2017). Eukaryotic DNA Replication Fork. Annu. Rev. Biochem. *86*, 417–438. https://doi.org/10.1146/annurev-biochem-061516-044709.

7. Zaher, M.S., Rashid, F., Song, B., Joudeh, L.I., Sobhy, M.A., Tehseen, M., Hingorani, M.M., and Hamdan, S.M. (2018). Missed cleavage opportunities by FEN1 lead to Okazaki fragment maturation via the long-flap pathway. Nucleic Acids Res. *46*, 2956–2974. https://doi.org/10.1093/nar/gky082.

8. Raducanu, V.-S., Tehseen, M., Al-Amodi, A., Joudeh, L.I., De Biasio, A., and Hamdan, S.M. (2022). Mechanistic investigation of human maturation of Okazaki fragments reveals slow kinetics. Nat. Commun. *13*, 6973. https://doi.org/10.1038/s41467-022-34751-2.

9. Thomas, M., White, R.L., and Davis, R.W. (1976). Hybridization of RNA to double-stranded DNA: formation of R-loops. Proc. Natl. Acad. Sci. USA *73*, 2294–2298. https://doi.org/10.1073/pnas.73.7.2294.

10. Hamperl, S., and Cimprich, K.A. (2016). Conflict Resolution in the Genome: How Transcription and Replication Make It Work. Cell *167*, 1455–1467. https://doi.org/10.1016/j.cell.2016.09.053.

11. Marnef, A., and Legube, G. (2021). R-loops as Janus-faced modulators of DNA repair. Nat. Cell Biol. *23*, 305–313. https://doi.org/10.1038/s41556-021-00663-4.

12. Roy, S., and Schlacher, K. (2019). SIRF: A Single-cell Assay for in situ Protein Interaction with Nascent DNA Replication Forks. Bio. Protoc. *9*, e3377. https://doi.org/10.21769/BioProtoc.3377.

13. Feng, H., Bao, S., Rahman, M.A., Weyn-Vanhentenryck, S.M., Khan, A., Wong, J., Shah, A., Flynn, E.D., Krainer, A.R., and Zhang, C. (2019). Modeling RNA-Binding Protein Specificity In Vivo by Precisely Registering Protein-RNA Crosslink Sites. Mol. Cell *74*, 1189–1204.e6. https://doi.org/10.1016/j.molcel.2019.02.002.